Final Report 299 42 210

Mapping of ecosystem specific long-term trends in deposition loads and concentrations of air pollutants in Germany and their comparison with Critical Loads and Critical Levels

Part 1: Deposition Loads 1990-1999

Dipl.-Geogr. Th. Gauger

Dipl.-Geogr. F. Anshelm

Dipl.-Geogr. Hartmut Schuster

Dr. Jan Willem Erisman

MSc. Alex T. Vermeulen

Dr. Geert P. J. Draaijers

MSc. Albert Bleeker

Dr. Hans-Dieter Nagel

Institut für Navigation
der Universität Stuttgart
Head of Institute: Prof. Dr.-Ing. A. Kleusberg

ON BEHALF OF
FEDERAL ENVIRONMENTAL AGENCY
(UMWELTBUNDESAMT), BERLIN

December 2002

Berichts-Kennblatt

1. Berichtsnummer UBA-FB 299 42 210	2. Endbericht	3.

4. Titel des Berichts

Kartierung ökosystembezogener Langzeittrends atmosphärischer Stoffeinträge und Luftschadstoffkonzentrationen in Deutschland und deren Vergleich mit Critical Loads und Critical Levels

5. Autor(en), Name(n), Vorname(n)

Gauger, Thomas	Erisman, Jan Willem	Bleeker, Albert
Anshelm, Frank	Vermeulen, Alex T.	Nagel, Hans-Dieter
Hartmut Schuster	Draaijers, Geert P. J.	

8. Abschlußdatum

15. Februar 2002

9. Veröffentlichungsdatum

Dezember 2002

6. Durchführende Institution (Name, Anschrift)

Institut für Navigation
Universität Stuttgart
Breitscheidstr. 2

D-70174 Stuttgart

10. UFOPLAN - Nr.

BMU/UBA 299 42 210

11. Seitenzahl

Teil 1: 207 **Teil 2:** 104

12. Literaturangaben

Teil 1: 128 **Teil 2:** 128

7. Fördernde Institution (Name, Anschrift)

Umweltbundesamt
Bismarckplatz1

D-14193 Berlin

13. Tabellen

Teil 1: 64 **Teil 2:** 6

14. Abbildungen + Karten

Teil 1: 98 **Teil 2:** 60

15. Zusätzliche Angaben

16. Kurzfassung

Der Abschlußbericht zum o. g. Forschungsvorhaben ist - bis auf eine enthaltene deutsche Zusammenfassung - in englischer Sprache abgefasst und gliedert sich in zwei Teile:

Teil 1: „Deposition Loads 1990-1999“

mit dem Schwerpunkt der Erfassung der Nass-, Trocken-, Wolkenwasser- und Gesamtdeposition von SO_X-S, NH_X-N, NO_Y-N, Cl, Na, Ca, Mg und K in Deutschland im Zeitraum 1990 – 1999 gestützt auf Monitoringdaten und die Nutzung von Inferentialmodellen für eine räumlich hoch aufgelöste Depositionskartierung.

Es werden Methoden, Eingangsdaten und Modellergebnisse der Erfassung von Eintragsraten der Naß-, Trocken-, Wolkenwasser- und Gesamtdeposition vorgestellt. Trends der Nass-, Trocken und Gesamtdeposition im Verlauf der Zehnjahresperiode 1990 bis 1999 werden ausführlich dargestellt einschließlich der graphischen Aufbereitung der einzelnen Kartierungsergebnisse, die das räumliche Muster des Depositionsgeschehens und seine Entwicklung im Lauf der Zeit abbilden. Eine Gegenüberstellung der Ergebnisse der Deutschen mit der EMEP Kartierung für SO_X-S, NH_X-N, NO_Y-N 1999 ist enthalten. Die Berechnung von Critical Loads und deren Überschreitung für potentielle Säure- und eutrophierende Stickstoffeinträge in Deutschland wird in einer kurzen Zusammenfassung präsentiert.

Die Bearbeitung dieses Beritsteils erfolgte in enger Kooperation zwischen dem Institut für Navigation, Stuttgart, ECN in Petten (NL), TNO-MEP in Apeldoorn (NL) und ÖKO-DATA in Strausberg.

Teil 2: „Mapping Critical Levels exceedances“

beschreibt die Methoden und Datengrundlagen der Berechnung und flächenhaften Kartierung von Luftschadstoffkonzentrationen und die Überschreitung von **Critical Levels** für die Schadgase O_3, SO_2 und NO_x , bezogen auf die Rezeptoren landwirtschaftliche Nutzpflanzen, Wald- und naturnahe Ökosysteme sowie die menschliche Gesundheit für den Zeitraum 1985 bis 1999.

17. Schlagwörter

Critical Loads - Critical Levels - Deposition - Immission - Überschreitung von Critical Loads - Überschreitung von Critical Levels - potentielle Säureeinträge - Stickstoffeinträge - Ozon - Ozon AOT40-Werte – Ozon AOT60-Werte – WHO-Luftqualitätsleitwert zum Schutz der Menschlichen Gesundheit - Schwefeldioxid - Stickstoffoxide -

18. Preis	19.	20.

1. Report No.
UBA-FB 299 42 210

2.
Final Report

3.

4. Report Title

Mapping of ecosystem specific long-term trends in deposition loads and concentrations of air pollutants in Germany and their comparison with Critical Loads and Critical Levels

5. Author(s), Family Name(s), First Name(s)

Gauger, Thomas	Erisman, Jan Willem	Bleeker, Albert
Anshelm, Frank	Vermeulen, Alex T.	Nagel, Hans-Dieter
Hartmut Schuster	Draaijers, Geert P. J.	

8. Report Date
February, 15th 2002

9. Publication Date
December 2002

6. Performing Organisation (Name, Address)

Institute of Navigation
Stuttgart University
Breitscheidstr. 2

D-70174 Stuttgart

10. UFOPLAN – Ref. No.
BMU/UBA 299 42 210

11. No. of Pages
Part 1: 207 **Part 2:** 104

12. No. of References
Part 1: 128 **Part 2:** 128

7. Sponsoring Agency (Name, Address)

Federal Environmental Agency
Bismarckplatz 1

D-14193 Berlin

13. No. of Tables
Part 1: 64 **Part 2:** 6

14. No. of Figures and Maps
Part 1: 98 **Part 2:** 60

15. Supplementary Notes

16. Abstract

This final report describes the results of the project “Mapping of ecosystem specific long-term trends in deposition loads and concentrations of air pollutants in Germany and their comparison with Critical Loads and Critical Levels ”.

Part 1: “Deposition Loads 1990 - 1999” has been carried out in close co-operation between INS, Stuttgart University, ECN, Petten, NL, TNO-MEP, Apeldoorn, NL and ÖKO-DATA, Strausberg. This Part of the report deals with mapping total deposition of von SO_X-S, NH_X-N, NO_Y-N, Cl, Na, Ca, Mg and K in Germany for the period 1990 to 1999 using monitoring data and inferential models on a small scale. Methods, data and results of

- the national scale approach of assessing wet, dry, cloud and total deposition on an ecosystem level in Germany,
- the trends of wet, dry and total deposition over the ten years time period from 1990 to 1999 and the graphical representation of the mapping result showing the spatial trend over Germany within the time period considered and
- a brief summary of Critical Loads and Critical Loads Exceedance calculations for Potential Acidity and Nutrient Nitrogen in Germany

are presented, including a synopsis of the German and EMEP 1999 mapping results for SO_X-S, NH_X-N, NO_Y-N.

Part 2: “Mapping Critical Levels exceedances“

refers to the mapping of air concentration and exceedances of **Critical Levels** of O_3, SO_2 , and NO_x in the years 1985 – 1999. The receptors “agricultural crops”, “forests”, “natural ecosystems” and “health effects” have been taken into account.

17. Keywords

Critical Loads - Critical Levels - Deposition - Air Concentration - Air Pollutants - Exceedance of Critical Loads - Exceedance of Critical Levels - Potential Acid Deposition - Nitrogen Deposition - Ozone AOT40 – Ozone AOT60 - WHO Guideline Level for the protection of human health - Sulphur Dioxide - Nitrogen Dioxide

18. Price

19.

20.

Contents

List of figures

List of tables

List of maps

1 Introduction

The research project “Mapping of ecosystem specific long-term trends in deposition loads and concentrations of air pollutants in Germany and their comparison with Critical Loads and Critical Levels” (BMU/UBA FE-No. 299 42 210) is carried out on behalf of Federal Environmental Agency, Berlin (Umweltbundesamt, UBA). The aim of the project is to support the German Federal Environmental Agency in calculation and verification of national data to be implemented in European scale Critical Loads and Levels maps. Special interest is put on the detection of long term trends in deposition loads and concentration of air pollutants in Germany. The results of this research project are gained by working in close co-operation with (1) Gesellschaft für Ökosystemanalyse und Umweltdatenmanagement mbH (ÖKO-DATA GmbH) located in Strausberg, (2) Netherlands Organization for Applied Scientific Research (TNO), Institute of Environmental Sciences, Energy Research and Process Innovation (TNO-MEP), Appeldoorn, and (3) Netherlands Energy Research Foundation (ECN), Petten.

Within the project national maps of air concentration levels and deposition loads are generated. The maps are used to calculate exceedances of scientifically derived thresholds, aimed to protect different receptors, the Critical Loads and Critical Levels, in Germany. The calculation of the maps is based upon measurement network data, additional model estimates and high resolution land use maps. Differences of air pollutant input to several receptors, ecosystems respectively, on the local scale can be identified and exceedances of Critical Levels and Critical Loads within different regions in Germany are determined. Moreover time-rows of pollutant maps are monitoring the effects of emission reduction and ecosystem specific long-term trends of air pollutants and exceedances can be derived.

The International Co-operative Program on Modelling and Mapping of Critical Loads & Levels and Air Pollution Effects, Risks and Trends (ICP Modelling and Mapping), formerly Task Force on Mapping, founded in 1988 under the leadership of the Federal Republic of Germany, has developed an effects-based approach, the concept of critical loads and levels, that allows to monitoring, mapping and evaluating the concentrations and loads of pollutants under various chemical parameters and biological conditions. The critical loads and levels are scientifically derived thresholds, aimed to protect different receptors (ICP MODELLING AND MAPPING, 2002).

The Critical Loads and Levels concept has been successfully applied to strategies for emission reductions under two protocols of the UN/ECE Convention on Long-range Transboundary Air Pollution (CLRTAP, Geneva, 1979): the 1994 Protocol on Further Reductions of Sulphur Emissions and the 1999 Gothenburg-Protocol to Abate Acidification, Eutrophication and Ground-level Ozone (‘multi-pollutant/multi-effect protocol’). The 1999 Gothenburg-Protocol for the first time sets the critical loads for acidity, nutrient nitrogen and critical levels or national ambient air quality standards for ozone as emission reduction targets (ICP MODELLING AND MAPPING, 2002). Article 1 of the Gothenburg Protocol defines the terms “Critical Load” and “Critical Levels”:

- "**Critical load**" means a quantitative estimate of an exposure to one or more pollutants below which significant harmful effects on specified sensitive elements of the environment do not occur, according to present knowledge.
- "**Critical levels**" mean concentrations of pollutants in the atmosphere above which direct adverse effects on receptors, such as human beings, plants, ecosystems or materials, may occur, according to present knowledge.

Objectives of the ICP Modelling and Mapping among others are to: support the Working Group on Effects (WGE) and the Convention (CLRTAP) by preparing, reviewing and assessing critical load and level maps and by performing data quality control; continuously update the critical loads and levels methodologies; maintain and update existing data bases; disseminate information and provide assistance for interpretation and use of critical load and level maps. In order to provide scientific and technical assistance to the ICP Modelling and Mapping, a Coordination Center for Effects (CCE) was established at the National Institute of Public Health and the Environment (RIVM) in Bilthoven, The Netherlands. The CCE solicits and co-ordinates the data of the 24 participating countries (ICP MODELLING AND MAPPING, 2002; CCE, 2002).

On the national scale this research and development is co-ordinated by the National Focal Centers (NFC). The NFC Mapping Germany is established at Federal Environmental Agency (Umweltbundesamt), Berlin, its collaborating institutions are ÖKO-DATA, Strausberg and Institute of Navigation (INS), Stuttgart University (CCE, 2002).

The outline of the methodologies of modelling and mapping air concentration, total deposition, critical levels and loads was published in the Manual on Methodologies and Criteria for Mapping Critical Levels/Loads (‘Mapping Manual’, UBA, 1966), which at present is undergoing refurbishment. The publication of an updated and revised version of the Mapping Manual, including several new developments and applications found on the base of international scientific discussion and experiences, will soon be available. The Mapping Manual and its updates are basic orientation for the work carried out within this project.

The scope of this research and development project is the mapping of long-term

- air concentration fields of sulphur dioxide (SO_2), nitrogen oxides (NO, NO_2, and NO_X), and ozone (O_3)
- Critical Levels for ecosystems and human health and their exceedances in Germany
- receptor specific total deposition fields of base cations, acidifying and eutrophicating compounds in Germany, used as input for ecosystem specific calculations of Critical Loads and Critical Loads exceedances

Emission, in-air transport and conversion of pollutants, **air concentration**, removal from the atmosphere (‘**total deposition**’) by wash-out and rain-out processes (‘**wet deposition**’), by direct deposition of particles and gases to terrestrial surfaces (‘**dry deposition**’), or direct capture of cloud and/or fog droplets containing airborne pollutants by receptor surfaces (‘**cloud&fog deposition**’), in principle can all be measured directly at certain sample points. There are different measurement networks spread over Germany, where basic measurands are quantified routinely. Additionally applied model calculations can generate fields of atmospheric conditions, atmospheric processes and atmospheric fluxes from basic measurement and successively modelled data.

Air pollution levels and loads as well as critical levels and loads need to be mapped in order to implement regionalized emission control strategies based on a cost-effective minimisation of effects. The risk of damage to ecosystems by air pollutants is determined neither by actual pollutant air concentrations or total deposition fluxes alone, nor by critical levels or critical loads alone. It is determined by the difference between actual and critical values, which is termed **exceedance of critical levels and loads** (UBA, 1996; SPRANGER ET AL. 2001).

Actual air pollutants, receptors and critical levels and loads are conveniently represented on maps (Figure 1.1). This allows to quantify combined effects of receptor and/or ecosystem specific factors in relation to current pollutant inputs in their spatial distribution.

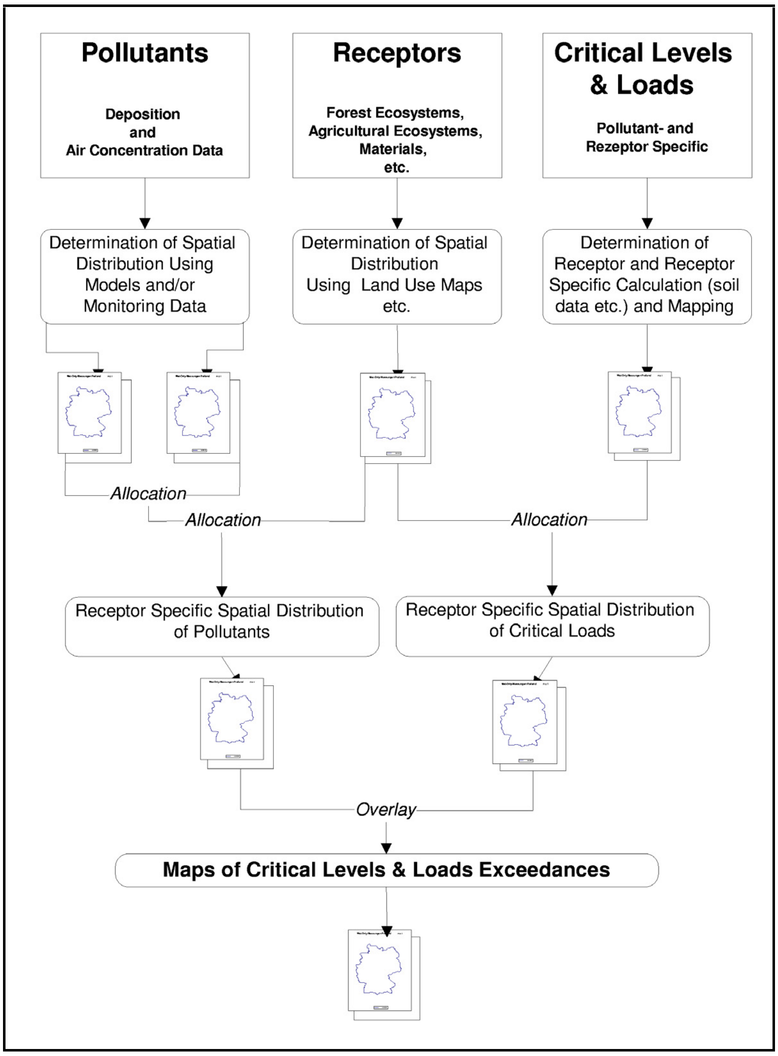

Figure 1.1: Outline of mapping critical loads and critical levels exceedances in Germany

The work carried out in this joint research and development project of INS and the subcontractors ECN, TNO-MEP and ÖKO-DATA in particular were:

by **INS, Stuttgart University**:

- the co-ordination of the work of the project partners, including data transfer within the project; organisation and presentation of project meetings (June 2000 in Petten, NL; April 2001 in Bilthoven, NL; December 2001 in Stuttgart, D); reporting and permanent contact to Federal Environmental Agency (UBA)
- the support of Federal Environmental Agency (UBA) by:
  - providing data and information needed at UBA or in parallel projects carried out on behalf of UBA,
  - providing data and information to other scientific and governmental institutions
  - participating in national and international expert work group sessions and workshops including oral and poster presentations of methods and interim results
- update of UBA/INS air concentration database
- classification of air concentration monitoring sites, mapping air concentration fields of SO_2, NO, NO_2 and mapping of critical levels exceedances for SO_2, NO_X, O_3
- mapping AOT60 and WHO120 guideline level for protection of human health
- critical levels for vegetation, modification of O_3 level I AOT40, approaching O_3 level II
- calculation of map statistics and trends in air concentration and critical levels exceedance over Germany
- update of UBA/INS wet deposition database, including quality checks and preparation of input data for mapping wet deposition
- update of DWD precipitation maps via UBA
- mapping wet deposition fields of SO_4-S, NO_3-N, NH_4-N, K, Ca, Mg, Na, Cl, and H for the years 1987 to 1999; calculation of preliminary maps of wet deposition fields of Cd and Pb 1996
- investigation of errors and uncertainties of wet deposition maps and calculation of map statistics and trends of wet deposition in Germany
- canopy budget model calculations used for validation of the mapping results of dry and total deposition, transfer of data from INS to TNO
- calculation of SO_2 air concentration fields based on measurements for dry deposition input data correction purposes
- calculation of dry deposition fluxes from air concentration and revised deposition velocity data per land use class (provided by ECN) and calculation of map statistics and trends of dry deposition in Germany
- calculation of total deposition fluxes from wet and dry deposition fluxes and map statistics and trends of total deposition in Germany
- deposition data transfer to ÖKO-DATA for critical loads and exceedance calculations
- co-ordination and compilation of the final report of the project

by **ECN, Petten**:

- transfer of input data and maps from the previous project to ECN
- update and thorough modification of the EDACS/IDEM model parameterisation modules
- update of meteorological input data
- acquisition of LRT air concentration data for 1985 and 1990 to 1996 at EMEP, Kjeller, Norway
- recalculation of dry deposition from the previous project, comparison of mapping and modelling results
- data acquisition of air concentration data from NERI (DEM/DEHM) for the years 1990 and 1996 to 2000, which were not available from EMEP LRT model calculations
- update of air concentration data and preparation of the data sets as input for IDEM model calculations
- modelling of dry deposition 1985 and 1990 to 2000
- preliminary modelling of cloud&fog deposition 1990 to 2000 on the basis of 1998 liquid water content model data
- modelling of dry deposition point data (forest stands)
- revision and recalculation of dry deposition velocity per land use class 1990 to 1999 and data transfer to INS
- programming of a map and data viewer for Germany, production of a prototype master CD-ROM
- reporting

by **TNO-MEP, Apeldoorn**:

- transfer of the EUTREND model from RIVM to TNO
- transfer of updated emission data from the German NH_3 emission database (1990 to 1998) from UBA emission inventory via IER, Stuttgart University (emission per Landkreis) and INS
- allocation of emissions to areas with agricultural land use per Kreis (5x5km^{2}grid)
- comparison of previous used and updated NH_3 emission data
- acquisition of other input data necessary for calculating NH_X air concentration and dry deposition using EUTREND
- EUTREND model calculations of NH_X dry deposition 1990 to 1998
- preparation of canopy budget model calculations for validation purposes, transfer of throughfall and stemflow data from INS to TNO
- calculation of comparison between modelled and measured dry and total deposition data
- reporting

by **ÖKO-DATA, Strausberg**:

- transfer of available data of wet, dry and total deposition estimates from INS to ÖKO-DATA
- calculation of critical loads and exceedance using total deposition data available for an update of the national data set provided to CCE, Bilthoven in 2001
- calculation of trends and emission reduction scenarios to derive estimates of the dynamics in deposition abatement affecting critical loads and exceedance calculation results
- transfer of CORINE Land Cover information and data in the grid and land use class resolutions needed for critical loads exceedance calculations to ECN and TNO-MEP via INS
- acquisition of different parameters necessary for dry and cloudwater deposition modelling from Level II forest intensive monitoring plot data at the Bundeslaender forest research institutions responsible for the measurements. Transfer of forest plot data to ECN in order to calculate site specific deposition and in order to derive validation data for mapping results respectively
- deposition data transfer from INS to ÖKO-DATA for critical loads and exceedance calculations, data validation at certain forest plots, comparison with previous model calculations and mapping results
- participating in national and international expert work group sessions and workshops including oral and poster presentations of methods, data and interim results
- reporting

2 Deposition of air pollutants used as input for Critical loads exceedance calculations

The application of the critical load concept is suitable to describe the threshold below which present loads have to be reduced for ecosystem recovery. By definition, the threshold values are measurable quantitative estimates showing the degree of tolerable exposure to one or more pollutants. These scientifically derived values reflect the state of present knowledge and are subject to revisions as science develops further.

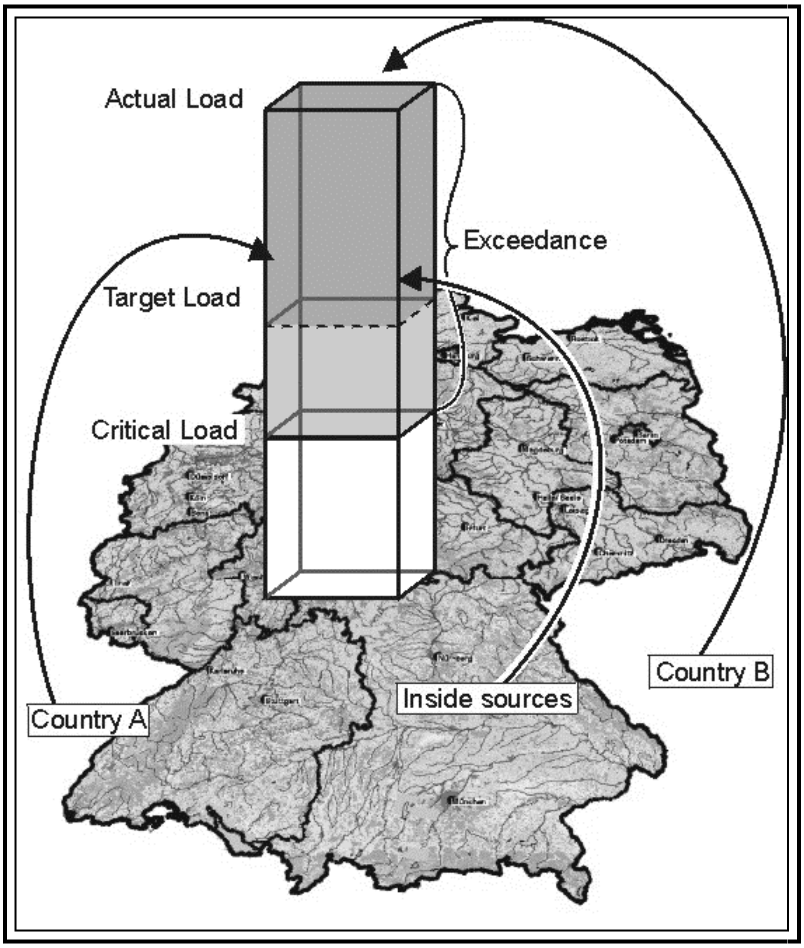

Figure 2.1: Illustration of the critical loads concept (ICP MODELLING AND MAPPING, 2002)

Figure 2.1 illustrates the concept on the example of Germany representing a ‘receptor’. The arrows stand for the transport of transboundary and inland emitted pollutants, which are deposited into the receptor system (actual load). The column is showing the critical load value in its bottom part, target loads represent interim emission reduction goals as a percentage reduction towards achieving critical loads (‘gap-closure’). Exceedance is the difference between critical load and actual deposition load. The critical loads represent tolerable, long-term deposition rates of pollutants that do not harm structure and function of ecosystems.

Acidification occurs due to the total deposition of sulphur (S) and nitrogen (N) compounds, resulting in destabilisation of soil processes or to direct vegetation damage. Significant damage can be expected to develop when certain chemical parameters of the soil solution, such as base cations, show a marked deviation from the steady-state conditions. The release of heavy metals and aluminium may increase the negative effects of acidification. Eutrophication will occur when nitrogen (N) inputs result in nutrient imbalances. The ecosystem then more likely is affected by climatic and other stresses, and eutrophication often affects the biodiversity of terrestrial and aquatic ecosystems because existing plant and animal communities are unable to adapt to the changes in chemical conditions.

The magnitude of any critical load depends on the structural and functional (geological, hydrological, pedological, biological, economical and ecological) factors and properties of the target ecosystem and receptor respectively, tat builds up the pollution load capacity at a given location. Thus, critical loads are different for each plant community, forest and soil type, climatic condition, etc.

Receptors (c.f. Map 2.1) for critical loads in this project are terrestrial ecosystems, including forests, and (semi-) natural vegetation, covering about 30% of Germany. Mapping of critical loads and their exceedance in Germany is carried out using the ‘Level I’ or mass-balance approach: A **simple mass balance** (‘SMB’) is used to calculate critical loads for acidity and nutrient nitrogen (Figure 2.2).

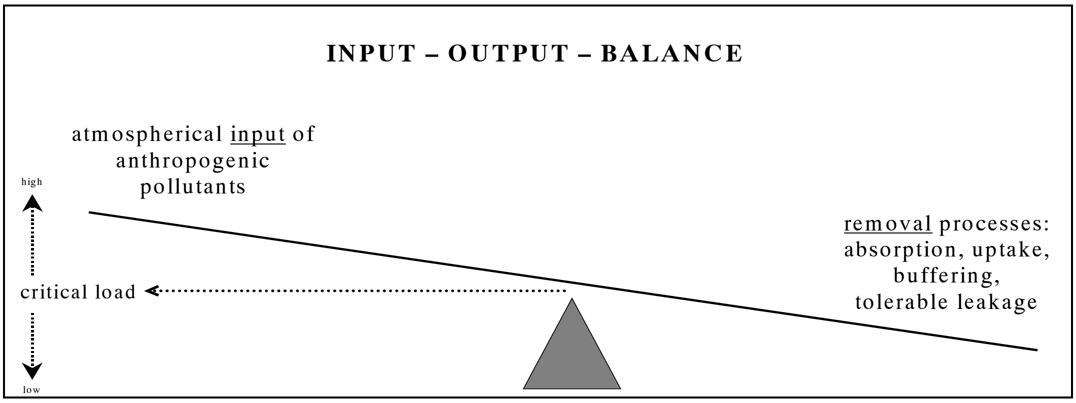

Figure 2.2: Application of a simple quantitative mass balance to derive critical loads

Critical loads for each ecosystem are determined using a simple quantitative mass balance method, where the balance is calculated between the mainly anthropogenic inputs of pollutants (sources) on the one side, and removal processes (sinks) on the other side, which consist in absorption, uptake, buffering or tolerable transfer into other environmental compartments. The critical load for potential acidity ($CL_{(ACpot)}$, Equation (2.1)) is set where the acid input can be neutralised by the total acid neutralisation capacity (ANC) of the ecosystem:

$$CL_{(AC_{pot})} = BC_w - BC_u + N_i + N_u + N_{de} - ANC_{le(crit)} \quad [\text{eq ha}^{-1}\ \text{a}^{-1}] \tag{2.1}$$

where:

$CL_{(ACpot)}$ = critical load for potential acidity
BC_w = base cations weathering derived from soil type and parent material class
BC_u = base cations uptake and removal by biomass under steady state conditions
N_i = long-term nitrogen immobilisation
N_u = nitrogen uptake and removal by biomass under steady state conditions
N_{de} = denitrification rate
$ANC_{le(crit)}$ = acceptable leaching of acid neutralisation capacity

Critical loads for nutrient nitrogen ($CL_{nut}(N)$) are determined by the given properties of the ecosystems. The maximum tolerable deposition (critical load) of nitrogen again is calculated at equilibrium between input and removal. Temporary deviations from equilibrium only are tolerable as long as the ecosystem is capable of recovering (steady state condition). Equation (2.2) shows the nitrogen cycle of terrestrial ecosystems on these terms:

$$CL_{nut}(N) = N_u + N_i + N_{de} + N_{l(acc)} \text{ [eq ha}^{-1}\text{ a}^{-1}\text{]} \qquad (2.2)$$

where:

$CL_{nut}(N)$ = critical load for nutrient nitrogen
N_u = nitrogen uptake and removal by biomass under steady state conditions
N_i = long-term nitrogen immobilisation
$N_{l(acc)}$ = acceptable leaching of nitrogen
N_{de} = denitrification rate

Details on the equations can be found in the 'Mapping Manual' (UBA, 1996) and in NAGEL & GREGOR (1999).The methods applied and current (preliminary) critical loads maps of Germany can be found in the CCE status reports (e.g. CCE, 2001) and in national reports (e.g. NAGEL ET AL. 2000), respectively.

The comparison of critical loads maps, calculated for a certain receptor-pollutant combination, with current deposition loads of the pollutant provides critical loads exceedance maps. To derive the exceedance of critical loads of nitrogen, $CL_{nut}(N)$ (Equation (2.2)) the difference to total depositions of nitrogen, N_{dep} (Equation (2.3)) is calculated. The exceedance of critical loads of potential acidity is calculated as difference of $CL_{(ACpot)}$ (Equation (2.1)) and total deposition of potential acidity, $AC_{(pot)dep}$ (Eqation. (2.4))

$$N_{dep} = NO_{ydep} + NH_{xdep} \text{ [eq ha}^{-1}\text{ a}^{-1}\text{]} \qquad (2.3)$$

$$AC_{(pot)dep} = (SO_{X(nss)dep} + N_{dep} + Cl_{(nss)dep}) - (Ca_{(nss)dep} + Mg_{(nss)dep} + K_{(nss)dep}) \text{ [eq ha}^{-1}\text{ a}^{-1}\text{]} \qquad (2.4)$$

where:

$SO_{X\,(nss)dep}$ = total deposition of non-sea-salt oxidised sulphur compounds (SO_2, SO_4^{2-})
NO_{Ydep} = total deposition of oxidised nitrogen compounds (NO, NO_2, HNO_3, NO_3)
NH_{Xdep} = total deposition of reduced nitrogen compounds (NH_3, NH_4^+)
N_{dep} = total deposition of nitrogen compounds ($NO_{ydep} + NH_{xdep}$)
$Cl_{(nss)dep}$ = wet deposition of non-sea-salt chloride (Cl^-)
$Ca_{(nss)dep}$ = total deposition of non-sea-salt calcium (Ca^{2+})
$Mg_{(nss)dep}$ = total deposition of non-sea-salt magnesium (Mg^{2+})
$K_{(nss)dep}$ = total deposition of non-sea-salt potassium (K^+)

In the definition of $\boldsymbol{AC_{(pot)dep}}$ the following **basic assumptions** are made:

- Several oxidative processes, mainly due to fossil fuel combustion, are underlying the acidifying effects of airborne sulphur and nitrogen. The products of in-air chemical reaction are deposited and taken up by the soil e.g. in form of nitric and sulphuric acid. The deposition of 1mol of oxidised nitrogen (NO_Y) is set equal to 1mol H^+, the deposition of 1mol of oxidised sulphur (SO_X) is set equal to 2mol H^+.

- Within the frame of the critical loads concept it is assumed, that on the long run all reduced nitrogen input (NH_X) is completely nitrified and exported from the ecosystem as nitrate (NO_3^-), thereby acidifying the system. Thus, with respect to soil acidification, a net-production of 1mol H^+ per 1mol NH_X is assumed.
- The anthropogenic chloride mainly are emitted as hydrochloric acid (HCl) and equal 1mol H^+ per 1mol of deposited chloride (Cl^-). However, the quantitatively most important natural source of deposited Cl^- is sea spray. Emission abatement of course aims at man-made emission. Moreover it can be assumed that all sea salt input is chemically neutral. Deposition originating from sea spray therefore is quantified by assuming that the ratio of Ca^{2+}, K^+, Mg^{2+}, SO_4^{2-} and Cl^- to sodium (Na^+) in bulk sea water is the same as in sea spray and all Na is of marine origin. It then is possible to correct the deposition for the sea-salt contribution accordingly (see Chapter 4.3.1). These corrected deposition values are attributable to predominantly anthropogenic sources and termed 'non-sea-salt' (e.g. $Cl_{(nss)}$). With respect to soil acidification it is assumed that 1mol H^+ per 1mol $Cl_{(nss)}$ is formed.
- The non-sea-salt deposition of base cations calcium (Ca^{2+}), potassium (K^+), and magnesium (Mg^{2+}) – all Na^+ is assumed to be of sea spray origin and not taken into account (see above and Chapter 4.3.1) – are assumed to neutralise the input of potential acidity ($AC_{(pot)dep}$). Natural background deposition of base cations in principle should not be included here. The rates emission reduction of acidifying compounds, negotiated and decided upon within the frame of CLRTAP, is to be deduced from their acidifying effects alone and must not be compensated by other anthropogenic emissions (e.g. base compounds emitted by coal combustion). Thus only the natural background deposition of base cations, which can be assumed as ecosystem property because it has a certain continuity in time and space, may be charged up against potential acid deposition. Unfortunately there is no adequate application quantifying natural and anthropogenic rates of base cat-ion deposition fluxes yet. The total deposition of non-sea-salt base cations (BC_{nss}) representing base cations attributable to natural *and* anthropogenic emission processes excluding neutral salts from sea spray therefore is used in this study to be charged up against potential acid deposition ($AC_{(pot)dep}$). The result is termed deposition of potential net acidity ($AC_{(pot)net}$).

The units used for deposition fluxes as well as for critical loads are ionic equivalents per hectare and year (eq ha^{-1} a^{-1}). The calculation on the base of ionic equivalents facilitates the direct comparison of deposited magnitudes of compounds and the of their quantities e.g. with regard of the acid balance.

An important aspect – aside an exact definition of the compounds being processed – is the use of the same spatial geometry for mapping deposition and critical loads. Deposition fluxes as well as critical loads have to be related to the same area and to the same receptor. Calculations of critical loads in Germany presently are carried out for the receptor ecosystems: coniferous forests, deciduous forests and mixed forests, natural grassland, acid fens and heathland wet grassland and mesotrophic peat bogs respectively (Table 2.1). The minimum requirements for gathering receptor specific total deposition are spatial resolutions corresponding to the receptor map used for critical loads calculations and mapping (Map 2.1).

Table 2.1: Receptors for critical loads calculations in Germany

Ecosystem type	**Percentage of receptor area (total Germany = 100%)**	**Percentage of total considered receptor area**
coniferous forest	16,0 %	52,9 %
deciduous forest	6,5 %	21,6 %
mixed forest	6,4 %	21,3 %
natural grassland	0,5 %	1,8 %
acid fens and heathland	0,3 %	1,0 %
wet grassland	0,1 %	0,4 %
mesotrophic peat bogs	0,3 %	1,0 %
total:	30,1 %	100,0 %

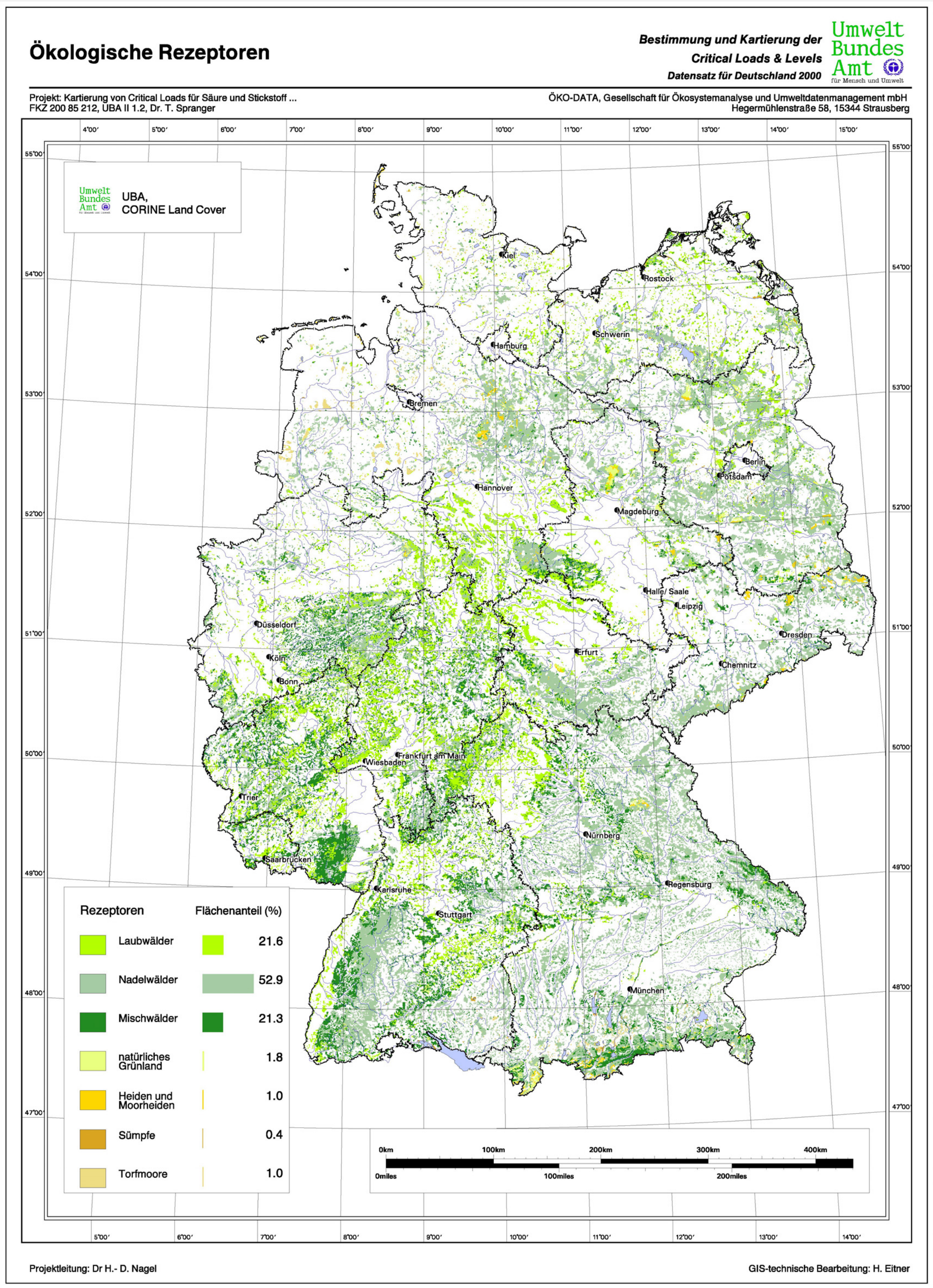

Map 2.1: Receptors used for critical loads and critical loads exceedance calculations in Germany

3 Methods applied for mapping total deposition loads

Detailed information on spatial variation of deposition and on ecosystems and their spatial distribution is needed to determine deposition fluxes on the ecosystem level. The three main different deposition processes of wet, dry and cloud&fog deposition contribute to total deposition fluxes. Total deposition is the sum of these three fluxes at a certain location. The magnitude of the contribution of each flux to total deposition is varying over time and geographical space, due to pollution gradients, variations in atmospherical properties and surface conditions.

- The removal of pollutants from the atmosphere via precipitation of rain and snow is termed **wet deposition**. The wet deposition process is mainly controlled by the concentration of the pollutants and the precipitation amount. The wet deposition amount is most independent from the structure and surface of the receptor. Briefly, at a given solute concentration, amount and intensity of precipitation, the magnitude of the wet deposition flux (the wet deposition load respectively) into a water surface will be the same as into e.g. a forested area. However, large-scale and regional scale gradients of wet deposition amounts over Germany can be found. The ‘rain-out’ of pollutants captured in rain droplets and ‘wash-out’ of in-air pollutants by the falling rain are constitutive processes for measured solute concentrations in precipitation. Thus, by installation of monitoring networks of sufficient spread and density of sampling sites to cover the spatial gradients of variation in solute concentrations, maps of wet deposition fields can be interpolated from these measurements.
- The direct deposition of particles and gases into terrestrial surfaces happening in periods without precipitation is termed **dry deposition**. Interactions between the receptor surfaces and airborne components strongly determine the load of dry deposition. The dry deposition processes are controlled by atmospheric conditions, the concentration of the gaseous and particulate pollutants in the ambient air as well as by the shape, area, roughness, and condition of the receptor’s surface. There are only few sites in Germany where dry deposition is monitored routinely. Moreover the high variability of dry deposition fluxes in time and space does not allow spatial interpolation of measured values. However, the knowledge on deposition processes derived from measurements can be parameterised and used in inferential deposition models, allowing the mapping of dry deposition fluxes.
- The flux of cloud and fog droplets to the receptor’s surfaces in this study is termed **cloud&fog deposition**. Concentrations in cloud droplets depend on air concentrations of gases and aerosols and their scavenging ratios and have been found highly variable in space and time. Cloud&fog droplet deposition was found to contribute considerably to total deposition at hillsides of mountain regions in Germany (BLEEKER ET AL. 2000).

Wet deposition is measured in local, regional and national monitoring networks in Germany. The wet deposition database which was set up at INS by comprehensive data acquisition at the institutions responsible for the different monitoring programmes (see Chapter 4.1 for further details). The scatter and density of open field wet deposition measurements is appropriate to map the spatial trend wet deposition fluxes over the area of Germany using kriging technique (see Chapter 4.3 for further details).

Estimates of total deposition into single forested areas may be derived by applying **canopy budget model** (termed **CBM** in this report) calculations (e.g. ULRICH 1983, ULRICH 1991; UBA 1996; DRAAIERS & ERISMAN 1995, DRAAIJERS ET AL. 1996B, DRAAIJERS ET AL. 1998; UN ECE & EC 2001). Basic data in CBM calculations are open space wet deposition and parallel throughfall and stemflow measurements at single forest stand areas. In a CBM the effect of canopy exchange processes (canopy leaching and/or uptake) , which are due to atmospheric input as well as to ecosystem properties is accounted for. Because of inner ecosystem cycling the data of throughfall and stemflow measurements and hence CBM estimates of dry and total deposition are explicitly site specific. Long-term routine measurements of throughfall and stemflow data provided from the Länder Forest Research Centres, from Water Management and Environmental Agencies, respectively, are integral part of INS deposition database (see Chapter 4.1).

Total deposition into forests is systematically higher than it is into other ecosystem types. This mainly is due to the structure (height, roughness, large surface area) of forest ecosystems which forms the so called ‘filtering effect’. The magnitude of this ‘filtering effect’ also is conditioned by air pollutant concentrations and meteorological parameters (wind speed, humidity, time of wetness etc.). The spatial variability of these parameters are virtually independent from spatial distribution of land use and ecosystem structure as well as from the spatial patterns of wet deposition rates. The processes controlling the fluxes dry, cloud&fog droplet and wet deposition are virtually independent from each other over space and no constant linear relation between the respective fluxes can be derived. Thus it is strongly recommended not to use e.g. constant ‘filtering factors’ for total deposition mapping (LÖVBLAD et al. 1993, UBA 1996, NAGEL&GREGOR 1999).

Inferential deposition models are available which are used to derive dry and cloud&fog deposition fluxes from information on emission and air concentration data which are linked to meteorological data and ecosystem information via parameterisations of the deposition processes. However, open field wet deposition measurements, throughfall and stemflow data together with the results of CBM estimates of dry and total deposition, which are only valid for single forest locations, can be used for inferential model evaluation purposes.

In the **German approach mapping total deposition** loads combines the interpolation of wet deposition measurements to derive wet deposition fields with small scale processing of receptor specific dry and cloud&fog deposition by using the inferential deposition models IDEM and EUTREND (Figure 3.1). The application of inferential models using basic data of different scale (i.e. LRT air concentration, meteorological data in high time resolution, small scale emission inventories, small scale receptor information) combined with interpolated measurement data (small scale air concentration, precipitation data and wet deposition) is the most promising method to derive small scale total deposition and critical loads exceedance (UBA 1996, LÖVBLAD ET AL. 1993). Details of the calculation of wet deposition fields are given in chapter 4, descriptions on the application of the IDEM and EUTREND model can be found in Chapter 5 of this report.

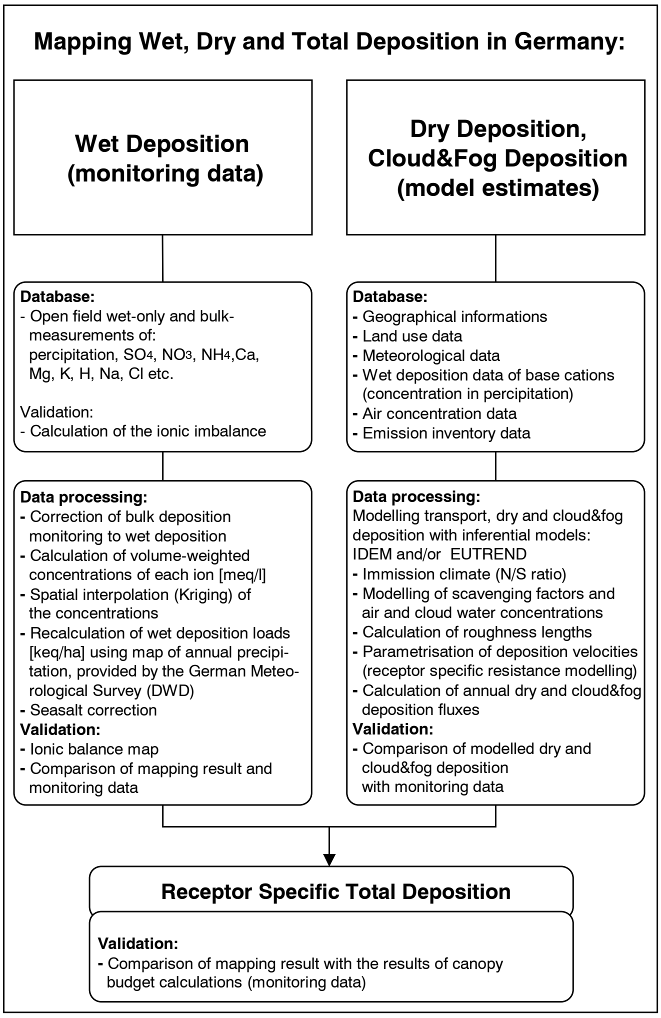

Figure 3.1: Mapping wet, dry, cloud &fog and total deposition in Germany

4 Wet deposition

Wet deposition is the vertical chemical input of airborne compounds to a ground surface via precipitation (rain, sleet, snow, hail). Airborne pollutants, which are attached to and dissolved in cloud droplets, rain drops and snow, respectively, are either transported downwards to the ground surface by 'rain-out', or they are taken up from the atmosphere by hydrometeors during the precipitation event ('wash-out'). Using **wet-only samplers** with funnels open to the atmosphere at precipitation events only to collect hydrometeors, is an adequate method **for measuring wet deposition fluxes**. Open top precipitation collectors permanently exposed to the atmosphere are referred to as **bulk deposition samplers**. **Bulk deposition fluxes** also include a surplus amount of dry deposited matter (particulates and gases) collected in dry periods. Bulk to wet-only conversion factors have been derived using parallel measurements (GAUGER ET AL. 2000) in order to correct measured bulk deposition to wet deposition fluxes (cf. Chapter 4.2.3).

The absence of precipitation is prerequisite for **dry deposition** processes, where gases and particulate matter is transported to and deposited directly on exposed surfaces (cf. Chapter 5). **Cloud&fog deposition** is the process where cloud and fog water droplets are directly intercepted by surfaces (cf. Chapter 5.2). Sophisticated micrometeorological measurements have to be applied in order to quantify dry and cloud&fog deposition in the field.

Throughfall and stemflow deposition are measured in forest stands and attributed to the deposition fluxes into the forest soil. Rainwater passing the forest canopy downwards to the ground is termed **throughfall deposition**. The throughfall water hereby is enriched with compounds washed from tree foliage and branches. The water running down tree trunks, also enriched with dissolved matter washed from the canopy and trunk, is termed **stemflow**.

4.1 Wet deposition database

Wet deposition is mapped using annual wet deposition monitoring data as basic input. Wet deposition in Germany is routinely measured in several local, regional and national monitoring programmes and networks. A wet deposition database has been set up at INS by comprehensive data acquisition at the institutions responsible for the monitoring. The database consists in wet deposition load data of the main components and heavy metals. Moreover, location parameters and additional information on each sample station provided is stored as meta data attached to the data records. The wet deposition database is split into three parts containing (a) precipitation monitoring, i.e. deposition data of samples analysed from wet and bulk samplers exposed in open field locations (b) deposition data of bulk throughfall and stemflow from deciduous forests and (c) deposition data of bulk throughfall from coniferous forests. The data sources of the German INS/UBA wet deposition database are listed in Chapter 4.1.2.

Bulk deposition, throughfall and stemflow fluxes are basic input for canopy budget model (CBM) calculations. The application of CBM allows to calculate estimates of dry, cloud&fog and total deposition for a forest stand by taking into account canopy exchange processes. An overview of canopy model calculations can be found in DRAAIERS ET AL. 1998. Wet-only and bulk deposition data, corrected to wet deposition fluxes, are used as input for mapping wet deposition fields. Throughfall and stemflow data are used to apply CBM calculations to derive dry and total deposition estimates, serving as evaluation data for modelled dry and total deposition maps.

4.1.1 Data acquisition and updates of the German wet deposition database

Comprehensive and iterative data acquisition has been started in 1993 in order to set up the wet deposition database. In the initial phase data published in literature were compiled to a data pool, consisting of data measured between 1979 to 1992. The authors and institutions responsible for monitoring deposition in a second phase were contacted in order to consolidate all available information on measurement networks and programmes in Germany and in the cross border areas. The monitoring institutions in a third phase were asked to provide annual deposition data measured using open field bulk and wet-only samplers as well as canopy throughfall and stemflow data.

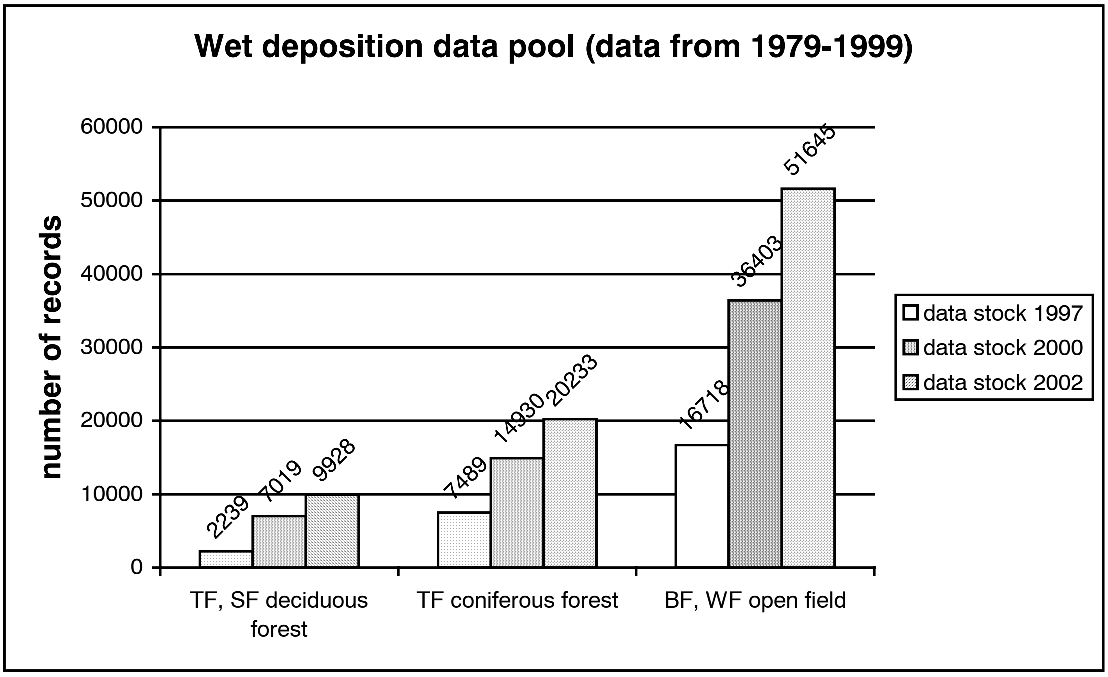

Figure 4.1: Updates of the wet deposition database 1997, 2000 and 2002
(TF = ThroughFall, SF = StemFlow, BF = Bulk Flux, WF = Wet-only Flux)

With the reflux of provided data the database serving for wet deposition mapping could be set up. The data pool then included 16718 records of main components (SO_4-S, NO_3-N, NH_4-N, K, Ca, Mg, Na, Cl, H, pH and annual precipitation) analysed 1979 to 1994 from open field bulk and wet-only measurements in Germany and Austria, 7.489 records of main components in throughfall measured in coniferous forests, and 2.239 records of main components in throughfall and stemflow sampled in deciduous forests in Germany (GAUGER ET AL. 1997).

In the following time period from 1997 to 1999 updates and thorough revisions of the database were carried out. A questionnaire was sent out to the institutions providing data in order to get more standardised information on the monitoring programmes and networks. The data pool was actualised and extended by about 19685 data records of open field bulk and wet-only measurements to a total of 36403, by about 7441 data records of throughfall measured in coniferous forests to a total of 14930, and 4780 records of throughfall and stemflow sampled in deciduous forests to total 7019 records, respectively. The database then consisted in data analysed within 1979 to 1996, including measurements of heavy metals (GAUGER ET AL. 2000).

The recent updates of the wet deposition database were carried out in this study. The main goal was to acquire monitoring data of the years 1997 to 1999 and to replace or add revised measurement data for all years covered. After this data acquisition the data pool was extended by about 15242 data records of open field bulk and wet-only measurements to a total of 51645, by about 5303 data records of throughfall measured in coniferous forests to a total of 20233, and 2909 records of throughfall and stemflow sampled in deciduous forests to total 9928 records respectively (Figure 4.1).

To meet the requirements of using the provided data for mapping wet deposition the institutions responsible for monitoring deposition were asked to provide measurement data

- of annual fluxes [in g ha^{-1} a^{-1}, kg ha^{-1} a^{-1}, eq ha^{-1} a^{-1}] and/or annual concentrations in precipitation [in mg l^{-1}, g l^{-1}] and annual precipitation amount [in l m^{-2}, mm], respectively, from complete measurements (e.g. samples of 52 weeks, 12 months per year, respectively)
- of: pH, conductivity, if analysed
- of the main compounds: SO_4-S, NO_3-N, NH_4-N, K, Ca, Mg, Na, Cl, F, H, PO_4-P if analysed
- of trace elements and metalloids: Al, As, Br, Cd, Co, Cu, Fe, Hg, Mn, Mo, Ni, Pb, Si, Tl, V, Zn, and others if analysed
- of organic compounds: DOC, TOC, PCB, PAK, HKW and others, if analysed
- derived from bulk and/or wet-only samplers in the open field and from throughfall and stemflow measurements in deciduous, coniferous, mixed forest stands
- if older data were not already provided and implemented into the wet deposition database beforehand, the data should cover the sampling periods from the beginning of the measurements until 1999
- and additional information (meta data, master data) on the samples, the sampling location (name of the site, co-ordinates, height above sea level, tree species, tree height, tree age, etc.), on the network and programme (beginning and end of measurements, main purpose, objectives and scientific goal of the monitoring), respectively

4.1.2 Wet deposition data sources

In Table 4.1 the 41 data providing institutions are listed, including a listing of main compounds analysed and of latest data set included into the data base.

Table 4.1: Data sources of deposition monitoring data in Germany and the neighbouring countries Austria and Czech republic provided to set up the deposition data base for wet deposition mapping (09/2001)

Region	**Institution**	**Acronym**	**SO_4**	**NO_3**	**NH_4**	**Cl**	**Na**	**Ca**	**Mg**	**K**	**H**	**PO_4**	**Pb**	**Cd**	**precipitation**	**conductivity**	**pH**	**open field monitoring**	**throughfall, stemflow**	**year of latest data set**
Germany	Umweltbundesamt, Fg. II 6,5 Meßnetz-Datenzentrale; Langen	UBA-b (bulk)	X	X	X	X	X	X	X	X	X	-	-	-	X	X	X	updated	n.a.	1999
Germany	Umweltbundesamt, Fg. II 6.5; Meßnetz-Datenzentrale; Langen	UBA-wo (wet-only)	X	X	X	X	X	X	X	X	X		X	X	X	X	X	updated	n.a.	1999
former GDR	Meteorologischer Dienst der DDR (via SLUG)	DDR-MD	X	X	-	X	X	X	X	X	X	-	-	-	X	-	-	sampling terminated	n.a.	1990
Germany	Institut für Troposphärenforschung e.V., Abt. Chemie; Leipzig	IFT	X	X	X	X	X	X	X	X	X				X			updated	n.a.	1999
Germany	Umweltforschungszentrum Leipzig-Halle GmbH, Sektion Analytik; Leipzig	UFZ	X	X	X	X		X	X	X	X				X		X	sampling terminated	sampling terminated	1994
Germany	*Bundesforschundsanstalt für Landwirtschaft BS-Völkenrode, Institut für agrarrelevante Klimaforschung; Müncheberg und Braunschweig; / FAL-AOE, Braunschweig*	*FAL*	*X*	*X*	*X*	*X*	*X*	*X*	*X*	*X*		*X*	*X*	*X*	*X*			*updated*	*n.a.*	*1993, 1996*
Germany	*Bundesforschungsanstalt für Holz- und Forstwirtschaft; Eberswalde (Simon & Westendorff)*	*BFH-EB*	*X*	*X*	*X*	*X*	*X*	*X*	*X*	*X*	*X*	*X*			*X*		*X*	*updated*	*updated*	*1989*
Schleswig-Holstein	Staatliches Umweltamt Itzehoe, Lufthygienische Überwachung Schleswig-Holstein former Gewerbeaufsichtsamt Schleswig-Holstein, Dez. Luftqualitätsüberwachung;	STUA-SH (former GAA-SH)	X	X	X	X	X	X	X	X	X		X	X	X		X	updated	n.a.	wet-only: 1999 bulk: 1998
Schleswig-Holstein	Landesamt für Natur und Umwelt des Landes Schleswig-Holstein, Abteilung Gewässer; Flintbeck	LANU-SH	X	X	X	X	X	X	X	X	X		X	X	X		X	updated	n.a.	1999
Schleswig-Holstein	*Christian-Albrechts-Universität Kiel, Öklologie-Zentrum (Jensen-Huß; Schimming; Spranger; Branding)*	*Univ. KI*	*X*	*X*	*X*	*X*	*X*	*X*	*X*	*X*	*X*				*X*			*updated*	*updated*	*1989, 1990*
Hamburg	*Freie und Hansestadt Hamburg - Umweltbehörde, Amt für Naturschutz und Landschaftspflege / Universität Hamburg, Institut für Bodenkunde (Lux)*	*Univ. HH*	*X*	*X*	*X*	*X*	*X*	*X*	*X*	*X*	*X*		*X*	*X*	*X*			*sampling terminated*	*sampling terminated*	*1992*
Hamburg	Deutscher Wetterdienst, Meteorologisches Observatorium Hohenpeißenberg	DWD	X	X	X	X									X		X	later data not deliverable / not affordable	n.a.	1993
Mecklenburg-Vorpommern	Landesamt für Umwelt und Natur, Abt. Immissionsschutz; Güstrow-Gülzow	LAUN-MV	X	X	X	X	X	X	X	X	X				X	X	X	updated	not yet available	1998 (1999 H+ only)
Mecklenburg-Vorpommern	Landesamt für Forstplanung; Schwerin	LAFOP-MV	X	X	X	X	X	X	X	X	X	X	X	X	X	X	X	not yet available	not yet available	- -
Niedersachsen	Niedersächsisches Landesamt für Ökologie, Dez.63 Luftreinhaltung, Dr. K.-P. Giesen; Hannover	NLÖ-H	X	X		X	X		X	X			X	X				updated	n.a.	1998
																				...

Region	**Institution**	**Acronym**	**SO_4**	**NO_3**	**NH_4**	**Cl**	**Na**	**Ca**	**Mg**	**K**	**H**	**PO_4**	**Pb**	**Cd**	**precipitation**	**conductivity**	**pH**	**open field monitoring**	**throughfall, stemflow**	**year of latest data set**
Niedersachsen	Niedersächsisches Landesamt für Ökologie, Abt. 6 Immissionsschutz; Hildesheim	NLÖ-HI	X	X	X	X	X			X					X			updated	updated	1999
Niedersachsen	Niedersächsische Forstliche Versuchsanstalt, Abt. Umweltkontrolle; Göttingen	NFVA	X	X	X	X	X	X	X	X	X				X		X	updated	updated	1999
Niedersachsen	*Bundesanstalt für Geowissenschaften und Rohstoffe; Hannover (FRANKEN ET.AL)*	*BGR*	*X*	*X*	*X*	*X*	*X*	*X*	*X*	*X*							*X*	*sampling terminated*	*sampling terminated*	*1995/ 1996*
Brandenburg	Landesumweltamt Brandenburg, Nebenstelle Lauchhammer	LUA-BB	X	X	X	X	X	X	X	X					X	X	X	updated	n.a.	1998
Brandenburg	Landesanstalt für Forstplanung, Brandenburg; Potsdam	LAFOP-BB																updated	updated	1999
Berlin	Senatsverwaltung für Stadtentwicklung und Umweltschutz, Abt. III A 31; Berlin	SenV-B.	X	X	X	X	X	X	X	X	X	X	X	X	X			updated	updated	1998
Sachsen-Anhalt	Landesamt für Umweltschutz Sachsen-Anhalt, Abt.5, Halle	LfU-ST	X	X	X	X	X	X	X	X	X				X	X	X	updated	n.a.	1998
Sachsen-Anhalt	Forstliche Versuchs- und Forschungsanstalt; Flechtingen	FVFA-ST																not yet available	not yet available	- -
Nordrhein-Westfalen	Landesanstalt für Ökologie, Bodenordnung und Forsten/Landesamt für Agrarordnung, Dez. Bioindikation, Biomonitoring; Recklinghausen	LÖBF/ LAFAO-NW	X	X	X	X	X	X	X	X	X	X			X			updated	updated	1999
Nordrhein-Westfalen	Landesanstalt für Umweltschutz (LUA, former LIS), Nordrhein-Westfalen, Abt. 3; Essen	LUA-NW	X	X	X	X	X	X	X	X	X				X			terminated	n.a.	1988
Nordrhein-Westfalen	Fraunhofer gesellschaft für Umweltchemie und Ökotoxikologie, Schmallenberg, Grafschaft	FhG	X	X	X	X	X	X	X	X	X				X	X		updated	n.a.	1999
Hessen	Hessische Landesanstalt f. Forsteinrichtung, Waldforschung und Waldökologie; Hannoversch Münden	HLFWW	X	X	X	X	X	X	X	X	X		X	X	X		X	updated	updated	1997
Hessen	Universität Frankfurt, Zentrum für Umweltforschung (ZUF)	Univ. F	X	X	X	X	X	X	X	X	X				X			sampling terminated	sampling terminated	1989
Sachsen	Sächsische Landesanstalt für Umwelt und Geologie, Abt. L1 Luft-Lärm-Strahlen; Radebeul	SLUG	X	X	X	X	X	X	X	X	X				X	X	X	updated	n.a.	1999
Sachsen	Sächsische Landesanstalt für Forsten; Graupa	SLAF	X	X	X	X	X	X	X	X	X	X	X	X	X			updated	updated	1999 HM: 1998
Sachsen	Technische Universität Dresden, Institut für Pflanzen- und Holzchemie; Tharandt	TU-DD	X	X	X	X	X	X	X	X	X				X	X	X	updated	updated	1996
Thüringen	Landesanstalt für Wald und Forstwirtschaft, Thüringen; Gotha	LWF-TN	X	X	X	X	X	X	X	X	X	X	X	X	X	X	X	updated	updated	1999
Rheinland-Pfalz	Forstliche Versuchsanstalt Rheinland-Pfalz, Abt. Waldschutz; Trippstadt	FVA-RP	X	X	X	X	X	X	X	X	X	X	X	X	X		X	updated	updated	1999
Bayern	Bayerische Landesanstalt für Wald- und Forstwirtschaft, Abt. Forsthydrologie, Freising	BLWF	X	X	X	X	X	X	X	X	X				X			updated	updated	1999
Bayern	Bayerische Landesanstalt für Umweltschutz; München	BLFU	X	X	X													updated	n.a.	1996
Bayern	Bayerisches Landesamt für Wasserwirtschaft; München	BLFW	X	X	X	X	X	X	X	X	X	X	X	X	X	X	X	updated	updated	1999
Saarland	Forstplanungsanstalt des Saarlandes; Saarbrücken/Univ. des Saarlandes, ZFU, AG-Forst; Duttweiler	FPA-SB	X	X	X	X	X	X	X	X	X	X	X		X		X	updated	updated	1999
Baden-Württemberg	Forstliche Versuchs- und Forschungsanstalt Baden-Württemberg; Freiburg i. B.	FVA-BW	X	X	X	X	X	X	X	X	X	X	X	X	X			updated	updated	1999
Baden-Württemberg	Landesanstalt für Umweltschutz Baden-Württemberg, Ref. 31 Luftreinhaltung Klima; Karlsruhe	LFU-BW	X	X			X								X			updated	n.a.	1996
Austria	Technische Universität Wien, Institut für Analytische Chemie, Abt. Umweltanalytik	TU Wien	X	X	X	X	X	X	X	X	X				X		X	updated	n.a.	1998
Czech Republic	Czech Hydrometeorological Institute (provided via SLUG)	CHMI	X	X	X	X	X	X	X	X	X				X			updated	n.a.	1998

Italics: Data from literature / publication

n.a.: not analysed

- - : no data provided

4.1.3 Overview on deposition monitoring networks in Germany

1987 to 1999 monitoring data from different deposition networks and programs were provided by about 41 institutions. A summarised overview of the scatter of the monitoring sites is given in Figure 4.2.

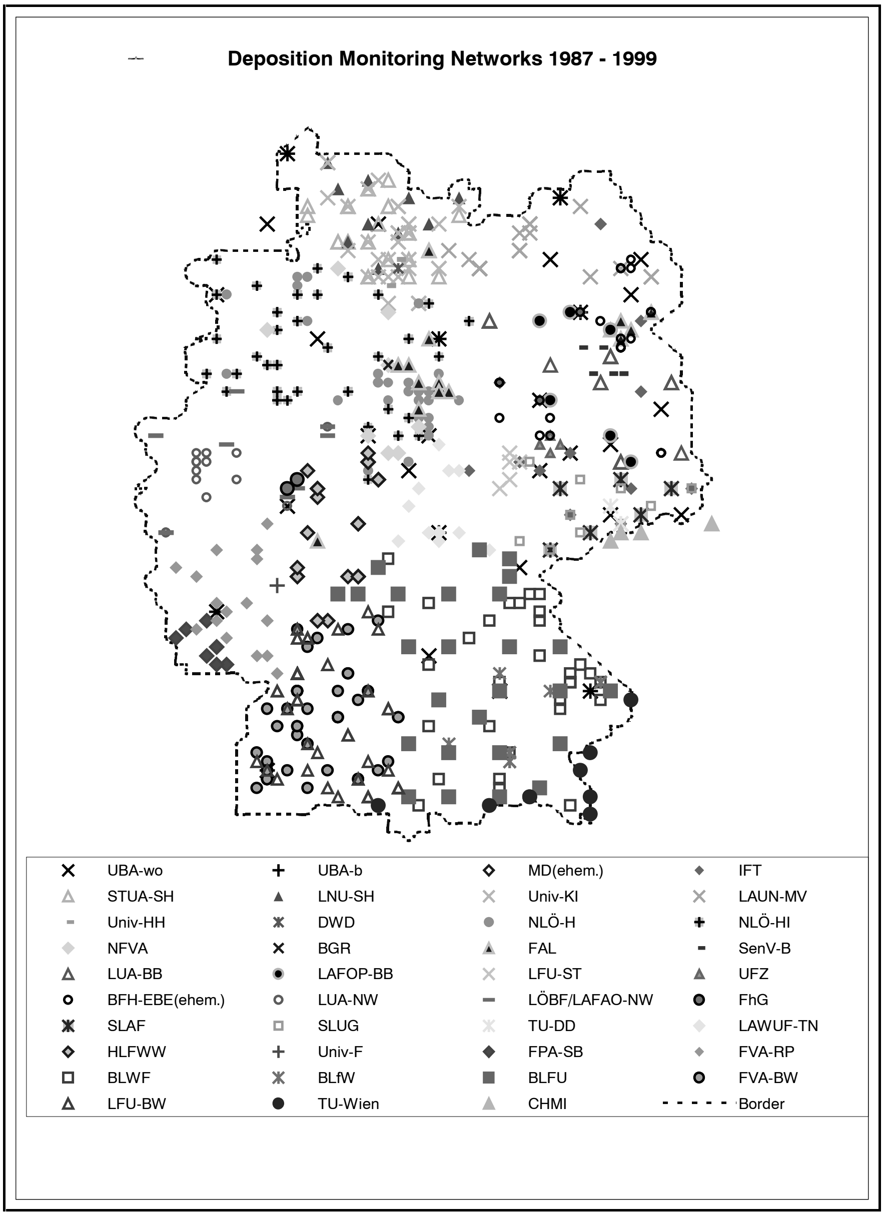

Figure 4.2: Distribution of open field deposition measurements (at least one year measurement within 1987-1999 at each point)

The scatter of the sample points is not regularly spread over Germany. Moreover not for every year and each site all main compounds were analysed and/or provided. Of course this is important for the quality of the wet deposition mapping results. Nevertheless there are enough data plots available for almost each compound needed and year considered in this study. Thorough analyses showed that number and scatter of annual wet deposition measurements are sufficient to obtain the spatial trends observed over Germany. Hence fields derived by spatial interpolation of measured solute concentration in precipitation as well as fluxes of wet deposition derived by multiplication of concentration maps with high resolution precipitation maps provide reliable results. More details on the quality of measurements can be found in Chapter 4.2.2, on the quality of the wet deposition mapping results can be found in chapter 4.3.2 respectively.

4.1.4 Deposition monitoring data measured in the open field, in coniferous forests and in deciduous forests

The main use of open field measurements is the mapping of wet deposition fluxes using kriging interpolation technique, whereas throughfall and stemflow measurements from forest plots are used to evaluate deposition fluxes calculated using inferential model technique (cf. Chapter 5.51).

Figure 4.3 shows the **open field deposition data stock** for 1987 to 1999 for all components included in the wet deposition data base (n = 46279) and provided by the institutions responsible for monitoring (listed in Table 4.1).

The columns of Figure 4.3 show that the number of main components measured in wet deposition is much higher than the number of e.g. measurements of heavy metals. The latter are mainly screening data analysed from the same sample as the main components. The number of data per compound is mainly due to different objectives of the different monitoring networks, and, of course due to costs for sampling and analyses. There are also some monitoring programmes included, where only SO_4^{2-}-S and NO_3^--N (and Cl^-) is analysed. Other smaller differences in the total amount of measurements are due to (a) the scale of data analysed, e.g. when some networks were set up, base cations were not analysed in the first years, due to (b) sample contamination and analytic errors, where only some components where affected, due to (c) incomplete delivery of data sets and (d) other errors respectively. This also applies for forest monitoring data.

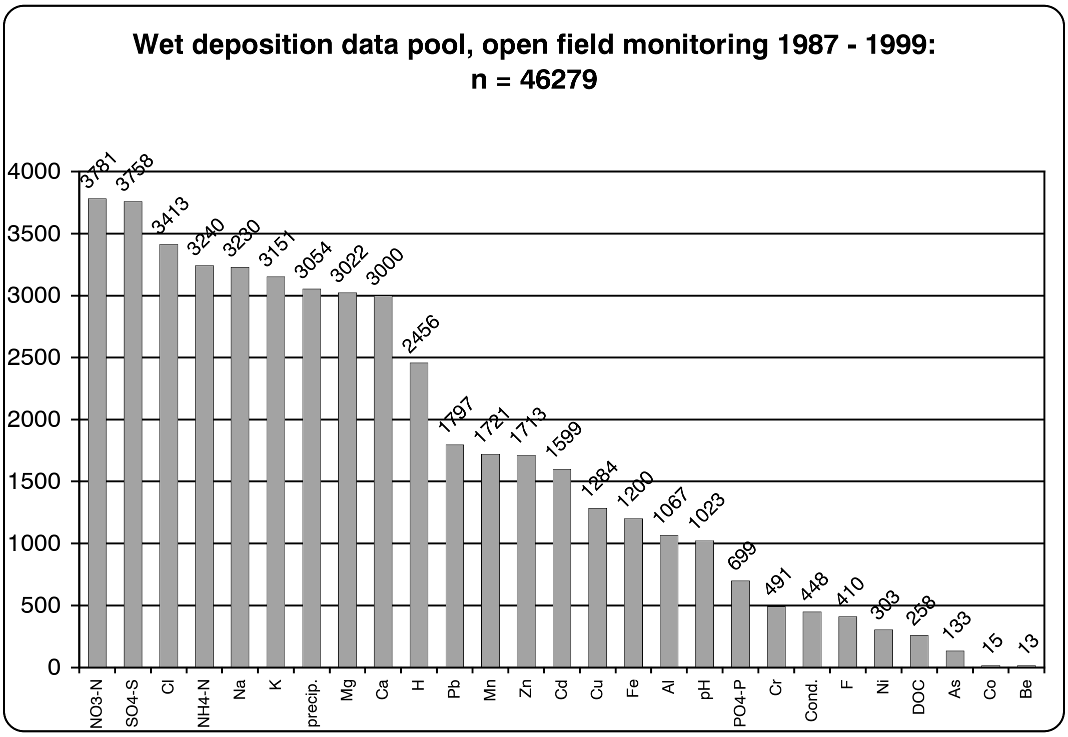

Figure 4.3: Open field wet deposition measurements 1987-1999

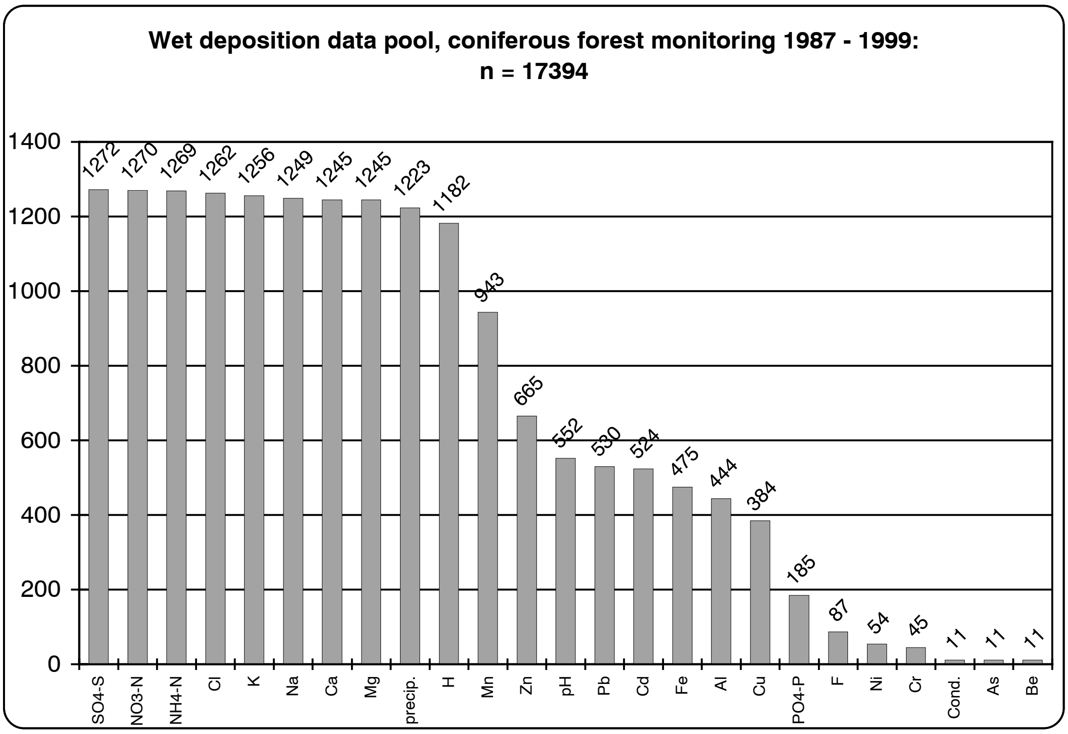

Figure 4.4: Coniferous forest throughfall measurements 1987-1999

The **data pool of coniferous forest monitoring data** for the same time period 1987 to 1999 (Figure 4.4) consists of 17394 throughfall data only. More or less the same amount of data for the nine main components and for precipitation (‘precip.’) can be found in this data pool. Heavy metals, which again are mainly screening data analysed from the same bulk throughfall sample like the main compounds, and other compounds in wet deposition are not analysed at and/or provided from every monitoring site.

The 1987 to 1999 **data pool of deciduous forest wet deposition** monitoring data consists of about 9366 throughfall and stemflow data (Figure 4.5). On the contrary to coniferous forests, where stemflow measurements are scarcely carried out anywhere in Germany because of the high intensity of maintenance and costs compared to the magnitude of fluxes, stemflow fluxes in deciduous forests are remarkable in magnitude and routinely analysed at several sites.

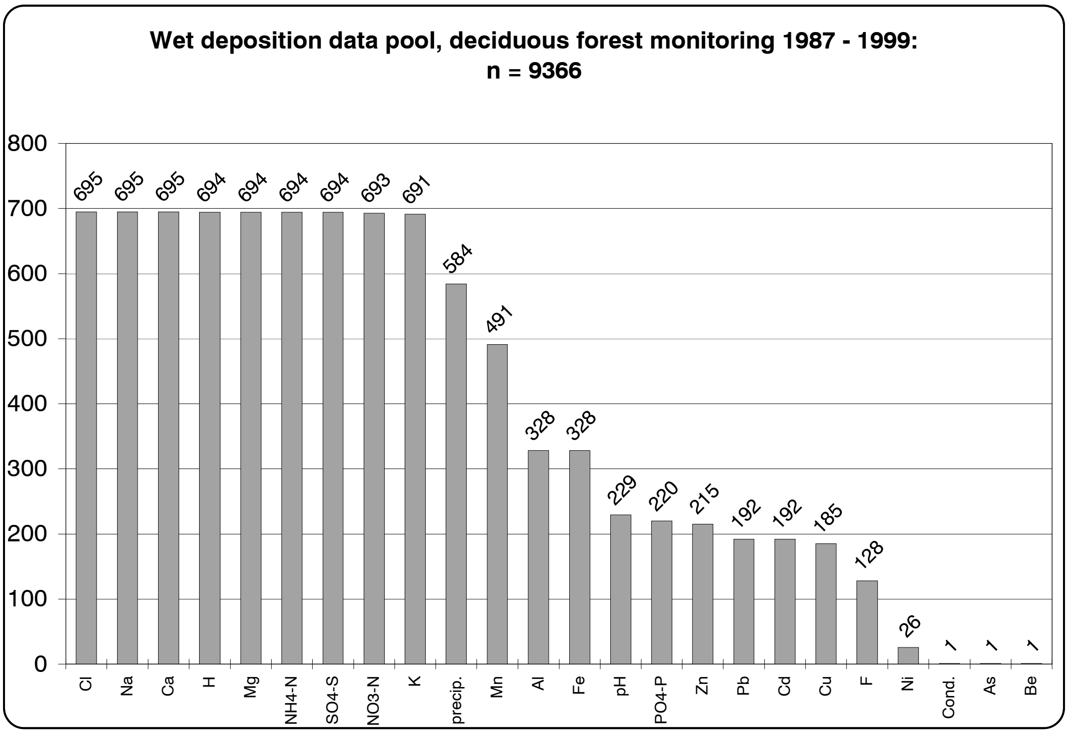

Figure 4.5: Deciduous forest throughfall and stemflow measurements 1987-1999

4.2 Data management

The wet deposition data are stored using relational tables of MS Excel. The use of this software application has some technical advantages, since most of the institutions providing data meanwhile are also using this application for storing their own database and/or for delivering the data. The use of relational tables allow to process most of the data conversions and calculations needed, e.g. for preparation of input data for mapping wet deposition.

4.2.1 Data conversion

Different conversions of data are necessary to realise a consistent data management and largely smooth preparation of measured annual deposition fluxes and concentrations in precipitation to provide input data for mapping wet deposition using GIS ARC/INFO and ArcView respectively.

The data provided by the institutions responsible for monitoring wet deposition either are wet deposition fluxes per area and year at the respective sample points [in μg ha^{-1} a^{-1}, mg ha^{-1} a^{-1}, g ha^{-1} a^{-1} or kg ha^{-1} a^{-1}], daily averages per year [in g m^{-2} d^{-1}, mg m^{-2} d^{-1} or μg m^{-2} d^{-1}], concentrations in precipitation [in μg l^{-1} a^{-1}, mg l^{-1} a^{-1}, g l^{-1} a^{-1}] or ion equivalents [in meq l^{-1} a^{-1}, eq l^{-1} a^{-1}, keq l^{-1} a^{-1}; meq ha^{-1} a^{-1}, eq ha^{-1} a^{-1}, keq ha^{-1} a^{-1}]. Fluxes of nitrogen, sulphur and phosphor compounds are either denoted as sulphate (SO_4^{2-}), nitrate (NO_3^-), ammonium (NH_4^+) and phosphate (PO_4^{2-}), or as phosphor, nitrogen and sulphur (PO_4-P, NO_3-N, NH_4-N, SO_4-S). Data of proton fluxes (H^+) are provided either as loads [e.g. kg H^+ ha^{-1} a^{-1}] or as precipitation weighted pH. Precipitation weighted conductivity [in μS cm^{-1}] – if provided – may be used for checking the data quality. Units for precipitation amounts most commonly are mm a^{-1} (= l m^{-2} a^{-1}).

Provided data are put into the database as annual wet deposition fluxes [in g ha^{-1} a^{-1}, kg ha^{-1} a^{-1}] of the compounds. With further data processing ion equivalents of each compound [in meq ha^{-1} a^{-1}, eq ha^{-}1 a^{-1}] are derived. Finally concentration in precipitation [in meq l^{-1} a^{-1}] is calculated using annual precipitation data at each sample site.

Data conversion keys, factors and equations used are presented in Table 4.2 and 4.3.

Table 4.2: Conversion keys for elements and compounds of S, N and P

$SO_4\text{-}S = SO_4 \cdot 0{,}3338$
$NO_3\text{-}N = NO_3 \cdot 0{,}2259$
$NH_4\text{-}N = NH_4 \cdot 0{,}7765$
$PO_4\text{-}P = PO_4 \cdot 0{,}3261$

$SO_4 = SO_4\text{-}S \cdot 2{,}9958$
$NO_3 = NO_3\text{-}N \cdot 4{,}4267$
$NH_4 = NH_4\text{-}N \cdot 1{,}2879$
$PO_4 = PO_4\text{-}P \cdot 3{,}0662$

Table 4.3: Conversion of masses and equivalents

	valency	**moar mass [g]**	**equivalent mass [g]**	**faktor keq → kg**	**faktor kg → keq**
Ca	2^+	40.08	20.04	20.04	0.050
Cd	2^+	112.40	56.20	56.20	0.018
Cl	1^-	35.45	35.45	35.45	0.028
H	1^+	1.01	1.01	1.01	0.992
K	1^+	39.10	39.10	39.10	0.026
Mg	2^+	24.31	12.15	12.15	0.082
Na	1^+	22.99	22.99	22.99	0.043
NH_4-N	1^+	14.01	14.01	14.01	0.071
NO_3-N	1^-	14.01	14.01	14.01	0.071
PO_4-P	2^-	30.97	15.49	15.49	0.065
Pb	2^+	207.20	103.60	103.60	0.010
SO_4-S	2^-	32.06	16.03	16.03	0.062

4.2.2 Data quality

In a liquid water phase the sum of anions and cations must be of the same magnitude because of the electroneutrality condition. The equilibrium of anion and cation equivalent concentration is commonly used to control the analytical procedure applied to measured content of precipitation. Hereby the quotient of anions and cations should be smaller than 20%, otherwise analytical errors are indicated. The quality of measured open field deposition data used for mapping wet deposition fields is checked by calculating the ion balance from the main components accordingly, using Equation 4.1:

$$\mathit{Ion\ Balance}\,[\%] = \frac{(NH_4^+ + Ca^{2+} + Mg^{2+} + K^+ + Na^+ + H^+) - (SO_4^{2-} + NO_3^- + Cl^-)}{(NH_4^+ + Ca^{2+} + Mg^{2+} + K^+ + Na^+ + H^+) + (SO_4^{2-} + NO_3^- + Cl^-)} \cdot 100\ [eq] \qquad (4.1)$$

Since analytical errors indicated by ion balances exceeding 20% can not be assigned to single compounds, the respective data sets are rejected. The number and source of data sets excluded from further processing are listed in Table 4.4.

Table 4.4: Data sets excluded from further processing due to the ionic imbalance exceeding 20%

data sets excluded from further processing because of ionic imbalance of main components >20% :							**excluded data sets per year:**
1987	**Brandenburg: 4** Simon& Westendorff	**Bayern: 3** BLWF	**Hessen: 1** Univ.-F				**8**
1988	**Brandenburg: 2** Simon& Westendorff	**Mecklenburg-Vorpommern: 3** Simon& Westendorff	**Bayern: 2** BLfW				**7**
1989	**Brandenburg: 4** Simon& Westendorff	**Mecklenburg-Vorpommern: 3** Simon& Westendorff	**Hessen: 2** HLFWW				**9**
1990	**Hessen: 11** HLFWW	**Baden-Württemberg: 3** FVA-BW					**14**
1991	**Hessen: 21** HLFWW	**Thüringen: 2** LaWuF-TN	**Nordrhein-Westfalen: 1** LUA-NW	**Bayern: 1** BLfW	**Österreich: 1** TU-Wien		**26**
1992	**Hessen: 21** HLFWW	**Thüringen: 5** LaWuF-TN	**Bayern: 3** BLfW	**Österreich: 3** TU-Wien	**Nordrhein-Westfalen: 1** LUA-NW	**Brandenburg: 1** UBA-wo	**34**
1993	**Hessen: 22** HLFWW	**Thüringen: 4** LaWuF-TN	**Österreich: 3** TU-Wien	**Bayern: 2** BLfW 1+BLWF 1			**31**
1994	**Hessen: 26** HLFWW	**Baden-Württemberg: 1** FVA-BW	**Bayern: 1** BLfW	**Österreich: 1** TU-Wien			**29**
1995	**Hessen: 7** HLFWW	**Österreich: 3** TU-Wien	**Bayern: 1** BLfW				**11**
1996	**Bayern: 3** BLfW 2+BLWF 1	**Sachsen: 2** LAF-SN 1 + TU-DD 1	**Niedersachsen: 1** NFVA 1				**6**
1997	**Bayern: 5** BLfW 2+BLWF 3	**Thüringen: 1** LaWuF-TN	**Österreich: 1** TU-Wien				**7**
1998	**Bayern: 10** BLfW 4+BLWF 6	**Thüringen: 2** LaWuF-TN	**Baden-Württemberg: 1** FVA-BW	**Nordrhein-Westfalen: 1** LUA-NW			**14**
1999	**Bayern: 16** UBA-wo 1 + BLfW3+BLWF12	**Saarland. 3** UNI-SB	**Nordrhein-Westfalen: 1** LUA-NW	**Thüringen: 1** LaWuF-TN			**21**
acronyms, data sources see Table 4.1							

Another check of the wet deposition input data is made by determining and rejecting outliers of each component in order to exclude high values which are due to very local circumstances or sample contamination. In the analysis carried out both statistical and the regional context of the measurements are taken into account.

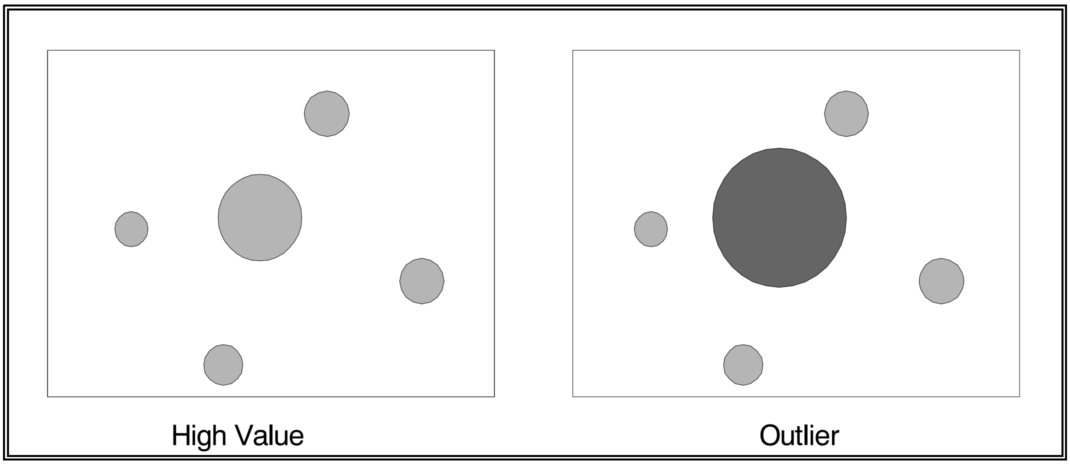

Figure 4.6: Illustration of the detection of outliers in a point map

Point maps were calculated in order to detect high outliers in the regional context of surrounding measurements. The difference between high values and outliers is illustrated in Figure 4.6. Very high values (outliers, respectively) can be attributed to local circumstances, where the measurements either are strongly influenced by local emissions of a certain compound or by contamination of the sample. Where applicable, additional information on the surroundings of the sample site, and/or on certain events near by the site in the respective year (e.g. construction activities or stormy weather conditions in an agrarian area in harvesting periods leading to high deposition of base cations, high sulphate deposition close to a power plant etc.) provided by the institutions responsible were also taken into account in order to detect suspected outliers. In addition to this investigation, a statistical analysis was applied. A statistical method applicable for detection of outliers is the ‘4-sigma-test’ (SACHS 1989), where the mean value ± 4 times the standard deviation of the population, both calculated without the suspected outliers, marks the upper and lower limit beyond which the outliers can be found. For practical purposes a comparison with quantiles of the populations of the input data was carried out (GAUGER ET AL. 2000). The 99-, 98, and 95-percentile were found to represent the upper limits observed using the ‘4-sigma-test’ for Na^+ and Cl^- values, of H^+, SO_4^{2-}-S, NO^{3-}-N and NH^{4+}-N and of the base cations Ca^+, K^+ and Mg^+, respectively (see Figure 4.7). The so detected outliers are excluded from further processing.

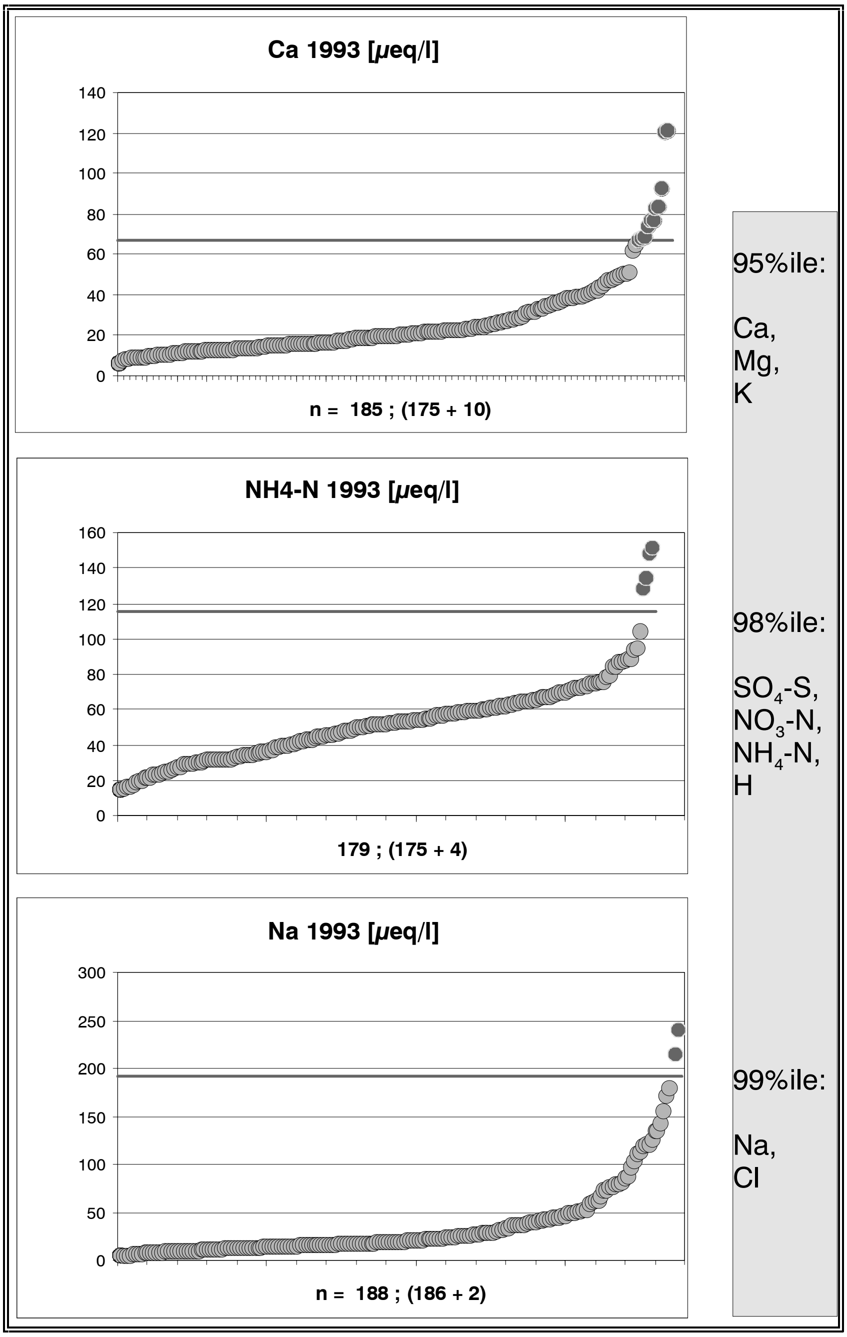

Figure 4.7: Example for elimination of outliers using quantiles of the population

4.2.3 Bulk to wet-only conversion

At those sampling points where bulk deposition samplers are used wet deposition is estimated by correcting bulk deposition fluxes for dry deposition into the funnels. Simultaneous bulk and wet deposition measurements in different parts of Germany were used to derive average conversion factors (Gauger et al. 2000) listed in Table 4.5. The ratios shown in Table 4.5 are used to calculate wet deposition fluxes from bulk deposition fluxes. According to the Mapping Manual (UBA 1996) only corrected bulk deposition data and measured wet deposition data are used as input for mapping wet deposition in Germany.

Table 4.5: Annual mean ratio of wet-only and bulk fluxes measured in Germany (Gauger et al. 2000)

	Mn	**K**	**Ca**	**PO_4-P**	**Fe**	**Al**	**Pb**	**Mg**	**Cd**	**Cu**	**NO_3-N**	**Na**	**Cl**	**SO_4-S**	**NH_4-N**	**Precip.**	**H**
simultaneous measurements, n =	11	26	26	6	8	8	11	25	12	8	27	26	26	27	26	20	15
average ratio wet-only / bulk	**0.57**	**0.60**	**0.63**	**0.63**	**0.67**	**0.70**	**0.71**	**0.72**	**0.73**	**0.82**	**0.83**	**0.86**	**0.87**	**0.89**	**0.89**	**0.94**	**1.22**
Minimum	0.26	0.16	0.35	0.44	0.05	0.15	0.25	0.37	0.55	0.43	0.62	0.51	0.56	0.68	0.63	0.71	0.83
Maximum	0.87	1.50	1.11	0.71	0.93	0.95	0.93	1.18	1.00	0.97	1.02	1.35	1.40	1.52	1.41	1.05	2.50
Standard deviation	0.16	0.27	0.20	0.09	0.25	0.24	0.20	0.21	0.14	0.16	0.11	0.20	0.17	0.17	0.17	0.09	0.46
Coefficient of variation (%)	28	45	32	14	37	34	28	29	19	20	13	23	20	19	19	10	38

The average contribution of dry deposited compounds varies between 43% for magnesium and 11% for sulphur and ammonium respectively. Wet deposition of protons (H^+) are found to be about 22% higher in wet-only deposition samples. This can be attributed to exchange processes with particles in bulk samples. The latter also are in most cases exposed for longer time periods than wet-only samples (e.g. weekly to monthly bulk and daily to weekly wet-only samples), which enhances this process. Precipitation amounts are on average about 6% higher in bulk samples compared to wet-only samples, which is due to the collecting efficiency of the sampler type. Permanent open bulk samplers also collect fog droplets and other precipitation in small amount and intensity, whereas wet-only samplers, due to the sensitivity of the sensor which controls the opening of the funnel tops, would not open or open later when precipitation events are starting (Gauger et al. 2000).

4.2.4 Input data used for mapping wet deposition 1990 to 1999

After data conversions and quality checks described above are finished, the input data sets for the mapping procedure are used in the GIS. Table 4.6 shows the respective number of 1990 to 1999 data (1) in the wet deposition database, (2) after data revision is made and (3) after averaging the values of closely neighbouring sites. The latter step of pre-processing the input data is made in order to accommodate the scatter of the sample points more equally over the whole area, since the following kriging interpolation necessitates to avoid clustered data points.

Table 4.6: Quantity of monitoring data used for mapping wet deposition

	1990			1991			1992			1993			1994		
	availabe data(1)	after revision (2)	input data(3)	availabe data(1)	after revision (2)	input data(3)	availabe data(1)	after revision (2)	input data(3)	availabe data(1)	after revision (2)	input data(3)	availabe data(1)	after revision (2)	input data(3)
SO4-S	251	245	204	150	149	134	218	213	188	277	271	231	303	296	259
NO3-N	253	247	205	152	151	136	234	229	203	281	275	236	306	299	261
NH4-N	221	216	180	120	119	108	174	170	155	215	210	188	242	237	212
Ca	182	172	138	120	119	107	160	151	136	216	205	175	222	210	182
Mg	180	170	134	118	117	105	156	148	134	209	198	173	220	208	177
K	217	206	170	118	117	107	179	170	154	234	222	194	240	227	194
Na	219	216	180	118	117	106	179	177	164	233	230	197	243	240	204
Cl	250	274	206	149	148	134	190	188	173	243	240	212	249	246	215
H	165	161	129	101	100	93	140	137	126	170	166	149	173	169	148
precip.			DWD map			DWD map			DWD map			DWD map			DWD map

	1995			1996			1997			1998			1999		
	availabe data(1)	after revision (2)	input data(3)	availabe data(1)	after revision (2)	input data(3)	availabe data(1)	after revision (2)	input data(3)	availabe data(1)	after revision (2)	input data(3)	availabe data(1)	after revision (2)	input data(3)
SO4-S	329	322	281	360	352	307	328	321	288	318	311	278	182	178	163
NO3-N	323	316	277	358	350	305	326	319	285	316	309	276	188	184	170
NH4-N	273	267	236	302	295	258	275	269	244	269	263	238	188	184	169
Ca	249	236	199	283	268	231	272	258	233	268	254	231	188	178	159
Mg	265	251	217	297	282	243	284	269	241	274	260	233	184	174	152
K	262	248	215	291	276	235	274	260	236	254	241	217	175	166	171
Na	272	269	229	310	306	259	289	286	257	280	277	249	188	186	171
Cl	268	265	234	295	292	256	282	279	251	281	278	250	186	184	163
H	186	182	159	185	181	159	199	195	179	189	185	168	139	136	122
precip.			DWD map			DWD map			DWD map			DWD map			DWD map

(1) = quantity of open field sampling data in the wet deposition data base

(2) = quantity of data after data revision (without outliers and ionic balance <21%)

(3) = quantity of data input for mapping after averaging closely neighbouring sample points (within each 5x5km^2 grid cell)

The scatter and density of open field wet deposition measurements is important for spatial representativity. Taking spatial variability of wet deposition fluxes of SO_4-S and NO_3-N into account it is assumed that the survey area should be covered with one site per 1000km^2 to 2000km^2, or, that a wet deposition monitoring network representative for main compounds should be arranged in a regular 40 km grid to derive spatial average estimates with standard errors of the mean below ±20% for SO_4-S and NO_3-N. Other compounds, e.g. Mg, Ca, H, and an orographically complex terrain would require a more dense network (KALLWEIT 1997, SAGER 1997). This means that a monitoring network covering all Germany with its acreage of about 357 thousand km^2 should consist of 178 wet deposition sites (one per 2000km^2), 268 sites (one per 1500km^2), 233 sites (one per 1600km^2) or 357 sites (one per 1000km^2), respectively, in a more or less regular scatter in order to approach the conventional requirements mentioned above.

The amount of open field wet deposition measurements provided as input to the INS/UBA wet deposition database and used (see ‘available data’ and ‘input data’ in Table 4.6) to derive wet deposition fields already more or less meets the conventional minimum requirements to derive fields of wet deposition fluxes, except for 1991, in most of the years mapped. The sample data are used to derive fields of precipitation weighted annual mean ion concentrations. When the concentration fields are mapped, wet deposition fluxes are calculated as the product of concentrations and the annual precipitation amount provided by Deutscher Wetterdienst (DWD) in 1x1km^2 grid resolution maps. The precipitation maps are modelled by DWD using a very large network of gauges (about 3500 sample sites) as primary input (cf. Chapter 4.3.1).

4.3 Calculation of wet deposition fields

4.3.1 Concept of mapping wet deposition

The concept of mapping wet deposition in Germany follows the recommendations of the Mapping Manual (UBA 1996). The horizontal variation of the chemical composition of precipitation in most cases is much smaller than the variation of precipitation amount.

Spatial patterns of rainfall composition is monitored in the wet deposition sampling networks (Chapter 4.2). The sample data are used to calculate precipitation weighted annual ion concentration fields for the main compounds SO_4^{2-}-S, NO_3^--N, NH_4^+-N, K^+, Ca^{2+}, Mg^{2+}, Na^+, Cl^- and H^+ using kriging technique. All concentration maps are calculated in a 5x5km² grid resolution except for the year 1991, where, due to the poorer amount of data (see Table 4.6), a coarser grid resolution of 10x10km² had to be chosen to derive wet concentration fields covering all Germany. Though the number and scatter of the measurement data plots are varying from year to year between 1987 and 1999, the monitoring sites cover most areas of Germany, both horizontally (scatter and density) and vertically (orography and exposition). In previous studies it has been proved possible to calculate regional distribution of the main compounds' ion concentration in precipitation in a 5x5km² grid with a minimum number of about 130 sites scattered more or less equally over the whole country (GAUGER ET AL. 1997). However, more data are needed, because the more equal the scatter of the monitoring sites and the more monitoring data are available, which do represent the spatial trend of wet deposition, the better the kriging interpolation result will be in terms of lower errors and uncertainties (see Chapter 4.3.2).

The outline of data processing using GIS is shown in Figure 4.8. Co-ordinates of the measurement sites and attributed concentration in precipitation are input to derive point maps showing the scatter and measured annual concentration of the different species in precipitation. This maps are giving an overview on possible horizontal lack of data, which is useful when analysing uncertainties of the mapping result, and they are also used for visual identification of outliers in their spatial context (see Chapter 4.2.2). In a second step the concentrations in precipitation of closely neighbouring sample points within each 5x5km² grid cell are averaged to one value and attributed to one point (see Chapter 4.2.4). These points are input for kriging interpolation procedure.

A **sea salt correction** is calculated for SO_4^{2-}-S, Cl^-, Ca^{2+}, K^+ and Mg^{2+}, using sodium as a tracer. The sea salt correction is calculated with the interpolated results, because sodium deposition is not measured at each monitoring site. Rainwater contains ions originating from sea water which is transported into the continent by sea spray. The sea salt correction is used to correct the measured ion content from a sample for the sea salt contribution. It is assumed that the ratio of Na to SO_4^{2-}-S, Cl^-, Ca^{2+}, K^+ and Mg^{2+} in the sample is the same as in sea water and that all Na is of marine origin. Table 4.7 shows the Na-ratios in sea water and the calculation of the sea salt correction.

The sea salt corrected values of SO_4^{2-}-S, Cl^-, Ca^{2+}, K^+ and Mg^{2+} are termed 'non sea salt' ('nss', e.g. $K_{(nss)}$). They are representing the deposition flux mainly attributable to anthropogenic processes excluding the natural sea spray input.

The interpolated precipitation weighted annual ion concentration fields are then resampled into 1x1km² grid maps and multiplied with a high resolution (1x1km²) precipitation map, provided by DWD. This DWD modelled maps of annual precipitation fields are derived using more than 3500 samples of the DWD precipitation monitoring network (MÜLLER-WESTERMEIER 1995). Since precipitation data show significant correlation to topography, regression coefficients between precipitation and topography (i.e. elevation, slope, land use) can be derived. By DWD modelling the precipitation data are reduced to a common reference level by using the spatially variable regression functions. Then the reduced data are interpolated (in a 1x1km² grid) and subsequently recalculated into the real topography by using the regression functions in a 1x1km² grid map covering all Germany (MÜLLER-WESTERMEIER 1995). The result of the intersection of fields of annual concentration in rainfall with the annual precipitation map is a 1x1km² wet deposition loads map, combining the maximum information on both spatially differentiated wet deposition and precipitation monitoring.

Table 4.7: S, Cl, Ca, K and Mg to Na ratios in sea water [eq/eq] and the calculation of the sea salt correction (UBA 1996)

Ca_{sw}/Na_{sw}	Mg_{sw}/Na_{sw}	K_{sw}/Na_{sw}	S_{sw}/Na_{sw}	Cl_{sw}/Na_{sw}
0,044	0,277	0,021	0,120	1,164
$Ca_{nss} = Ca_{dep} - (Na_{dep} \cdot 0,044)$	$Mg_{nss} = Mg_{dep} \; (Na_{dep} \cdot 0,277)$	$K_{nss} = K_{dep} - (Na_{dep} \cdot 0,021)$	$S_{nss} = S_{dep} - (Na_{dep} \cdot 0,120)$	$Cl_{nss} = Cl_{dep} - (Na_{dep} \cdot 1,164)$

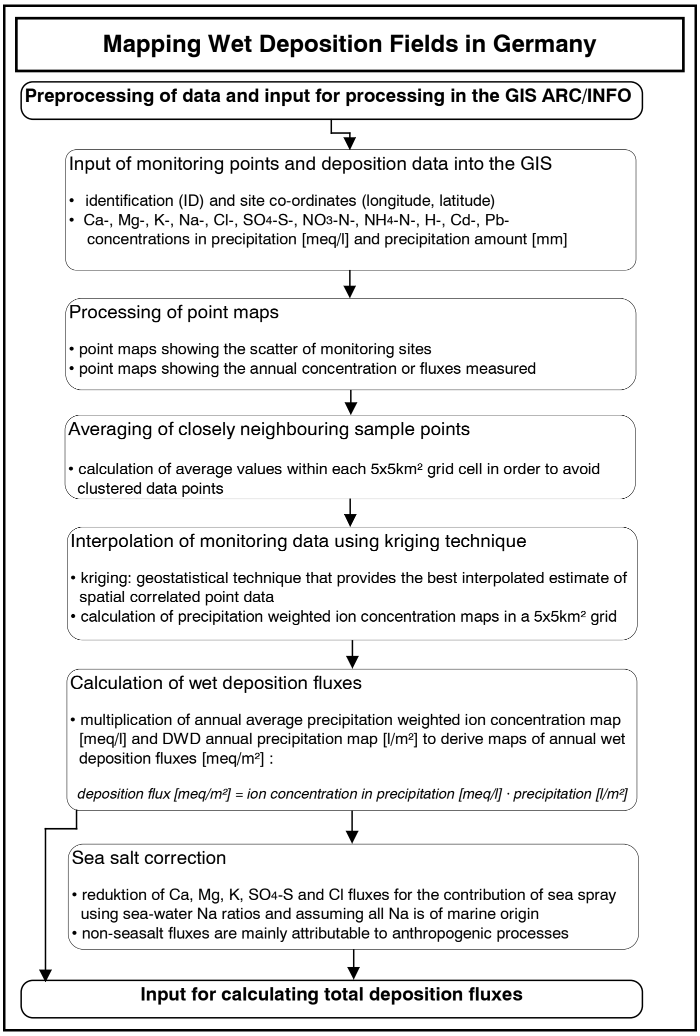

Figure 4.8: Outline of mapping wet deposition using GIS

4.3.2 Quality of the wet deposition mapping results

An overview of consistency of the wet deposition mapping results for each year treated is carried out by calculating ionic balance maps. Within each grid of the maps the ion balance of all main compounds mapped is calculated (see Equation 4.1). The outcome in this ion balance map then should show values more or less in the same range of the input data. Moreover it is possible to get back ion balance values at those locations of monitoring plots where only incomplete data sets where provided for the wet deposition data base, or where not all main compounds are analysed from the sample, and only the interpolated estimate is substituting the missing wet deposition values at this specific locations.

The ion balance calculated from the wet deposition maps of 1990 to 1999 is shown in Map 4.1. The range of the ion balance for the wet deposited main components in 1990-1999 shows satisfying results. Each year imbalances between 0 and ±10% cover most parts of Germany. However, higher imbalances (±10% to ±20%) are found in some areas around and between individual sites with already higher ionic imbalances in the monitoring data. In 1992, 1994 and 1996-1999 the range of ion imbalances lies between ±20%, which is the limit set for the input data used (see chapter 4.2.2). Maximum ion imbalances (beyond ±20%) are only found in small areas in the years 1990, 1993 and 1995, and in 1991 in a more extended area in eastern Germany.

In 1990 three small areas with an ionic imbalance beyond ±20% can be observed in North Rhine-Westphalia, in Hesse and in Baden-Württemberg respectively, which are due to lack of data in these areas and/or already high ion imbalances at the monitoring sites surrounding these areas.

Wet deposition mapping of the year 1991 was treated different compared to the other years, because, due to the lack of sufficient data especially in the eastern part of Germany, the interpolation of site data was carried out in a 10x10km² gird instead of 5x5km², and the mapping of H^+ could not be carried out. The relatively high ionic imbalances beyond ±20% in 1991 hence are due to lack of data, missing H^+ estimates and due to higher uncertainties of the estimates of other main compounds in precipitation derived by kriging interpolation.

In 1993 in a small area at the southern border of Germany , and in 1995 in a small area in the south-eastern most part of Germany ion imbalances beyond ±20% can be observed, which again are due to the lack of data in this areas and higher imbalances of the monitoring data at sites situated around.

A site specific comparison between mapped and measured data has been carried out for wet deposition loads. The results of this comparison are shown for 1990-1999 in Table 4.8, and for the year 1999 in the graphs of Figure 4.9. This comparison mainly reflects the effect of data preprocessing, interpolation and intersection of wet concentration with the precipitation map at the points of the open field wet deposition monitoring.

In the graphs in Figure 4.9 the comparisons of measured and modelled 1999 wet deposition are presented. In this comparison all open field sample points in Germany are included, where data were provided for 1999.

Table 4.8: Comparison of measured and mapped wet deposition loads 1990-1999

1990	**SOx-S**	**NOy-N**	**NHx-N**	**Ca**	**K**	**Mg**	**H**	**Na**	**Cl**	**precip.**
n	232	234	203	160	194	159	150	204	236	210
m	0,94	0,94	0,95	0,92	0,97	0,95	0,96	1,01	0,99	0,94
r	0,68	0,73	0,92	0,87	0,84	0,91	0,59	0,97	0,99	0,86
R²	0,47	0,53	0,85	0,76	0,71	0,83	0,35	0,94	0,97	0,73
1991	**SOx-S**	**NOy-N**	**NHx-N**	**Ca**	**K**	**Mg**	**H**	**Na**	**Cl**	**precip.**
n	139	140	109	106	104	105	--	109	140	143
m	0,95	0,95	0,95	0,81	0,92	0,88	--	0,94	0,99	0,94
r	0,69	0,69	0,83	0,32	0,70	0,70	--	0,95	0,96	0,77
R²	0,48	0,48	0,69	0,10	0,49	0,49	--	0,90	0,91	0,60
1992	**SOx-S**	**NOy-N**	**NHx-N**	**Ca**	**K**	**Mg**	**H**	**Na**	**Cl**	**precip.**
n	207	223	164	147	166	145	131	172	183	167
m	0,94	0,91	0,93	0,95	0,95	0,97	0,97	0,96	0,97	0,94
r	0,49	0,56	0,64	0,77	0,49	0,86	0,76	0,97	0,93	0,79
R²	0,24	0,31	0,41	0,59	0,24	0,74	0,58	0,94	0,87	0,62
1993	**SOx-S**	**NOy-N**	**NHx-N**	**Ca**	**K**	**Mg**	**H**	**Na**	**Cl**	**precip.**
n	258	262	197	192	209	186	153	219	228	203
m	0,91	0,91	0,92	0,93	0,92	0,88	0,97	0,93	0,91	0,93
r	0,57	0,74	0,77	0,75	0,57	0,73	0,76	0,94	0,96	0,84
R²	0,32	0,55	0,59	0,56	0,33	0,53	0,58	0,88	0,93	0,71
1994	**SOx-S**	**NOy-N**	**NHx-N**	**Ca**	**K**	**Mg**	**H**	**Na**	**Cl**	**precip.**
n	282	284	222	198	213	195	156	227	233	219
m	0,91	0,67	0,96	0,92	0,96	0,96	1,00	0,93	0,91	0,96
r	0,49	0,57	0,63	0,49	0,51	0,82	0,86	0,96	0,93	0,78
R²	0,24	0,32	0,40	0,24	0,26	0,67	0,73	0,92	0,86	0,61
1995	**SOx-S**	**NOy-N**	**NHx-N**	**Ca**	**K**	**Mg**	**H**	**Na**	**Cl**	**precip.**
n	297	297	250	220	232	239	168	253	251	244
m	0,91	0,92	0,94	0,86	0,93	0,94	1,01	0,97	0,93	0,93
r	0,66	0,66	0,60	0,27	0,54	0,78	0,85	0,97	0,91	0,83
R²	0,44	0,43	0,36	0,07	0,30	0,61	0,73	0,95	0,83	0,69
1996	**SOx-S**	**NOy-N**	**NHx-N**	**Ca**	**K**	**Mg**	**H**	**Na**	**Cl**	**precip.**
n	342	340	284	258	264	277	173	297	284	269
m	0,86	0,87	0,89	0,79	0,90	0,88	1,04	0,91	0,89	0,95
r	0,61	0,68	0,61	0,33	0,67	0,68	0,80	0,96	0,95	0,82
R²	0,37	0,47	0,37	0,11	0,44	0,46	0,63	0,93	0,91	0,67
1997	**SOx-S**	**NOy-N**	**NHx-N**	**Ca**	**K**	**Mg**	**H**	**Na**	**Cl**	**precip.**
n	305	303	253	243	245	258	181	272	265	240
m	0,94	0,93	0,95	0,88	1,00	0,97	1,07	0,92	0,93	0,97
r	0,66	0,71	0,78	0,24	0,73	0,72	0,81	0,96	0,94	0,79
R²	0,43	0,51	0,61	0,06	0,54	0,51	0,66	0,91	0,88	0,62
1998	**SOx-S**	**NOy-N**	**NHx-N**	**Ca**	**K**	**Mg**	**H**	**Na**	**Cl**	**precip.**
n	296	293	247	239	226	248	172	264	265	227
m	0,92	0,91	0,91	0,93	0,91	0,92	1,02	0,92	0,92	0,94
r	0,65	0,78	0,76	0,55	0,49	0,83	0,82	0,96	0,95	0,81
R²	0,42	0,61	0,58	0,30	0,24	0,69	0,67	0,93	0,90	0,65
1999	**SOx-S**	**NOy-N**	**NHx-N**	**Ca**	**K**	**Mg**	**H**	**Na**	**Cl**	**precip.**
n	175	178	178	172	162	172	132	182	180	124
m	0,92	0,92	0,92	0,92	0,93	0,91	0,97	0,95	0,95	0,96
r	0,78	0,80	0,84	0,74	0,60	0,84	0,93	0,99	0,99	0,89
R²	0,61	0,64	0,70	0,55	0,37	0,70	0,86	0,98	0,97	0,79

n = number of points
linear regression line between field estimate (y) and map (x); y = 0 when x = 0: y = m·x; **m** = slope
r = Pearson correlation coefficient
R² = coefficient of determination

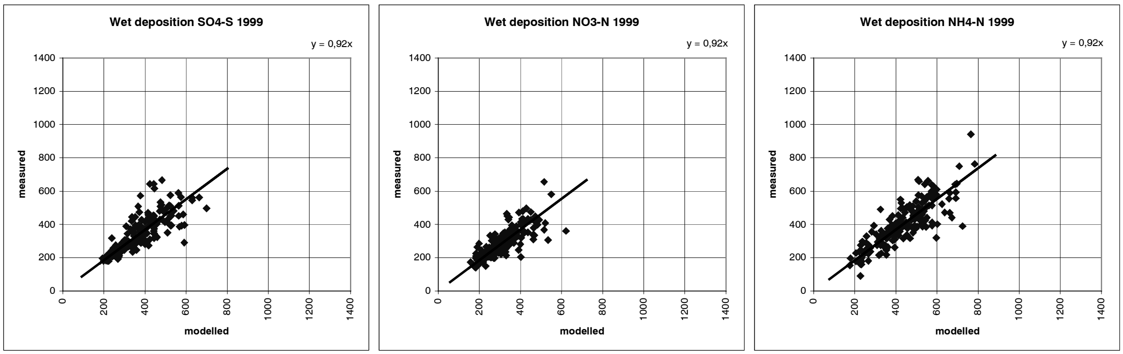

Wet deposition SO_4-S [eq ha^{-1}] **Wet deposition NO_3-N [eq ha^{-1}]** **Wet deposition NH_4-N [eq ha^{-1}]**

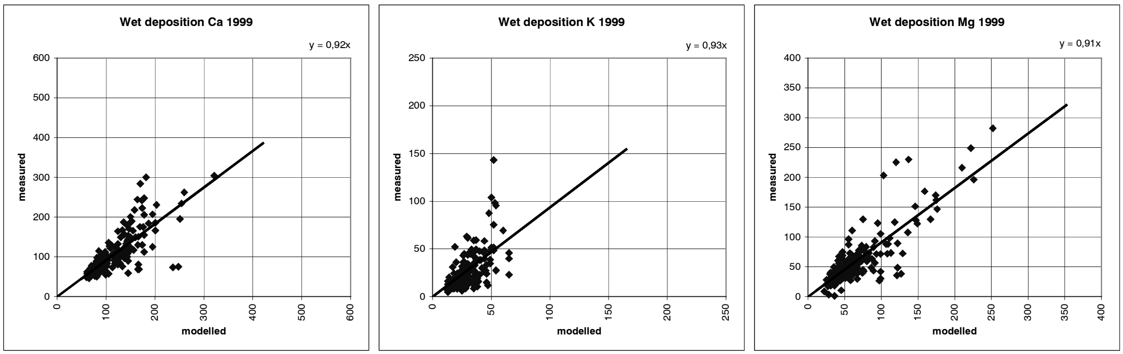

Wet deposition Ca [eq ha^{-1}] **Wet deposition K [eq ha^{-1}]** **Wet deposition Mg [eq ha^{-1}]**

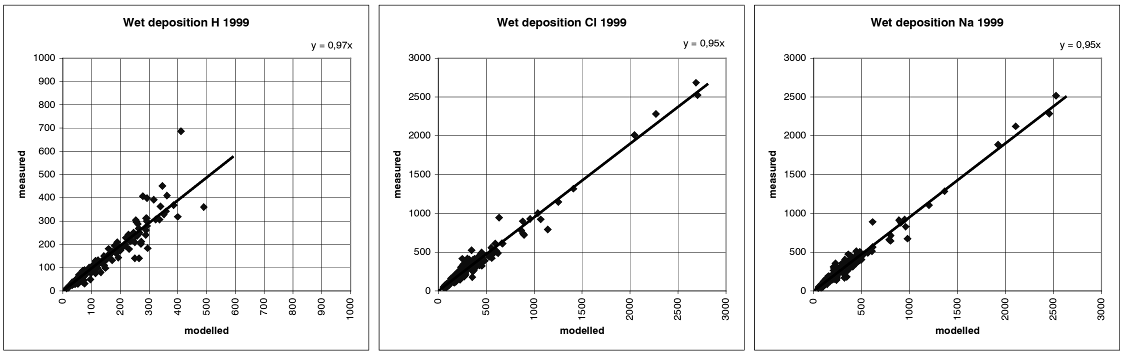

Wet deposition H [eq ha^{-1}] **Wet deposition Cl [eq ha^{-1}]** **Wet deposition Na [eq ha^{-1}]**

Figure 4.9: Comparison of measured (y) and modelled (x) wet deposition at open field sample point locations

The main source of error affecting the results of the wet deposition mapping procedure, however, lies in the spatial distribution of the wet deposition networks' sample sites, since a lack of site relative to variation of deposition over a larger area enhances uncertainty of the interpolated estimate.

4.4 Wet Deposition Mapping Results

Samples of open field wet deposition of the major ions sulphur (SO_4-S), nitrate (NO_3-N) and ammonium (NH_4-N), the base cations calcium (Ca), magnesium (Mg), potassium (K) and sodium (Na), chloride (Cl) and protons (H) present in precipitation are used to map 5x5km² annual mean wet concentration fields using kriging technique. These precipitation weighted annual wet concentration fields are representing patterns of concentration of all main compounds over Germany and can be used to calculate fields of ion balance to provide an overview on the quality of the mapping result.

Wet deposition fluxes (wet deposition loads in eq ha^{-1} a^{-1}) is then calculated as the product of the 5x5km² wet concentration fields and 1x1km² precipitation maps obtained from the German meteorological survey (Deutscher Wetterdienst, DWD).

Table 4.9: Maps of wet deposition 1990-1999

Wet Deposition	**1987**	**1988**	**1989**	**1990**	**1991**	**1992**	**1993**	**1994**	**1995**	**1996**	**1997**	**1998**	**1999**
SO_4-S, SO_4-$S_{(nss)}$	**X**	**X**	**X**	**X**	**X**	**X**	**X**	**X**	**X**	**X**	**X**	**X**	**X**
NO_3-N	**X**	**X**	**X**	**X**	**X**	**X**	**X**	**X**	**X**	**X**	**X**	**X**	**X**
NH_4-N	**X**	**X**	**X**	**X**	**X**	**X**	**X**	**X**	**X**	**X**	**X**	**X**	**X**
Ca, $Ca_{(nss)}$	**X**	**X**	**X**	**X**	**X**	**X**	**X**	**X**	**X**	**X**	**X**	**X**	**X**
Mg, $Mg_{(nss)}$	**X**	**X**	**X**	**X**	**X**	**X**	**X**	**X**	**X**	**X**	**X**	**X**	**X**
K, $K_{(nss)}$	**X**	**X**	**X**	**X**	**X**	**X**	**X**	**X**	**X**	**X**	**X**	**X**	**X**
Na	**X**	**X**	**X**	**X**	**X**	**X**	**X**	**X**	**X**	**X**	**X**	**X**	**X**
Cl, $Cl_{(nss)}$	**X**	**X**	**X**	**X**	**X**	**X**	**X**	**X**	**X**	**X**	**X**	**X**	**X**
H	**X**	**X**	**X**	**X**	**- -**	**X**	**X**	**X**	**X**	**X**	**X**	**X**	**X**
N = $(NO_3\text{-}N + NH_4\text{-}N)$	**X**	**X**	**X**	**X**	**X**	**X**	**X**	**X**	**X**	**X**	**X**	**X**	**X**
Potential Acidity $AC_{pot} = (S_{(nss)} + N + Cl_{(nss)})$	**X**	**X**	**X**	**X**	**X**	**X**	**X**	**X**	**X**	**X**	**X**	**X**	**X**
BC = $(Ca + K + Mg)$, $BC_{(nss)} = (Ca_{(nss)} + K_{(nss)} + Mg_{(nss)})$	**X**	**X**	**X**	**X**	**X**	**X**	**X**	**X**	**X**	**X**	**X**	**X**	**X**
Potential Net Acidity $AC_{pot\ (net)} = ((S_{(nss)}+N+Cl_{(nss)})–BC_{(nss)})$	**X**	**X**	**X**	**X**	**X**	**X**	**X**	**X**	**X**	**X**	**X**	**X**	**X**
DWD 1x1km² precipitation map	**X**	**X**	**X**	**X**	**X**	**X**	**X**	**X**	**X**	**X**	**X**	**X**	**X**
$_{(nss)}$ =non-seasalt (sea salt corrected)	**X = processed , - - = not processed / processing not possible**												

An overview on all wet deposition maps calculated within this study is given in Table 4.9.

To calculate exceedances of Critical Loads for nutrient nitrogen and acidity it is necessary to calculate wet deposition fields of total nitrogen (N = $(NO_3\text{-}N + NH_4\text{-}N)$) of potential acidity ($Ac_{pot} = (S_{(nss)} + N + Cl_{(nss)})$), the sum of base cations (BC = $(Ca + K + Mg)$), and potential net acidity ($AC_{pot(net)} = ((S_{(nss)} + N + Cl_{(nss)}) - BC)$).

In Table 4.10 and Figure 4.10 an overview is given on the mapping results. Table 4.10 shows the single mapping results for each ions and the years 1990 to1999 given as average annual wet deposition loads in Germany. Included are the sum of the major anions and cations as well as the result of the ion balance calculation, where the difference between the sum of cations and anions is given as mean annual average of the not analysed fraction.

Table 4.10: Average annual wet deposition of main compounds in precipitation in Germany 1990-1999

	1990	**1991**	**1992**	**1993**	**1994**	**1995**	**1996**	**1997**	**1998**	**1999**
Na in eq ha^{-1} a^{-1}	354.1	230.3	226.2	249.8	245.7	251.2	160.9	178.8	226.2	217.9
H in eq ha^{-1} a^{-1}	261.7	n. a.	261.4	243.0	237.9	227.4	168.7	128.2	171.8	129.5
Ca in eq ha^{-1} a^{-1}	198.7	209.4	176.5	188.3	168.1	130.0	118.5	122.9	136.8	115.9
K in eq ha^{-1} a^{-1}	39.5	33.7	38.3	37.1	32.3	35.5	29.1	27.8	32.8	25.7
Mg in eq ha^{-1} a^{-1}	90.7	76.3	69.5	79.6	72.2	69.5	55.7	54.2	59.8	56.6
NHx-N in eq ha^{-1} a^{-1}	464.8	386.3	395.8	422.3	420.8	410.9	385.4	344.3	382.9	378.3
SOx-S in eq ha^{-1} a^{-1}	659.4	545.9	559.6	590.2	530.4	476.3	384.3	335.4	376.8	310.5
NOy-N in eq ha^{-1} a^{-1}	291.2	274.0	291.2	311.9	298.0	289.7	269.9	246.7	287.3	269.7
Cl in eq ha^{-1} a^{-1}	385.7	256.2	245.9	273.1	296.1	299.4	186.1	217.9	262.5	249.2
Cations in eq ha^{-1} a^{-1}	1.410	936	1.168	1.220	1.177	1.125	918	856	1.010	924
Anions in eq ha^{-1} a^{-1}	1.336	1.076	1.097	1.175	1.125	1.066	840	800	927	829
not analysed:	**1990**	**1991**	**1992**	**1993**	**1994**	**1995**	**1996**	**1997**	**1998**	**1999**
in eq ha^{-1} a^{-1}	-73	+140	-71	-45	-52	-59	-78	-56	-84	-95
in %	-3	+7	-3	-2	-2	-3	-4	-3	-4	-5

n. a. = not analysed

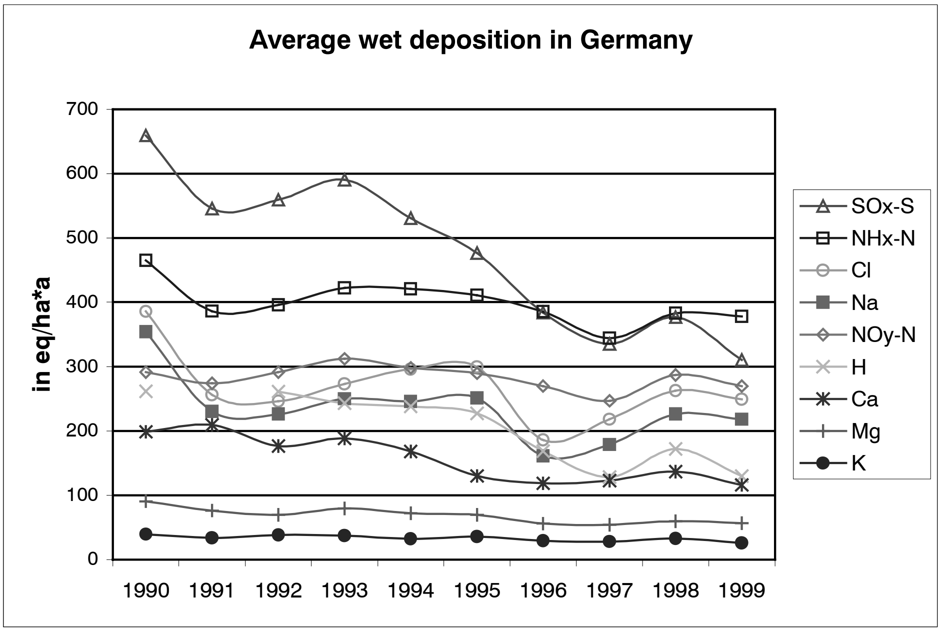

Figure 4.10: Average annual wet deposition of main compounds in Germany 1990-1999

The wet deposition loads of the total sum of all major compounds declined for about 34% from 1990 to 1999. This decline is dominated by the sharp fall of sulphur (SO_4-S), where the annual average wet deposition load in 1999 is about 53% lower than in 1990 (Figure 4.10).

The trends in Na^+ and Cl^- wet deposition are very similar (Figure 4.10). Na is assumed to be 100% of marine origin, and it is deposited together with chlorine as seasalt input. The curve of chlorine lies above the sodium line, which is due to slightly higher Cl^- fractions in sea water. Moreover the shape of both curves is not fully parallel. This indicates, that Cl^- also originates from other sources than from sea spray only. Those non-seasalt chloride deposition is assumed to be completely due to anthropogenic HCl emissions (UBA 1996).

The annual variation of the average wet deposition of Na^+, Cl^- and H^+ is shown in Table 4.11 as percentage change from the previous year. There is no clear trend in Na^+ and Cl^- wet deposition, which mainly reflects the variation in inland transport of sea salt from the North Sea by marine air masses and storms, which is different in the single years.

The wet deposition loads of protons (H^+) declined by 51% from 1990 to 1999. The shape of the H^+ curve is almost parallel (i.e. correlated) with the curve of sulphur wet deposition.

Table 4.11: Budgets of average annual wet deposition of Na, Cl and H in Germany 1990-1999

Wet Deposition	Na [eq ha^{-1} a^{-1}]	% change from previous year	Cl [eq ha^{-1} a^{-1}]	% change from previous year	H [eq ha^{-1} a^{-1}]	% change from previous year
1990	354		386		262	
1991	230	-35.0	256	-33.6	*n. a.*	*n. a.*
1992	226	-1.8	246	-4.0	261	-0.1
1993	250	+10.5	273	+11.1	243	-7.0
1994	246	-1.6	296	+8.4	238	-2.1
1995	251	+2.2	299	+1.1	227	-4.4
1996	161	-36.0	186	-37.8	169	-25.8
1997	179	+11.1	218	+17.1	128	-24.0
1998	226	+26.5	263	+20.5	172	+34.0
1999	218	-3.7	249	-5.1	130	-24.6
% change from 1990 to 1999		-38		-35		-51

n. a. = not analysed

The trend of annual average NH_X-N and NO_Y-N wet deposition 1990 to1999 shows more or less parallel curves (Figure 4.10), which, over the whole time period, are only slightly moving downward. The run of the NO_Y-N curve, however, in most of the years can be found on an about one third lower level than the NH_X-N curve. From 1996 on the NH_X-N curve lies above the SO_X-S curve (Figure 4.10), which illustrates that, with respect to the magnitude of average wet deposition loads over all Germany, NH_X-N is more and more becoming the most important acidifying compound.

Table 4.12: Budgets of average annual wet deposition of SO_X-S, NH_X-N, NO_Y-N and N in Germany 1990-1999

Wet Deposition	SO_X-S [eq ha^{-1} a^{-1}]	% change from previous year	NH_X-N [eq ha^{-1} a^{-1}]	% change from previous year	NO_Y-N [eq ha^{-1} a^{-1}]	% change from previous year	N [eq ha^{-1} a^{-1}]	% change from previous year
1990	659		465		291		756	
1991	546	-17.2	386	-16.9	274	-5.9	660	-12.7
1992	560	+2.5	396	+2.5	291	+6.3	687	+4.0
1993	590	+5.5	422	+6.7	312	+7.1	734	+6.9
1994	530	-10.1	421	-0.4	298	-4.5	719	-2.1
1995	476	-10.2	411	-2.4	290	-2.8	701	-2.5
1996	384	-19.3	385	-6.2	270	-6.8	655	-6.5
1997	335	-12.7	344	-10.7	247	-8.6	591	-9.8
1998	377	+12.3	383	+11.2	287	+16.5	670	+13.4
1999	310	-17.6	378	-1.2	270	-6.1	648	-3.3
% change from 1990 to 1999		-53		-19		-7		-14

The 53% decline of average wet deposited SO_X-S over Germany between 1990 and 1999 is interrupted by a slight increase in 1992 (+2.5%) and 1993 (+5.5%), and an increase of +12% from 1997 to 1998 (c.f. Table 4.12 and Figure 4.10).

The average wet deposition loads of base cations Ca, Mg and K over the time period 1990 to 1999 show a more or less continuous decline in magnitude (c.f. Table 4.13 and Figure 4.10). Calcium, mainly (more than 90%) originating from terrestrial and anthropogenious emission sources, in all the years shows highest wet deposition rates, and contributes between 55% and 66% to the sum of base cations (BC = Ca + Mg + K). The annual average wet deposition load of Ca 1999 is about 42% lower than in 1990. In contrast, average potassium (K) wet deposition rates, originating mainly (more than 80%) from terrestrial and vegetation sources, are lowest in magnitude. The average K contribution to the sum of base cations in 1990 to 1999 ranges from 11% to about 15%. The annual average wet deposition load of K 1999 is about 35% lower than in 1990. Average Mg wet deposition declined by 38% from 1990 to 1999. The magnesium contribution to the sum of base cations in wet deposition ranges from about 24% to 30%. Mg mainly (more than 70%) originates from sea spray.

Table 4.13: Budgets of average annual wet deposition of Ca, Mg, K and BC in Germany 1990-1999

Wet Deposition	**Ca [eq ha^{-1} a^{-1}]**	**% change from previous year**	**K [eq ha^{-1} a^{-1}]**	**% change from previous year**	**Mg [eq ha^{-1} a^{-1}]**	**% change from previous year**	**BC [eq ha^{-1} a^{-1}]**	**% change from previous year**
1990	199		40		91		329	
1991	209	+5.4	34	-14.7	76	-15.8	319	-2.9
1992	176	-15.7	38	+13.6	69	-9.0	284	-11.0
1993	188	+6.7	37	-3.1	80	+14.5	305	+7.3
1994	168	-10.7	32	-13.0	72	-9.3	273	-10.6
1995	130	-22.7	35	+10.0	69	-3.7	235	-13.8
1996	118	-8.9	29	-17.9	56	-19.8	203	-13.5
1997	123	+3.7	28	-4.6	54	-2.7	205	+0.8
1998	137	+11.3	33	+18.0	60	+10.4	229	+12.0
1999	116	-15.2	26	-21.8	57	-5.4	198	-13.6
% change from 1990 to 1999		-42		-35		-38		-40

The wet deposition mapping results and trends within the 10 years period 1990 to 1999 are presented in more detail in the following sub chapters: for base cations (Chapter 4.4.1), and for acidifying components and nutrient nitrogen (Chapter 4.4.2). 1990 to 1999 maps of wet deposition are shown in Chapter 4.5.

4.4.1 Wet deposition fluxes and trends of base cations (Na; Ca, K, Mg, BC)

The deposition of Sodium (Na) is assumed to be 100% of marine origin. Sodium compounds are deposited as neutral salt and their elements do neither contribute to acidification nor to acid neutralisation. Na fluxes are mapped, because Na is used as a tracer for calculating the seasalt contribution to the wet flux of Ca, K, Mg, Cl and SO_4-S (cf. sea salt correction, chapter 4.3.1). The marine compounds of these species are also deposited as neutral salt and thus are assumed not to be physiologically active within the receptor ecosystems.

The deposited sum of non-seasalt base cations ($BC_{(nss)} = Ca_{(nss)} + K_{(nss)} + Mg_{(nss)}$) are physiologically active. If not deposited as neutral salt, Ca, K and Mg can improve the nutrient status with respect to eutrophication, and they counteract deposition of potential acid.

Following the Critical Load approach, anthropogenic base cation deposition should not be accounted for. The aim of the Convention is to minimise emissions of acidifying components irrespective of other man made emissions. The emission abatement of acidifying compounds has to be derived from their effects alone. Thus it is not permissible to charge up base cations against acidifying components, if both are emitted from anthropogenic sources, even though those base cations would also buffer acidity. Only the deposited natural background level of base cations should be used as a magnitude counteracting man made acidifying input into ecosystems, because it has a relatively large continuity in time and space and can be assumed to be a quality of the ecosystems. Unfortunately there are no methods or data (e.g. emission inventories of base cations) yet available to clearly quantify all fractions of anthropogenic and natural deposition loads of base cations besides the sea salt fraction. Therefore the non-seasalt fraction ($BC_{(nss)}$) is only attributable to natural *and* anthropogenic emission processes excluding sea spray. (UBA 1996; GAUGER ET AL. 1997; KÖBLE UND SPRANGER 1999, GAUGER ET AL. 2000).

4.4.1.1 Wet deposition of sodium (Na)

In the graph of Figure 4.11 the mapped minimum, maximum and annual mean wet deposition of Sodium (Na) in the years 1990 to 1999 in Germany is shown. A relatively large interannual variability of the average wet deposition rates up to 36% from one year to the next can be observed. The highest annual wet deposition of Na is found in 1990 with 292 kt (8.14 kg ha^{-1} a^{-1}), the lowest in 1996 with about 132 kt (3.70 kg ha^{-1} a^{-1}). The spatial pattern of high and low fluxes (Map 4.2) clearly reflects the marine origin of Na. Sodium wet deposition each year shows a regular spatial gradient with highest wet deposition loads at the coastal region of the North Sea (NW) and lowest wet deposition loads in continental most inland areas of Germany (SE). In inland areas only orographic obstacles (mountain areas and the alpine region) receive higher Na loads than their surrounding areas, due to long-range transport of marine air masses. The magnitude of annual sodium deposition in Germany mainly is due to the occurrence of storm events from north-west in winter time, where higher amounts of sea salt are transported inland (cf. UBA 1997).

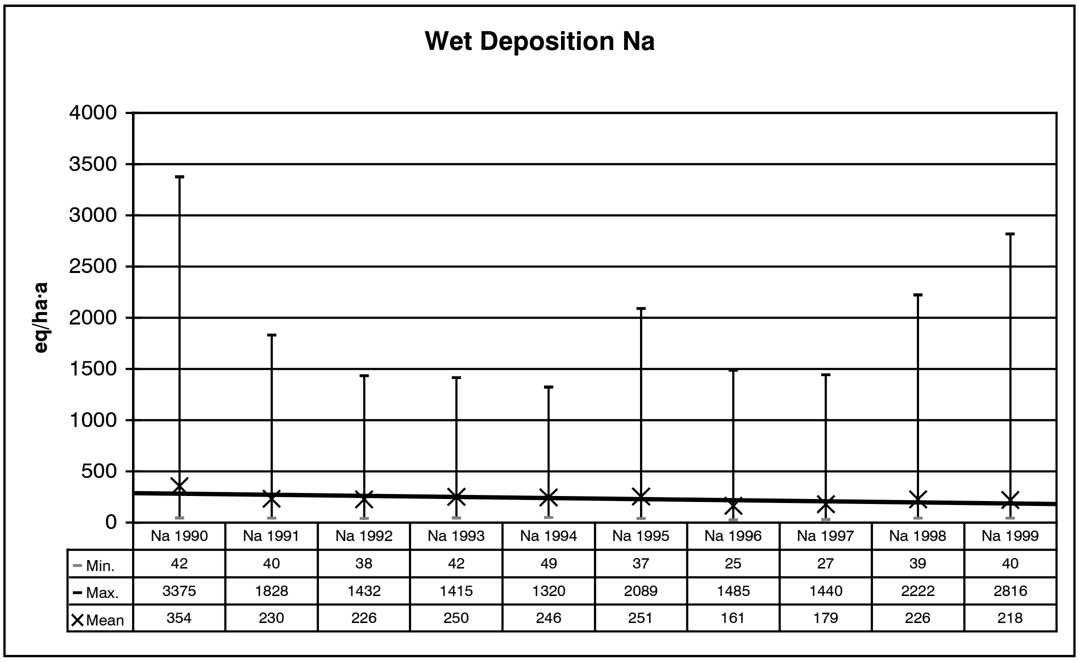

	Na 1990	Na 1991	Na 1992	Na 1993	Na 1994	Na 1995	Na 1996	Na 1997	Na 1998	Na 1999
− Min.	42	40	38	42	49	37	25	27	39	40
− Max.	3375	1828	1432	1415	1320	2089	1485	1440	2222	2816
× Mean	354	230	226	250	246	251	161	179	226	218

Figure 4.11: Minimum, maximum and annual mean wet deposition of sodium (Na) 1990-1999

4.4.1.2 Wet deposition of non-seasalt calcium ($Ca_{(nss)}$)

The annual average wet deposition of non-seasalt calcium ($Ca_{(nss)}$) within the period from 1990 to 1999 has decreased about 42% (Figure 4.1.1.2). This equals an absolute decrease of about 55.1 kt from 131.5 kt (3.67 kg ha^{-1} a^{-1}) in 1990 to 76.3 kt (2.13 kg ha^{-1} a^{-1}) in 1999. Over the ten years period a discontinuous downward trend, showing decreases as well as increases between the single years, can be observed. The range of data (see Min. and Max. in Figure 4.12), however, becomes significantly smaller from the early to the latest 1990s, due to the decline of maximum values. This, in its overall modelled pattern, is illustrated in the wet deposition maps of $Ca_{(nss)}$ 1990-1999 (Map 4.3).

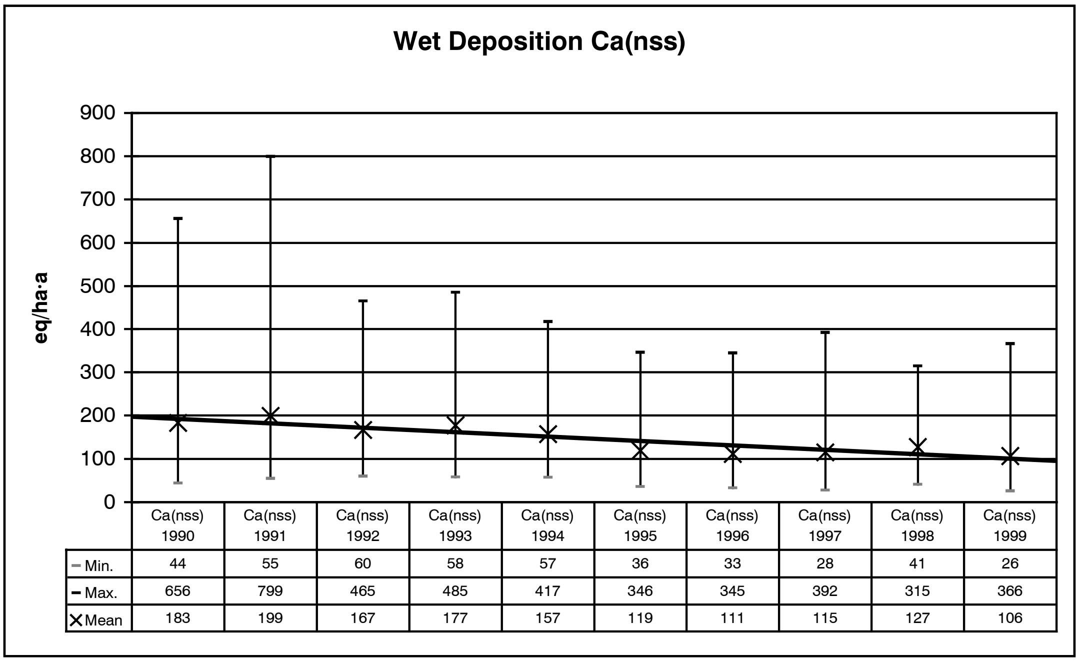

	Ca(nss) 1990	Ca(nss) 1991	Ca(nss) 1992	Ca(nss) 1993	Ca(nss) 1994	Ca(nss) 1995	Ca(nss) 1996	Ca(nss) 1997	Ca(nss) 1998	Ca(nss) 1999
– Min.	44	55	60	58	57	36	33	28	41	26
– Max.	656	799	465	485	417	346	345	392	315	366
✕ Mean	183	199	167	177	157	119	111	115	127	106

Figure 4.12: Minimum, maximum and annual mean wet deposition of non-seasalt calcium ($Ca_{(nss)}$) 1990-1999

The magnitudes of the sea salt fraction of wet deposited calcium is listed in Table 4.14. Here again, as it is shown for the non-seasalt fraction of wet deposited Ca, a discontinuous, but over the ten year period obvious downward trend of the absolute value of wet deposited sea salt calcium can be observed. This, of course, is due to the inland spread of sea spray originating mainly from the North Sea (cf. Sodium, Chapter 4.4.1.1). The wet deposition load of sea salt Ca ranges from 7.1 eq ha^{-1} a^{-1} (0.14 kg ha^{-1} a^{-1}) in 1996 to 15.6 eq ha^{-1} a^{-1} (0.31 kg ha^{-1} a^{-1}) in 1990, and in most of the years the average wet deposition load of sea salt Ca in Germany is around 0.2 kg ha^{-1} a^{-1}. The relative sea salt Ca share, shown as percentage of the total wet deposited Ca, over the time period is slightly rising (cf. Table 4.14). There are several natural and anthropogenic, local and remote sources of (measured) non-seasalt calcium in wet deposition. Thus uncertainties in the attribution to different emission sources are high, due to lacking data and research. The slight rising fraction of seasalt Ca while the amount of deposited non-seasalt $Ca_{(nss)}$ is decreasing (cf. Figure 4.12), however, can carefully be interpreted as additional indication of continuing emission abatement of anthropogenic calcium.

Table 4.14: Average seasalt fraction of calcium wet deposition 1990-1999

Average seasalt fraction of Ca wet deposition	**1990**	**1991**	**1992**	**1993**	**1994**	**1995**	**1996**	**1997**	**1998**	**1999**
in kt a^{-1}	11.2	7.3	7.1	7.9	7.8	7.9	5.1	5.6	7.1	6.9
eq ha^{-1} a^{-1}	15.6	10.1	10.0	11.0	10.8	11.1	7.1	7.9	10.0	9.6
in kg ha^{-1} a^{-1}	0.31	0.20	0.20	0.22	0.22	0.22	0.14	0.16	0.20	0.19
% of the total Ca wet deposition	7.8%	4.8%	5.6%	5.8%	6.4%	8.5%	6.0%	6.4%	7.3%	8.3%

4.4.1.3 Wet deposition of non-seasalt potassium ($K_{(nss)}$)

The annual average wet deposition of non-seasalt potassium ($K_{(nss)}$) within the period from 1990 to 1999 has decreased about 34% (Figure 13). This equals an absolute decrease of 15.4 kt from 44.9 kt (1.25 kg ha^{-1} a^{-1}) in 1990 to 29.5 kt (0.82 kg ha^{-1} a^{-1}) in 1999.

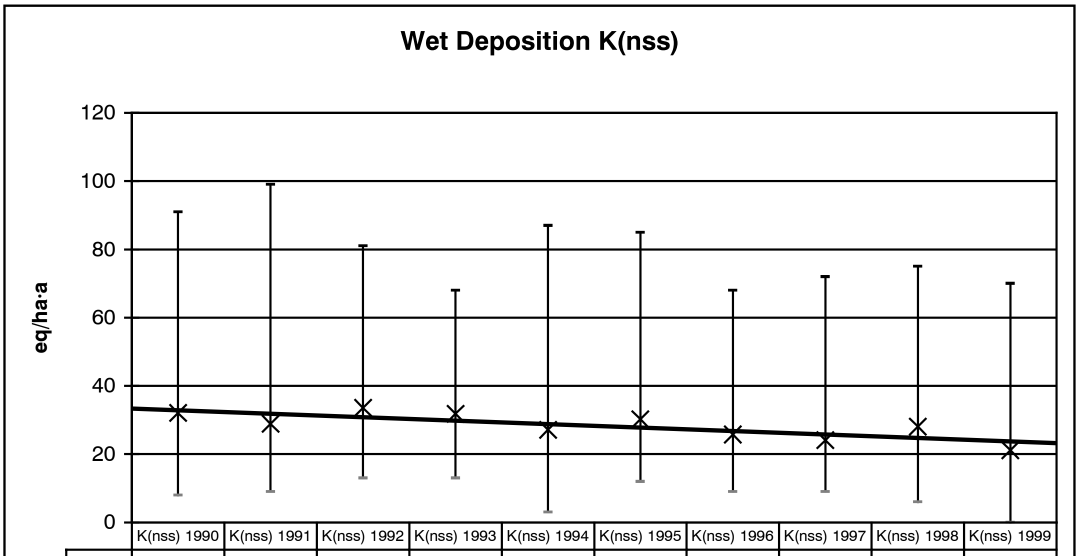

	K(nss) 1990	K(nss) 1991	K(nss) 1992	K(nss) 1993	K(nss) 1994	K(nss) 1995	K(nss) 1996	K(nss) 1997	K(nss) 1998	K(nss) 1999
- Min.	8	9	13	13	3	12	9	9	6	0
- Max.	91	99	81	68	87	85	68	72	75	70
× Mean	32	29	34	32	27	30	26	24	28	21

Figure 4.13: Minimum, maximum and annual mean wet deposition of non-seasalt potassium ($K_{(nss)}$) 1990-1999

The spatial pattern of wet deposited non-seasalt potassium ($K_{(nss)}$) is shown in the maps from 1990 to 1999 (Map 4.4). Aside anthropogenic sources and soil particulates, non-seasalt potassium also is emitted by vegetation.

The annual average percentage of the seasalt fraction of K ranges from 11.6% to 18.8% compared to the total wet deposition of K (Table 4.15).

Table 4.15: Average seasalt fraction of Potassium wet deposition 1990-1999

Average seasalt fraction of K wet deposition	**1990**	**1991**	**1992**	**1993**	**1994**	**1995**	**1996**	**1997**	**1998**	**1999**
in kt a^{-1}	10.4	14.1	6.6	7.3	7.2	7.4	4.79	5.3	6.7	6.4
eq ha^{-1} a^{-1}	7.4	4.8	4.7	5.2	5.2	5.3	3.4	3.8	4.8	4.6
in kg ha^{-1} a^{-1}	0.29	0.19	0.19	0.21	0.20	0.21	0.13	0.15	0.19	0.18
% of the total K wet deposition	18.8%	14.4%	12.4%	14.1%	16.0%	14.9%	11.6%	13.5%	14.5%	17.8%

4.4.1.4 Wet deposition of non-seasalt magnesium ($Mg_{(nss)}$)

The annual average wet deposition of non-seasalt magnesium ($Mg_{(nss)}$) within the period from 1990 to 1999 has decreased about 62% (Figure 4.14). This equals an absolute decrease of 5.4 kt from 8.7 kt (0.24 kg ha^{-1} a^{-1}) in 1990 to 3.3 kt (0.09 kg ha^{-1} a^{-1}) in 1999.

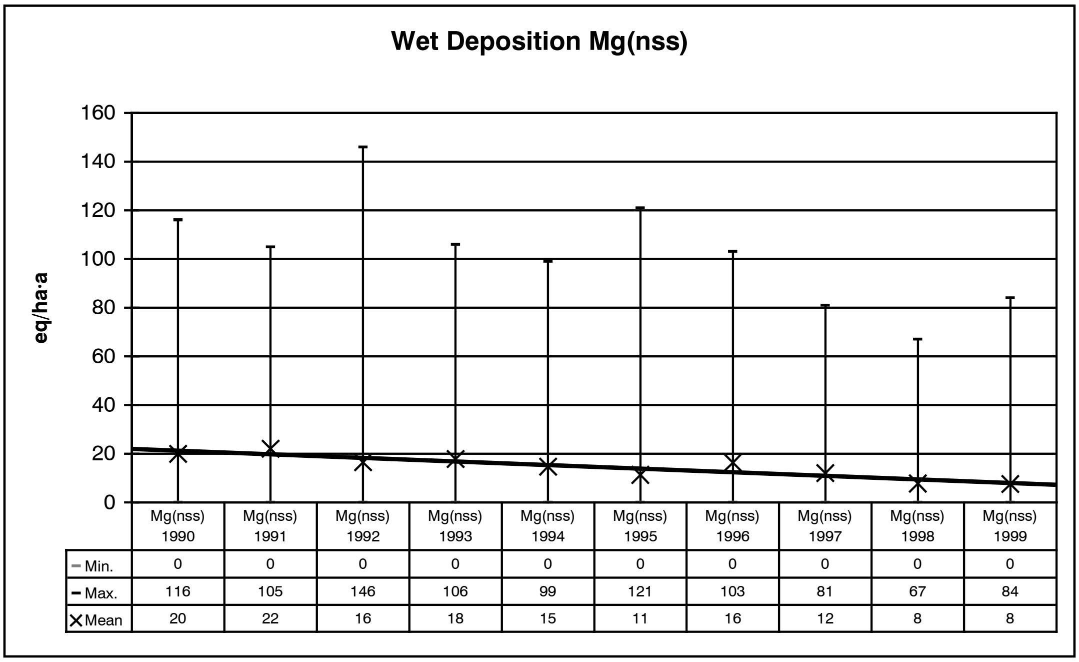

	Mg(nss) 1990	Mg(nss) 1991	Mg(nss) 1992	Mg(nss) 1993	Mg(nss) 1994	Mg(nss) 1995	Mg(nss) 1996	Mg(nss) 1997	Mg(nss) 1998	Mg(nss) 1999
− Min.	0	0	0	0	0	0	0	0	0	0
− Max.	116	105	146	106	99	121	103	81	67	84
× Mean	20	22	16	18	15	11	16	12	8	8

Figure 4.14: Minimum, maximum and annual mean wet deposition of non-seasalt magnesium ($Mg_{(nss)}$) 1990-1999

The spatial patterns of non-seasalt magnesium wet deposition ($Mg_{(nss)}$) is shown in the 1990 to 1999 Map 4.5. Main terrestrial sources of Mg are mineral particulates from soils, industry and (brown) coal combustion. The annual average percentage of the seasalt fraction of Mg ranges from 70.6% to 86.7% compared to the total wet deposition of Mg (Table 4.16).

Table 4.16: Average seasalt fraction of Magnesium wet deposition 1990-1999

Average seasalt fraction of Mg wet deposition	**1990**	**1991**	**1992**	**1993**	**1994**	**1995**	**1996**	**1997**	**1998**	**1999**
in kt a^{-1}	30.8	25.2	23.1	26.9	25.0	25.3	17.1	18.4	22.7	21.4
eq ha^{-1} a^{-1}	70.8	54.3	53.0	61.8	57.5	58.1	39.3	42.2	52.1	49.1
in kg ha^{-1} a^{-1}	0.86	0.66	0.64	0.75	0.70	0.71	0.48	0.51	0.63	0.60
% of the total Mg wet deposition	78.1%	71.1%	76.3%	77.7%	79.7%	83.7%	70.6%	77.8%	87.1%	86.7%

4.4.1.5 Wet deposition of the sum of base cations ($BC_{(nss)}=Ca_{(nss)}+K_{(nss)}+Mg_{(nss)}$)

The annual average wet deposition of the sum of non-seasalt base cations ($BC_{(nss)}$) within the period from 1990 to 1999 has decreased about 43% (Figure 4.15). This equals an absolute decrease of average 235 eq ha^{-1} a^{-1} in 1990 to 135 eq ha^{-1} a^{-1} in 1999.

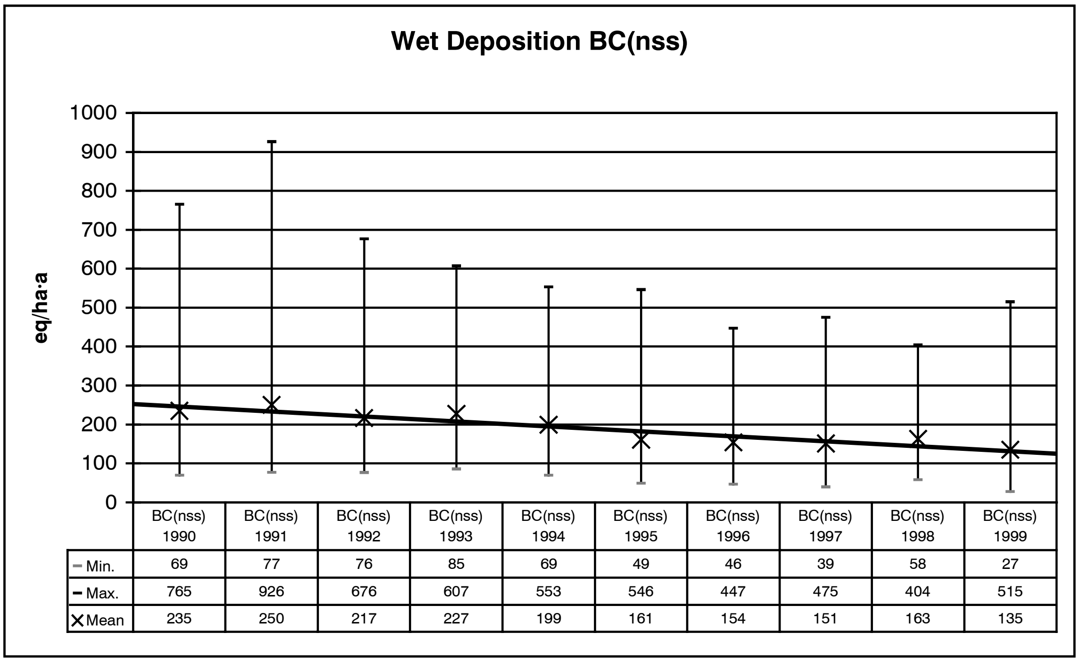

	BC(nss) 1990	BC(nss) 1991	BC(nss) 1992	BC(nss) 1993	BC(nss) 1994	BC(nss) 1995	BC(nss) 1996	BC(nss) 1997	BC(nss) 1998	BC(nss) 1999
– Min.	69	77	76	85	69	49	46	39	58	27
– Max.	765	926	676	607	553	546	447	475	404	515
× Mean	235	250	217	227	199	161	154	151	163	135

Figure 4.15: Minimum, maximum and annual mean wet deposition of non-seasalt base cations ($BC_{(nss)} = Ca_{(nss)} + K_{(nss)} + Mg_{(nss)}$) 1990-1999

The spatial patterns of the non-seasalt base cations 1990 to 1999 are shown in Map 4.6.

The annual average percentage of the seasalt fraction of BC in the single years ranges from 21.7% to 31.9% compared to the total wet deposition of BC (Table 4.17). The sea salt fraction of the BC wet deposition flux shows a rising tendency over the period considered within this study.

Table 4.17: Average seasalt fraction of base cation wet deposition 1990-1999

Average seasalt fraction of BC wet deposition	**1990**	**1991**	**1992**	**1993**	**1994**	**1995**	**1996**	**1997**	**1998**	**1999**
in eq ha^{-1} a^{-1}	93.8	69.2	67.7	78.0	73.5	74.5	49.8	53.8	66.8	63.3
% of the total BC wet deposition	28.5%	21.7%	23.8%	25.6%	27.0%	31.7%	24.5%	26.3%	29.1%	31.9%

Calcium is the dominating compound of the sum of base cations. The mean fraction of $Ca_{(nss)}$ of wet deposited base cations 1990 to 1999 is relatively close to 80% (72.5% - 78.8%, c.f. Table 4.18). The magnitude of the $K_{(nss)}$ fraction ranges between 11.5% and 18.8%, whereas the fraction of $Mg_{(nss)}$ is the smallest, ranging from 4.8% to 10.7% within the period from 1990 to 1999.

Table 4.18: Average non-seasalt calcium ($Ca_{(nss)}$), potassium ($K_{(nss)}$) and magnesium ($Mg_{(nss)}$) fraction of the sum of wet deposited non-seasalt base cations ($BC_{(nss)}$)

	1990	**1991**	**1992**	**1993**	**1994**	**1995**	**1996**	**1997**	**1998**	**1999**
mean fraction of $Ca_{(nss)}$	77.9%	79.6%	76.9%	78.1%	79.0%	74.1%	72.5%	76.1%	78.0%	78.8%
mean fraction of $K_{(nss)}$	13.6%	11.5%	15.5%	14.0%	13.6%	18.8%	16.8%	15.9%	17.3%	15.6%
mean fraction of $Mg_{(nss)}$	8.5%	8.8%	7.6%	7.8%	7.4%	7.1%	10.7%	8.0%	4.8%	5.6%
total	100%	100%	100%	100%	100%	100%	100%	100%	100%	100%

4.4.2 Wet deposition fluxes of acidifying components and nitrogen

4.4.2.1 Wet deposition of non-seasalt sulphur (SO_4-$S_{(nss)}$)

Average non-seasalt sulpur (SO_4-$S_{(nss)}$) wet deposition declined by about 54% within the ten year time period from 1990 to 1999 (c.f. Figure 4.16). This equals a reduction of the total SO_4-$S_{(nss)}$ wet deposition on Germany by 191 kt from 354 kt (9.89 kg ha^{-1} a^{-1}) in 1990 to 163 kt (4.56 kg ha^{-1} a^{-1}) in 1999.

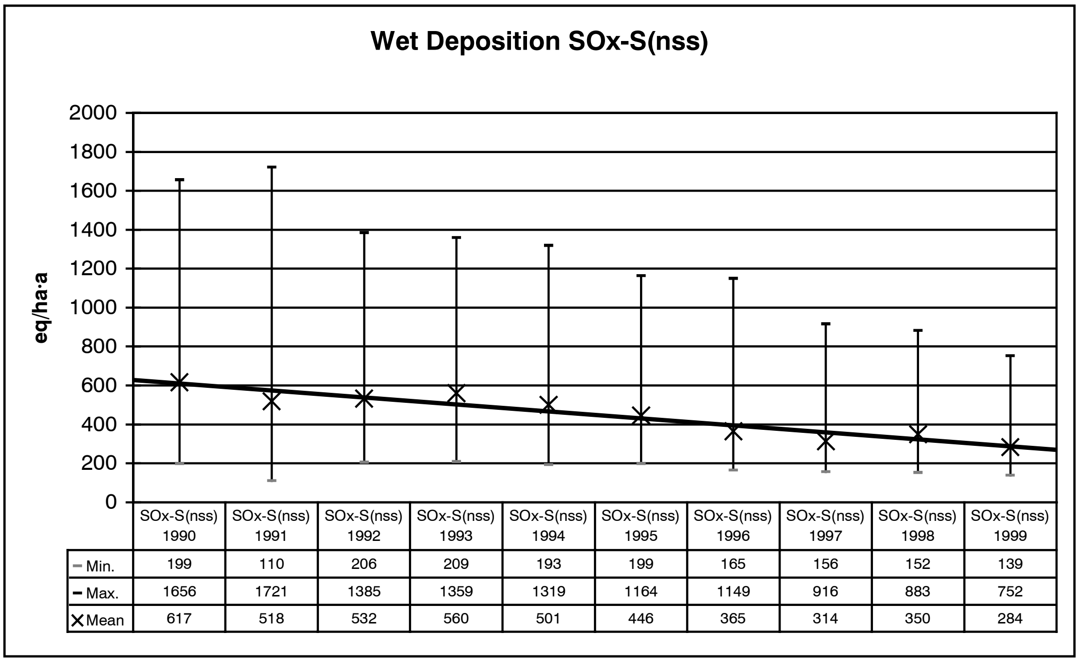

	SOx-S(nss) 1990	SOx-S(nss) 1991	SOx-S(nss) 1992	SOx-S(nss) 1993	SOx-S(nss) 1994	SOx-S(nss) 1995	SOx-S(nss) 1996	SOx-S(nss) 1997	SOx-S(nss) 1998	SOx-S(nss) 1999
– Min.	199	110	206	209	193	199	165	156	152	139
– Max.	1656	1721	1385	1359	1319	1164	1149	916	883	752
✕ Mean	617	518	532	560	501	446	365	314	350	284

Figure 4.16: Minimum, maximum and annual mean wet deposition of non-seasalt sulphur (SO_4-$S_{(nss)}$) 1990-1999

The spatial patterns of non-seasalt sulphur wet deposition are shown in Map 4.7. Here the decline of peak values becomes obvious between 1990 and 1999, especially in the eastern half of Germany, and reflects ongoing sulphur emission abatement.

The average seasalt fraction of wet deposited sulphur ranges from 4.9% to 8.4% (c.f. Table 4.19) and is mainly deposited close to the North Sea (see Chapter 4.4.1.1, Na).

Table 4.19: Average seasalt fraction of sulphur wet deposition 1990-1999

Average seasalt fraction of SO_4-S wet deposition	**1990**	**1991**	**1992**	**1993**	**1994**	**1995**	**1996**	**1997**	**1998**	**1999**
in t/a	24.394	15.862	15.580	17.208	16.926	17.306	11.082	12.315	15.582	15.008
in eq/ha	42,5	27,6	27,1	30,0	29,5	30,1	19,3	21,5	27,1	26,1
in kg/ha	0,68	0,44	0,44	0,48	0,47	0,48	0,31	0,34	0,44	0,42
% of the total SO_4-S wet deposition	6,4%	5,1%	4,9%	5,1%	5,6%	6,3%	5,0%	6,4%	7,2%	8,4%

4.4.2.2 Wet deposition of reduced nitrogen (NH_4-N)

Annual average wet deposition rates of reduced nitrogen (NH_4-N) are shown in Figure 4.1. A decline of the peak values of NH_4-N wet fluxes can be observed From 1990 (1703 eq ha^{-1} a^{-1} = 23.9 kg ha^{-1} a^{-1}) to 1992 (956 eq ha^{-1} a^{-1} = 13.4 kg ha^{-1} a^{-1}). Maximum values in the following years vary between 1082 eq ha^{-1} a^{-1} = 15.2 kg ha^{-1} a^{-1} (1993) and 837 eq ha^{-1} a^{-1} = 11.7 kg ha^{-1} a^{-1} (1999) without showing a trend in any direction. The Annual average NH_4-N wet deposition, however, declined by about 19% from 233 kt (6.5 kg ha^{-1} a^{-1}) 1990 to 190 kt (5.3 kg ha^{-1} a^{-1}) in 1999.

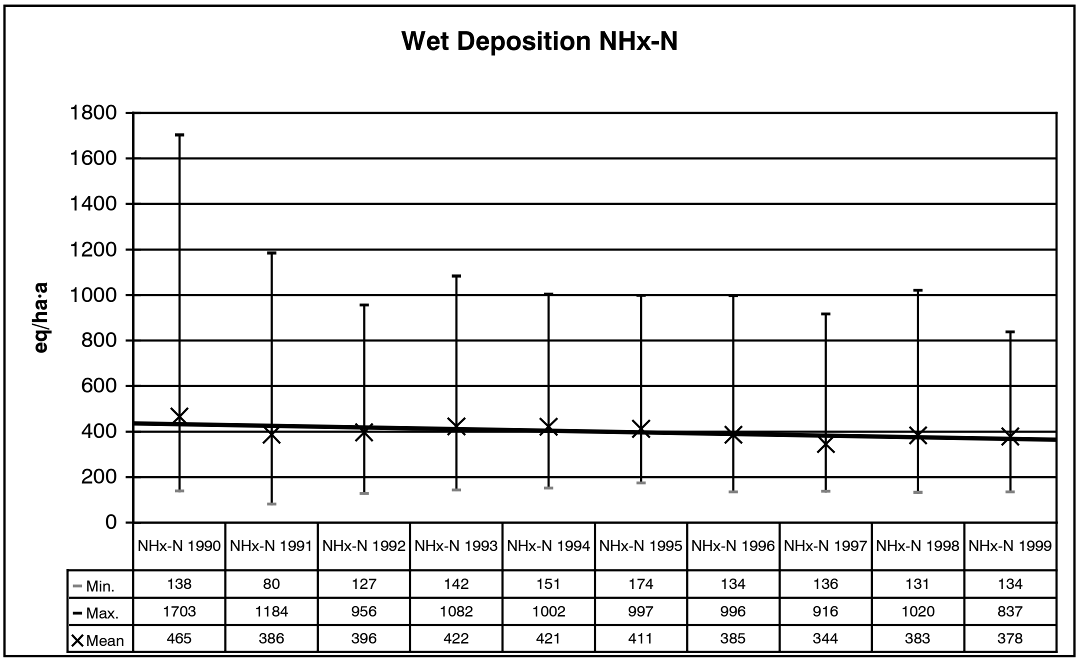

	NHx-N 1990	NHx-N 1991	NHx-N 1992	NHx-N 1993	NHx-N 1994	NHx-N 1995	NHx-N 1996	NHx-N 1997	NHx-N 1998	NHx-N 1999
− Min.	138	80	127	142	151	174	134	136	131	134
− Max.	1703	1184	956	1082	1002	997	996	916	1020	837
× Mean	465	386	396	422	421	411	385	344	383	378

Figure 4.17: Minimum, maximum and annual mean wet deposition of reduced nitrogen (NH_4-N) 1990-1999

The maps (Map 4.8) show the spatial pattern of NH_4-N wet deposition from 1990 to 1999. The maps show rather year to year variations then changes in the general spatial pattern. Areas with wet fluxes of NH_X-N above the annual average are mainly found in the north-western and in the south-eastern parts of Germany, respectively. Only the more or less obvious decline in the magnitude of wet deposited ammonium in the eastern part of Germany can be found, which can be attributed to the reduction of livestock after the political and economic changes starting there at the end of 1989.

4.4.2.3 Wet deposition of oxidised nitrogen (NO_3-N)

The annual average wet deposition of nitrate (NO_3-N) 1999 only shows an about 7% lower value than 1990 (Figure 4.18). This is smaller than some changes from one year to the next over the whole ten year period (c.f. Table 4.12). Obviously no trend over time can be found here.

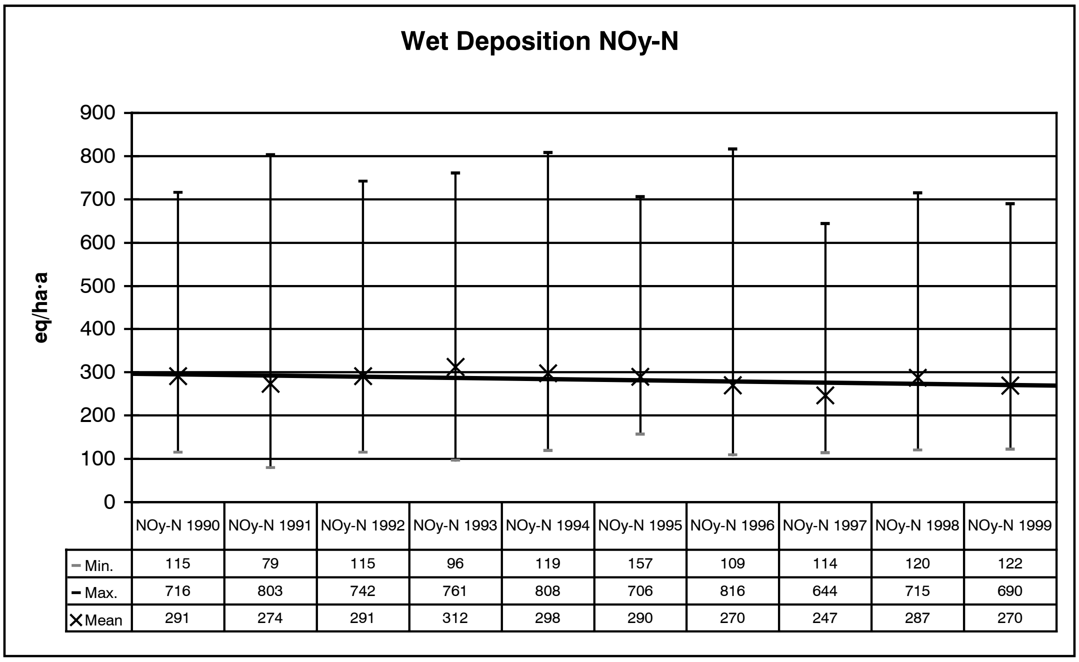

	NOy-N 1990	NOy-N 1991	NOy-N 1992	NOy-N 1993	NOy-N 1994	NOy-N 1995	NOy-N 1996	NOy-N 1997	NOy-N 1998	NOy-N 1999
- Min.	115	79	115	96	119	157	109	114	120	122
- Max.	716	803	742	761	808	706	816	644	715	690
× Mean	291	274	291	312	298	290	270	247	287	270

Figure 4.18: Minimum, maximum and annual mean wet deposition of oxidised nitrogen (NO_3-N) 1990-1999

The spatial patterns in 1990 to 1999 are presented in the maps in Map 4.9. From the first five years 1990 to 1994 show a slightly different spatial trend of NO_3-N wet deposition than the latest five can be found: mainly in the eastern part of Germany more often values below 3.5 kg ha^{-1} a^{-1} are covering larger areas in 1995 to 1999.

4.4.2.4 Wet deposition of total nitrogen (N = NH_4-N + NO_3-N)

A straight trend in wet deposition of nitrogen (N) over time can hardly be found in the annual average map values. Only decline in the maximum values between 1990 and 1999 (Figure 4.19), and a decline of the average N wet deposition from 1993 to 1997 can be observed (cf. Table 4.12). The difference between 1990 and 1999 is an about 14% lower average N wet deposition. In 1990 about 397 kt N (10.6 kg ha^{-1} a^{-1}) were deposited with the wet flux in Germany, whereas in 1999 the average magnitude of wet deposition of N was 9.1 kg ha^{-1} a^{-1} (325 kt N), respectively.

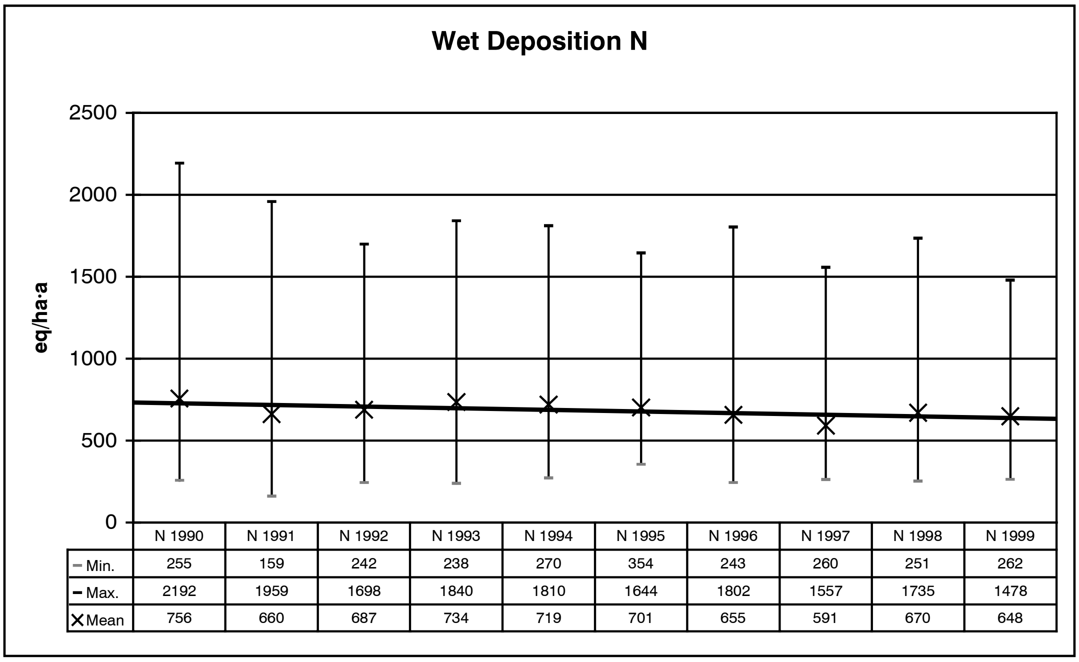

	N 1990	N 1991	N 1992	N 1993	N 1994	N 1995	N 1996	N 1997	N 1998	N 1999
– Min.	255	159	242	238	270	354	243	260	251	262
– Max.	2192	1959	1698	1840	1810	1644	1802	1557	1735	1478
× Mean	756	660	687	734	719	701	655	591	670	648

Figure 4.19: Minimum, maximum and annual mean wet deposition of total nitrogen (N) 1990-1999

The spatial pattern of N wet deposition 1990 to 1999 is presented in the maps in Map 4.11. N wet deposition above the annual averages in all the years are mainly found in the north-western and south-eastern areas in Germany. The patterns are more similar to those of NH_X-N wet deposition than to those of NO_Y-N, which indicates the difference in magnitude of both compounds.

The average fraction of reduced (NH_X-N) and oxidised (NO_Y-N) nitrogen of the total wet deposited N is shown in Table 4.20, where the average wet flux of N is composed by more or less 60% NH_X-N, and close to 40% NO_Y-N, respectively.

Table 4.20: Average NH_X-N and NO_Y-N fraction of total wet deposited N

Average fraction of N wet deposition	**1990**	**1991**	**1992**	**1993**	**1994**	**1995**	**1996**	**1997**	**1998**	**1999**
mean fraction of NH_X –N	61,5%	58,5%	57,6%	57,5%	58,5%	58,6%	58,8%	58,3%	57,1%	58,4%
mean fraction of NO_Y –N	38,5%	41,5%	42,4%	42,5%	41,5%	41,4%	41,2%	41,7%	42,9%	41,6%
total	100%	100%	100%	100%	100%	100%	100%	100%	100%	100%

4.4.2.5 Wet deposition of non-seasalt chlorine ($Cl_{(nss)}$)

Chlorine mainly originates from sea spray (c.f. Table 4.21). Annual average non-seasalt chlorine ($Cl_{(nss)}$) wet deposition loads are relatively low in magnitude(c.f. Figure 4.20). It is assumed, that wet deposition of non-seasalt chlorine is completely due to anthropogenic HCl emissions. Moreover it is assumed that dry deposition of HCl locally is relevant close to emission sources only. Hence $Cl_{(nss)}$ wet deposition is attributed to total deposition of anthropogenic chlorine.

Average $Cl_{(nss)}$ wet deposition 1999 is remarkable 77% lower than in 1990. In 1990 59.5 kt (1.66 kg ha^{-1} a^{-1}) $Cl_{(nss)}$ were wet deposited in Germany, in 1999 only 13.9 kt (0.39 kg ha^{-1} a^{-1}) (c.f. Figure 4.20). The annual percentage changes, however, are varying very much (Table 4.22), and hence a trend over the whole ten years period can not be determined. In the maps of annual average $Cl_{(nss)}$ wet deposition 1990 to 1999 (Map 4.12) also rather different spatial patterns of low and spots of high value areas can be found than a trend within certain German regions.

Table 4.21: Average seasalt fraction of chlorine wet deposition 1990-1999

Average seasalt fraction of Cl wet deposition	**1990**	**1991**	**1992**	**1993**	**1994**	**1995**	**1996**	**1997**	**1998**	**1999**
in kt a^{-1}	430.1	371.5	293.0	329.4	337.8	337.1	221.8	254.1	310.1	302.4
in eq ha^{-1} a^{-1}	338.8	233.0	230.8	259.4	266.1	265.5	174.7	200.2	244.3	238.2
in kg ha^{-1} a^{-1}	12.01	8.26	8.18	9.20	9.43	9.41	6.19	7.10	8.66	8.44
% of the total Cl wet deposition	87,8%	90,9%	93,9%	95,0%	89,9%	88,7%	93,9%	91,9%	93,0%	95,6%

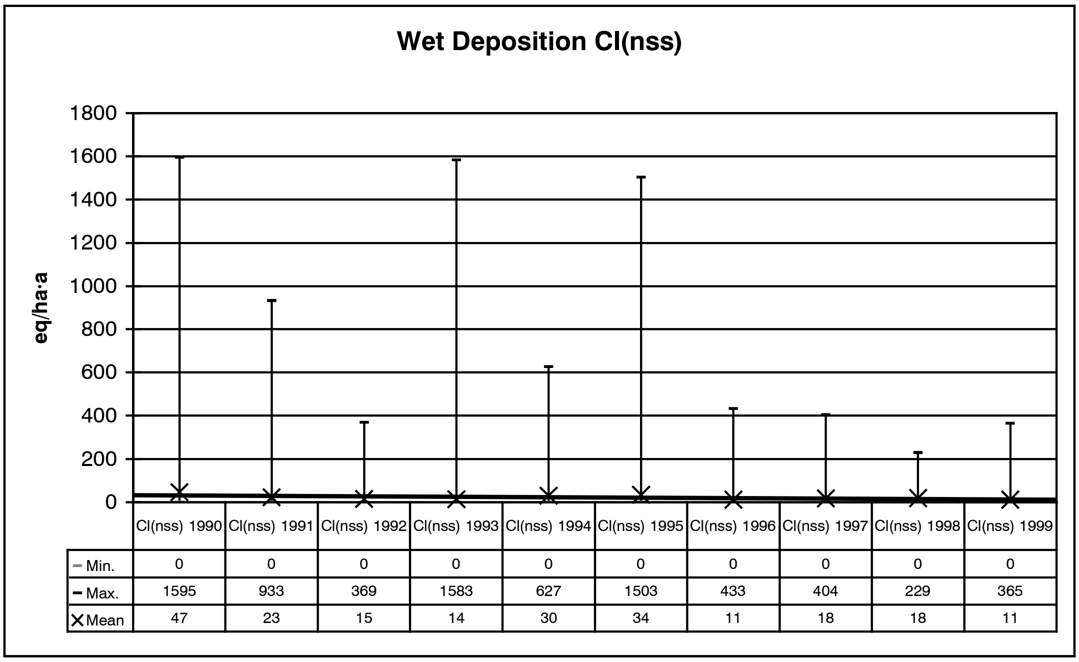

Figure 4.20: Minimum, maximum and annual mean wet deposition of non-seasalt chlorine ($Cl_{(nss)}$) 1990-1999

Table 4.22: Budgets of average non-seasalt wet deposition of chlorine ($Cl_{(nss)}$) 1990-1999

Annual average $Cl_{(nss)}$ wet deposition	**1990**	**1991**	**1992**	**1993**	**1994**	**1995**	**1996**	**1997**	**1998**	**1999**	**% change from 1990 to 1999**
in kg ha^{-1} a^{-1}	1.66	0.82	0.54	0.48	1.06	1.20	0.41	0.63	0.65	0.39	**-77**
% change from previous year		**-51**	**-35**	**-10**	**+120**	**+13**	**-66**	**+55**	**+3**	**-40**	

4.4.2.6 Wet deposition of potential acidity ($AC_{pot} = S_{(nss)} + N + Cl_{(nss)}$)

Potential acidity (AC_{pot}) is defined as the sum of non-seasalt sulphur, total nitrogen and non-seasalt chlorine (UBA 1996). Wet deposition of AC_{pot} declined by about 34% from 1990 to1999 (c.f. Figure 4.21).

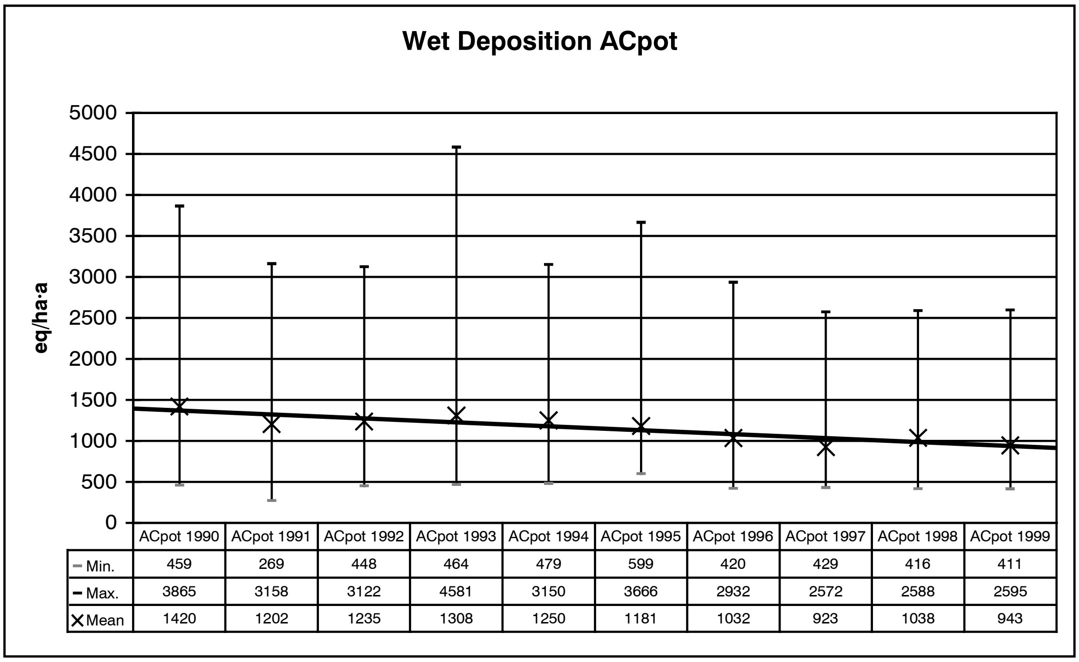

	ACpot 1990	ACpot 1991	ACpot 1992	ACpot 1993	ACpot 1994	ACpot 1995	ACpot 1996	ACpot 1997	ACpot 1998	ACpot 1999
- Min.	459	269	448	464	479	599	420	429	416	411
- Max.	3865	3158	3122	4581	3150	3666	2932	2572	2588	2595
× Mean	1420	1202	1235	1308	1250	1181	1032	923	1038	943

Figure 4.21: Minimum, maximum and annual mean wet deposition of potential acid (AC_{pot}) 1990-1999

The trend to lower average wet potential acidity input (Figure 4.21) is mainly due to the reduction of SO_X-$S_{(nss)}$ deposition, which declined by 54% within the ten years period 1990 to 1999 (Chapter 4.4.2.1), whereas the average reduction of wet deposited N in the same time only is found to be 14% (Chapter 4.4.2.3).

In Table 4.23 the average fractions of wet deposited acidifying compounds are listed. The contribution of $Cl_{(nss)}$ is the smallest with a range between 1% and 3% in the different years. The fraction of SO_X-$S_{(nss)}$ is contributing by 43% to 30% with an obvious decline between 1990 and 1999. In contrast the contribution of total N to wet deposition of AC_{pot} is rising from 53% 1990 to 69% in 1999. This is due to both, the fraction of reduced nitrogen (NH_X-N) and oxidised nitrogen (NO_Y-N), which show only slightly falling absolute values, and hence a rising relative contribution to AC_{pot} (c.f. Figure 4.22 and Table 4.23). From 1996 onward the NH_X-N fraction is bigger than the SO_X-$S_{(nss)}$ fraction of potential acidity.

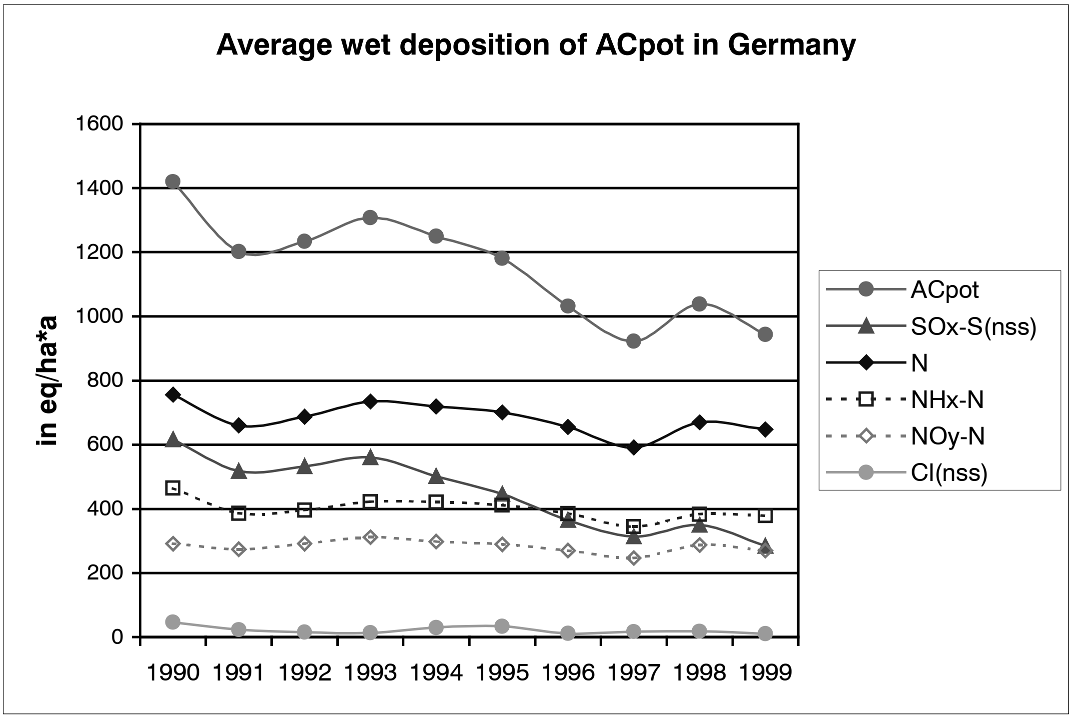

Figure 4.22: Average potential acidity and fractions of acidifying compounds in wet deposition 1990-1999

Table 4.23: Average fractions of acidifying compounds in wet deposition 1990-1999

Average fraction of...	**1990**	**1991**	**1992**	**1993**	**1994**	**1995**	**1996**	**1997**	**1998**	**1999**
SO_4-$S_{(nss)}$ in eq/ha	617	518	532	560	501	446	365	314	350	284
SO_4-$S_{(nss)}$ as % of the total AC_{pot} wet deposition	43%	43%	43%	43%	40%	38%	35%	34%	34%	30%
N in eq/ha	756	660	687	734	719	701	655	591	670	648
N as % of the total AC_{pot} wet deposition	53%	55%	56%	56%	58%	59%	64%	64%	65%	69%
$Cl_{(nss)}$ in eq/ha	47	23	15	14	30	34	11	18	18	11
$Cl_{(nss)}$ as % of the total AC_{pot} wet deposition	3%	2%	1%	1%	2%	3%	1%	2%	2%	1%
NH_X-N in eq/ha	465	386	396	422	421	411	385	344	383	378
NH_X-N as % of the total AC_{pot} wet deposition	33%	32%	32%	32%	34%	35%	37%	37%	37%	40%
NO_Y-N in eq/ha	291	274	291	312	298	290	270	247	287	270
NOY-N as % of the total AC_{pot} wet deposition	21%	23%	24%	24%	24%	25%	26%	27%	28%	29%

The spatial patterns of AC_{pot} in the single years AC_{pot} 1990-1999 are presented in Map 4.12.

4.4.2.7 Wet deposition of potential net-acidity ($AC_{pot(net)}=(S_{(nss)}+N+Cl_{(nss)})-BC_{(nss)}$) and acid neutralisation ($=BC_{(nss)}\cdot 100/AC_{pot}$ [%])

The sum of base cations ($BC_{(nss)} = Ca_{(nss)} + K_{(nss)} + Mg_{(nss)}$) is subtracted from potential acidity (AC_{pot}) in order to calculate potential net acidity ($AC_{pot(net)}$). By doing so, the of potential acid neutralisation is accounted for. Hence the wet deposition loads of $AC_{pot(net)}$ are lower than the wet deposition loads of AC_{pot}. The relative magnitudes (annual min. max. and mean % values) of acid neutralisation by wet deposition of $BC_{(nss)}$ are presented in Figure 4.23.

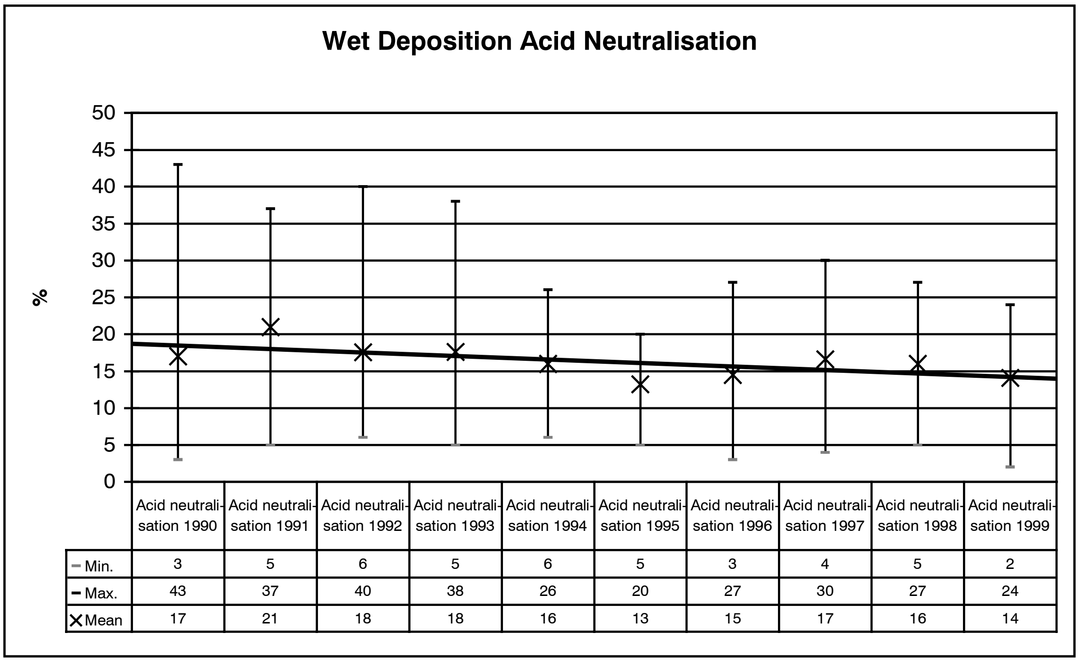

	Acid neutralisation 1990	Acid neutralisation 1991	Acid neutralisation 1992	Acid neutralisation 1993	Acid neutralisation 1994	Acid neutralisation 1995	Acid neutralisation 1996	Acid neutralisation 1997	Acid neutralisation 1998	Acid neutralisation 1999
- Min.	3	5	6	5	6	5	3	4	5	2
- Max.	43	37	40	38	26	20	27	30	27	24
× Mean	17	21	18	18	16	13	15	17	16	14

Figure 4.23: Minimum, maximum and annual mean acid neutralisation in wet deposition 1990-1999

The difference between the 1990 and 1999 average wet deposition of potential net acidity ($AC_{pot(net)}$) is a 376 eq ha^{-1} a^{-1} (37%) lower flux (Figure 4.24).

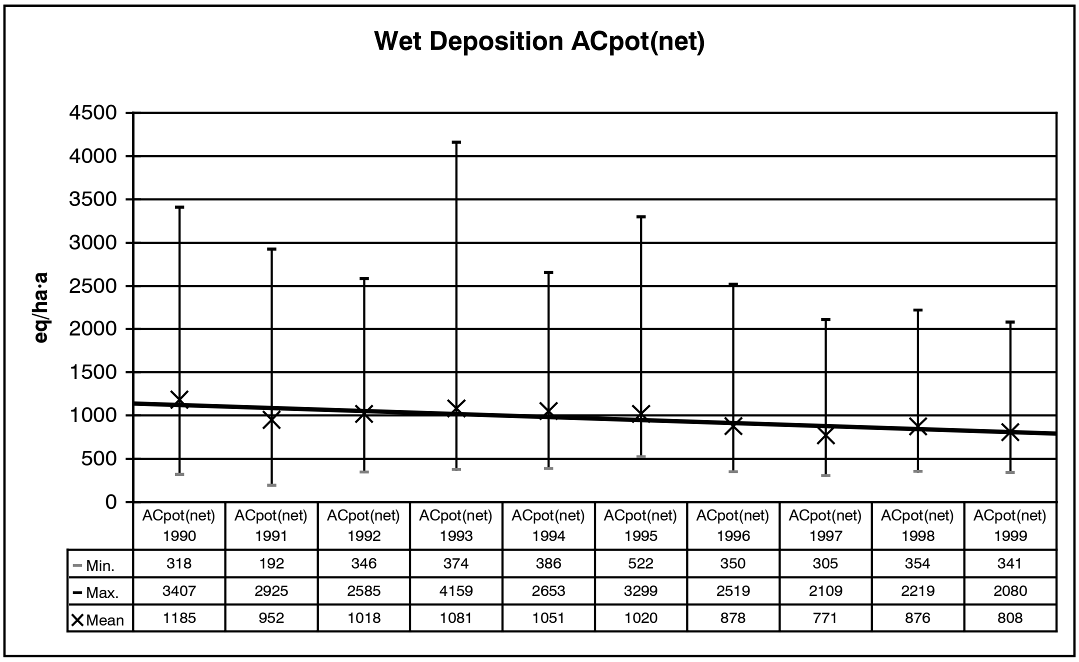

	ACpot(net) 1990	ACpot(net) 1991	ACpot(net) 1992	ACpot(net) 1993	ACpot(net) 1994	ACpot(net) 1995	ACpot(net) 1996	ACpot(net) 1997	ACpot(net) 1998	ACpot(net) 1999
- Min.	318	192	346	374	386	522	350	305	354	341
- Max.	3407	2925	2585	4159	2653	3299	2519	2109	2219	2080
× Mean	1185	952	1018	1081	1051	1020	878	771	876	808

Figure 4.24: Minimum, maximum and annual mean wet deposition of potential net acidity ($AC_{pot(net)}$) 1990-1999

The spatial patterns of $AC_{pot(net)}$ 1990-1999 are presented in Map 4.13. The decline of peak values (Figure 4.24) are represented in the maps by obviously less high value areas, especially in the second half of the ten years period. Regions with wet $AC_{pot(net)}$ fluxes above the average in the later years are found in the north-western parts of Germany (covering Schleswig-Holstein, Lower Saxony and North Rhine-Westphalia), while in the other parts of Germany fluxes above the annual average are mainly restricted to higher altitude mountain areas (Map 4.13).

4.5 Maps of wet deposition 1990-1999

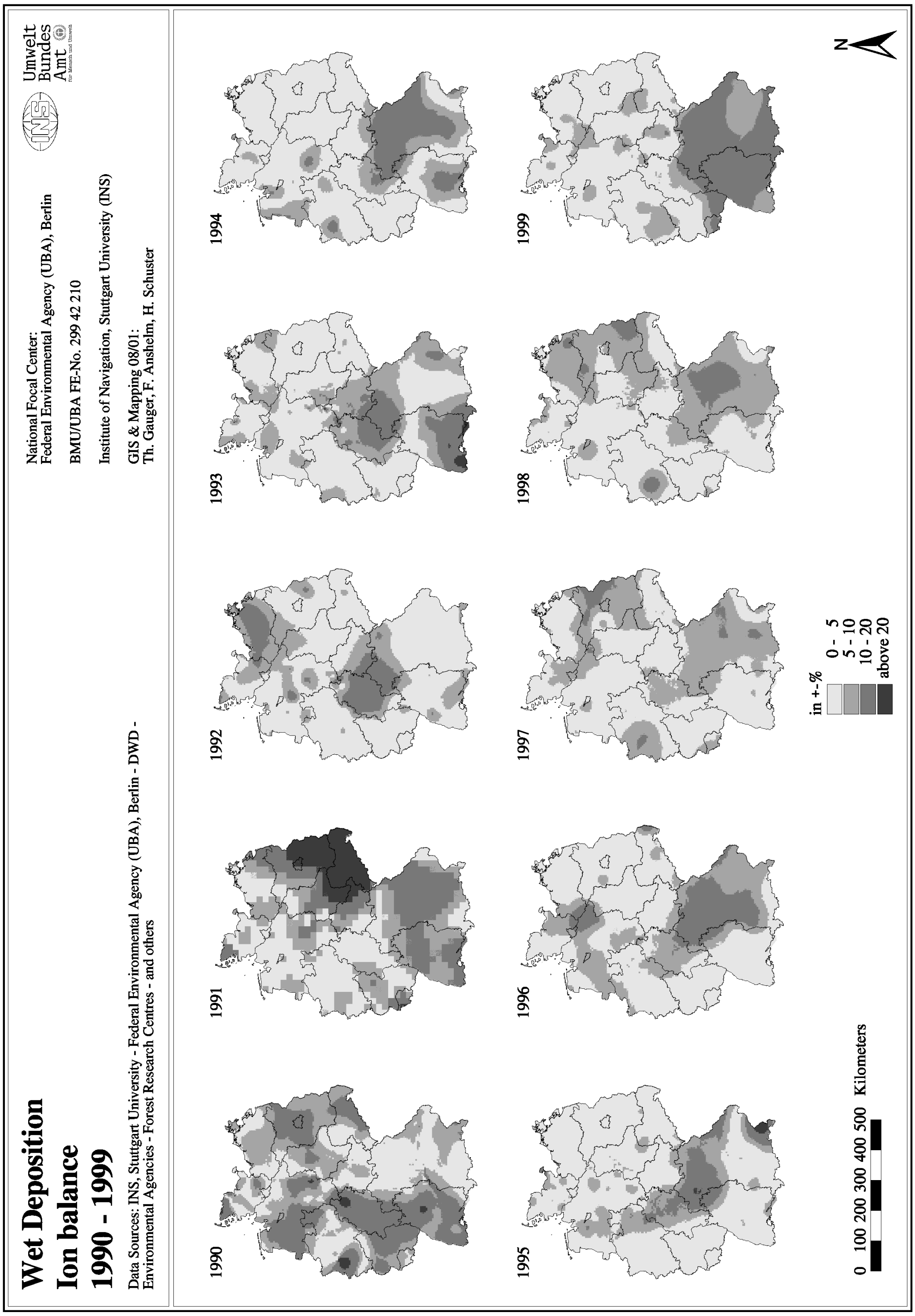

Map 4.1: Ion balance [in %] calculated from wet deposition maps of the main compounds in precipitation 1990 – 1999

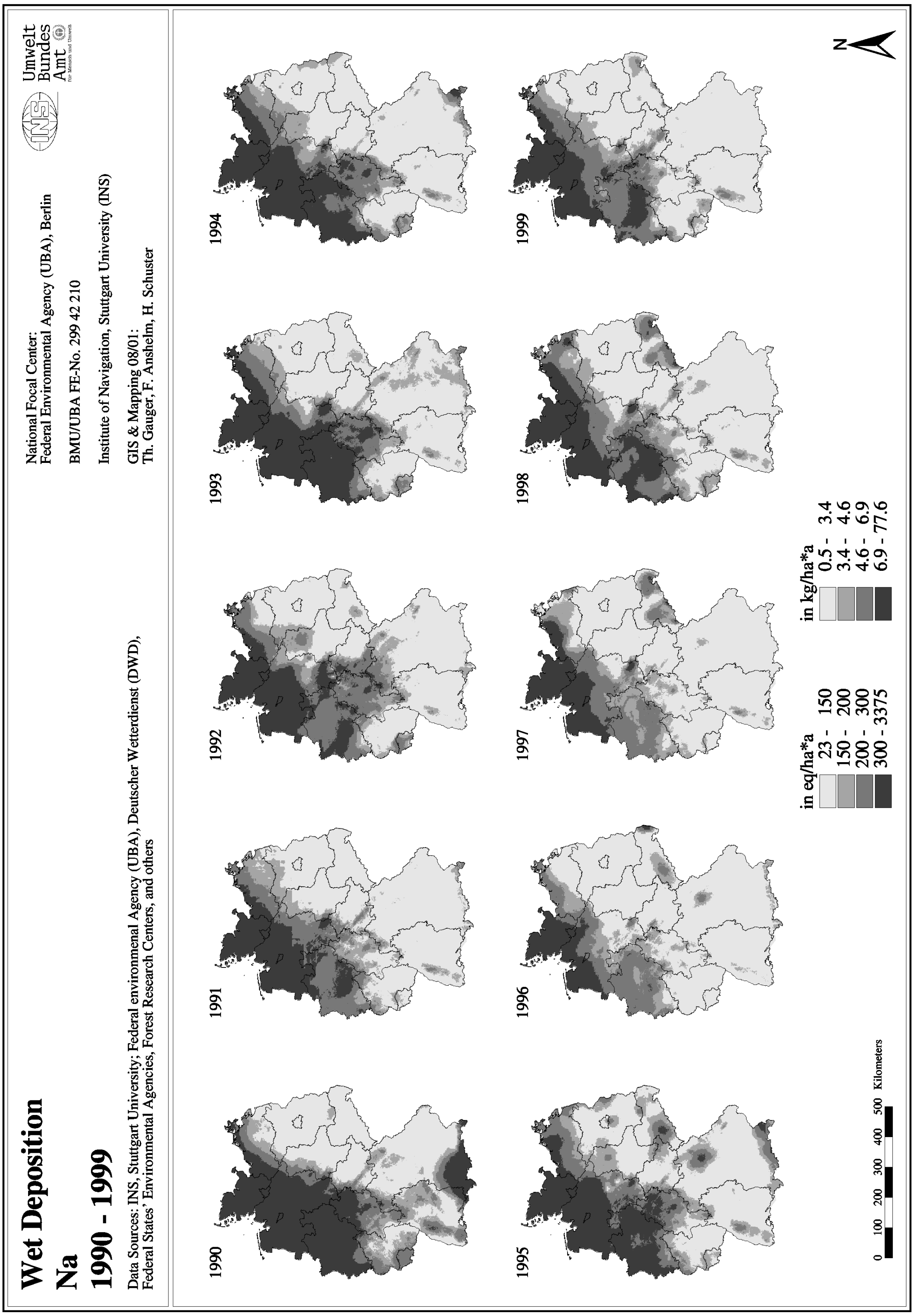

Map 4.2: Wet deposition of Na 1990 – 1999

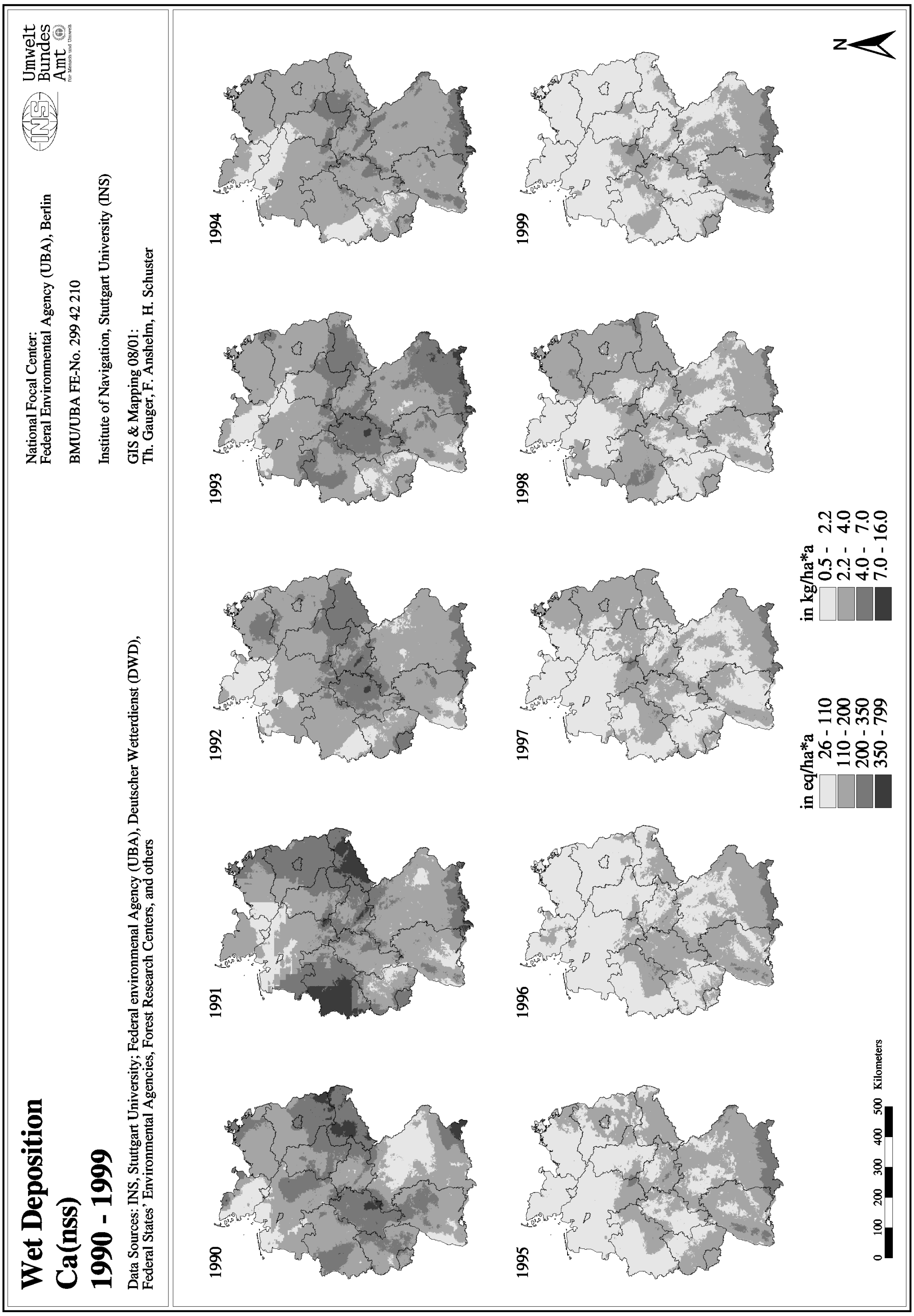

Map 4.3: Wet deposition of $Ca_{(nss)}$ 1990 – 1999

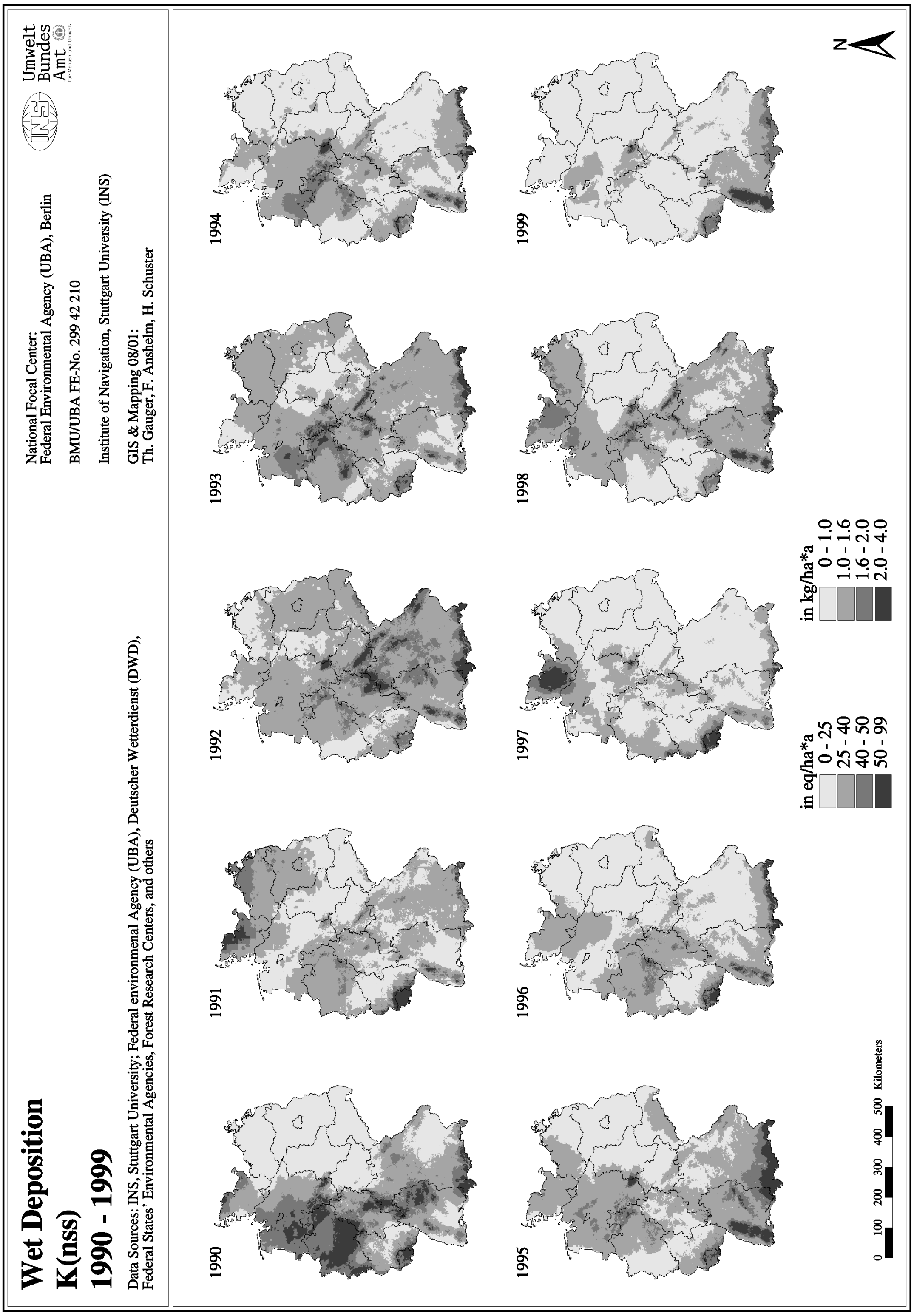

Map 4.4: Wet deposition of $K_{(nss)}$ 1990 – 1999

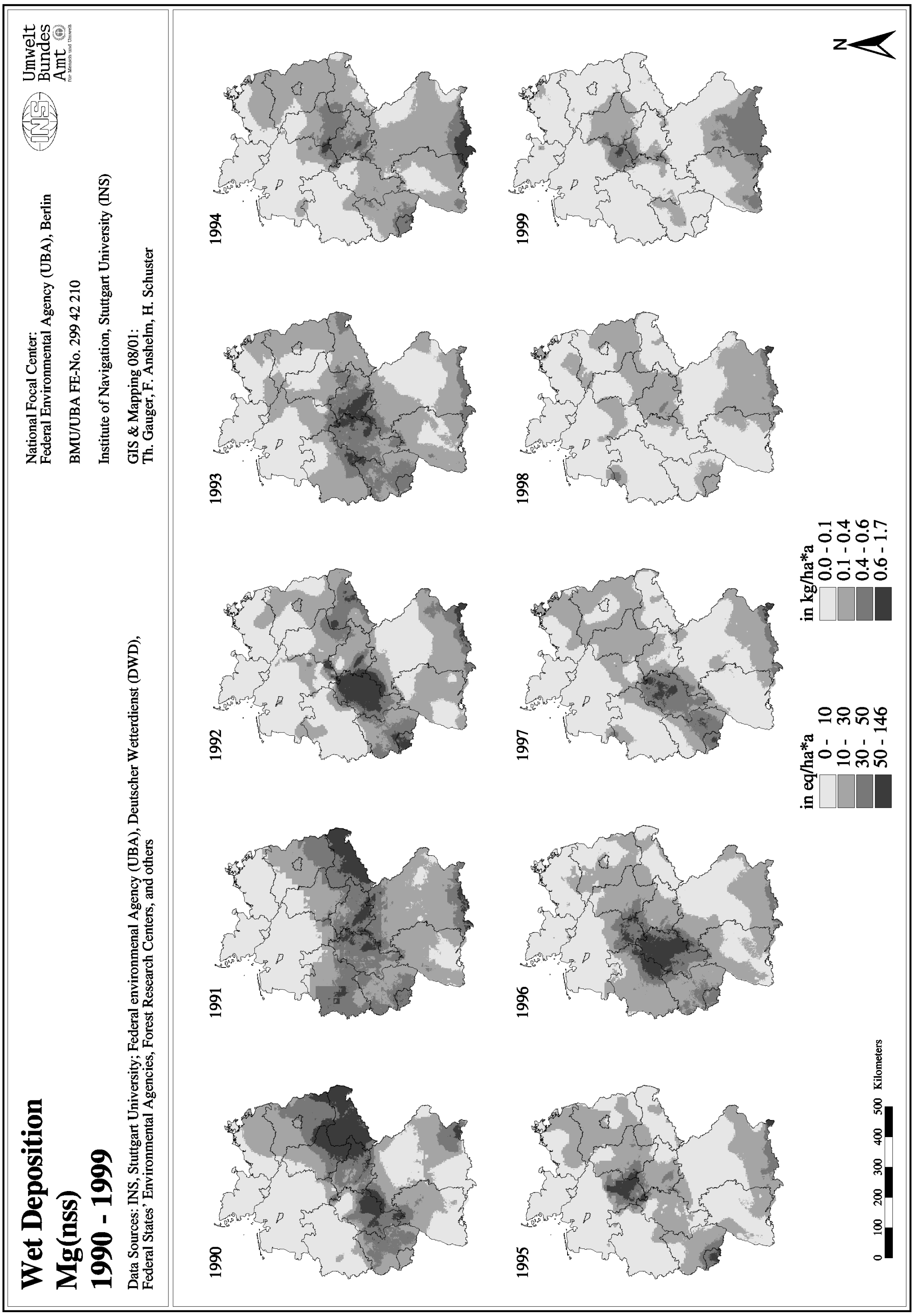

Map 4.5: Wet deposition of $Mg_{(nss)}$ 1990 – 1999

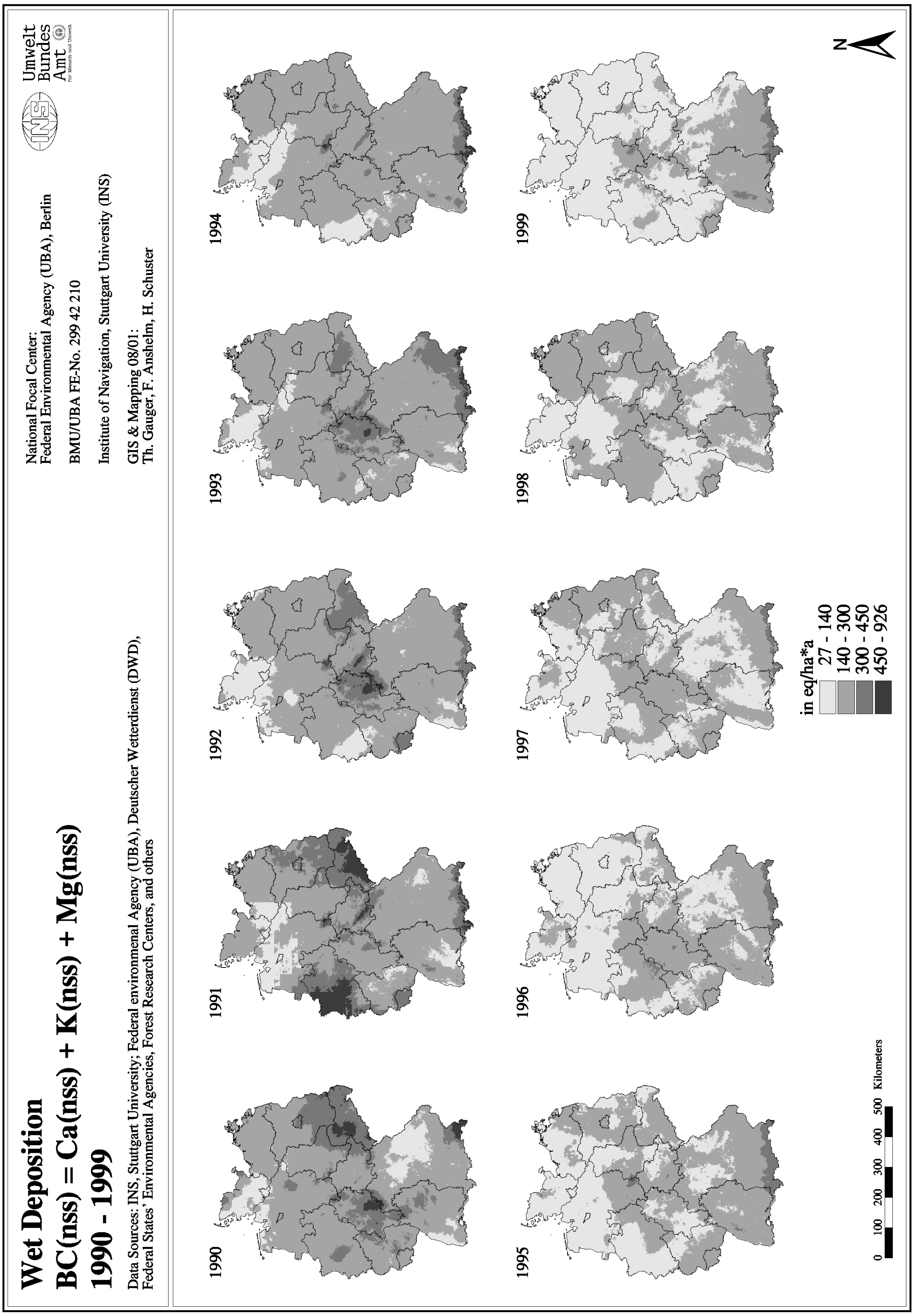

Map 4.6: Wet deposition of $BC_{(nss)}$ 1990 – 1999

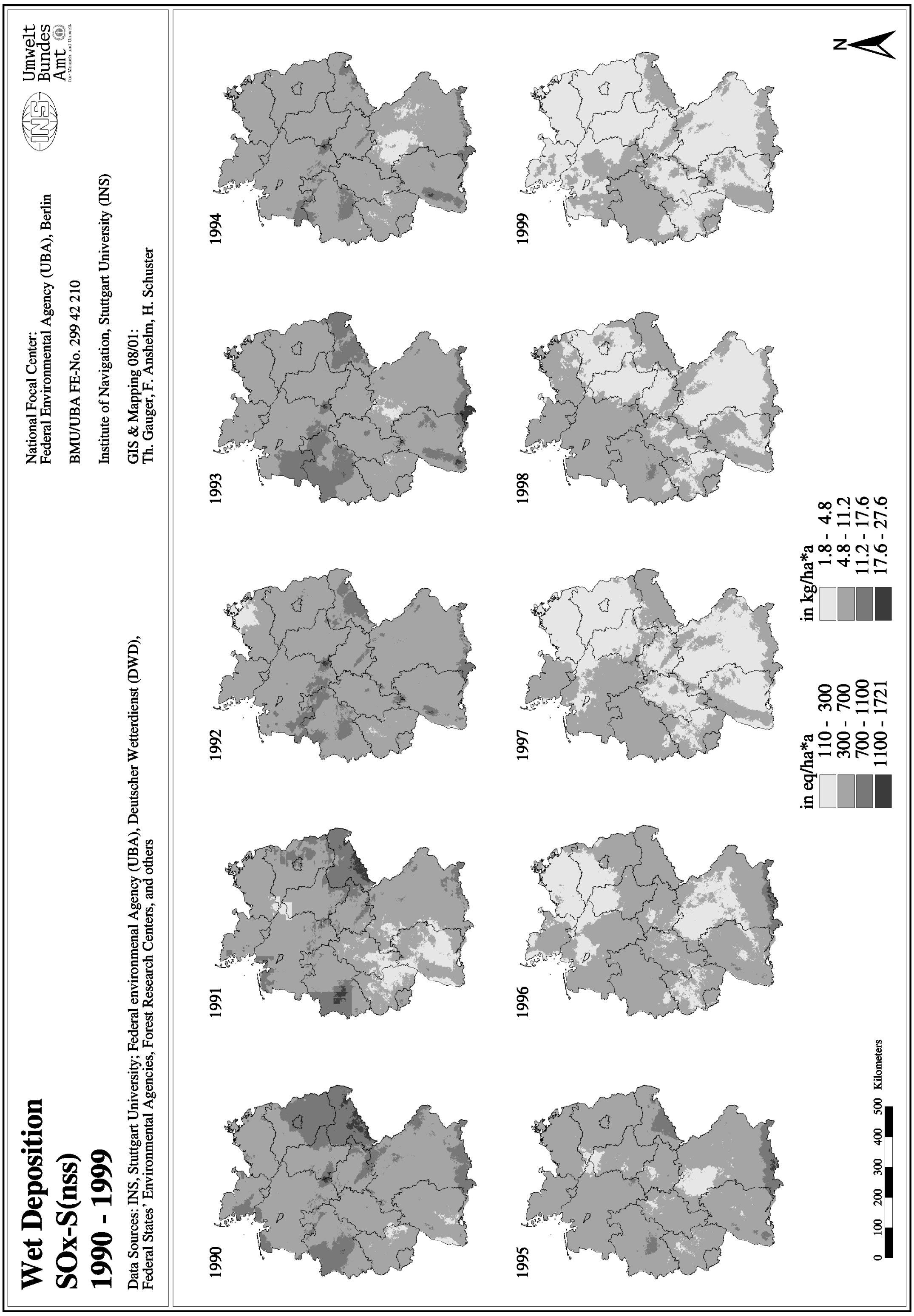

Map 4.7: Wet deposition of SO_X-$S_{(nss)}$ 1990 – 1999

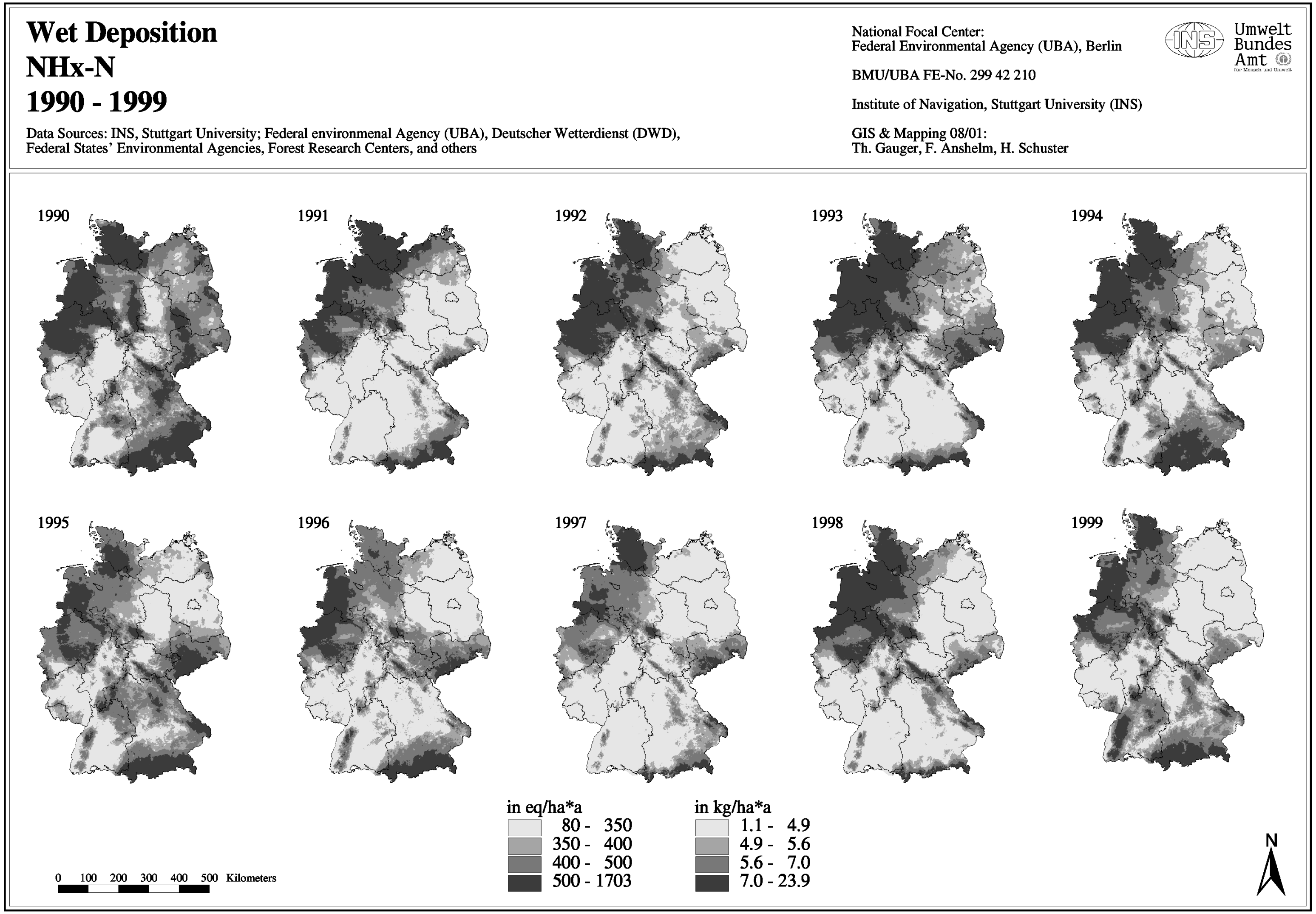

Map 4.8: Wet deposition of NH_X-N 1990 – 1999

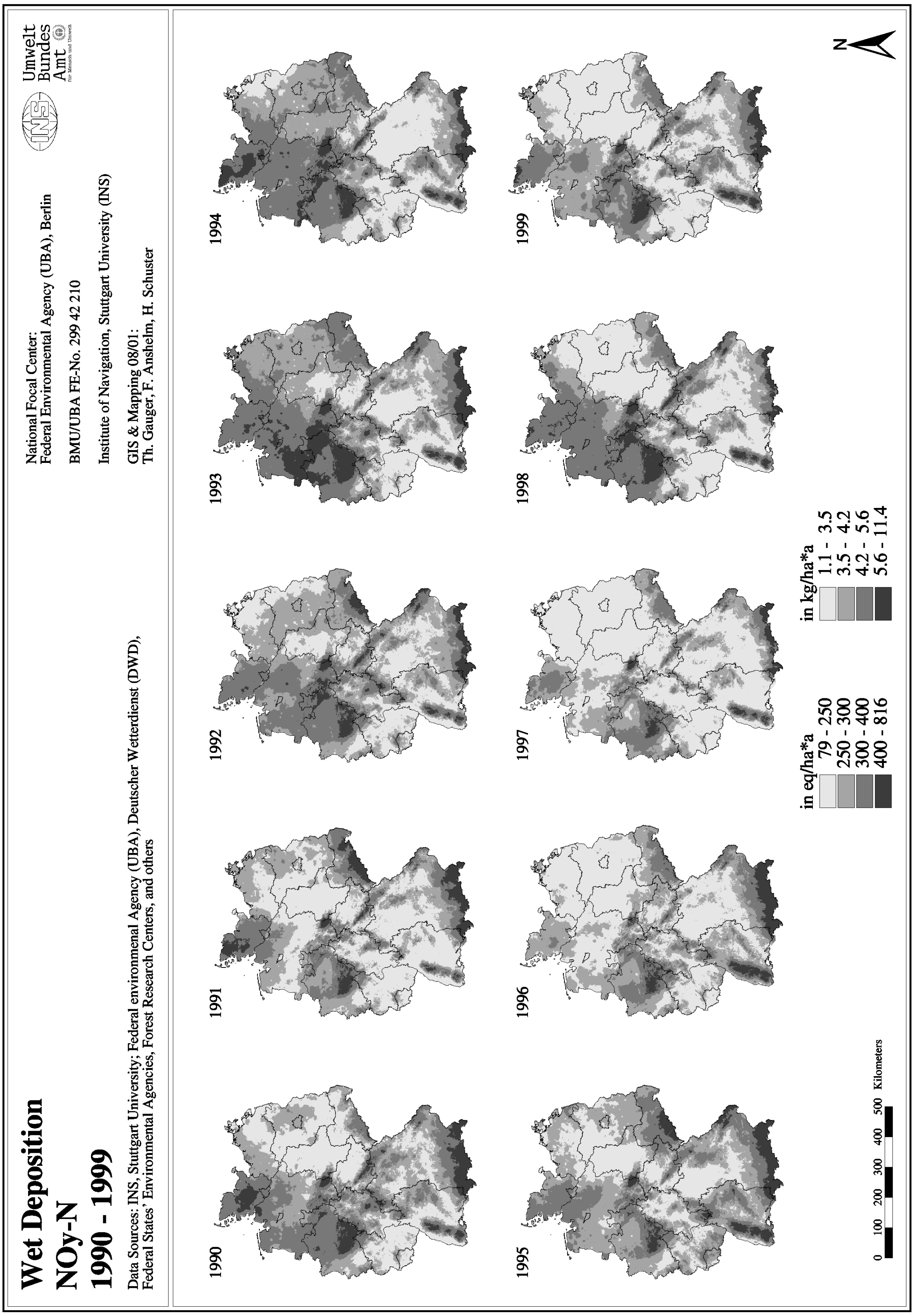

Map 4.9: Wet deposition of NO_Y-N 1990 – 1999

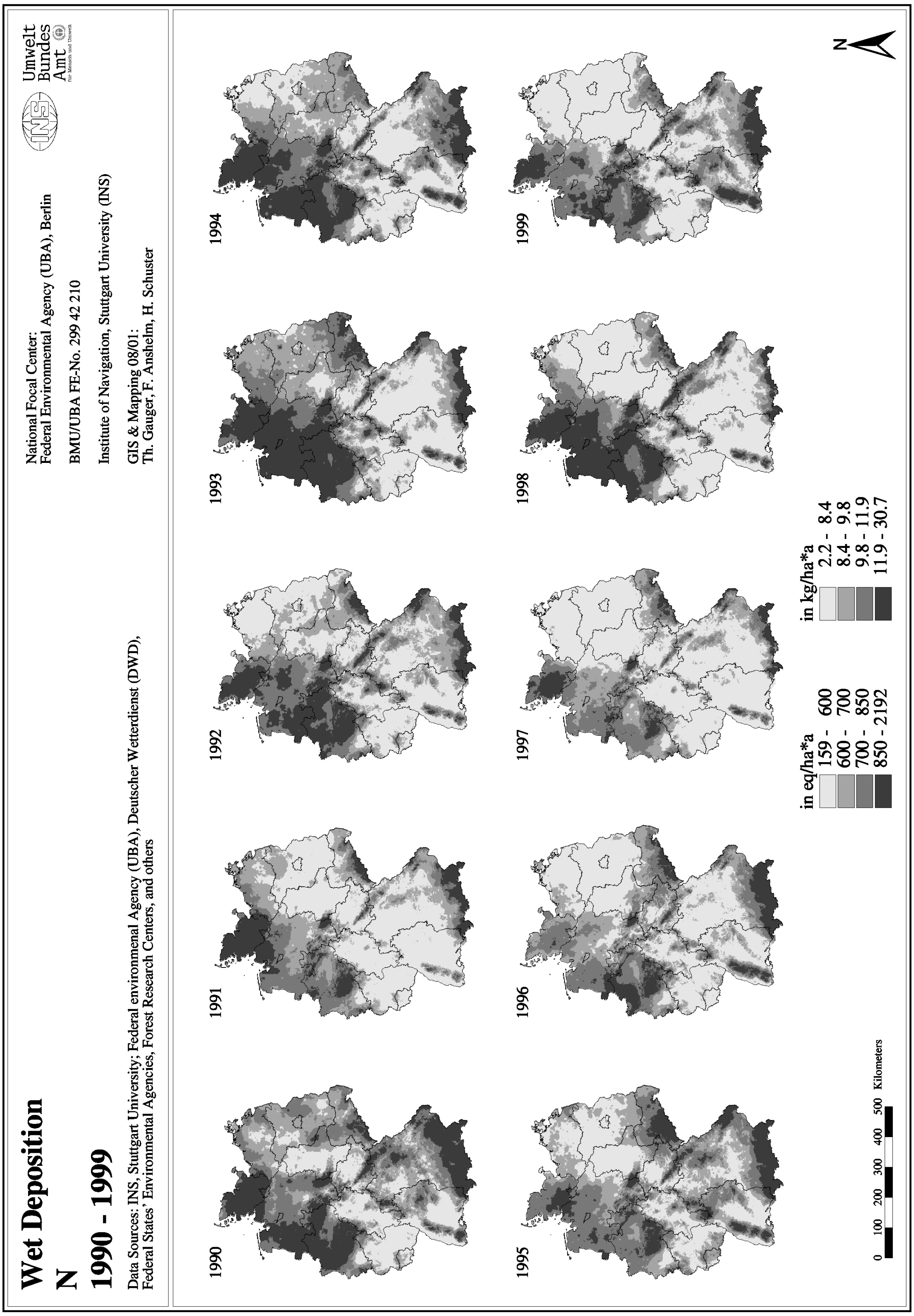

Map 4.10: Wet deposition of N 1990 – 1999

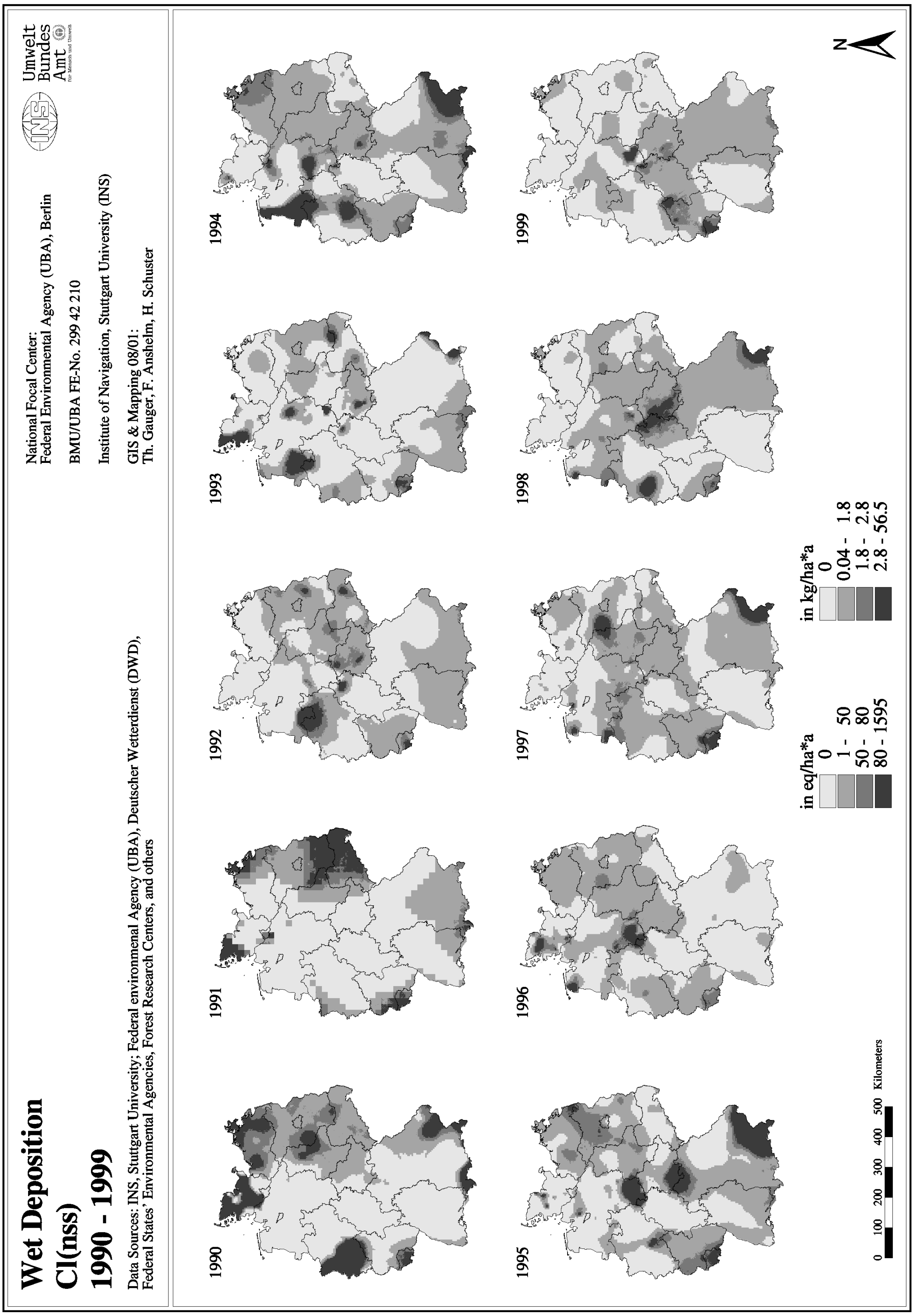

Map 4.11: Wet deposition of $Cl_{(nss)}$ 1990 – 1999

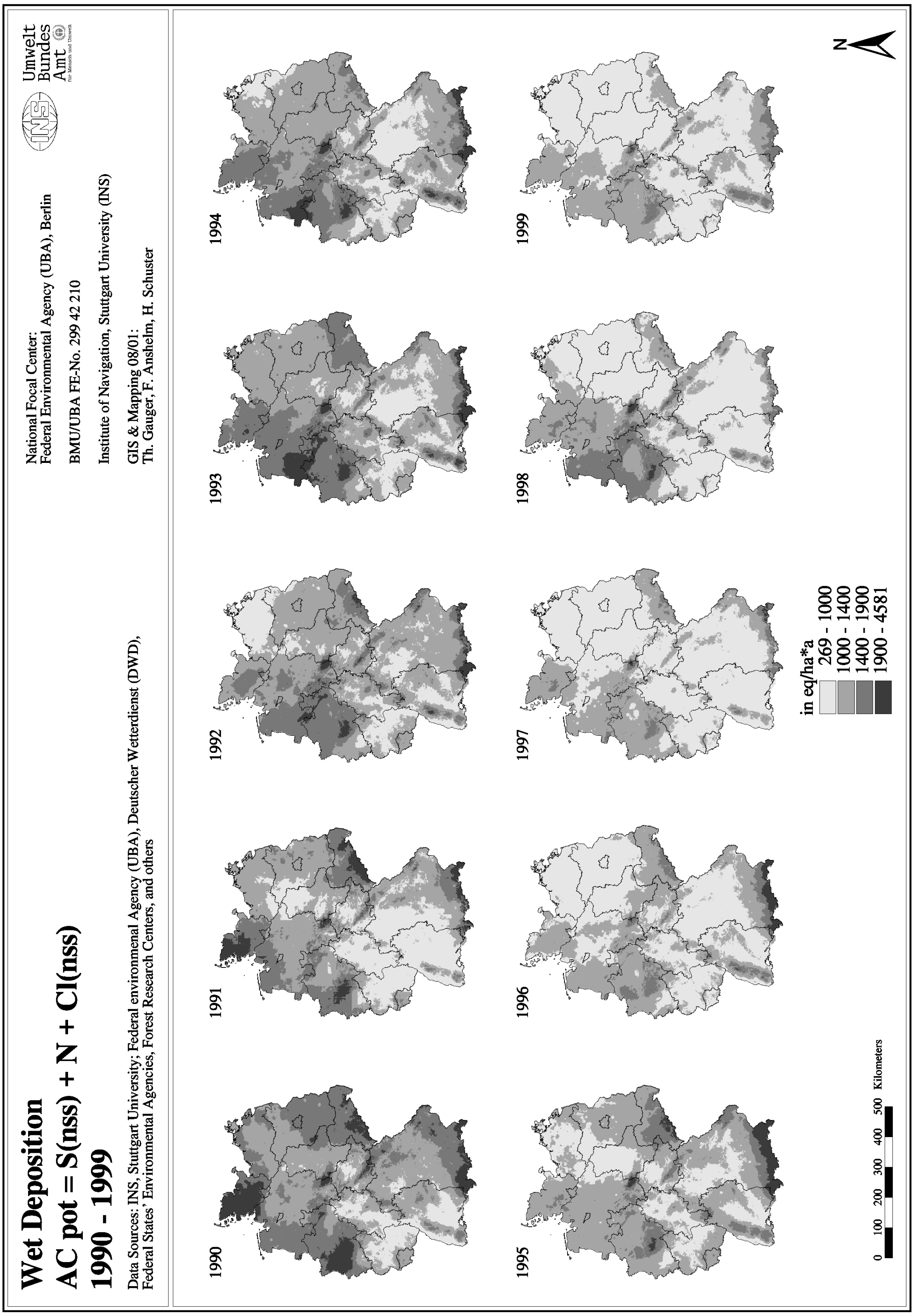

Map 4.12: Wet deposition of AC_{pot} 1990 – 1999

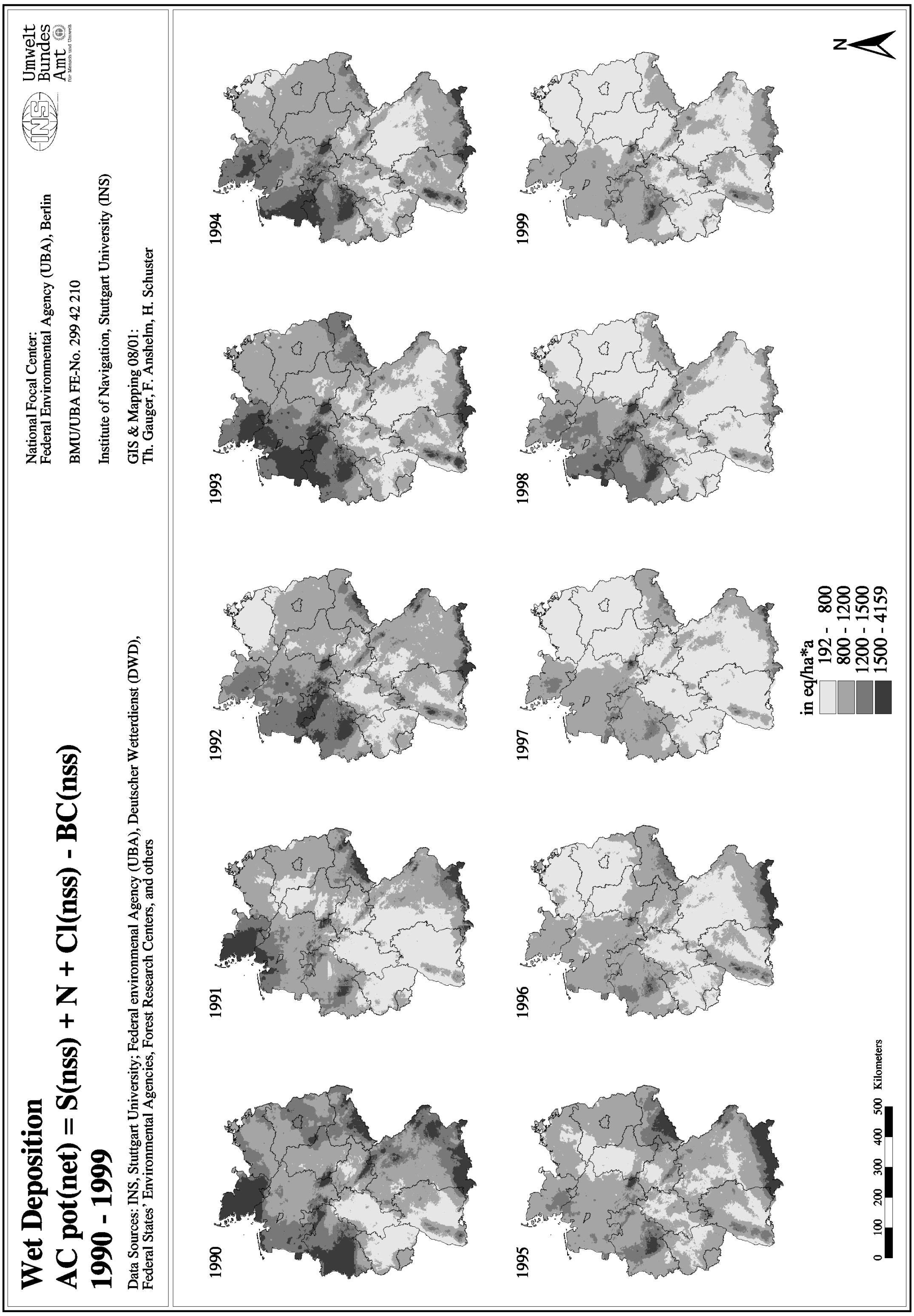

Map 4.13: Wet deposition of $AC_{pot(net)}$ 1990 – 1999

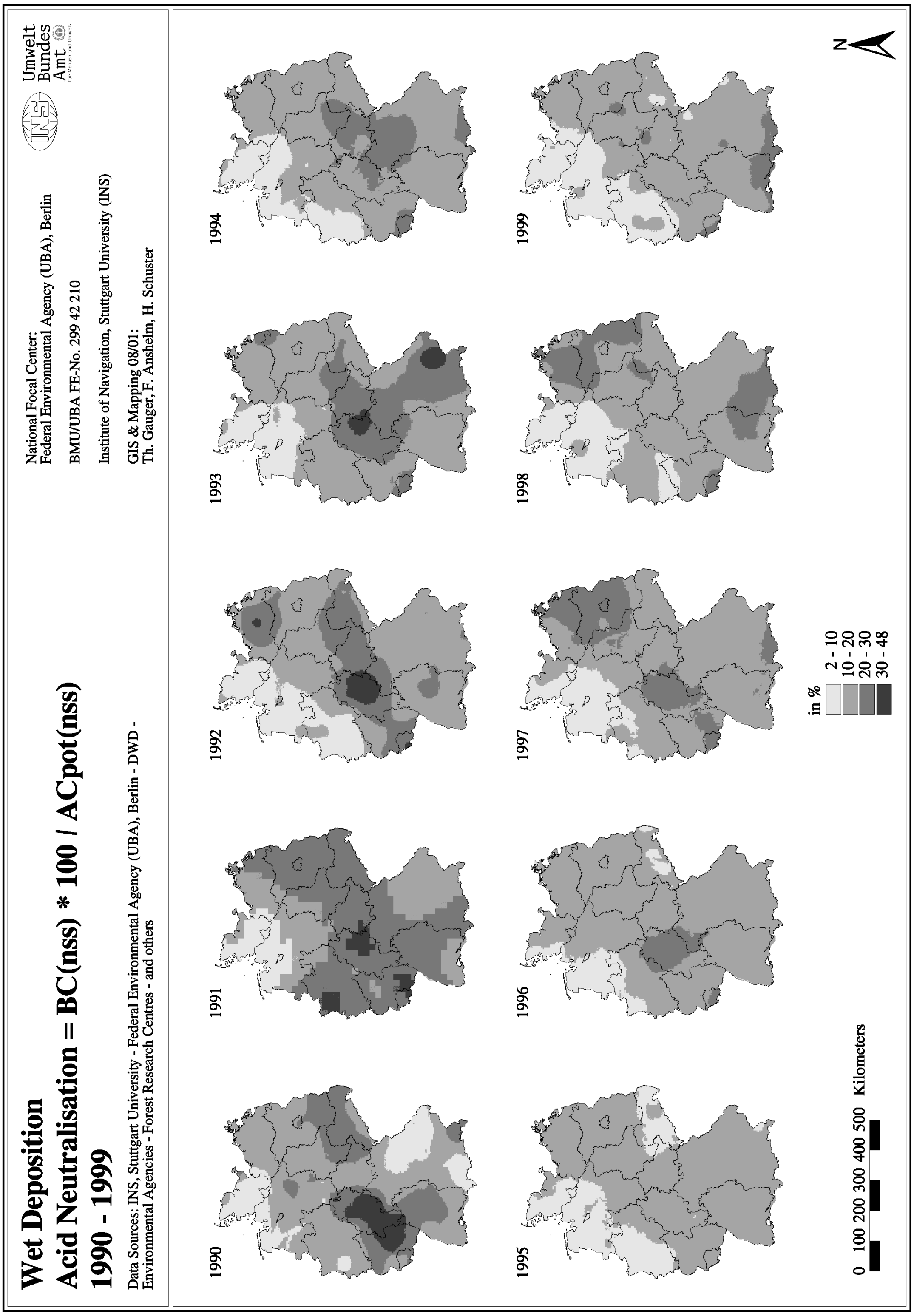

Map 4.14: Neutralisation of wet deposited AC_{pot} by $BC_{(nss)}$ 1990 – 1999

5 Mapping dry deposition

5.1 General

The dry deposition of the components considered in this project is calculated by a model called the Integrated DEposition Model (IDEM) using the so called dry deposition inference method (ERISMAN, 1992; ERISMAN & BALDOCCHI, 1994; VAN PUL ET AL, 1992, 1995). The dry deposition sub-model that was built into IDEM is based on the DEPAC module. DEPAC stands for DEPosition of Acidifying Components. The IDEM model is built around this dry deposition scheme and integrates the retrieval of spatial data concerning land use etc., and time dependent data like meteorological and concentration data with the deposition calculations. The method followed is roughly the same as in the EDACS model that was used in a previous project (VAN PUL, 1995; BLEEKER ET AL., 2000), except for usage of different and higher resolution meteorological and modelled concentration data, some small changes and corrections in DEPAC, and the added integrative viewer program to enable dissemination of the calculated data on CD. The outline of the IDEM model is presented in Figure 5.1.

Dry deposition fluxes are calculated in IDEM by calculation of dry deposition velocities and applying these on modelled concentrations for the same height. In the inference method it is assumed that a constant flux layer exists between a reference height and the surface. To fulfil this condition air and surface layer need to be in equilibrium, no chemical reactions take place in the surface layer and no advection is present. Only then is the deposition flux at the reference height equal to that at the surface. The reference height has to be chosen so that it lies within the surface layer and that the concentration at that height is not severely influenced by local deposition, so that using concentration data from a relatively coarse resolution model or measurement network is allowed. In IDEM and EDACS the reference height is taken at 50m above ground level (ERISMAN, 1992).

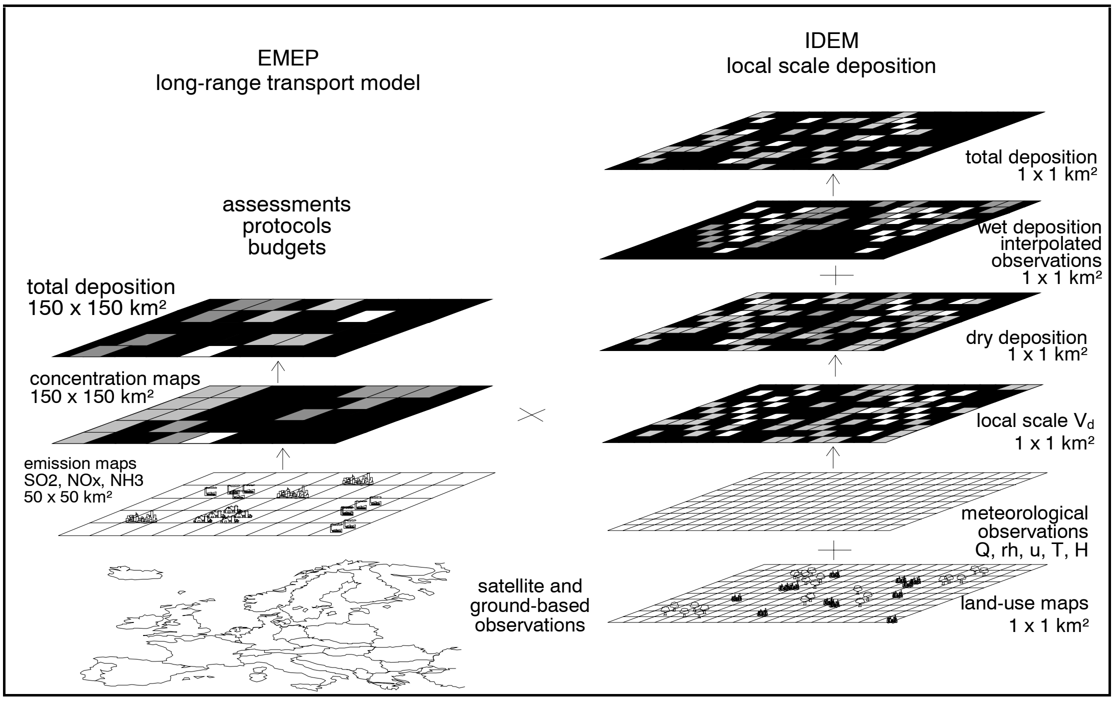

Figure 5.1: Outline of the EMEP and IDEM model (from BLEEKER ET AL. 2000, modified)

5.1.1 IDEM Domain

The IDEM model domain for the calculations described in this report was a 1x1km² grid covering Germany. The grid consists of 750 data points in West-East direction and 1000 data points in North-South direction. IDEM was provided with land use data and data describing the German Federate State ('Bundesland') for each pixel. The 6 land-use classes that were used, and the corresponding roughness lengths used per land use class are explained in Table 5.1. The regional average tree heights ('TH') used to calculate roughness lengths of forests is listed in Table 5.2.

Table 5.1: IDEM land use types

Land use type	Roughness length (m)		Canopy height (m)
	summer	winter	
Arable (agriculture)	0.1	0.05	0.5
Coniferous forest	0.085 x TH*		see Table 5.2
Deciduous forest	0.06 x TH*	0.09 x TH*	see Table 5.2
Mixed forest	0.085 x TH*		see Table 5.2
Water	0.0002		n.a.
Urban	1.0		n.a.

* TH = Tree Height (m); n.a. = not available

Table 5.2: Average tree height per tree type and per Bundesland

Bundesland	Deciduous	Coniferous	Mixed
Brandenburg	19.3	14.6	15.3
Mecklenburg-Vorpommern	21.0	16.8	18.4
Sachsen	17.1	15.2	15.6
Sachsen-Anhalt	19.6	15.2	16.6
Thuringen	21.1	16.4	17.9
Schleswig-Holstein	19.3	16.4	18.0
Niedersachsen	17.7	14.8	15.9
Saarland	17.8	17.8	17.7
Rheinland-Pfalz	18.6	18.4	18.5
Hessen	21.8	19.8	20.8
Baden-Wurtemberg	21.6	22.1	21.7
Bayern	18.2	21.0	20.2
Nordrhein-Westphalen	18.7	17.4	18.1
Germany average	19.4	17.4	18.0

In Figure 5.2 the land use categories on the 1x1km² grid over Germany are shown.

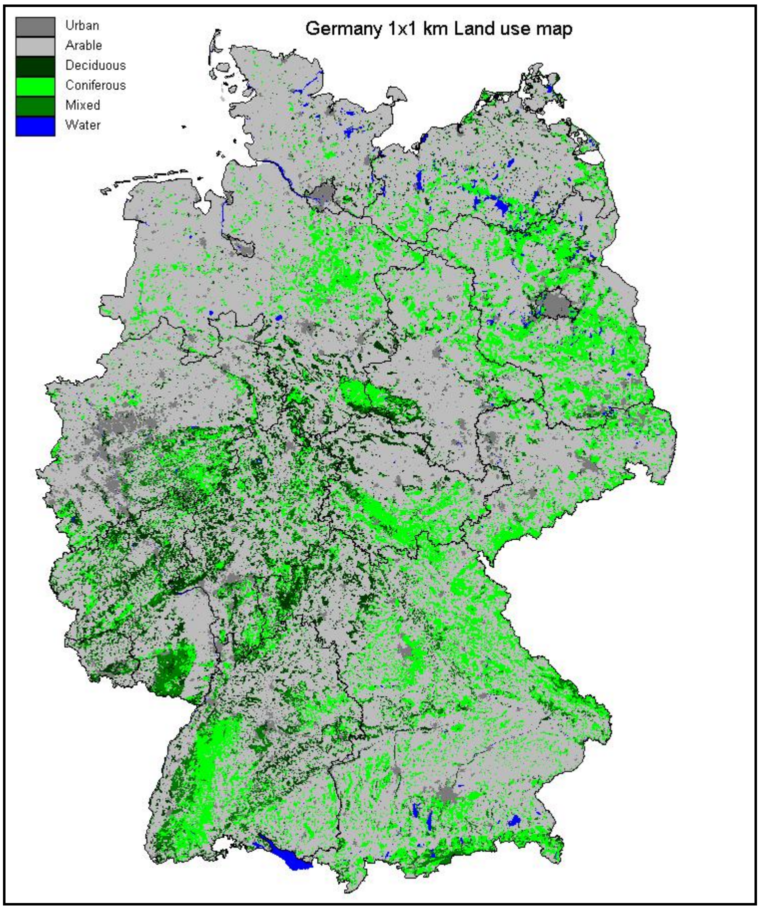

Figure 5.2: Land use categories on the 1x1km² grid over Germany (source: CORINE LAND COVER)

5.1.2 IDEM Components

In IDEM the dry deposition velocities are calculated for the following components:

- Ammonia; NH_3
- Ammonium; NH_4
- Sulphur dioxide; SO_2
- Sulphate (aerosol); SO_4
- Nitrogen monoxide; NO
- Nitrogen dioxide; NO_2
- Nitric Acid; HNO_3
- Nitrate aerosol; NO_3
- Base Cations; Na, Mg, Ca, K

The following definitions are used for certain groups of components:

- **NO_Y** = $NO+NO_2+HNO_3+NO_3$
- **NH_X** = NH_3+NH_4
- **SO_X** = SO_2+SO_4
- **Potential Acid** = $NO_Y+NH_X+SO_X$
- **BC** = Ca+K+Mg

5.1.3 IDEM meteorological input

IDEM requires detailed meteorological input data. In the calculations described in this report, data was used from the ECMWF MARS (European Centre for Medium-Range Weather Forecasts Meteorological Archival Retrieval System) [http://www.ecmwf.int/] database. For the years 1985 and 1990-1994 re-analysed data was used. For the further period (1995-1999) the re-analysed data was not yet available, so the standard analysed fields from the MARS database were used. The resolution of the data is 0.5 by 0.5 degree longitude and latitude. The time interval between the records is six hours. The data is stored in so called GRIB (GRId in Binary format) files. IDEM accesses these GRIB files directly using text index files to locate the requested data in the compressed binary GRIB data files. The de-assimilation of assimilated analysed data in the ECMWF databases is carried out by slightly modified software provided by Paul James [http://www.forst.tu-muenchen.de/EXT/LST/METEO/stohl/flextra/ecmwf_extr.html]. The data fields required by IDEM are listed in Table 5.3.

Table 5.3: IDEM required fields in meteorological input

Abbreviation	***Description***	***Abbreviation***	***Description***
WU	Wind speed in EW direction at 10 m	**LSP**	Large scale precipitation
WV	Wind speed in NS direction at 10 m	**SD**	Snow depth
MSL	Atmospheric pressure at surface level	**GLRad**	Global radiation
T2	Temperature at 2 m height	**TCC**	Total Cloud Cover
HF	Sensible Heat flux	**SSWE**	Surface stress in WE direction
TS	Soil temperature	**SSNS**	Surface stress in NS direction
CVP	Convective precipitation		

Atmospheric stability is determined by mechanically induced turbulence caused by the friction of wind at the surface and thermally induced turbulence caused by cooling or heating of the surface by exchange of long wave (infrared) radiation. The thermal turbulence is expressed as a function of the sensible heat flux (HF), the mechanical turbulence is expressed as a function of the friction velocity (u^*). It is possible to derive the atmospheric stability from the ECMWF input, as this contains values for both Sensible Heat flux and friction velocity (through SSWE, SSNS; cf. Table 5.3). The values obtained are, however, values that are representative for the 0.5 by 0.5 degree grid cell. In IDEM we derive from wind speed, cloud cover, radiation and local surface roughens a localised version of the energy balance on the 1x1km^2 grid and use this in the dry deposition calculation scheme. The surface energy budget scheme from Beljaars & Holtslag (1990) is used in an optimised version. This leads to a presumably much higher accuracy then using the ECMWF values.

The IDEM model interpolates all meteorological data to the 1x1km^2 grid using weighted distance averaging. This avoids visual block effects in some of the calculated data when sharp gradients in for example wind speed exist between 0.5x0.5 degree meteo grid data cells.

5.1.4 IDEM Concentration input

The model can use concentration data in the latitude-longitude projection as well as in the EMEP projection. For the years 1985 and 1990-1996 data was obtained from EMEP, calculated using the EMEP Lagrangian transport model (Sandnes, 1993). The EMEP data has a resolution of 150x150km^2 and uses a special EMEP projection method.

For the years 1990 and 1996-2000 concentration data became available from NERI, calculated using the DEM model (1990, 1996-1998) and the DEHM model (1999 and further), with a data resolution of 0.5 by 0.5 degree. Both NERI models are Eulerian models.

Also the concentration data can be and is for the calculations in this report interpolated to the 1x1km^2 grid using weighted distance averaging. The concentration data is used by IDEM in the same native binary format in which the input files were provided by EMEP and NERI, respectively. The latter uses the Grid Analysis and Display System (GrADS) binary format [http://grads.iges.org/grads/grads.html].

5.1.5 IDEM Dry Deposition Module: DEPAC

The approach followed in this project for estimating dry deposition velocity involves using larger scale atmospheric models and gridded fields of surface meteorological data to produce a regular grid of deposition velocity values.

Air quality models used to study acid deposition and photochemical oxidants contain modules to estimate dry deposition velocities. Wesely (1989) and Walmsley & Wesely (1996) described the model used within RADM (Regional Acid Deposition Model; Chang et al., 1987), Padro et al. (1991) evaluated the model included in ADOM (Acid Deposition and Oxidant Model; Pleim et al., 1984; Venkatram et al., 1988) and Voldner et al. (1986) developed a dry deposition parameterisation for use in the Canadian Lagrangian acid deposition model. The ADOM and RADM dry deposition modules have appeared in several applications. For example, the RADM module has been adapted for the California Institute of Technology photochemistry airshed model (Harley et al., 1993), the Urban Airshed Model (UAM; SAI, 1996), studies involving the California Ozone Deposition Experiment (CODE; Massman et al., 1994; Pederson et al., 1995), the Global CHemistry Model (GChM; Leucken et al., 1991; Benkovitz et al., 1994), and EURopean Air Pollution Dispersion model system in western Europe (EURAD; Hass et al., 1995). The ADOM module has, for example, been used in the CALGRID photochemical oxidant model (Yamartino et al., 1992).

Several models have been developed in Europe. Van Pul et al. (1995) described a model, EDACS (European Deposition of Acidifying Components on Small scale), that has been developed for routine estimates of dry deposition across a regular grid covering Europe. Meteorological inputs for this model are derived through interpolation of surface meteorological observations and land-use data that are provided on a 10x20km^2 grid. This work represents the first attempt to apply a model for routine estimation of spatially (1/6^{o}x1/6^o) and temporally (6h) resolved dry deposition that is suitable for combination with wet deposition measurements for determination of annual total deposition. EDACS and the Dutch Empirical Acid Deposition Model (DEADM) have been used with long-range modules to map modelled deposition amounts for sulphur and nitrogen compounds (e.g., ERISMAN & DRAAIJERS, 1995). Concern over the accuracy of estimates of particulate deposition have led to several experimental efforts (e.g., ERISMAN ET AL., 1997). In addition, dry deposition routines for general circulation models coupled with chemistry modules have been carried out for the European Centre HAmburg Model (ECHAM; GANZEVELD & LELIEVELD, 1995).

In areas that contain sharp contrasts in surface characteristics, edge effects, and hilly terrain, the assumptions inherent in the micrometeorological formulations that are commonly used in large-scale and site-specific models are questionable. In mountainous terrain or where patchy forest conditions exist, the approach of measuring the amounts and chemical composition of throughfall and stemflow in forests at specific sites is considered more reliable for some substances, especially sulphur, than the micrometeorological methods (DRAAIJERS ET AL., 1994; LOVETT, 1994; VELTKAMP & WYERS, 1997).

5.1.6 Theory of dry deposition parameterisation

Several articles have reviewed the state of the science in evaluating dry deposition (BALDOCCHI, 1993; ERISMAN ET AL., 1994B; ERISMAN & DRAAIJERS, 1995; RUIJGROK ET AL., 1995; WESELY & HICKS, 2000). WESELY AND HICKS (2000) indicated that although models have been improving and can perform well at specific sites under certain conditions, there remain many problems and more research is needed. In spite of these problems, given the necessary meteorological and surface/vegetative data, there are a number of models for estimating deposition velocity (V_d) that have been shown to produce reasonable results using currently available information.

Dry deposition processes for gaseous species are generally understood better than for particles. Several dry deposition model formulations have been reported in the literature. These include big-leaf models (HICKS ET AL., 1987; BALDOCCHI ET AL., 1987), multi-layer models (BALDOCCHI, 1988; MEYERS ET AL., 1998) and general dry deposition models (ERISMAN ET AL., 1996). Some of these models have been developed for estimating V_d at specific sites and are used within the framework of monitoring networks (CLARKE ET AL., 1997; MEYERS ET AL., 1991).

Computation of the dry deposition rate of a chemical species requires that the concentration c of the substance of interest is known through model computations or measurement. In most modelling schemes, the mass flux density F is found as

$$F = -V_d(z) \cdot c(z) \tag{5.1}$$

where $c(z)$ is the concentration at height z and V_d is the dry deposition velocity. Estimates of deposition velocities V_d constitute the primary output of dry deposition models, both for large-scale models and site-specific methods of inferring dry deposition from local observations of concentrations, meteorological conditions, and surface conditions (CHANG ET AL., 1987; VENKATRAM ET AL., 1988; MEYERS ET AL., 1991; GANZEVELD AND LELIEVELD, 1995). z is the reference height above the surface. If the surface is covered with vegetation, a zero-plane displacement is included: $z=z-d$. d is usually taken as 0.6-0.8 times the vegetation height (THOM, 1975). The absorbing surface is often assumed to have zero surface concentration and the flux is therefore viewed as being linearly dependent on atmospheric concentration. This holds only for depositing gases and not for gases that might be also emitted, such as NH_3 and NO. For these gases a nonzero surface concentration, a compensation point c_p, might exist, which can be higher than the ambient concentration, in which case the gas is emitted. For these gases the flux is estimated as

$$F = -V_d(z) \cdot [c(z) - c_p] \tag{5.2}$$

V_d provides a measure of conductivity of the atmosphere-surface combination for the gas and it is widely used to parameterise gas uptake at the ground surface (WESELY & ., 1977; HICKS ET AL., 1989; FOWLER ET AL., 1989). To describe the exchange of a range of gases and particles with very different chemical and physical properties, a common framework is provided, the resistance analogy (THOM, 1975; GARLAND, 1977; WESELY & HICKS, 1977; FOWLER, 1978; BALDOCCHI ET AL., 1987). In this framework, V_d is calculated as the inverse of three resistances:

$$V_d(z) = \frac{1}{R_a(z-d) + R_b + R_c} \qquad (5.3)$$

The three resistances represent bulk properties of the lower atmosphere or surface. R_a, R_b and R_c must be described by parameterisations. Although this approach is practical, it can lead to over-simplification of the physical, chemical, and biological properties of the atmosphere or surface that affect deposition.

The term R_a represents the aerodynamic resistance above the surface for the turbulent layer. R_a is governed by micrometeorological parameters and has the same value for all substances. R_a depends mainly on the local atmospheric turbulence intensities. Turbulence may be generated through mechanical forces of friction with the underlying surface (forced convection) or through surface heating (buoyancy or free convection). Unless wind speed is very low, free convection is small compared to mechanical turbulence.

The term R_b represents the quasi-laminar resistance to transport through the thin layer of air in contact with surface elements, and is governed by diffusivity of the gaseous species and air viscosity. For surfaces with bluff roughness elements, values of R_b are considerably larger than for relatively permeable, uniform vegetative cover, and the appropriate formulations should be used (TUOVINEN ET AL., 1998).

Considerable variation from model to model is associated with the methods used to evaluate the surface or canopy resistance R_c for the receptor itself. R_c represents the capacity for a surface to act as a sink for a particular pollutant, and depends on the primary pathways for uptake such as diffusion through leaf stomata, uptake by the leaf cuticular membrane, and deposition to the soil surface. This makes R_c complicated, because it depends on the nature of the surface and how the sink capacities for specific surfaces vary as a function of the local microclimate.

The resistance analogy is not used for particles. For sub-micron particles, the transport through the boundary layer is more or less the same as for gases. However, transport of particles through the quasi-laminar layer can differ. Whereas gases are transported primarily through molecular diffusion, particle transport and deposition basically take place through sedimentation, interception, impaction and/or Brownian diffusion. Sedimentation under the influence of gravity is especially significant for receptor surfaces with horizontally oriented components. Interception occurs if particles moving in the mean air motion pass sufficiently close to an obstacle to collide with it. Like interception, impaction occurs when there are changes in the direction of airflow, but unlike interception a particle subject to impaction leaves the air streamline and crosses the laminar boundary layer with inertial energy imparted from the mean airflow. The driving force for Brownian diffusion transport is the random thermal energy of molecules. Transport is a function of atmospheric conditions, characteristics of the depositing contaminant and the magnitude of the concentration gradient over the quasi-laminar layer (DAVIDSON AND WU, 1990).

Which type of transport process dominates is largely controlled by the size distribution of the particles (SEHMEL, 1980; SLINN, 1982). For particles with a diameter <0.1µm, deposition is controlled by diffusion, whereas deposition of particles with a diameter >10µm is more controlled by sedimentation. Deposition of particles with a diameter between 0.1 and 1µm is determined by the rates of impaction and interception and depends heavily on the turbulence intensity. To describe particle dry deposition, the terms $(R_b+R_c)^{-1}$ on the right-hand side of Equation (5.3) must be replaced with a surface deposition velocity or conductance, and gravitational settings must be handled properly.

Dry deposition models or modules require several types of inputs from observations or from simulations of atmospheric chemistry, meteorology, and surface conditions. To compute fluxes, the concentrations of the substances must be known. Inputs required from meteorological models are values of friction velocity u^*, atmospheric stability via the Monin-Obukhov length scale L, aerodynamic surface roughness z_0, and aerodynamic displacement height d. Most dry deposition models also need solar radiation or, preferably, photosynthetically active radiation; ambient air temperature at a specified height; and measures of surface wetness caused by rain and dewfall. All models require a description of surface conditions, but the level of detail depends on the model chosen. Descriptions could include broad land use categories, plant species, leaf area index (LAI), greenness as indicated by the normalised difference vegetation index, various measures of plant structure, amount of bare soil exposed, and soil pH.

5.1.7 Description of the land use information

The deposition velocity for each chemical species can differ by close to an order of magnitude between some landuse classes. In the daytime, SO_2 and O_3 have higher deposition velocities over surface types or canopy types with large leaf area indices (LAIs) due to uptake through the leaf stomata. This uptake is greater in the summer or growing season compared to the autumn. The effect of canopy wetness on dry deposition velocities can be significant. Surface roughness also has an important role due to its influence on aerodynamic resistance. This is particularly noticeable for HNO_3 and SO_4^{2-}, for which stomata opening and closing is not important.

5.1.8 Aerodynamic and Quasi-laminar Boundary Layer Resistances

The atmospheric resistance to transport of gases across the constant flux layer is assumed to be similar to that of heat (e.g., HICKS ET AL., 1989). R_a is approximated following the procedures used by GARLAND (1978):

$$R_a(z-d)=\frac{1}{\kappa\cdot u^*}\cdot\left[\ln\left(\frac{z-d}{z_o}\right)-\psi_h\left(\frac{z-d}{L}\right)+\psi_h\left(\frac{z_o}{L}\right)\right] \tag{5.4}$$

in which κ is the Von Karman constant (0.4), u^* is the friction velocity, which is calculated from the output of the meteorological model, L is the Monin-Obukhov length, d is the displacement height and z_0 is the roughness length, which is defined independently for each land use and season category. $\psi_h[(z-d)/L]$ is the integrated stability function for heat. These can be estimated using procedures described in BELJAARS AND HOLTSLAG (1990). Under the same meteorological conditions, the aerodynamic resistance is the same for all gases and in fact also for aerosols. Only for aerosols with a radius > 5µm does the additional contribution of gravitational settling become significant. When the wind speed increases, the turbulence usually increases as well and consequently R_a becomes smaller.

The second atmospheric resistance component R_b is associated with transfer through the quasi-laminar layer in contact with the surface. The transport through the laminar boundary layer takes place for gases by molecular diffusion and for particles by several processes: Brownian diffusion, interception, impaction and by transport under influence of gravitation. None of the processes for particles are as efficient as the molecular diffusion of gas molecules. This is because molecules are much smaller than aerosols and therefore have much higher velocities. For particles with radii <0.1µm Brownian diffusion is the most efficient process, whereas impaction and interception are relatively important for those with radii >1µm. For particles with radii between 0.1 and 1µm the transport through the laminar boundary layer is slowest (R_b is largest). The laminar boundary layer resistance is for most surface types more or less constant (forest, at sea for a wind speed < 3m/s) or decreases with wind speed (low vegetation).

R_b quantifies the way in which pollutant or heat transfer differs from momentum transfer in the immediate vicinity of the surface. The quasi-laminar layer resistance R_b can be approximated by the procedure presented by HICKS ET AL. (1987):

$$R_b = \frac{2}{\kappa \cdot u_*} \cdot \left(\frac{Sc}{\Pr} \right)^{2/3} \tag{5.5}$$

where Sc and Pr are the Schmidt and Prandtl number, respectively. Pr is 0.72 and Sc is defined as $Sc = \upsilon / D_i$, with υ being the kinematic viscosity of air (0.15 cm^2 s^{-1}) and D_i the molecular diffusivity of pollutant i and thus component specific. The Schmidt and Prandtl number correction in the equation for R_b is listed in Table 5.4 for different gases. Molecular and Brownian diffusivities for a selected range of pollutants, and the deduced values of Schmidt number are listed in Table 5.5. Usually R_b values are smaller than R_a and R_c. Over very rough surfaces such as forest canopies, however, R_a may approach small values and the accuracy of the R_b estimate becomes important. This is especially the case for trace gases with a small or zero surface resistance.

Table 5.4: Schmidt and Prandtl number correction in equation for R_b (HICKS ET AL., 1987) for different gaseous species, and the diffusion coefficient ratio of water to the pollutant i (PERRY, 1950).

Component	$D^*_{H_2O} / D_i$	**(Sc/Pr)$^{2/3}$**
SO_2	1.9	1.34
NO	1.5	1.14
NO_2	1.6	1.19
NH_3	1	0.87
HNO_2	1.7	1.24
HNO_3	1.9	1.34
HCl	1.5	1.14
PAN	2.8	1.73
H_2O	1	0.87
O_3	1.5	1.14

$^* D_{H_2O} = 2.27 \cdot 10^{-5} m^2 s^{-1}$

Table 5.5: Molecular (for gases) and Brownian (for particles) diffusivities (D; $cm^2\ s^{-1}$) for a range of pollutants, and the deduced values of Schmidt number (Sc). The viscosity of air is taken to be 0.15 $cm^2\ s^{-1}$. From HICKS ET AL. (1987).

Component	***D***	***Sc***
Gaseous species		
H_2	0.67	0.22
H_2O	0.22	0.68
O_2	0.17	0.88
CO_2	0.14	1.07
NO_2	0.14	1.07
O_3	0.14	1.07
HNO_3	0.12	1.25
SO_2	0.12	1.25
Particles (unit density)		
0.001 µm radius	$1.28\ 10^{-2}$	$1.17\ 10^{1}$
0.01	$1.35\ 10^{-4}$	$1.11\ 10^{3}$
0.1	$2.21\ 10^{-6}$	$6.79\ 10^{4}$
1	$1.27\ 10^{-7}$	$1.18\ 10^{6}$
10	$1.38\ 10^{-8}$	10^{7}

5.1.9 Surface resistance parameterisation for gases

The surface or canopy resistance R_c is the most difficult of the three resistances to describe, and is often the controlling resistance of deposition flux. The analytical description of R_c has been difficult since it involves physical, chemical and biological interaction of the pollutant with the deposition surface. Over a given area of land, numerous plant, soil, water, and other material surfaces are present, each with a characteristic resistance to uptake of a given pollutant.

R_c values presented in the literature are primarily based on measurements of V_d and on chamber studies. By determining R_a and R_b from the meteorological measurements, R_c can be calculated as the residual resistance. Values of R_c can then be related to surface conditions, time of day, etc., yielding parameterisations. However, measurements using existing techniques are still neither accurate nor complete enough to obtain R_c values under most conditions. Furthermore, R_c is specific for a given combination of pollutants, type of vegetation and surface conditions, and measurements are available only for a limited number of combinations.

The surface resistance of gases consists of other resistances (Figure 5.3), either determined by the actual state of the receptor, or by a memory effect. R_c is a function of the canopy stomatal resistance R_{stom} and mesophyll resistance R_m; the canopy cuticle or external leaf resistance R_{ext}; the soil resistance R_{soil} and in-canopy resistance R_{inc}, and the resistance to surface waters or moorland pools R_{wat}. In turn, these resistances are affected by leaf area, stomatal physiology, soil and external leaf surface pH, and presence and chemistry of liquid drops and films. Based on values from the literature for the stomatal resistance (WESELY, 1989), and on estimated values for wet (due to rain and to an increase in relative humidity) and snow-covered surfaces, the following parameterisation (with the stomatal resistance, external leaf surface resistance and soil resistance acting in parallel) can be applied for routinely measured components (ERISMAN ET AL., 1994b):

vegetative surface:

$$R_c = \left[\frac{1}{R_{stom} + R_m} + \frac{1}{R_{inc} + R_{soil}} + \frac{1}{R_{ext}} \right]^{-1} \tag{5.6}$$

water surfaces:

$$R_c = R_{wat} \tag{5.7}$$

bare soil:

$$R_c = R_{soil} \tag{5.8}$$

snow cover:

$$R_c = R_{snow} \tag{5.9}$$

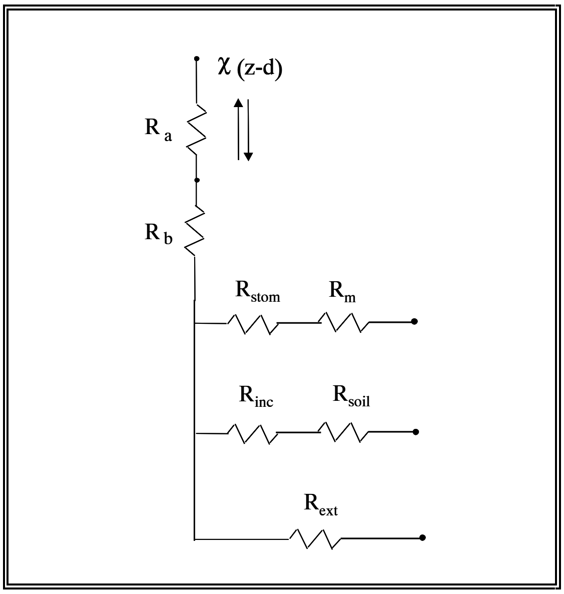

Figure 5.3: Resistance analogy approach in dry deposition models.

Table 5.6 shows some surface resistance values for soil surfaces (R_{soil}), snow-covered surfaces (R_{snow}) and water surfaces (R_{wat}).

Table 5.6: Surface resistance values (s m^{-1}) for soil surfaces (R_{soil}), snow-covered surfaces (R_{snow}) and water surfaces (R_{wat}). From ERISMAN ET AL. (1994B).

Gas	Soil surfaces, R_{soil}		Water surfaces,	Soil or water	Snow-covered surfaces	
	Wet	Dry	R_{wat}	pH	R_{snow}	Temperature (°C)
SO_2 and	0	1000	0	>4	70 (2-T)	-1<T<1
HNO_2	500	R_{ext}	500	<4	500	T<-1
	250	Emission:		>8	70 (2-T)	-1<T<1
NH_3	0	500	500	<8	500	T<-1
	emission:	50		----	2000	----
NO	1000	emission:	0	----	2000	----
NO_2 and	2000	1000	2000	>2	0	T>-5
PAN	0	1000	2000		100	T<-5
HNO_3 and		0	0	----	2000	----
HCl	500		2000			
O_3		100				

It is not clear whether R_m is relevant at ambient concentrations (ERISMAN ET AL., 1994b). Therefore, they consider the sum of R_{stom} and R_m to be a new resistance R_{st}, a stomatally controlled resistance which would equal the true stomatal resistance R_{stom} if $R_m=0$. Similarly, they defined a new resistance $R_{fs}=R_{inc}+R_{soil}$, a non-stomatal resistance to express that the uptake could be either direct foliage uptake or soil uptake. Thus, Equation (5.6) reduces to

$$R_c = \frac{R_{st} \cdot R_{fs}}{R_{st} + R_{fs}} \tag{5.10}$$

Combining equations (5.3) and (5.10) yields

$$\frac{1}{V_d} = R_a + R_b + \frac{R_{st} \cdot R_{fs}}{R_{st} + R_{fs}} \tag{5.11}$$

for daytime situations. During the night, when stomata are closed, $R_{st}=\infty$ is assumed and Equation (5.11) can be reduced to

$$\frac{1}{V_d} = R_a + R_b + R_{fs} \tag{5.12}$$

R_{cut} denotes local leaf cuticular resistance. In BROOK ET AL. (1999):

$$R_{cut}(SO_2) = R_{cut}(LUC, season); \quad (5.13)$$

$$R_{cut}(HNO_3) = 20\ sm^{-1}. \quad (5.14)$$

LUC denotes land use class. Under wet surface conditions after rainfall or dew R_{cut} is replaced by R_{wcut}, which denotes wet cuticle resistance. For SO_2, under wet/dew conditions it is assumed a constant value of 50 sm^{-1} for both dew-covered and rainfall conditions:

$$R_{wcut}(SO_2) = 50\ sm^{-1} \quad (5.15)$$

HNO_3 uptake is rapid regardless of wetness.

R_g denotes ground surface resistance, which varies depending upon whether the surface is soil, water or snow/ice and whether it is wet or dry.

$$R_g(SO_2) = 100\ sm^{-1} \quad (5.16)$$

$$R_g(HNO_3) = 20\ sm^{-1} \quad (5.17)$$

For all surface conditions (dry, wet or snow) a small value of 20 sm^{-1} is used for the ground resistance of HNO_3. For wet soil, a constant value of 100 sm^{-1} is used for SO_2. There is little information available for resistance over snow or ice surfaces. From the limited amount of data available (see BROOK ET AL., 1999) a value of 200 s m^{-1} is set for $R_g(SO_2)$ *for* snow covered surfaces:

$$R_g(SO_2) = 200\ sm-1 \quad (5.18)$$

5.1.9.1 Stomatal (R_{stom}) and mesophyll (R_m) resistances

Most gases enter plants through stomata. As gas molecules enter the leaf, deposition occurs as molecules react with the moist cells in the sub-stomatal cavity and the mesophyll. Stomatal resistance decreases hyperbolically with increasing light and increases linearly with increasing vapour pressure deficits (JARVIS, 1976). Soil water deficits cause stomata to close after some threshold deficit level is exceeded. Low and high temperatures cause stomatal closure; stomatal opening is optimal at a vegetation-specific temperature. Leaf age, nutrition and adaptation are other factors affecting stomatal resistance (JARVIS, 1976). Elevated exposure to SO_2 causes stomata to close, whereas exposure to both O_3 and NH_3 may increase stomatal opening. Stomatal resistance is different for different types of vegetation.

The stomatal resistance for water vapour, R_{stom}, is a function of the photosynthetically active radiation (*PAR*), air temperature (*T*), leaf water potential (ψ), vapour pressure deficit (*VPD*), and can be calculated using a scheme described by BALDOCCHI ET AL. (1987). This scheme is based on a model presented by JARVIS (1976) for the computation of the stomatal resistance to water vapour transfer of a leaf that is biologically and physically realistic. It is a multiplicative model which is expressed in terms of stomatal conductance (g_s), the inverse of R_{stom}. In this scheme the bulk leaf stomatal conductance is written as:

$$g_s = f(PAR) \cdot f(T) \cdot f(VPD) \cdot f(\psi) \tag{5.19}$$

Values of the functions $f(T)$, $f(\psi)$ and $f(VPD)$ range from 0 to 1. $f(PAR)$ is the influence of photosynthetically active radiation on the stomatal conductance, and depends on the LUC-dependent parameters of the minimum stomatal resistance, $R_s(min)$; the light response constant, b_{rs}, equal to the *PAR* flux density at twice the minimum stomatal resistance; the leaf area index, *LAI*; and variations in *PAR* (table 5.7). The response of stomatal resistance to *PAR* is estimated using a rectangular hyperbola relationship (TURNER AND BEGG, 1974):

$$f(PAR) = \frac{1}{r_s(min)} \cdot \frac{1}{1 + b_{rs}(PAR)/PAR} \tag{5.20}$$

PAR is estimated as a fraction of the short-wave incoming radiation, *Q*:

$$PAR = 0.5 \cdot Q \tag{5.21}$$

Stomatal conductance increases with increasing temperature until a threshold temperature, after which it decreases. This dependence on temperature is the result of energy balance feedbacks between humidity and transpiration of the leaf (SCHULZE AND HALL, 1982) and the influence of temperature on enzymes associated with stomatal operation (JARVIS AND MORISON, 1981). The response of stomatal conductance to temperature (*T*) is computed using the relationship presented by JARVIS (1976):

$$f(T) = \left[\frac{T - T_{min}}{T_{opt} - T_{min}}\right] \cdot \left[\frac{T_{max} - T}{T_{max} - T_{opt}}\right]^{\beta} \tag{5.22}$$

where, according to JARVIS (1976), and ERISMAN ET AL. (1994b)

$$\beta = \left(T_{max} - T_{opt}\right)/\left(T_{max} - T_{min}\right) \tag{5.23}$$

However, according to BALDOCCHI ET AL. (1987), and BROOK ET AL. (1999)

$$\beta = \left(T_{max} - T_{opt}\right)/\left(T_{opt} - T_{min}\right) \tag{5.24}$$

$T_{min}(i)$, $T_{max}(i)$ indicates minimum and maximum temperatures at which stomatal closure occurs, and the optimum temperature $T_{opt}(i)$ indicates the temperature of maximum stomatal opening (Table 5.7).

The influence of vapour pressure deficit on stomatal conductance $f(VPD)$ is represented by

$$f\left(VPD\right) = 1 - b_{vpd} \cdot VPD \tag{5.25}$$

b_{vpd} is a constant (Table 5.7), while VPD, vapour pressure deficit, is estimated from relative humidity $rh(\%)$ by (BELJAARS AND HOLTSLAG, 1990)

$$VPD = \left(1 - rh/100\right) \cdot es \tag{5.26}$$

es is the saturated water vapour pressure (mbar):

$$es = 6.1365 \cdot \exp\left(\frac{17.502 \cdot T}{240.97 + T}\right) \tag{5.27}$$

According to MONTEITH (1975), the saturated water vapour pressure es (in kPa) at temperature t (^{o}C) can be calculated using:

$$\begin{aligned} es = {} & 0.611371893 + 0.044383935 \cdot t \\ & + 0.001398175 \cdot t^2 + 0.000029295 \cdot t^3 \\ & + 0.000000216 \cdot t^4 + 0.000000003 \cdot t^5 \end{aligned} \tag{5.28}$$

The bulk stomatal resistance is approximated with

$$R_{stom} = \frac{1}{LAI \cdot g_s} \tag{5.29}$$

which will lead to an overestimation of R_{stom} caused by partial shading of leaves (BALDOCCHI ET AL., 1987).

Modelling the stomatal resistance in a detailed manner is only possible if enough information is available. This might be a problem for the water potential and for the leaf area index *LAI*. For those regions where such data are not available the parameterisation for the stomatal resistance given by WESELY (1989) may be used. This parameterisation is derived from the method by BALDOCCHI ET AL. (1987) and only needs data for global radiation Q (W m^{-2}) and surface temperature T_s (^{o}C):

$$R_{stom} = R_i \cdot \left\{ 1 + \left[\frac{200}{Q + 0.1} \right]^2 \right\} \cdot \left\{ \frac{400}{T_s \cdot (40 - T_s)} \right\} \tag{5.30}$$

Values for R_i can be obtained from a look-up table for different land use categories and seasons, as listed in Table 5.8 (from WESELY, 1989).

Table 5.7: Constants used in ERISMAN ET AL. (1994B) to compute R_{stom} for several vegetation types (adopted from BALDOCCHI ET AL., 1987).

Variable	**Units**	**Spruce**	**Oak**	**Corn**	**Soybean**
R_s *(min)*	s m^{-1}	232	145	242	65
b_{rs}*(PAR)*	W m^{-2}	25	22	66	10
T_{min}	^{o}C	-5	10	5	5
T_{max}	^{o}C	35	45	45	45
T_{opt}	^{o}C	9	24-32	22-25	25
b_{vpd}	k Pa^{-1}	-0.0026	0	0	0
ψ_o	M Pa	-2.1	-2.0	-0.8	-1.1

Table 5.8: Internal resistance (R_i) used in ERISMAN ET AL. (1994B) to compute the stomatal resistance for different seasons and land use types. Entities of -999 indicate that there is no air-surface exchange via that resistance pathway (adopted from WESELY, 1989).

Seasonal Category	**1**	**2**	**4**	**5**	**6**	**7**	**9**	**10**
Midsummer with lush vegetation	-999	60	70	130	100	-999	80	100
Autumn with unharvested cropland	-999	-999	-999	250	500	-999	-999	-999
Late autumn after frost, no snow	-999	-999	-999	250	500	-999	-999	-999
Winter, snow on ground and subfreezing	-999	-999	-999	400	800	-999	-999	-999
Transitional spring with partially green short annuals	-999	120	140	250	190	-999	160	200

(1) Urban land, (2) agricultural land, (4) deciduous forest, (5) coniferous forest, (6) mixed forest including wetland, (7) water, both salt and fresh, (9) non-forested wetland, (10) mixed agricultural and range land

After the passage through the stomatal opening, transfer of pollutant must take place between the gas phase of the stomatal cavity and the apoplast fluids. Parameterisations for R_m usually include a dependency on the Henry constant of the compound (e.g., WESELY, 1989). It was considered independent of land use class and season, and BALDOCCHI ET AL. (1987) estimated that R_m should be between 10 and 50 s m^{-1}. However, many water soluble compounds, such as HNO_3 and SO_2 are assumed to dissolve easily into the apoplast fluid due to a high or moderate (respectively) Henry coefficient and/or efficient conversion and transport after dissolution. Therefore R_m for HNO_3 and SO_2 (also for O_3) is generally assumed to be negligible (VOLDNER ET AL., 1986; WESELY, 1989, ERISMAN ET AL., 1994B; NOAA, 1997). For NH_3, R_m is usually also set to zero. This approximation may be well acceptable for unfertilised vegetation. However, it may be far from realistic if fertilisation causes a high ammonium content in the apoplast, leading to frequent and significant emissions. In that case, it may be necessary to account for R_m, unless the concentration in the stomata is estimated or calculated directly as a compensation point. In general, the mesophyll resistances R_m for all the gases are assumed to be zero, because of insufficient knowledge.

This general framework for the water vapour stomatal resistance can be used to describe stomatal uptake for each gas by correcting the R_{stom} using the ratio of the diffusion coefficient of the gas involved to that of water vapour (D_{H_2O} / D_i; Table 5.4) and adding the mesophyll resistance:

$$R_{stom,x} = R_{stom} \cdot \frac{D_{H_2O}}{D_x} + R_m \qquad (5.31)$$

5.1.9.2 External leaf uptake (R_{ext})

Many studies have shown that the external leaf surface can act as an effective sink, especially for soluble gases at wet surfaces (HICKS ET AL., 1989; FOWLER ET AL., 1991; ERISMAN ET AL., 1993A, 1994A). Under some conditions the external leaf sink can be much larger than the stomatal uptake. When R_{ext} is negligible, R_c also becomes negligible, dominating the other resistances.

SO_2

SO_2 dry deposition is enhanced over wet surfaces (Garland & Branson, 1977; Fowler & Unsworth, 1979; Fowler, 1985; Vermetten et al., 1992; Erisman et al., 1993b; Erisman & Wyers, 1993). Erisman et al. (1994b) derived an R_{ext} parameterisation for wet surfaces (due to precipitation and an increase in relative humidity) of heather plants:

- during or just after precipitation:

$$R_{ext} = 1 \text{ s m}^{-1} \tag{5.32}$$

- in all other cases:

$$R_{ext} = \begin{cases} 25000 \cdot e^{-0.0693 \cdot rh} & \text{rh} \le 81.3\% \\ 58 \cdot 10^{10} \cdot \mathrm{e}^{-0.278 \cdot \mathrm{rh}} & \text{rh} > 81.3\% \end{cases} \tag{5.33}$$

where rh is the relative humidity. The previous equation is applied to air temperatures above -1°C. Below this temperature it is assumed that surface uptake decreases and R_{ext} is set at 200 ($-1>T>-5$°C), or 500 ($T<-5$°C) s m^{-1}. R_{ext} will be zero for some hours after precipitation has stopped. This time limit varies with season and depends on environmental conditions. Drying of vegetation is approximated to take 2h during daytime in summer and 4h in winter. During night-time, vegetation is expected to be dry after 4h in summer and after 8h in winter (Erisman et al., 1993a).

NH_3

While most other gaseous pollutants have a consistently downward flux, NH_3 is both emitted from and deposited to land and water surfaces. For semi-natural vegetation, fluxes are usually directed to the surface, whereas fluxes are directed away from the surface over agricultural grassland treated with manure. For arable cropland fluxes may be bi-directional depending on atmospheric conditions and the stage in the cropping cycle (Sutton, 1990). Nitrogen metabolism has been shown to produce NH_3 and as a result there is a compensation point (Farquhar et al., 1980) at which deposition might change into emission when ambient concentrations fall below the compensation concentration and vice versa.

To describe NH_3 exchange it is necessary to consider natural and managed vegetation separately. For managed vegetation the compensation point approach seems to be most promising for use in models. However, the current state of knowledge is insufficient to define canopy resistance terms or compensation points reliable over different surface types and under different environmental conditions relevant for model parameterisation (LÖVBLAD ET AL., 1993). Furthermore, the compensation point is expected to be a function of many (undefined) factors and not a constant value.

Ammonia generally deposits rapidly to semi-natural (unfertilised) ecosystems and forests. Results show R_c values mostly in the range of 0-50 s m^{-1} (DUYZER ET AL., 1987, 1992; SUTTON ET AL. 1992; ERISMAN ET AL., 1993B). There is a clear effect of canopy wetness and relative humidity on R_c values (ERISMAN & WYERS, 1993). Under very dry, warm conditions (rh<60%, T>15°C) deposition to the leaf surface may saturate, so that exchange is limited to uptake through stomata, even allowing for the possibility of emission at low ambient concentrations. In this context a larger R_c may be appropriate (~50 s m^{-1}). Table 5.9 shows some values for R_{ext} for NH_3, for different land use categories.

Table 5.9: R_{ext} for NH_3 (s m^{-1}) over different vegetation categories in Europe. Negative values for R_{ext} denote emission for estimating a net upward flux. From ERISMAN AND DRAAIJERS (1995).

Land use category		Day		Night	
		Dry	Wet	Dry	Wet
Pasture during grazing:	summer	-1000	-1000	1000	1000
	winter	50	20	100	20
Crops and ungrazed pasture:	summer	$-R_{stom}$	50	200	50
	winter	$-R_{stom}$	100	300	100
Semi-natural ecosystems and forests		-500	0	1000	0

Winter conditions: T>-1 °C, otherwise R_{ext}=200 s m^{-1} (-1>T>-5 °C) or R_{ext}=500 s m^{-1} (T<-5 °C)

NO_X

A very small stomatal uptake might be observed for NO at ambient concentrations. Fluxes are, however, very low and uptake is therefore neglected (WESELY ET AL., 1989; LÖVBLAD & ERISMAN, 1992). Uptake of NO_2 seems to be under stomatal control with no internal resistance. In EUGSTER AND HESTERBERG (1996) it is addressed that, for deposition of NO_2, R_{ext} is assumed to be very large (FOWLER ET AL., 1991) and can be set to infinity. R_{ext} is set at 9999 s m^{-1}.

HNO_3

The difficulty of measuring nitric acid (HNO_3) concentrations at ambient levels has limited the number of flux measurements of these gases. Recent investigations, however, consistently show that for vegetative surfaces these gases deposit rapidly, with negligible surface resistances.

Deposition of HNO_3 seems to be limited by the aerodynamic resistance only. For this gas the external surface resistance is found to be negligible: R_{ext} is set at 1 s m^{-1}.

5.1.9.3 In-canopy transport (R_{inc})

Deposition to canopies includes vegetation and soil. Early studies assumed that deposition to soils under vegetation was relatively small (5-10% of the total flux; FOWLER, 1978). Recent work shows that a substantial amount of material can be deposited to the soil below vegetation. This substantial transfer occurs because large-scale intermittent eddies are able to penetrate through the vegetation and transport material to the soil.

The in-canopy aerodynamic resistance R_{inc} for vegetation is modelled according to data from VAN PUL AND JACOBS (1993):

$$R_{inc} = \frac{b \cdot LAI \cdot h}{u^*} \tag{5.34}$$

where *LAI* is the one-sided leaf area index (set to one for a deciduous forest in winter), *h* the vegetation height and *b* an empirical constant taken as 14 m^{-1}. The previous equation is only applied to tall vegetation. For low vegetation R_{inc} is assumed to be negligible. The resistance to uptake at the soil under the canopy R_{soil} is modelled similarly to the soil resistance to bare soils. This will probably underestimate uptake to surfaces under forests (partly) covered with vegetation. Parameters used for the calculation of R_{inc} are summarised in Table 5.10.

Table 5.10: Parameters for the calculation of R_{inc}, for simple vegetation classes by WILSON AND HENDERSON-SELLERS (1985) to translate OLSON ET AL. (1985).

Vegetation type	***LAI***	***b***	***h***
Desert	-9999	-9999	-9999
Tundra	6	-9999	-9999
Grassland	6	-9999	-9999
Grassland + shrub cover	6	-9999	-9999
Grassland + tree cover	6	-9999	-9999
Deciduous forest	5	14	20
Coniferous forest	5	14	20
Rain forest	-9999	-9999	-9999
Ice	-9999	-9999	-9999
Cultivation	5	14	1
Bog or marsh	-9999	-9999	-9999
Semi-desert	-9999	-9999	-9999
Bare soil	-9999	-9999	-9999
Water	-9999	-9999	-9999
Urban	-9999	-9999	-9999

5.1.9.4 Deposition to soil (R_{soil}) and water surfaces (R_{wat})

SO_2

Deposition of SO_2 to soil decreases at a soil pH below 4 and increases with relative humidity (GARLAND, 1977). In SPRANGER ET AL. (1994) R_{soil} dependence on pH and relative humidity is calculated as

$$R_{soil} = e^{9.471-0.0235\cdot rh-0.578\cdot pH} \tag{5.35}$$

When surface temperatures fall below zero or the surface is covered with snow, R_c values increase up to 200-500 s m^{-1}. The deposition of SO_2 to snow-covered surfaces depends on pH, snow temperature and probably the amount of SO_2 already scavenged by the snow pack. ERISMAN ET AL. (1994B) found the following relations for snow-covered surfaces:

$$R_{snow}=500 \text{ s m}^{-1} \qquad \text{at } T<-1^{\circ}\text{C}$$

$$R_{snow}=70(2-T) \text{ s m}^{-1} \qquad \text{at } -1<T<1^{\circ}\text{C} \tag{5.36}$$

NH_3

Deposition of NH_3 to soil, snow and water surfaces is similar to that of SO_2, only the pH dependence is different. Resistances to unfertilised moist soils will be very small provided that the soil pH is below 7. Fertilised soils, or soils with a high ammonium content, will show emission fluxes, depending on the ambient concentration of NH_3. Resistances to water surfaces will be negligible if the water pH is below 7. Resistances to snow will be similar to that of SO_2 at pH<7. Resistances will increase rapidly above a pH of 7.

NO_X

For NO at ambient concentrations, emission from soils is observed more frequently than deposition. This emission, the result of microbial activity in the soil, is dependent on soil temperature, water content and ambient concentrations of NO (HICKS ET AL., 1989). Emissions are to be expected at locations with low ambient NO and NO_2 concentrations (<5ppb).

The surface resistance for NO_2 to soil surfaces is found to be about 1000-2000 sm^{-1} (WESELY, 1989). If the soil is covered by snow, the resistance will become even higher. Resistances of NO_2 to water surfaces are also expected to be high due to the low solubility of this gas.

HNO_3

Resistances to water surfaces (pH>2) and soils for HNO_3 are assumed to be negligible. A surface resistance for HNO_3 to snow surfaces at temperatures below –5°C is expected. Resistances for HNO_2 are assumed to follow those of SO_2.

R_{soil}, R_{snow} and R_{wat} values for different gases are summarised in Table 5.6.

5.1.10 Particles

The process of dry deposition of particles differs from that of gases in two respects:

- Deposition depends on particle size since transfer to the surface involves Brownian diffusion, inertial impaction/interception and sedimentation (all of which are a strong function of particle size).
- Presumably the surface resistance for particles less than 10µm diameter (HICKS & GARLAND, 1983) is negligible small to all surfaces.

For submicron particles, the transport through the boundary layer is more or less the same as for gases. However, transport of particles through the quasi-laminar layer can differ. For particles with a diameter <0.1µm, deposition is controlled by diffusion, whereas deposition of particles with a diameter >10µm is more controlled by sedimentation. Deposition of particles with a diameter between 0.1 and 1µm is determined by the rates of impaction and interception and depends heavily on the turbulence density.

RUIJGROK ET AL. (1997) proposed another parameterisation derived from measurements over a coniferous forest. In this approach, which is simplified from SLINN's (1982) model, V_d is not only a function of u_*, but also of relative humidity (*rh*) and surface wetness. Inclusion of *rh* allows to account for particle growth under humid conditions and for reduced particle bounce when the canopy is wet. Dry deposition velocity is expressed as:

$$\frac{1}{V_d} = R_a + \frac{1}{V_{ds}} \qquad (5.37)$$

where R_a is the aerodynamic resistance, which is the same as for gaseous species, and V_{ds} is the surface deposition velocity.

For tall canopies V_{ds} is parameterised by RUIJGROK ET AL. (1997) as

$$V_{ds} = E \cdot \frac{u_*^2}{u_h} \tag{5.38}$$

where u_h is the wind speed at the top of the canopy, which is obtained by extrapolating the logarithmic wind profile from Z_R to the canopy height h. u_h can be expressed as:

$$u_h = \frac{u_*}{k}\left(\ln\left(\frac{10 \cdot z_0 - d}{z_0}\right) - \psi_h\left(\frac{10 \cdot z_0 - d}{L}\right) + \psi_h\left(\frac{z_0}{L}\right)\right) \tag{5.39}$$

E is the total efficiency for canopy capture of particles, and is parameterised separately for dry and wet surfaces (RUIJGROK ET AL., 1997).

For dry surfaces, for SO_4^{2-} particles (BROOK ET AL., 1999):

$$E = \begin{cases} 0.005\,\mathrm{u}_*^{0.28} & \mathrm{rh} \le 80\% \\ 0.005\,\mathrm{u}_*^{0.28} \cdot \left[1 + 0.18 \cdot \exp\dfrac{rh - 80}{20}\right] & \mathrm{rh} > 80\% \end{cases} \tag{5.40}$$

For wet surfaces, for SO_4^{2-} particles (BROOK ET AL., 1999):

$$E = \begin{cases} 0.08\,\mathrm{u}_*^{0.45} & \mathrm{rh} \le 80\% \\ 0.08\,\mathrm{u}_*^{0.45} \cdot \left[1 + 0.37 \cdot \exp\dfrac{rh - 80}{20}\right] & \mathrm{rh} > 80\% \end{cases} \tag{5.41}$$

rh (relative humidity) is taken at the reference height.

ERISMAN AND DRAAIJERS (1995) used the following general form for the calculation of V_d:

$$V_d = \frac{1}{R_a + \dfrac{1}{V_{ds}}} + V_s \tag{5.42}$$

where V_s is the deposition velocity due to sedimentation, to represent deposition of large particles, and V_{ds} can be estimated from Equation (5.38). Relations for E for different components and conditions are given in Table 5.11. These were derived from model calculations and multiple regression analysis (ERISMAN & DRAAIJERS, 1995).

Table 5.11: Parameterisations of E values for different components and conditions.
From ERISMAN AND DRAAIJERS (1995).

	Wet surface		Dry surface	
Compound	$rh \leq 80\%$	$rh > 80\%$	$rh \leq 80\%$	$rh > 80\%$
NH_4^+	$0.066 \cdot u_*^{0.41}$	$0.066 \cdot u_*^{0.41} \cdot \left[1 + 0.37 \cdot e^{\frac{rh-80}{20}}\right]$	$0.05 \cdot u_*^{0.23}$	$0.05 \cdot u_*^{0.23} \cdot \left[1 + 0.18 \cdot e^{\frac{rh-80}{20}}\right]$
SO_4^{2-}	$0.08 \cdot u_*^{0.45}$	$0.08 \cdot u_*^{0.45} \cdot \left[1 + 0.37 \cdot e^{\frac{rh-80}{20}}\right]$	$0.05 \cdot u_*^{0.28}$	$0.05 \cdot u_*^{0.28} \cdot \left[1 + 0.18 \cdot e^{\frac{rh-80}{20}}\right]$
NO_3^-	$0.10 \cdot u_*^{0.43}$	$0.10 \cdot u_*^{0.43} \cdot \left[1 + 0.37 \cdot e^{\frac{rh-80}{20}}\right]$	$0.063 \cdot u_*^{0.25}$	$0.063 \cdot u_*^{0.25} \cdot \left[1 + 0.18 \cdot e^{\frac{rh-80}{20}}\right]$
Na^+, Ca^{2+}, Mg^{2+}	$0.679 \cdot u_*^{0.56}$	$0.679 \cdot u_*^{0.56} \cdot \left[1 + 0.37 \cdot e^{\frac{rh-80}{20}}\right]$	$0.14 \cdot u_*^{0.12}$	$0.14 \cdot u_*^{0.12} \cdot \left[1 - 0.09 \cdot e^{\frac{rh-80}{20}}\right]$

For the large particles (Na^+, Ca^{2+}, Mg^{2+}) and for low vegetation (for all particles), the sedimentation velocity has to be added:

$$
\begin{aligned}
V_s &= 0.0067\, m \cdot s^{-1} && \mathrm{rh} \leq 80 \\
V_s &= 0.0067 \cdot e^{\frac{0.0066 \cdot rh}{1.058 - rh}}\ m \cdot s^{-1} && \mathrm{rh} > 80\%
\end{aligned}
\tag{5.43}
$$

5.2 IDEM Cloud deposition module

In mountainous and hilly regions cloud droplet deposition occurs frequently. This gives rise to another source of acidifying input to especially forest ecosystems, as these intercept cloud droplets very efficiently. In hilly regions low clouds occur more frequently then in the lower regions because of the upward movements of moist air, leading to so called orographic clouds, usually when moist oceanic air is pushed into the continent with westerly flows. The frequency with which these conditions exist in hilly regions is higher then the frequency of conditions in which radiative fog exists, a type of fog also known in lower regions. Radiative fog usually exists under low wind conditions, whereas orographic clouds usually are produced at moderate to high wind speeds with corresponding higher turbulent exchange.

Chemical composition of hill clouds and radiative fog have also been found to be quite different, with higher concentrations in radiative fog.

The presence of clouds on the more remote hilly forested regions is poorly described by measurements and/or models. In this project an attempt was made to use the best available meteorological information to obtain approximations of the mean Liquid Water Content (LWC) due to clouds in hilly regions, using the 0.5 by 0.5 degree ECMWF analysed data.

For this, vertical information on the LWC from the ECMWF model was obtained for the year 1998. The data used provides 31 so called sigma layers, of which the first ten are in the lower 2500 meter above the mean surface height. Another input used was DTM (Digital Terrain Model; BGR 1998) data for Germany with a resolution of 1x1km^2.

In Figure 5.4 the used elevation map is shown.

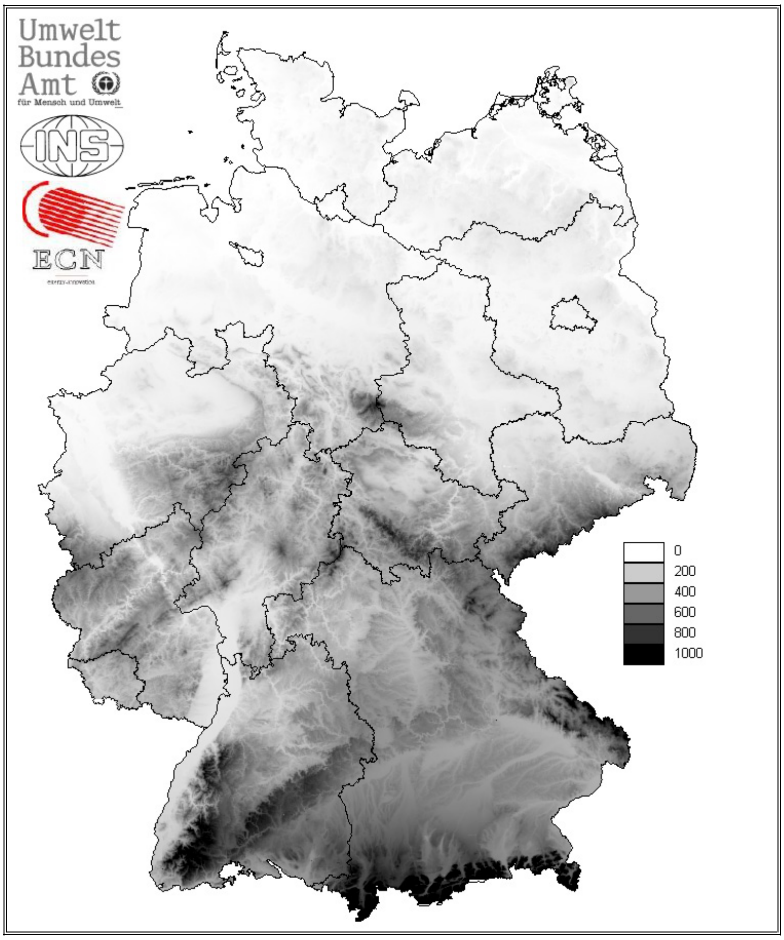

Figure 5.4 Digital elevation model on 1x1km² scale for Germany [in m ASL] (source: BGR 1998).

For each ECMWF grid cell the lowest height in the corresponding DTM cells was used as the base level of the sigma co-ordinates. Then for each time step in the LWC data (6 hours) the value of the LWC at the level of each 1x1km² grid cell was calculated by vertical interpolation of the sigma level values converted to height above surface using the standard atmosphere vertical pressure gradient. This leads to an average LWC per 1x1km² grid cell for the whole year.

In Figure 5.5 the resulting mean LWC for the 1x1km² grid is shown.

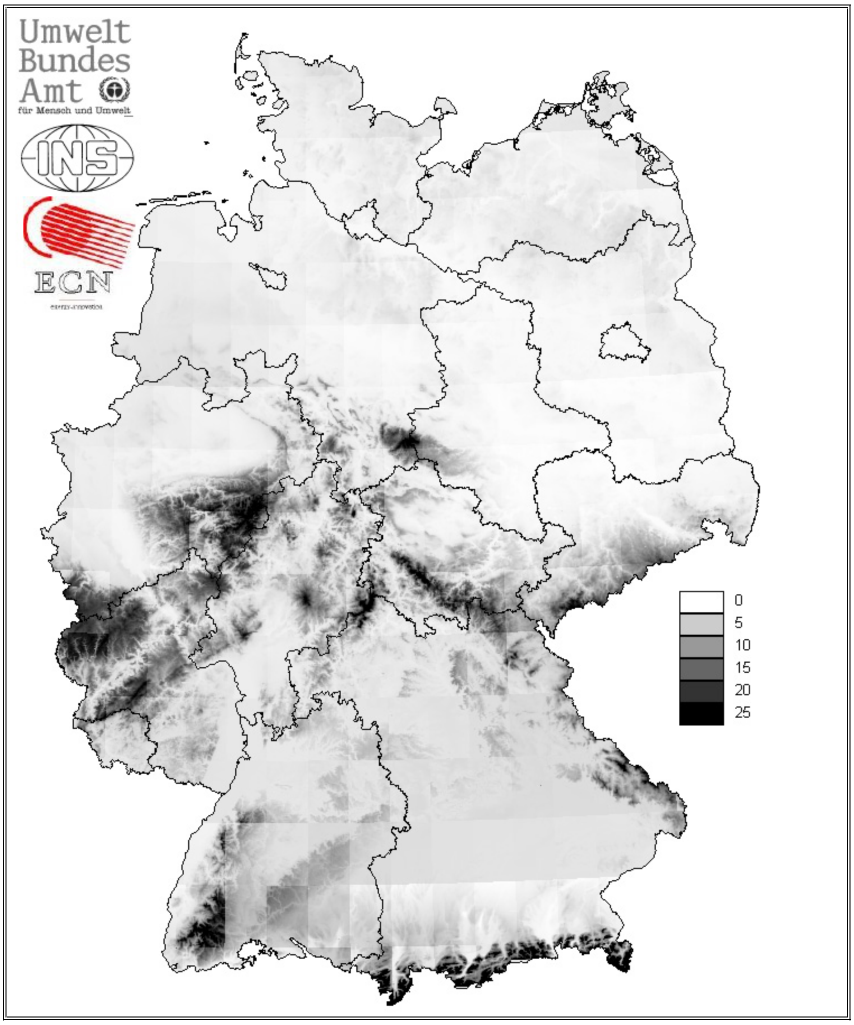

Figure 5.5 Mean LWC [g/kg] due to clouds over the year 1998 on the 1x1km² grid

The dry deposition rate and the deposition for fog/cloud droplets can be approximated by (REYNOLDS ET AL., 1997):

$$\begin{aligned} v_d &= \frac{1}{r_a} \\ F &= C_{cloud} * LWC * v_d \end{aligned} \qquad (5.44)$$

Where C_{cloud} is the cloud water concentration of the compound studied. This cloud water concentration can be derived from a large number of observations of the ratio between rain water concentrations and cloud water concentrations as a function of height above sea level. To derive those factors the kriged rain water concentration data for 1993 from INS was used (BLEEKER ET AL., 2000). The best fit of the relationships between rain water concentration and cloud concentrations as a function of height as the values of the constants a and b in the next equation are shown in the next table (Table 5.12):

$$\frac{C_{cloud}}{C_{rain}} = a.z^{b} \tag{5.45}$$

Table 5.12: Best fit for the values of constant a and b in Equation (5.45) used (BLEEKER ET AL., 2000)

Component	a	b
SO_4	341	-0.64
NO_3	912	-0.77
NH_4	25.6	-0.24
H	15.3	-0.24
Na	$9.1\ 10^{5}$	-1.90
Mg	$6.0\ 10^{7}$	-2.50
Ca	$1.3\ 10^{5}$	-1.60
K	$2.2\ 10^{3}$	-0.99
Cl	$3.0\ 10^{6}$	-2.09

As these functions lead to unrealistic high cloud water concentrations at heights below 250 ASL, the procedure to derive cloud/fog deposition fluxes was only applied to areas above 250 m ASL.

The resulting estimated potential acid deposition flux due to fog/cloud water deposition is shown in Figure 5.6, using the 1998 year average of R_a, the 1998 year average kriged rain water concentration and the 1998 year average LWC on the 1x1km² grid over Germany, all calculated in this project in the way described in this chapter.

Table 5.13 shows the 1998 potential acid fluxes by cloud deposition as a function of land use class and Bundesland.

As can be seen from Figure 5.6 the high elevation locations receive high fog water deposition fluxes because of the high mean LWC, but because the concentrations on the cloud water are calculated to be very low for the high sites, the total deposition per compound is low. Only for the middle high areas with heights between 250 and 750 meter significant cloud potential acid fluxes are calculated, these areas are of course also the most important forested regions of Germany. As can be seen clearly from Table 5.13 and Figure 5.6, the forested regions receive up to 800-1000 eq ha^{-1} a^{-1}, while the average over Germany is only 61 eq ha^{-1} a^{-1}.

Table 5.13: Annual average potential acid deposition flux by fog/cloud deposition for the Bundeslaender with areas above 250 meter ASL [eq ha^{-1} a^{-1}]

Land use class Federal States of Germany	Urban	Arable	Deciduous	Coniferous	Mixed	Water	Total
Lower Saxony	10	1	435	239	355	0	54
North Rhine-Westphalia	44	10	508	878	977	3	170
Hesse	41	15	350	400	438	2	158
Rhineland-Palatinate	69	19	158	178	163	1	77
Baden-Wurttemberg	27	5	38	30	58	1	19
Bavaria	42	7	147	120	138	1	46
Saarland	26	9	10	12	10	4	11
Saxony	61	11	117	296	150	1	76
Saxony -Anhalt	8	1	217	170	319	1	40
Thuringia	94	12	428	438	443	2	149
Germany	32	6	243	179	249	0	61

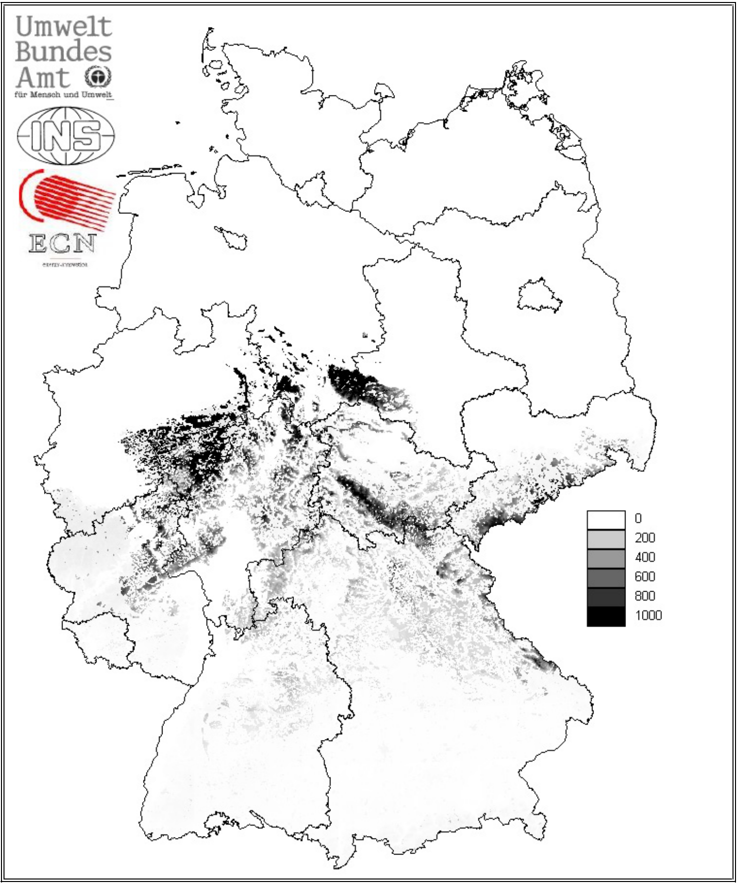

Figure 5.6 Total non-sea salt potential acid deposition by cloud water deposition [eq ha^{-1} a^{-1}]

5.3 The EUTREND model

The model used for the calculation of the concentration of both NH_3 and NH_4 is the so-called EUTREND model, which is an European version of the Operational Priority Substances (OPS) model (VAN JAARSVELD, 1995). The model concept has been used in studies of deposition to the North Sea (VAN JAARSVELD ET AL., 1986, WARMENHOVEN ET AL., 1989), the Rhine catchment area (BAART & DIEDEREN, 1991) and Europe, the so called ESQUAD study (VAN DEN HOUT, 1994). The model was originally developed for the calculation of transport and deposition of acidifying compounds such as ammonia (ASMAN & VAN JAARSVELD, 1992). In these studies the more general model concept was also validated by comparing model results with measurements of concentrations in air and in precipitation (VAN JAARSVELD, 1989).

5.3.1 Outline of the EUTREND Model

The version used here (EUTREND v1.17) covers the entire European continent with its marginal seas and calculates concentrations and depositions as functions of surface characteristics. The model is able to describe both short and long-distance transport by combining a Lagrangian trajectory model with a Gaussian plume model. The advection in this model is based on meteorological data (6-hour time step, 1000 and 850 hPa pressure levels) obtained through the Netherlands Meteorological Institute (KNMI) from the European Centre for Medium range Weather Forecasts (ECMWF) in Reading, England. The basic resolution of these data is 1° longitude x 0.5° latitude. Small scale processes such as dispersion, dry and wet deposition are described on the basis of surface observations of wind speed, cloud cover, temperature, humidity and precipitation. These surface observation data are obtained (mainly as 6-hourly values) from databases kept by ECMWF, the American National Centre for Atmospheric Research (NCAR) and DWD (Deutscher Wetterdienst). The spatial resolution of these small scale processes is limited by the (local) density of the meteorological stations. For Europe as a whole, data of more than 1300 stations is available. For practical purposes the EUTREND model distinguishes 50 'climatological areas' in Europe, but the model can also be used on a sub-European scale with the same number of climatological areas.

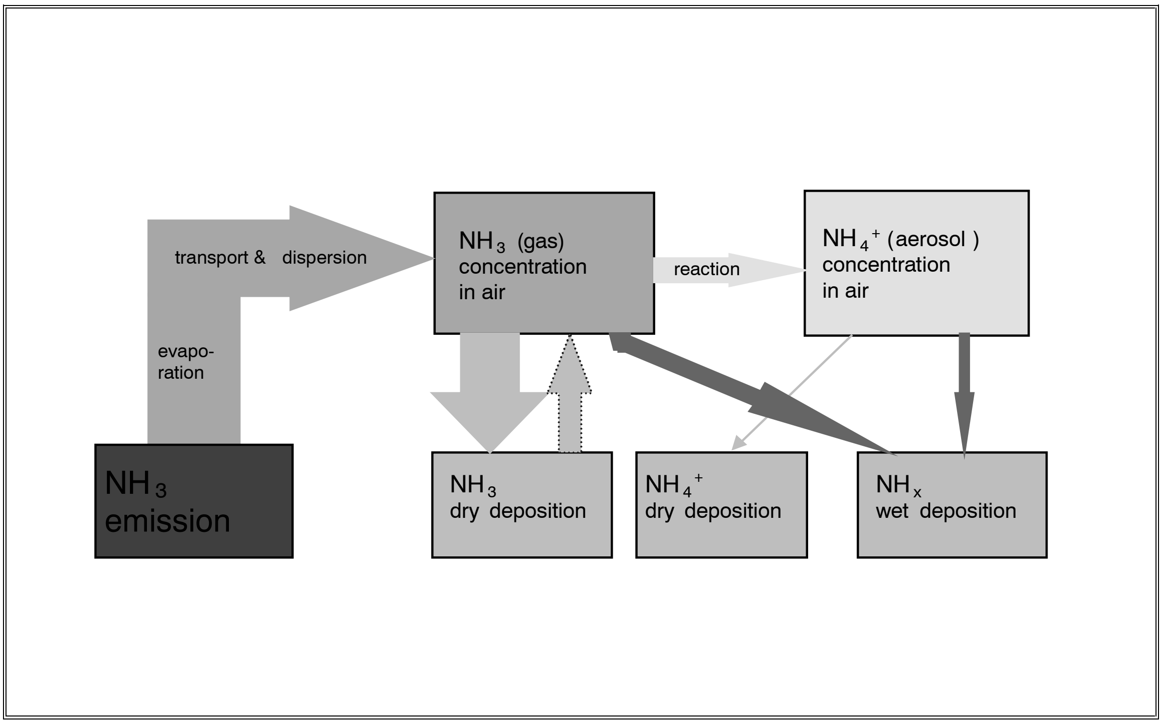

Figure 5.7: The atmospheric cycle of ammonia. The width of the arrows are representative for the relative importance of the processes.

Atmospheric processes included in the model are: emission, dispersion, advection, chemical conversion and wet and dry deposition. In Figure 5.7 the atmospheric cycle of ammonia is given. An important aspect with regard to dispersion and advection is that the model describes long range transport using well mixed trajectories, while local transport and dispersion is described using a Gaussian plume model. The latter model describes the air concentration as a function of source height and meteorology related dispersion parameters but – in case of high stacks – it also allows for (temporarily) transport of pollutants above the so-called mixing layer. Dry deposition is modelled using the so-called resistance approach, in which the dry deposition velocity is constructed from resistances of both the atmosphere and the receiving surface.

Chemical reaction rates are in the model independently of concentration levels, which means that only linear chemistry can be described. A general description of the modelled processes is given in VAN JAARSVELD (1995). The model can be applied with a variable spatial resolution, using a fixed receptor grid or using a set of individual receptor points. In this case each receptor point is characterised by its co-ordinates, land use class and roughness length.

Based on previous studies, some extensions were made to the original EUTREND model. The most important one is the introduction of local land use and surface roughness effects on dry deposition. These parameters now can be specified either in grid-form or as properties of receptors.

5.3.2 Ammonia in the EUTREND model

Modelling the dispersion and deposition of ammonia and ammonium is special in a way that ammonia is emitted as part of an evaporation process e.g. when manure is applied on the land. This means that there is a correlation between the meteorological condition and the emission rate is such a way that the dispersion (and also the dry deposition velocity) is high when the emission rate is high. In these terms one can speak of a feedback between atmospheric concentrations and emissions.

Another important aspect is the low height at which ammonia enters the atmosphere (zero level for emissions due manure application and 2-6m for emissions from stables). Due to the initial transport close to the surface a significant part of the ammonia will be dry deposited close to the source. The problem is illustrated in Figure 5.8 where the (cumulative) deposited fraction of ammonia is given as a function of the downwind distance from a release height of 1m. Under average meteorological conditions already 20% of the emitted ammonia will be dry deposited within the first 1000m and 50% within 60km. From Figure 5.8 it can also be seen that the dominant deposition form in the first 100km is dry deposition while for larger distances wet deposition of secondary formed ammonium will be the dominant form.

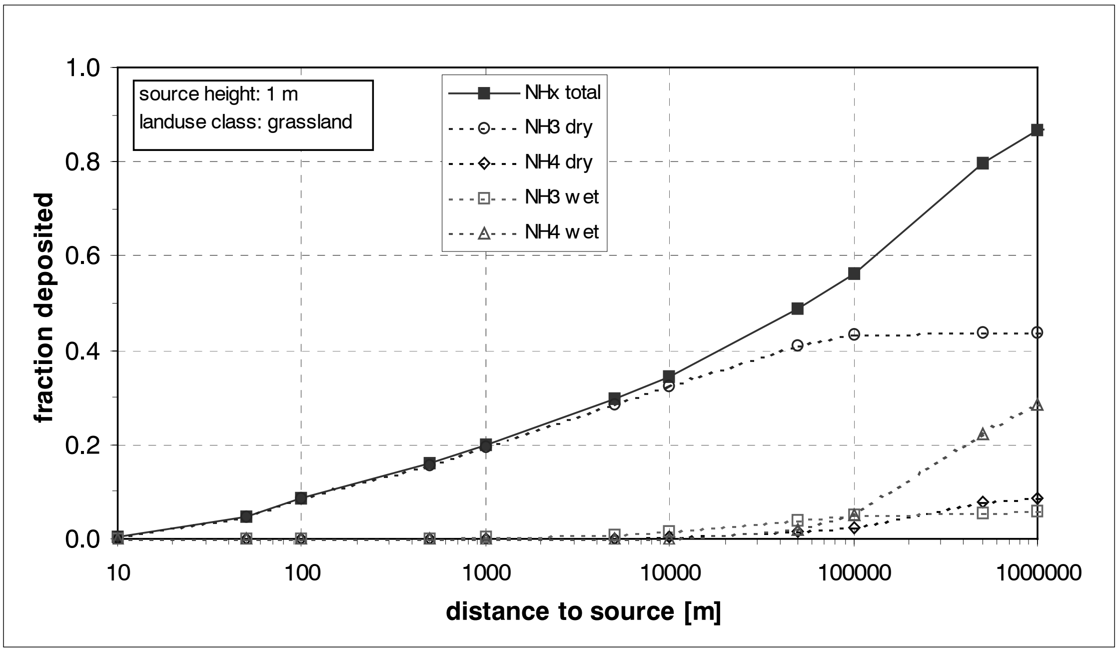

Figure 5.8: Cumulative deposition of ammonia and ammonium due to an ammonia point source as a function of downwind distance (ASMAN & VAN JAARSVELD, 1992)

5.3.3 Differences between the EUTREND model and the EMEP Lagrangian model

The aspects of low emission heights are addressed in the EUTREND model through a local Gaussian plume model superimposed on a trajectory model. In single-layer trajectory models such as the EMEP model, the locally emitted NH_3 will be immediately mixed up over the entire boundary layer, causing an underestimation of atmospheric concentrations close to the surface and hence an underestimation of the dry deposition flux. On the basis of this difference in model approach one may expect that the EUTREND model will calculate significantly higher surface concentrations for substances like NH_3 and NO_X. One solution to address the effects of local and low level sources in the EMEP model is the introduction of a local deposition factor. This means that a certain fraction of the emission is directly attributed to deposition in the same grid cell. The local deposition factor depends on the grid size used in the model. In case of the EMEP Langrangian model with its 150x150km^2 resolution the factor would be (according to Figure 5.8) in the order of 50%. It is clear that in such an approach the calculated deposition depends heavily on the local deposition factor. In the present study local scale emissions on a

$5x5km^2$ grid are used. Even then, approximately 25% of a grid cell emission will be deposited within the same grid cell.

5.3.3.1 Comparison with observations

In order to validate the outcome of the EUTREND model (including the emissions used) the results should be compared with measurements. Comparisons on the basis of atmospheric ammonia concentrations would be the most direct action but such measurements where not available. A recent comparison of results of a similar model approach with measurements in the Netherlands for the period 1993-1998 revealed a relatively high spatial correlation (R^2 = 0.9; 7 stations) but an underestimation of NH_3 concentrations of almost 30%. Similar results were obtained for the modelled wet deposition (R^2 = 0.9; 14 stations).

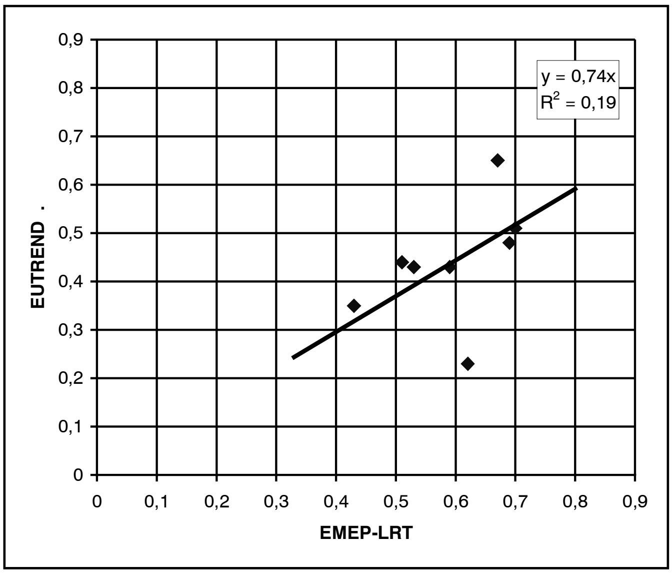

Figure 5.9: Comparison of modelled concentration in precipitation with observations of the EMEP network for the year 1994

In the previous study (Bleeker et al, 2000) the measured wet deposition in the EMEP network was used for validation purposes. For the 8 stations, which were in operation in 1994, the concentrations were calculated on the basis of NH_3 emission in Germany and other European countries. The results are given in Figure 5.9. The largest discrepancy was found for the EMEP station Westerland, which is a coastal station at the German Bight. It turns out that the model approach gives 25% lower concentrations in precipitation. This result is consistent with the Dutch situation. One of the suggestions is a general underestimation of ammonia emissions, especially those of manure application.

5.3.4 EUTREND Input data used

For the EUTREND concentration calculations, local scale ammonia emissions for Germany were used. For this purpose emissions for the period 1990-1998 were used that originate from the CORINAIR database and were given as total animal emission per territorial unit (German Kreis) (source: allocation of animal numbers and emissions to Kreis units based on CORINAIR, performed by IER of the University of Stuttgart). These emissions have been allocated to areas with agricultural land use using a Geographic Information System (ArcView). A land use map on a resolution of 1x1km^2, derived from CORINE Land cover data and provided by ÖKO-DATA/INS was used as a basis. This map was first classified into two classes, i.e. agricultural and non-agricultural land use. Then the fraction of agricultural land use per territorial unit was calculated, and subsequently the emission per agricultural land use cell within each territorial unit. Animal emissions account for about 86% of the total ammonia emission. In order to accommodate for other emissions, i.e. emissions from fertiliser application (9%), industry (1%) and others (traffic, combustion plants and denox, together 4%) these emissions were equally spread over the agricultural land use cells. The emissions on a 1x1km^2 resolution were then aggregated to 5x5km^2 grid cells, the resolution used in the EUTREND model. The result of this procedure is shown in Figure 5.10, while total emissions per Bundesland are given in Table 5.14.

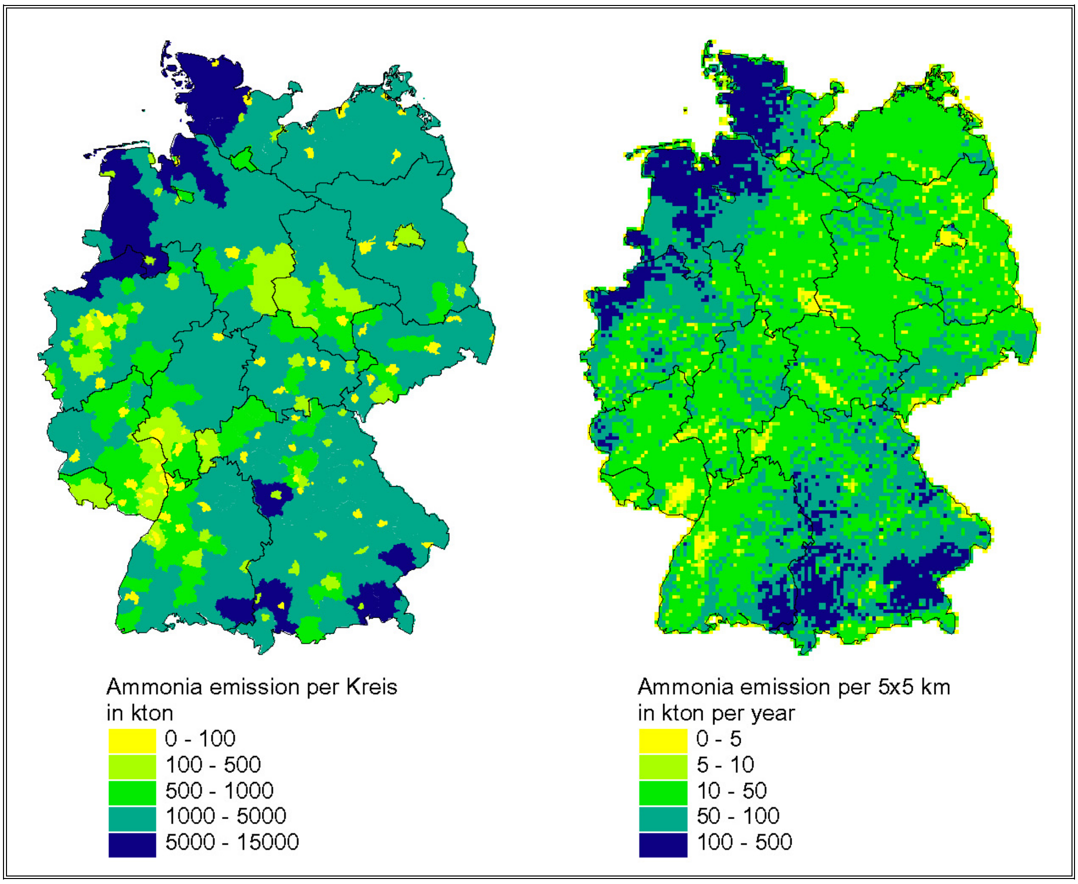

Figure 5.10: Ammonia emission per Kreis (left) and per 5x5km² grid cell (right) for 1998.

Table 5.14: Total agricultural ammonia emission per Bundesland (in kt/year)

Federal States of Germany	**Total ammonia emission (in kt/year)**								
	1990	**1991**	**1992**	**1993**	**1994**	**1995**	**1996**	**1997**	**1998**
Berlin	0.6	0.5	0.4	0.4	0.4	0.4	0.4	0.4	0.4
Brandenburg	36.8	32.7	31.6	31.1	31.4	32.0	32.1	31.7	32.1
Mecklenburg-West Pommerania	33.1	29.4	28.4	28.0	28.3	28.7	28.7	28.4	28.8
Saxony	33.8	29.7	28.6	28.1	28.2	27.8	27.8	27.4	27.7
Saxony -Anhalt	25.4	22.6	21.8	21.4	21.7	21.6	21.7	21.4	21.7
Thuringia	24.4	21.6	20.8	20.5	20.6	20.3	20.3	20.1	20.3
Schleswig-Holstein	59.6	52.5	50.6	49.8	49.8	49.9	49.9	49.1	49.5
Hamburg	0.7	0.6	0.6	0.5	0.5	0.6	0.6	0.5	0.5
Lower Saxony	132.8	116.9	112.8	111.0	111.0	110.9	111.1	109.4	110.3
Bremen	0.9	0.8	0.8	0.7	0.7	0.7	0.7	0.7	0.7
North Rhine-Westphalia	82.7	72.2	69.5	68.1	68.1	66.5	66.6	65.4	66.0
Hesse	30.2	26.5	25.6	25.1	25.2	25.2	25.3	24.9	25.1
Rhineland-Palatinate	25.1	22.1	21.4	21.0	21.1	21.1	21.1	20.9	21.1
Baden-Wurttemberg	68.7	60.2	58.0	56.9	56.9	56.3	56.4	55.6	56.0
Bavaria	201.8	177.3	171.1	168.3	168.0	166.0	166.3	163.6	164.7
Saarland	3.1	2.8	2.6	2.6	2.6	2.6	2.6	2.6	2.6

Comparing the emissions listed in Table 5.14 with the emissions used in the previous study (BLEEKER ET AL., 2000), shows that the present emissions are overall about 15% higher than the previous ones. This is also shown in Figure 5.11, where the difference between these emissions is shown. In this figure a distinction is made between former East and West Germany. Especially for the former East Germany there is a relatively large difference between the present and previous emissions (about 25%). These differences will subsequently result in concentrations and fluxes that are equally larger in comparison to the previous study.

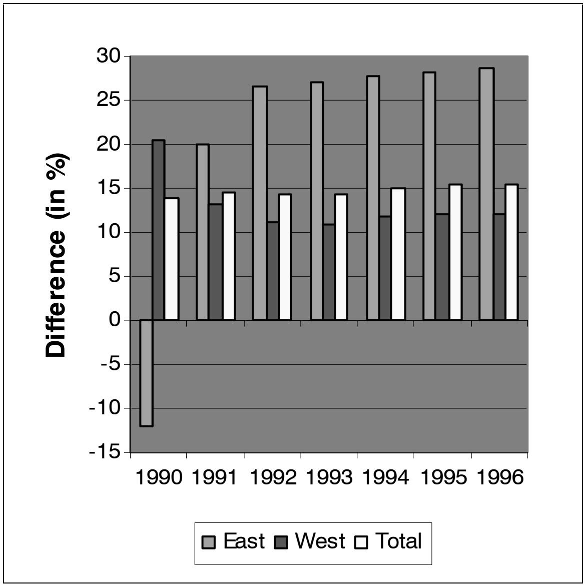

Figure 5.11: Difference between the ammonia emissions used in this study and those used in BLEEKER ET AL. (2000).

Using the methods described above, only the German contribution is accounted for. In border areas (especially near the Dutch border) this may give serious underestimates. Therefore, in order to account for the foreign contribution, the EUTREND model was also run using a European emission database excluding Germany. For the Netherlands and Belgium the resolution of these emissions is also 5x5km². For other countries a 75x75km² resolution was used according to ASMAN (1992). Actual emission data for 1994 were taken from EMEP. The concentration and deposition thus derived were added to the results obtained using the German emission data.

5.4 Dry deposition of Base Cations (Ca, K, Mg; Na)

Contrary to the other components SO_X, NO_Y and NH_X, no modelled or measured concentrations in air exist for base cations. As these components may contribute quite effectively to reducing the acidic input to ecosystems by their anion buffering capacity it is important to have a good estimate also of their dry deposition fluxes.

The concentrations in air of the base cations (Ca, K, Mg; Na)are derived indirectly using concentrations in rain water. As explained in Chapter 4 kriged maps have been produced in the framework of this project on a scale of 1x1km² over Germany for the acidifying components and the base cations. So called Scavenging Ratios (*SR*) have been applied to derive from these maps the concentration for the base cations. The scavenging ratio is simply expressed as:

$$SR = \rho \frac{C_{rain}}{C_{air}} \tag{5.46}$$

Where ρ is the density of air [g m^{-3}], C_{air} is the concentration in air [µg m^{-3}] and C_{rain} is the concentration in rain water [mg l^{-1}]. Alkaline particles usually fall in the size range between 0.1 and 2 µm. The *SR* depends on the mean mass diameter (*MMD* [µm]) of the particles (KANE ET AL, 1994):

$$SR = 188 * e^{0.227*MMD} \tag{5.47}$$

Combination of Equation 5.42 and Equation 5.43 yields a simple relationship between the concentration in air and that in rain.

The *MMD* of particles depends on many factors of which the most important one is the distance to the source as several processes like coagulation, condensation and uptake of humidity leads to growth of the *MMD* of particles over time. Also the concentration in rain water increases with the distance to the sources as in and below cloud scavenging increase with distance from the source. Assuming a simple linear relations ship between the *MMD* and the concentration in rain several authors derived best-fit relationships. From DRAAIJERS ET AL. (1996) the following relationships were taken (Table 5.15):

Table 5.15: Best fit constants for the linear relationship between Mean Mass Diameter (*MMD*) and the concentrations in rain for the studied (base) cations Na, Mg, Ca and K

$MMD=A*C_{rain}+B$	*A*	*B*
Na	0.574	6.082
Mg	2.778	5.694
Ca	1.520	6.316
K	2.740	4.096

The procedure as sketched above will derive mean concentrations at the same time resolution as the data for the rain water concentration. In our case this is a resolution of one year. Therefore dry deposition fluxes of the base cations only could be calculated as year average values by applying the year averaged dry deposition rate for base cations on the year average concentration in air of these base cations as derived by scavenging ratios from year average rain water concentration.

5.5 SO_2 dry deposition correction procedure

In the previous project (BLEEKER ET AL. 2000) it was suggested to base future SO_2 dry deposition estimates more on SO_2 air concentration maps interpolated from available measurements. This is done by a correction procedure, correcting the dry deposition estimates of SO_2 based on the difference between modelled and measured air concentrations. Only few of the nationally available background sites of the monitoring networks in Germany are routinely used for validation purposes of modelled air concentration data, which are standard dry deposition model input data. The correction procedure applied uses air concentration fields derived from 42 to 74 independant rural background SO_2 air concentration monitoring data.

At the beginning of the project it was expected that new EMEP Eulerian model air concentrations (in 50x50km² grid) would be available. It turned out that those data were not yet available. For the years 1985 and 1990-1996 data was obtained from EMEP, calculated using the EMEP Lagrangian transport model (in 150x150km² grid) and for the years 1990 and 1996-2000 NERI DEM/DEHM model data (in 0.5°x0.5° grid) became available (cf. Chapter 5.1.4).

Since annual average SO_2 air concentration maps interpolated from measurements in Germany are available at INS (c.f. Part 2 of this report), a comparison between this measurement based maps and SO_2 air concentration maps from EMEP and NERI, respectively, was carried out. The results of this comparison (Figure 5.12) were taken for the SO_X correction:

$$SO_{2\ \mathrm{corrected}} = SO_2 \text{ x Factor } [\%] / 100 \qquad (5.48)$$

Average SO_2 correction factors and the magnitudes of the correction in the individual years 1990-1999 are listed in Table 5.16. The spatial patterns of the correction are shown in Figures 5.12 and 5.13.

Table 5.16: Average SO_2 correction factors and correction in the air concentration maps

	Average SO_2 correction factors	Minimum	Mean	Maximum
			correction [µg/m³]	
1990	179%	-0.9	+8.0	+45.0
1991	165%	-5.7	+8.3	+34.0
1992	124%	-3.7	+2.9	+15.9
1993	134%	-3.8	+3.3	+13.5
1994	128%	-2.7	+1.7	+11.9
1995	99%	-4.9	-3.0	+10.0
1996	126%	-2.3	+1.4	+16.0
1997	188%	-4.6	+2.4	+8.7
1998	148%	-4.3	+0.3	+1.8
1999	214%	-4.5	+1.8	+3.8

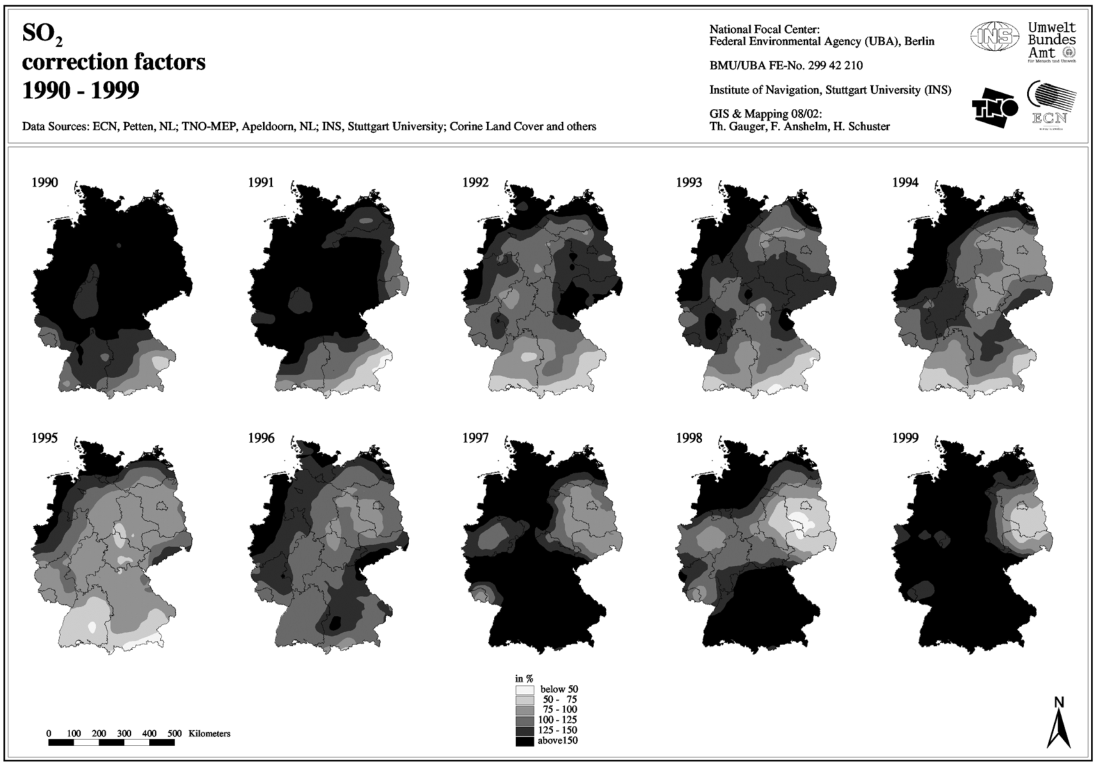

Figure 5.12: SO_2 correction factors for the individual years 1990-1999 [%]

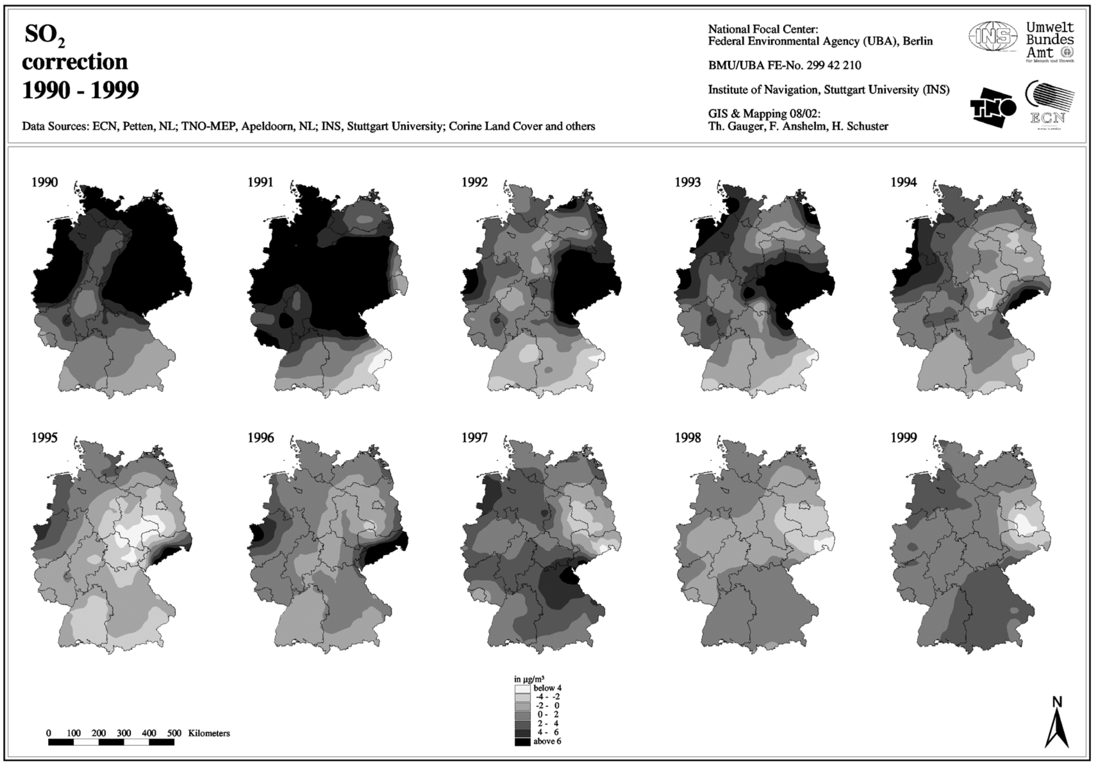

Figure 5.13: SO_2 correction in the individual years 1990-1999 [$\mu g/m^3$]

5.6 Dry deposition mapping results

An overview on all dry deposition maps calculated for the period 1990-1999 within this study is given in Table 5.17. To calculate exceedances of Critical Loads for nutrient nitrogen, acidity and net acidity (cf. Chapter 2) it is necessary to calculate dry deposition fields of total nitrogen (N) of potential acidity (Ac_{pot}), the sum of base cations (BC, $BC_{(nss)}$), and potential net acidity ($AC_{pot(net)}$).

Table 5.17: Maps of dry deposition 1990-1999

Dry Deposition	**1990**	**1991**	**1992**	**1993**	**1994**	**1995**	**1996**	**1997**	**1998**	**1999**
$SO_X\text{-}S_{(nss)}$	**X**	**X**	**X**	**X**	**X**	**X**	**X**	**X**	**X**	**X**
$NO_Y\text{-}N$	**X**	**X**	**X**	**X**	**X**	**X**	**X**	**X**	**X**	**X**
$NH_X\text{-}N$	**X**	**X**	**X**	**X**	**X**	**X**	**X**	**X**	**X**	**X**
Ca, $Ca_{(nss)}$	**X**	**X**	**X**	**X**	**X**	**X**	**X**	**X**	**X**	**X**
Mg, $Mg_{(nss)}$	**X**	**X**	**X**	**X**	**X**	**X**	**X**	**X**	**X**	**X**
K, $K_{(nss)}$	**X**	**X**	**X**	**X**	**X**	**X**	**X**	**X**	**X**	**X**
Na	**X**	**X**	**X**	**X**	**X**	**X**	**X**	**X**	**X**	**X**
$N = (NO_3\text{-}N + NH_4\text{-}N)$	**X**	**X**	**X**	**X**	**X**	**X**	**X**	**X**	**X**	**X**
Potential Acidity $AC_{pot} = (S_{(nss)} + N)$	**X**	**X**	**X**	**X**	**X**	**X**	**X**	**X**	**X**	**X**
$BC = (Ca + K + Mg)$, $BC_{(nss)} = (Ca_{(nss)} + K_{(nss)} + Mg_{(nss)})$	**X**	**X**	**X**	**X**	**X**	**X**	**X**	**X**	**X**	**X**
Potential Net Acidity $AC_{pot\ (net)} = ((S_{(nss)} + N) - BC_{(nss)})$	**X**	**X**	**X**	**X**	**X**	**X**	**X**	**X**	**X**	**X**
$_{(nss)}$ =non-seasalt (sea salt corrected)	**X = processed**									

The main mapping results of the dry deposition model calculations described in the preceding Chapters (Chapter 5.1 to 5.5) are presented in the following subchapters and illustrated by the graphical representation of the modelled dry deposition data sets in Chapter 5.8.

5.6.1 Dry deposition fluxes and trends of base cations (BC = Ca + K + Mg)

Dry deposition of base cations (BC) is calculated by summing up the fluxes of Ca, K and Mg. The annual average modelled dry deposition of BC and its components 1990-1999 including percentage changes is listed in Table 5.18, the same for non-sea salt base cations (BC$_{(nss)}$) is shown in Table 5.19, respectively. The trend of BC and BC$_{(nss)}$ dry deposition, respectively, shows a decline lasting 3 to 4 years from 1991 to 1994/1995 and then continuing on from 1995/1996 to 1999.

Table 5.18: Budgets of average annual dry deposition of Ca, Mg, K and BC in Germany 1990-1999

Dry Deposition	Ca [eq ha^{-1} a^{-1}]	% change from previous year	K [eq ha^{-1} a^{-1}]	% change from previous year	Mg [eq ha^{-1} a^{-1}]	% change from previous year	BC [eq ha^{-1} a^{-1}]	% change from previous year
1990	212		136		73		420	
1991	243	+14,9	143	+5,6	72	-0,9	459	+9,2
1992	196	-19,3	141	-1,7	58	-19,5	395	-13,8
1993	191	-2,5	127	-9,7	61	+4,7	379	-4,0
1994	173	-9,9	109	-14,0	55	-10,4	336	-11,3
1995	150	-13,3	131	+19,3	59	+8,5	339	+0,9
1996	154	+3,0	125	-4,2	55	-6,7	334	-1,5
1997	154	-0,3	112	-10,3	51	-8,5	316	-5,4
1998	141	-8,2	107	-4,8	44	-13,4	292	-7,8
1999	135	-4,2	96	-9,9	48	+10,3	280	-4,1
% change from 1990 to 1999		-36		-29		-34		-33

Table 5. 19: Budgets of average annual dry deposition of Ca$_{(nss)}$, Mg$_{(nss)}$, K$_{(nss)}$ and BC$_{(nss)}$ in Germany 1990-1999

Dry Deposition	Ca$_{(nss)}$ [eq ha^{-1} a^{-1}]	% change from previous year	K$_{(nss)}$ [eq ha^{-1} a^{-1}]	% change from previous year	Mg$_{(nss)}$ [eq ha^{-1} a^{-1}]	% change from previous year	BC$_{(nss)}$ [eq ha^{-1} a^{-1}]	% change from previous year
1990	198		114		19		331	
1991	234	+17.8	126	+10.5	22	+17.9	382	+15.3
1992	187	-20.1	125	-0.7	14	-39.2	325	-14.9
1993	182	-2.7	111	-11.0	15	+7.8	307	-5.4
1994	163	-10.4	93	-16.0	12	-19.5	268	-12.8
1995	138	-15.4	112	20.6	10	-12.8	260	-2.7
1996	145	+5.4	111	-0.9	16	+56.9	273	+4.7
1997	145	-0.3	98	-11.7	12	-26.0	255	-6.5
1998	132	-8.7	93	-5.5	6	-47.3	231	-9.3
1999	125	-5.8	80	-14.3	6	+1.0	211	-9.0
% change from 1990 to 1999		-37		-30		-66		-36

5.6.1.1 Dry deposition of non-seasalt base cations ($BC_{(nss)}$)

Dry deposition of non-sea salt base cations ($BC_{(nss)}$) in Germany declined by 36% between 1990 and 1999. This equals an absolute decrease of average 120 eq ha^{-1} a^{-1} from 331 eq ha^{-1} a^{-1} in 1990 to 211 eq ha^{-1} a^{-1} in 1999 (Figure 5.14).

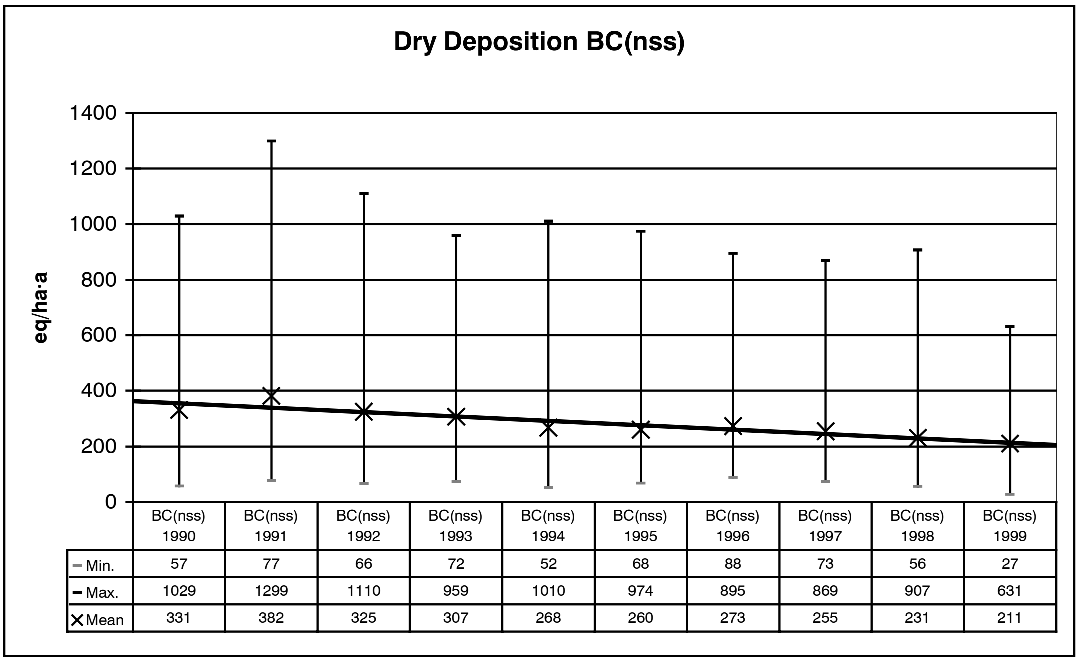

	BC(nss) 1990	BC(nss) 1991	BC(nss) 1992	BC(nss) 1993	BC(nss) 1994	BC(nss) 1995	BC(nss) 1996	BC(nss) 1997	BC(nss) 1998	BC(nss) 1999
- Min.	57	77	66	72	52	68	88	73	56	27
- Max.	1029	1299	1110	959	1010	974	895	869	907	631
× Mean	331	382	325	307	268	260	273	255	231	211

Figure 5.14: Minimum, maximum and annual mean dry deposition of non-seasalt base cations ($BC_{(nss)} = Ca_{(nss)} + K_{(nss)} + Mg_{(nss)}$) 1990-1999

The annual average composition of $BC_{(nss)}$ is listed in Table 5.20. $Ca_{(nss)}$ is the dominating compound of dry deposited non-seasalt base cations ($BC_{(nss)}$) with a mean fraction of about 58% (53% to 61%). The mean fraction of $K_{(nss)}$ 1990-1999 is about 38%, with a range between 33% and 43% in the single years. $Mg_{(nss)}$ only contributes to average 4.5% (2.7 to 5.9%) to $BC_{(nss)}$ within this ten years period.

Table 5.20: Average non-seasalt calcium ($Ca_{(nss)}$), potassium ($K_{(nss)}$) and magnesium ($Mg_{(nss)}$) fraction of the sum of wet deposited non-seasalt base cations ($BC_{(nss)}$)

	1990	**1991**	**1992**	**1993**	**1994**	**1995**	**1996**	**1997**	**1998**	**1999**
mean fraction of $Ca_{(nss)}$	59,9%	61,2%	57,4%	59,1%	60,8%	52,9%	53,3%	56,8%	57,2%	59,2%
mean fraction of $K_{(nss)}$	34,4%	32,9%	38,4%	36,1%	34,8%	43,2%	40,8%	38,5%	40,1%	37,8%
mean fraction of $Mg_{(nss)}$	5,7%	5,8%	4,2%	4,8%	4,4%	3,9%	5,9%	4,7%	2,7%	3,0%
total	100%	100%	100%	100%	100%	100%	100%	100%	100%	100%

The spatial patterns of $BC_{(nss)}$ wet deposition 1990-1999, where the overall reduction of the dry deposition flux of $BC_{(nss)}$ from 1990 to 1999 can be observed, are presented in Map 5.1.

5.6.2 Dry deposition fluxes and trends of acidifying compounds and nitrogen

Eutrophication occurs due to atmospheric input of nitrogen, that causes nutrient imbalances, while acidification is caused by deposition loads of sulphur and nitrogen compounds. Average annual dry deposition 1990 to 1999 and the percentage changes for sulphur (SO_X-$S_{(nss)}$), reduced, oxidised and total nitrogen (NH_X-N, NO_Y-N, N), respectively, are shown in Table 5.21. Over the period from 1990 to 1999, the dry deposition of all acidifying compounds declined. Modelled average SO_X-$S_{(nss)}$ dry deposition has fallen by 72%, NO_Y-N by 55%, NH_X-N by 12% and total N dry deposition by 28%, respectively, within the ten years period since 1990. Since 1992 on average more nitrogen than sulphur is deposited with the dry flux in Germany (Table 5.21).

Table 5.21: Budgets of average annual dry deposition of SO_X-$S_{(nss)}$, NH_X-N, NO_Y-N and N in Germany 1990-1999

Dry Deposition	**SO_X-$S_{(nss)}$ [eq ha^{-1} a^{-1}]**	**% change from previous year**	**NH_X-N [eq ha^{-1} a^{-1}]**	**% change from previous year**	**NO_Y-N [eq ha^{-1} a^{-1}]**	**% change from previous year**	**N [eq ha^{-1} a^{-1}]**	**% change from previous year**
1990	2284		1066		654		1719	
1991	2205	-3.4	887	-16.8	650	-0.5	1537	-10.6
1992	1727	-21.7	962	+8.5	660	+1.4	1622	+5.5
1993	1733	+0.3	948	-1.6	625	-5.2	1573	-3.1
1994	1202	-30.6	989	+4.3	649	+3.7	1637	+4.1
1995	1081	-10.1	1007	+1.8	606	-6.6	1612	-1.5
1996	1067	-1.3	918	-8.8	563	-7.1	1481	-8.1
1997	1152	+7.9	934	+1.7	689	+22.4	1623	+9.6
1998	577	-49.9	1036	+10.9	522	-24.3	1558	-4.0
1999	638	+10.6	942	-9.1	292	-44.0	1234	-20.8
% change from 1990 to 1999		-72		-12		-55		-28

5.6.2.1 Dry deposition of non-seasalt sulphur (SO_X-$S_{(nss)}$)

The 72% decline of modelled average dry deposition of non-seasalt sulphur (SO_X-$S_{(nss)}$) between 1990 and 1999 is shown in Figure 5.15. From 1306·kt a^{-1} (36.6 kg ha^{-1} a^{-1}) 1990 the average dry deposition of SO_X-$S_{(nss)}$ fell by 941 kt (26.4 kg ha^{-1} a^{-1}) to 365 kt/a (10.2 kg ha^{-1} a^{-1}) in 1999. The trend of average decline shows stagnation from 1992 to 1993 and from 1996 to1997, while the maximum values in those years are falling. The relatively high maximum value in 1996 may indicate higher SO_2 emissions and air concentrations (cf. Chapter 3.1 in Part 2 of this report), due to colder winter temperatures and longer firing periods. From 1998, where the lowest mean estimates can be observed, to 1999 an about 11% rise of the average values can be found, while the decline of maximum values holds on.

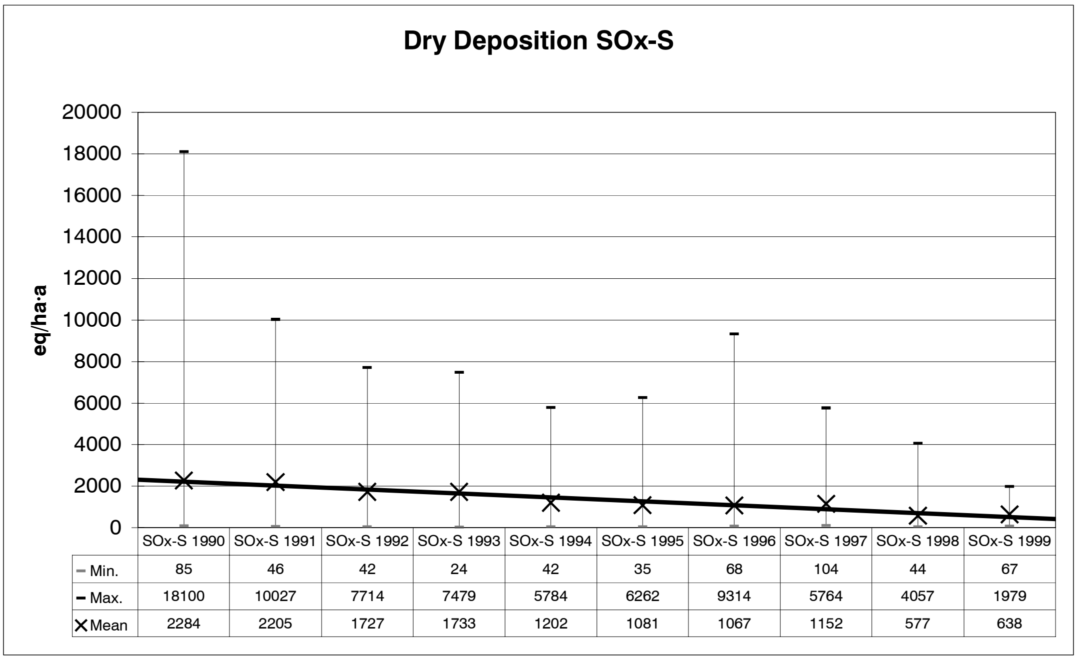

	SOx-S 1990	SOx-S 1991	SOx-S 1992	SOx-S 1993	SOx-S 1994	SOx-S 1995	SOx-S 1996	SOx-S 1997	SOx-S 1998	SOx-S 1999
- Min.	85	46	42	24	42	35	68	104	44	67
- Max.	18100	10027	7714	7479	5784	6262	9314	5764	4057	1979
× Mean	2284	2205	1727	1733	1202	1081	1067	1152	577	638

Figure 5.15: Minimum, maximum and annual mean dry deposition of non-seasalt sulphur (SO_X-$S_{(nss)}$) 1990-1999

The spatial patterns of change in SO_X-$S_{(nss)}$ dry deposition 1990 to 1999 are illustrated in Map 5.2. From the maps it can be seen that regional gradients in magnitude of annual average SO_X-$S_{(nss)}$ dry deposition fluxes become less explicit from 1990 to 1999, which is due to falling maximum values within the whole period (cf. Figure 5.15).

5.6.2.2 Dry deposition of reduced nitrogen (NH_X-N)

There can no trend be found in the annual mean estimates of reduced nitrogen in Germany in the period from 1990 to 1999 (cf. Figure 5.16). The 12% lower NH_X-N dry deposition on Germany in 1999 compared to 1990, which is equal to an absolute reduction of 61.9 kt, 124 eq ha^{-1} a^{-1} or 1.7 kg ha^{-1} a^{-1}, respectively, is more or less within the range of the changes between the single years of the time period considered (cf. Table 5.21). From the maximum values (Figure 5.16) also no trend in one direction can be derived.

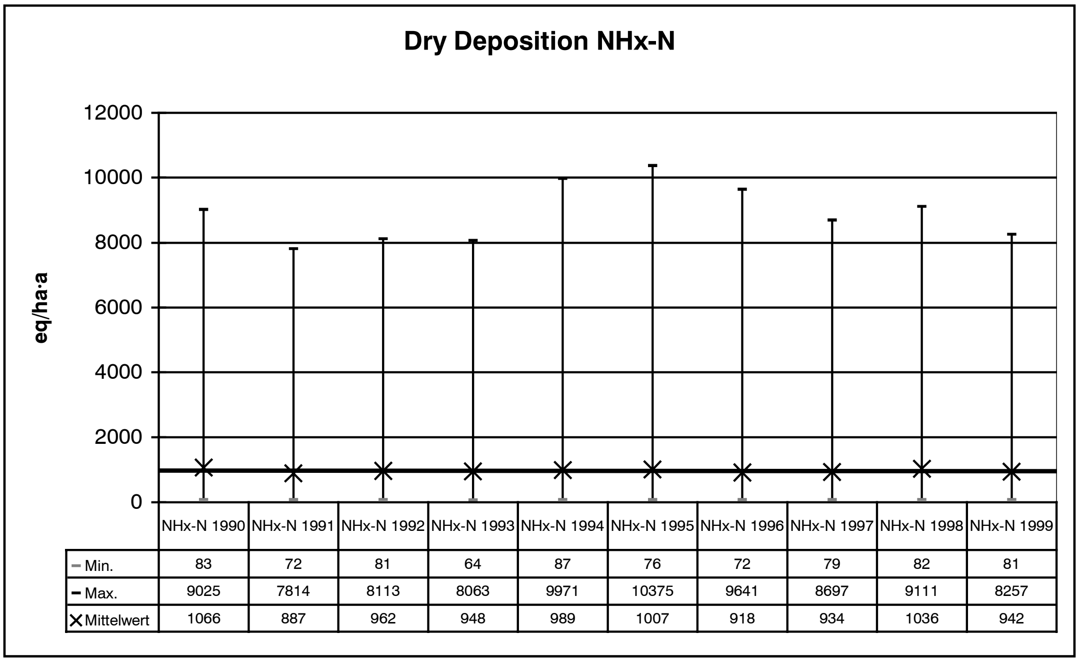

	NHx-N 1990	NHx-N 1991	NHx-N 1992	NHx-N 1993	NHx-N 1994	NHx-N 1995	NHx-N 1996	NHx-N 1997	NHx-N 1998	NHx-N 1999
- Min.	83	72	81	64	87	76	72	79	82	81
- Max.	9025	7814	8113	8063	9971	10375	9641	8697	9111	8257
× Mittelwert	1066	887	962	948	989	1007	918	934	1036	942

Figure 5.16: Minimum, maximum and annual mean dry deposition of reduced nitrogen (NH_X-N) 1990-1999

The overall spatial patterns of NH_X-N dry deposition is presented in Map 5.3. Modelled dry deposition fluxes of NH_X-N in all years are highest in those regions with intensive animal husbandry in the north-western and south-eastern most parts of Germany. Small patterns of locally high NH_X-N dry deposition can be observed in forested areas scattered over all Germany, while (forested) mountain areas remote from agricultural land are less pronounced in these maps compared to e.g. dry deposition of NO_Y-N (Map 5.4). This is due to the shorter range of transport from ammonia emission sources to dry deposition areas, which is taken into account by the emission database used in combination with the EUTREND model applied (cf. Chapter 5.3).

5.6.2.3 Dry deposition of oxidised nitrogen (NO_Y-N)

The change in average modelled dry NO_Y-N deposition between 1990 and 1999 is a decline of 55% (cf. Table 5.21). The annual average modelled NO_Y-N dry deposition only slightly changes between 1990 and 1996, while from 1997 to 1999 a rapid decrease by about 58% can be found, starting from a higher average level than it was in 1990 (Figure 5.17). According to this mapping results the total amount of dry deposited NO_Y-N declined from 327 kt a^{-1} (9.2 kg ha^{-1} a^{-1}) in 1990 by 181 kt (5.2 kg ha^{-1} a^{-1}) to 146 kt a^{-1} (4.1 kg ha^{-1} a^{-1}) in 1999.

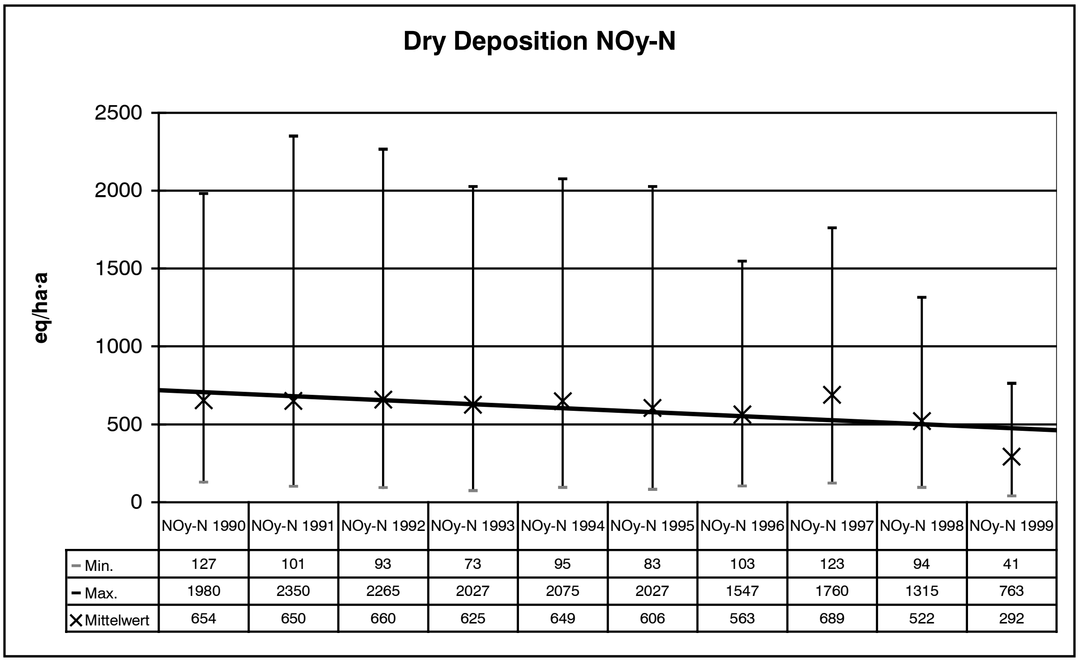

	NOy-N 1990	NOy-N 1991	NOy-N 1992	NOy-N 1993	NOy-N 1994	NOy-N 1995	NOy-N 1996	NOy-N 1997	NOy-N 1998	NOy-N 1999
– Min.	127	101	93	73	95	83	103	123	94	41
– Max.	1980	2350	2265	2027	2075	2027	1547	1760	1315	763
× Mittelwert	654	650	660	625	649	606	563	689	522	292

Figure 5.17: Minimum, maximum and annual mean dry deposition of oxidised nitrogen (NO_Y-N) 1990-1999

The patterns of NO_Y-N dry deposition fluxes are presented in Map 5.3. Generally pronounced in the maps by relative to the surrounding areas high dry deposition loads are urban areas and areas which are situated in higher altitude and forested. Between 1990 and 1996 only small changes in the spatial distribution and magnitude of the NO_Y-N dry deposition loads can be found. From 1997 to 1999 an overall decline of dry deposition of NO_Y-N can be found, which is mainly due to the trend in air concentration input data (cf. Chapter 6,2).

5.6.2.4 Dry deposition of total nitrogen (N= NH_X-N + NO_Y-N)

Annual average dry deposition of total nitrogen, calculated as the sum of reduced and oxidised nitrogen compounds (N= NH_X-N + NO_Y-N), over Germany from 1990 to 1999 declined by 28%. The total amount of dry deposited nitrogen declined from 860 kt a^{-1} (24.1 kg ha^{-1} a^{-1}) in 1990 by 243 kt (6.8 kg ha^{-1} a^{-1}) to 617 kt a^{-1} (17,3 kg ha^{-1} a^{-1}) 1999 (cf. Figure 5.16). The trend of reduction is not very obvious, since the annual changes of average dry deposition of N between 1990 and 1998 are ranging between +9.6% and –10.6% (cf. Table 5.21). Only from 1990 to 1999 the reduction is by about -20.1%, which is mainly due to the reduction in modelled reduced nitrogen dry deposition (Chapter 5.6.2.3).

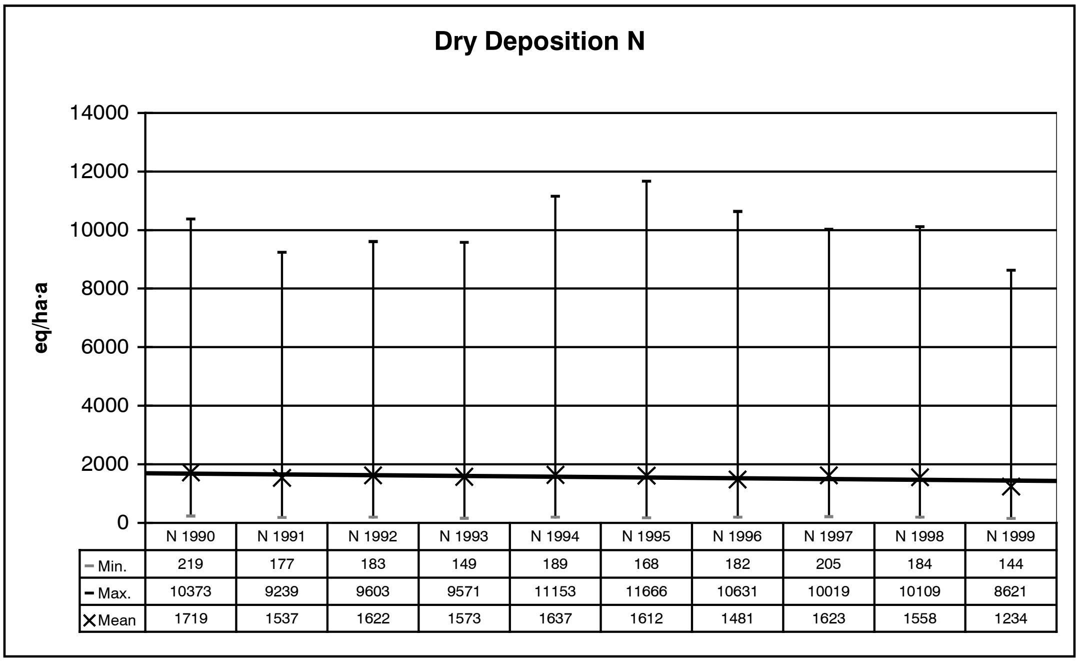

	N 1990	N 1991	N 1992	N 1993	N 1994	N 1995	N 1996	N 1997	N 1998	N 1999
– Min.	219	177	183	149	189	168	182	205	184	144
– Max.	10373	9239	9603	9571	11153	11666	10631	10019	10109	8621
× Mean	1719	1537	1622	1573	1637	1612	1481	1623	1558	1234

Figure 5.18: Minimum, maximum and annual mean dry deposition of total nitrogen (N) 1990-1999

Table 5.22: Average NH_X-N and NO_Y-N fraction of dry deposited total N

Average fraction of nitrogen (N) dry deposition	**1990**	**1991**	**1992**	**1993**	**1994**	**1995**	**1996**	**1997**	**1998**	**1999**
mean fraction of NH_X –N	62.0%	57.7%	59.3%	60.2%	60.4%	62.4%	62.0%	57.6%	66.5%	76.3%
mean fraction of NO_Y –N	38.0%	42.3%	40.7%	39.8%	39.6%	37.6%	38.0%	42.4%	33.5%	23.7%
total	100%	100%	100%	100%	100%	100%	100%	100%	100%	100%

The average fractions of reduced and oxidised nitrogen to total dry deposited nitrogen is listed in Table 5.22. Over the whole time period considered NH_X-N and NO_Y-N contribute with average 62% and 38% (5/8 and 3/8), respectively, to total dry deposited nitrogen. The average fraction of NH_X-N is around 60%, of NO_Y-N around 40% between 1990 and 1997, respectively, whereas from 1998 to 1999 it is changing to 76% NH_X-N and 24% NO_Y-N. The latter is due to changes in the air concentration input data to the model calculations (cf. Chapter 6.2).

The spatial patterns of N dry deposition are presented in Map 5.4. Regions of higher dry deposition of total nitrogen in all the years are found in the north-west and south-east of Germany, while regions of lower values are found in a band reaching from the south-west of Germany over the centre to the Baltic Sea and the north-east. The observable scatter of small peak value patterns can be identified as higher altitude and/or forested areas.

5.6.2.5 Dry deposition of potential acidity ($AC_{pot} = S_{(nss)} + N$)

Dry deposition of potential acidity is calculated as sum of non-seasalt sulphur and total nitrogen ($AC_{pot} = S_{(nss)} + N$). The average dry deposition fluxes of AC_{pot} from 1990 to 1999 have diminished by about 53% (cf. Table 5.24). This is equal to a reduction by average 2131 eq ha^{-1} a^{-1} from 4003 eq ha^{-1} a^{-1} in 1990 to 1872 eq ha^{-1} a^{-1} in 1999 (Figure 5.19). The spatial patterns of AC_{pot} dry deposition are presented in Map 5.6.

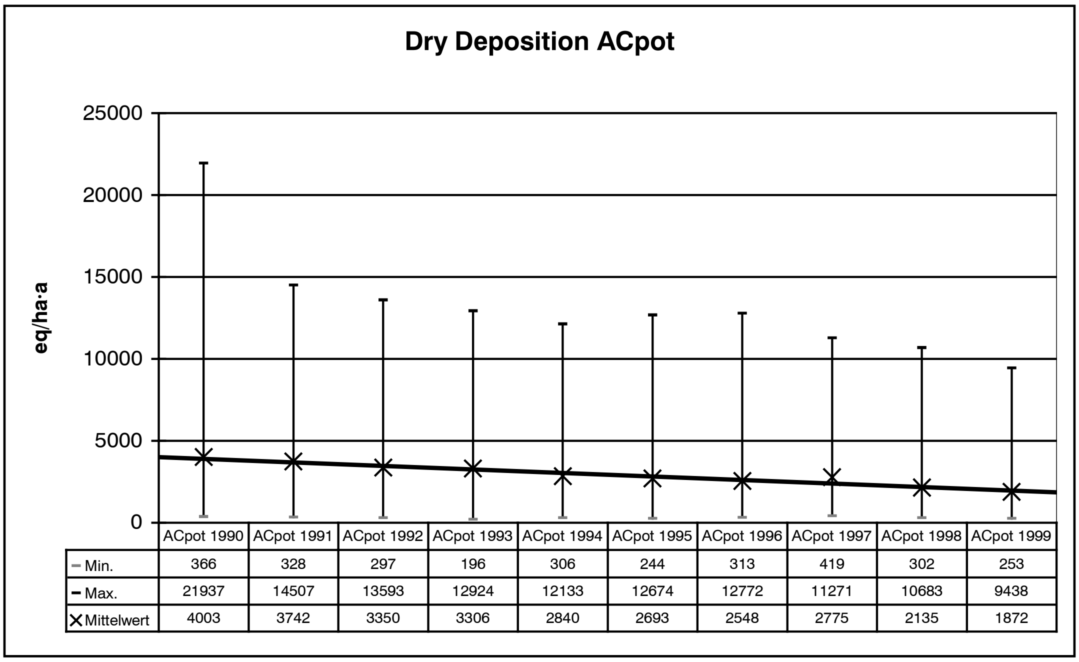

	ACpot 1990	ACpot 1991	ACpot 1992	ACpot 1993	ACpot 1994	ACpot 1995	ACpot 1996	ACpot 1997	ACpot 1998	ACpot 1999
– Min.	366	328	297	196	306	244	313	419	302	253
– Max.	21937	14507	13593	12924	12133	12674	12772	11271	10683	9438
× Mittelwert	4003	3742	3350	3306	2840	2693	2548	2775	2135	1872

Figure 5.19: Minimum, maximum and annual mean dry deposition of potential acidity (AC_{pot}) 1990-1999

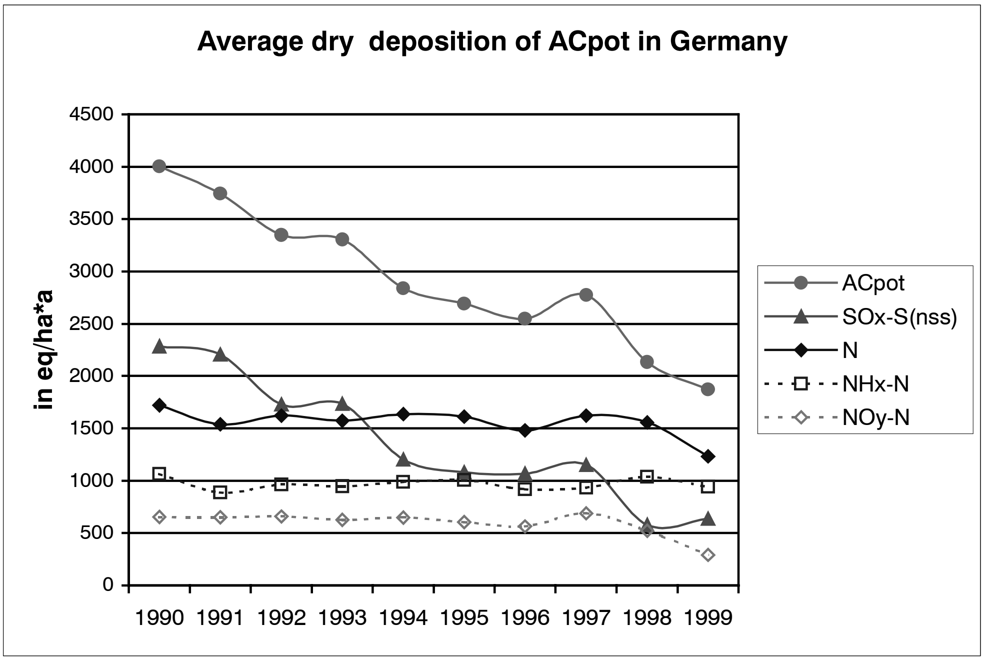

Figure 5.20: Average dry deposition of AC_{pot} and its compounds in Germany 1990-1999

The annual average composition of the dry fluxes of AC_{pot} in Germany 1990 to 1999 is shown in Figure 5.20, the average fractions of the single compounds of AC_{pot} are listed in Table 5.23.

From the curves in Figure 2.20 it clearly can be seen, that from 1994 on, due to the falling dry SO_X-$S_{(nss)}$ fluxes, N has taken over the role of the main acidifying compound, and in 1998 and 1999 the average modelled estimates of NH_X-N are higher than those of SO_X-$S_{(nss)}$.

Table 5.23: Average fractions of acidifying compounds of dry deposition 1990-1999

Average fraction of...	**1990**	**1991**	**1992**	**1993**	**1994**	**1995**	**1996**	**1997**	**1998**	**1999**
SO_X-$S_{(nss)}$ in eq ha^{-1} a^{-1}	2284	2205	1727	1733	1202	1081	1067	1152	577	638
SO_X-$S_{(nss)}$ as % of the total ACpot dry deposition	57%	59%	52%	52%	42%	40%	42%	42%	27%	34%
N in eq ha^{-1} a^{-1}	1719	1537	1622	1573	1637	1612	1481	1623	1558	1234
N as % of the total AC_{pot} dry deposition	43%	41%	48%	48%	58%	60%	58%	58%	73%	66%
NH_X-N in eq ha^{-1} a^{-1}	1066	887	962	948	989	1007	918	934	1036	942
NH_X-N as % of the total AC_{pot} dry deposition	27%	24%	29%	29%	35%	37%	36%	34%	49%	50%
NO_Y-N in eq ha^{-1} a^{-1}	654	650	660	625	649	606	563	689	522	292
NO_Y-N as % of the total AC_{pot} dry deposition	16%	17%	20%	19%	23%	22%	22%	25%	24%	16%

5.6.2.6 Dry deposition of potential net-acidity ($AC_{pot(net)}=(S_{(nss)}+N+Cl_{(nss)})-BC_{(nss)}$) and acid neutralisation ($=BC_{(nss)}\cdot 100/AC_{pot}$ [%])

Potential net acidity is calculated by subtracting the fluxes of non-seasalt base cations ($BC_{(nss)}$) from the sum of potential acidifying compounds (AC_{pot}) in order to account for potential acid neutralisation (cf. Chapter 2). Hence dry deposition loads of $AC_{pot(net)}$ are lower than dry deposition loads of AC_{pot}. The difference between the average dry deposition of $AC_{pot(net)}$ in 1990 and in 1999 is a 55% (2011 eq ha^{-1} a^{-1}) lower flux (Figure 5.21, Table 5.24).

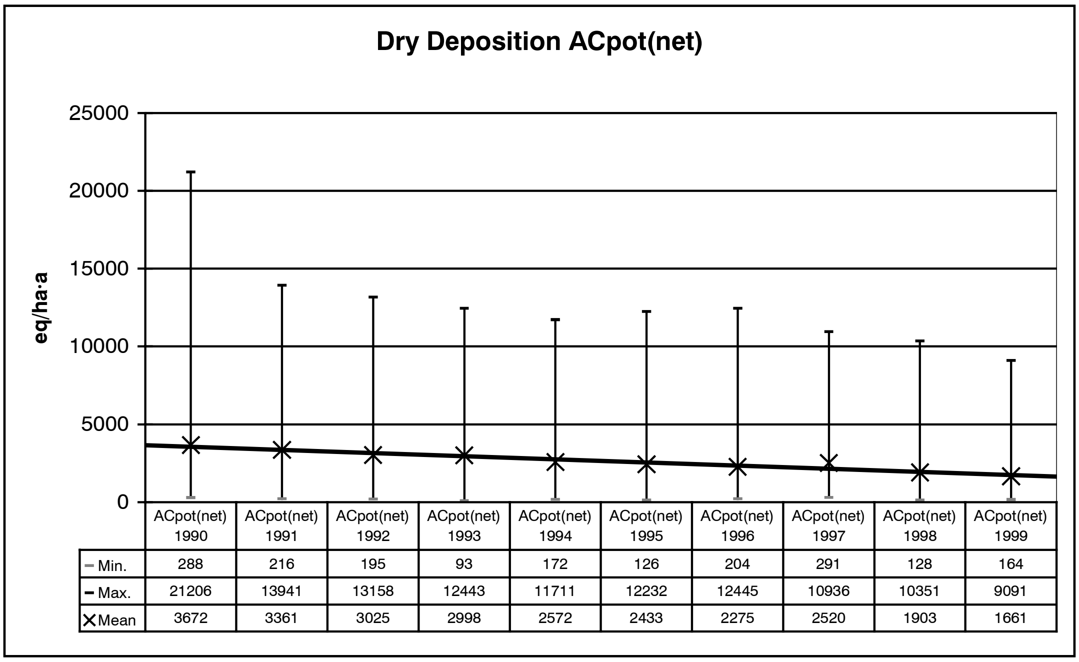

	ACpot(net) 1990	ACpot(net) 1991	ACpot(net) 1992	ACpot(net) 1993	ACpot(net) 1994	ACpot(net) 1995	ACpot(net) 1996	ACpot(net) 1997	ACpot(net) 1998	ACpot(net) 1999
- Min.	288	216	195	93	172	126	204	291	128	164
- Max.	21206	13941	13158	12443	11711	12232	12445	10936	10351	9091
× Mean	3672	3361	3025	2998	2572	2433	2275	2520	1903	1661

Figure 5.21: Minimum, maximum and annual mean dry deposition of potential net acidity ($AC_{pot(net)}$) 1990-1999

Acid neutralisation by dry deposition of non-seasalt base cations ($BC_{(nss)}$) in the period 1990-1999 is shown in Figure 5.22. The annual average values of acid neutralisation are rising from 9% in 1990 to 12% in 1999. The spatial patterns of $AC_{pot(net)}$ are shown in Map 5.7, acid neutralisation by dry deposition of $BC_{(nss)}$ 1990 to 1999 are presented in Map 5.8, respectively.

Budgets of average dry deposition of AC_{pot}, $AC_{pot(net)}$ and acid neutralisation by $BC_{(nss)}$ within the ten years period considered are listed in Table 5.26.

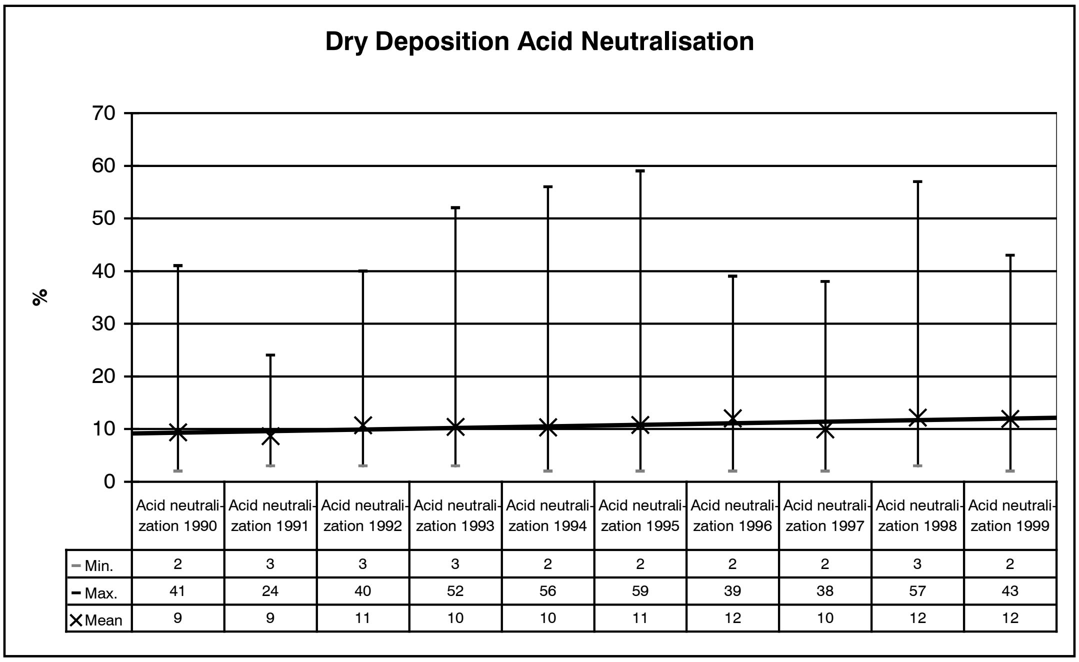

	Acid neutralization 1990	Acid neutralization 1991	Acid neutralization 1992	Acid neutralization 1993	Acid neutralization 1994	Acid neutralization 1995	Acid neutralization 1996	Acid neutralization 1997	Acid neutralization 1998	Acid neutralization 1999
Min.	2	3	3	3	2	2	2	2	3	2
Max.	41	24	40	52	56	59	39	38	57	43
× Mean	9	9	11	10	10	11	12	10	12	12

Figure 5.22: Minimum, maximum and annual mean dry deposition of acid neutralisation 1990-1999

Table 5.24: Budgets of average annual dry deposition of AC_{pot}, $AC_{pot(net)}$ and acid neutralisation by $BC_{(nss)}$ in Germany 1990-1999

Dry Deposition	AC_{pot} [eq ha^{-1} a^{-1}]	% change from previous year	$AC_{pot(net)}$ [eq ha^{-1} a^{-1}]	% change from previous year	$BC_{(nss)}$ [eq ha^{-1} a^{-1}]	% change from previous year	Acid neutralisation [%]
1990	4003		3672		331		9
1991	3742	-6.5	3361	-8.5	382	+15.3	9
1992	3350	-10.5	3025	-10.0	325	-14.9	11
1993	3306	-1.3	2998	-0.9	307	-5.4	10
1994	2840	-14.1	2572	-14.2	268	-12.8	10
1995	2693	-5.2	2433	-5.4	260	-2.7	11
1996	2548	-5.4	2275	-6.5	273	+4.7	12
1997	2775	+8.9	2520	+10.7	255	-6.5	10
1998	2135	-23.1	1903	-24.5	231	-9.3	12
1999	1872	-12.3	1661	-12.7	211	-9.0	12
% change from 1990 to 1999		-53		-55		-36	

From the data presented in Table 5.24 it can be seen that the decline of average dry deposition fluxes of potential Acidity (1990-99: -53%) is faster than the decline of non-seasalt base cations (-36%) over the same time period, hence the decline of potential net acidity (1990-99: -55%) is slightly faster than of potential acidity, since acid neutralisation is rising from 9% in 1990 to 12% in 1999 (cf. Figure 5.22).

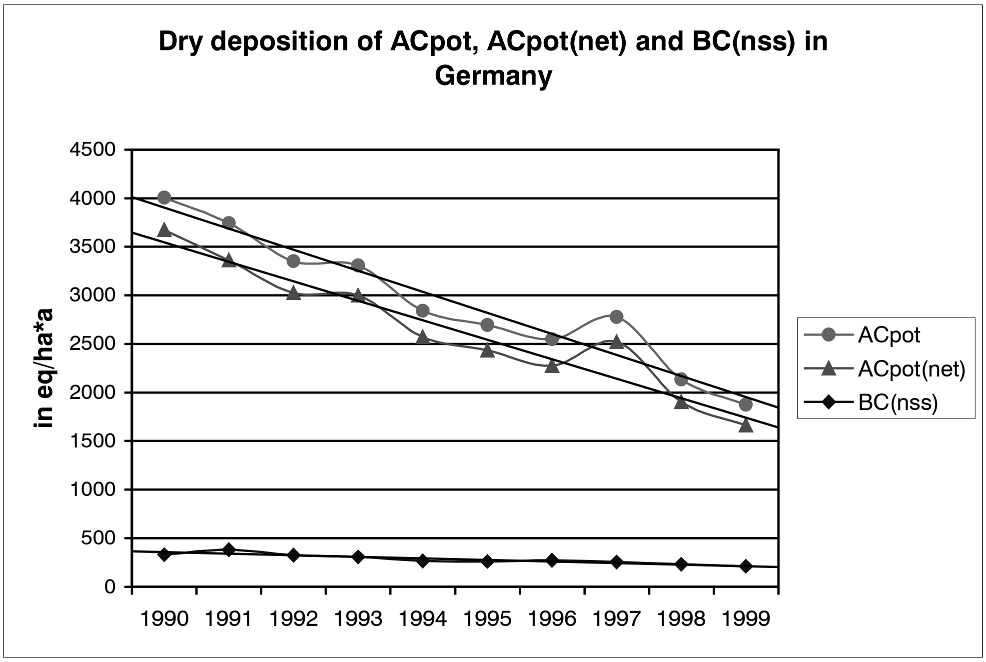

Figure 5.22: Average dry deposition of AC_{pot}, $AC_{pot(net)}$, and $BC_{(nss)}$ in Germany 1990-1999

5.7 Maps of dry deposition 1990-1999

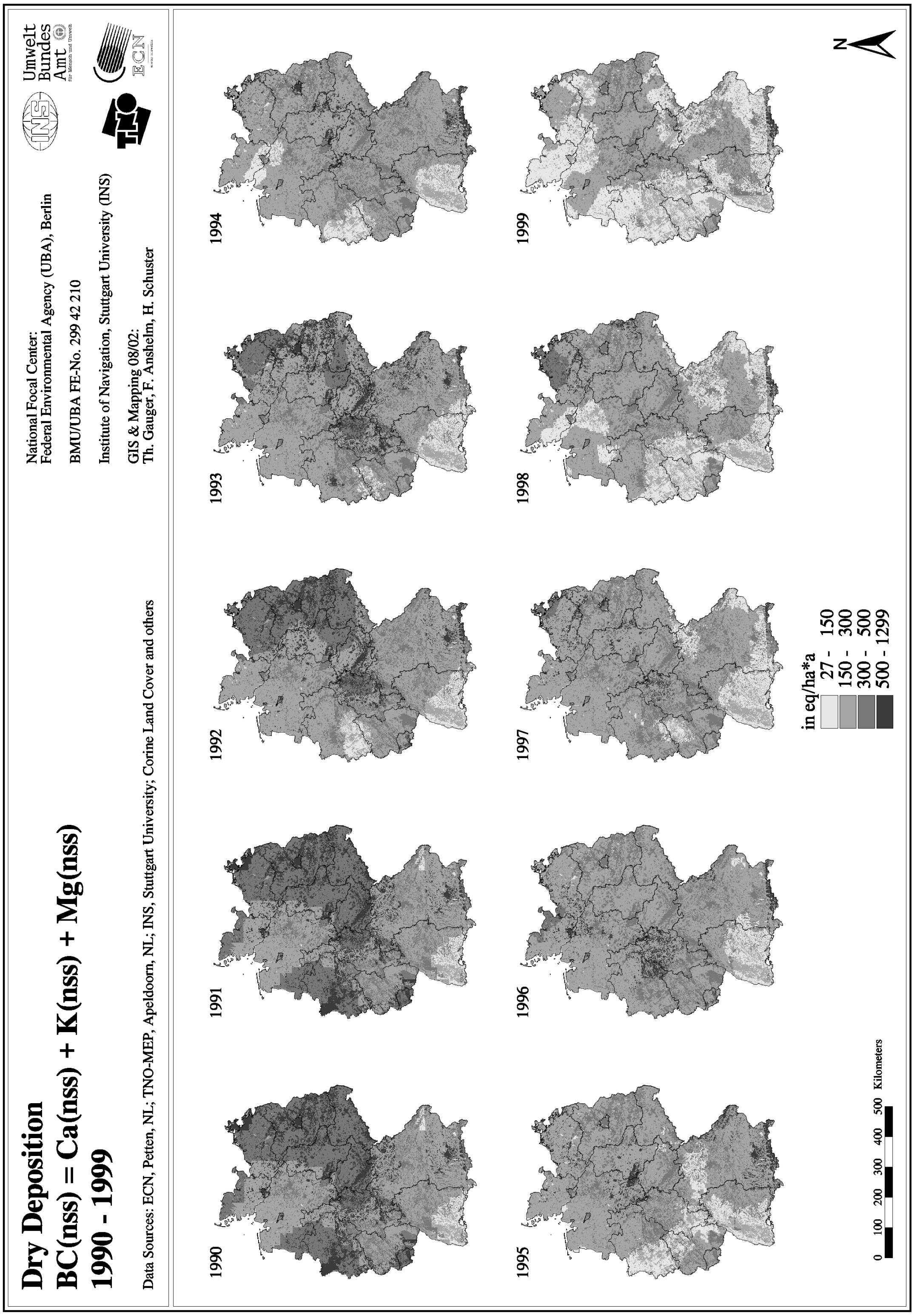

Map 5.1: Dry deposition of $BC_{(nss)}$ 1990-1999

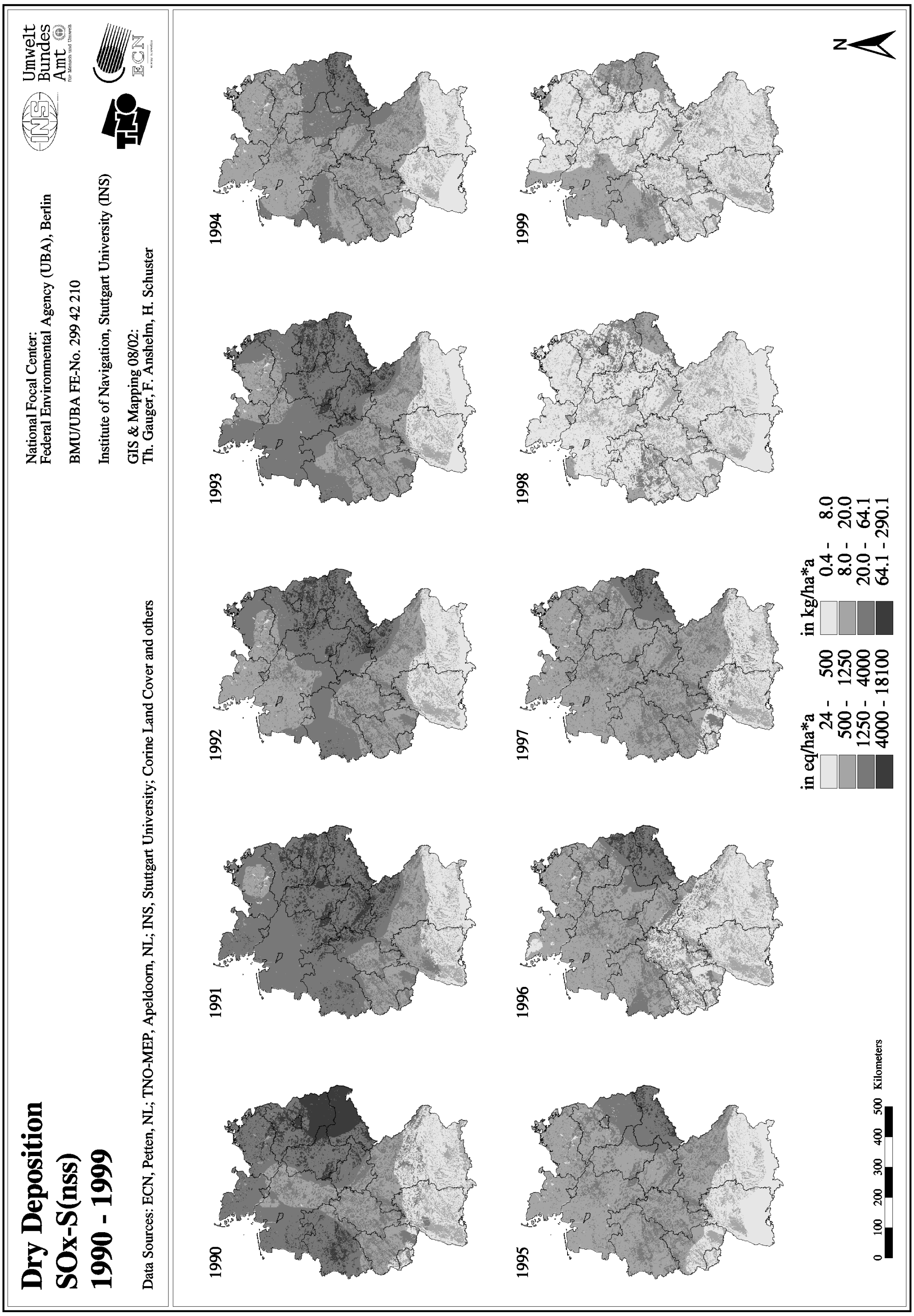

Map 5.2: Dry deposition of SO_X-S 1990-1999

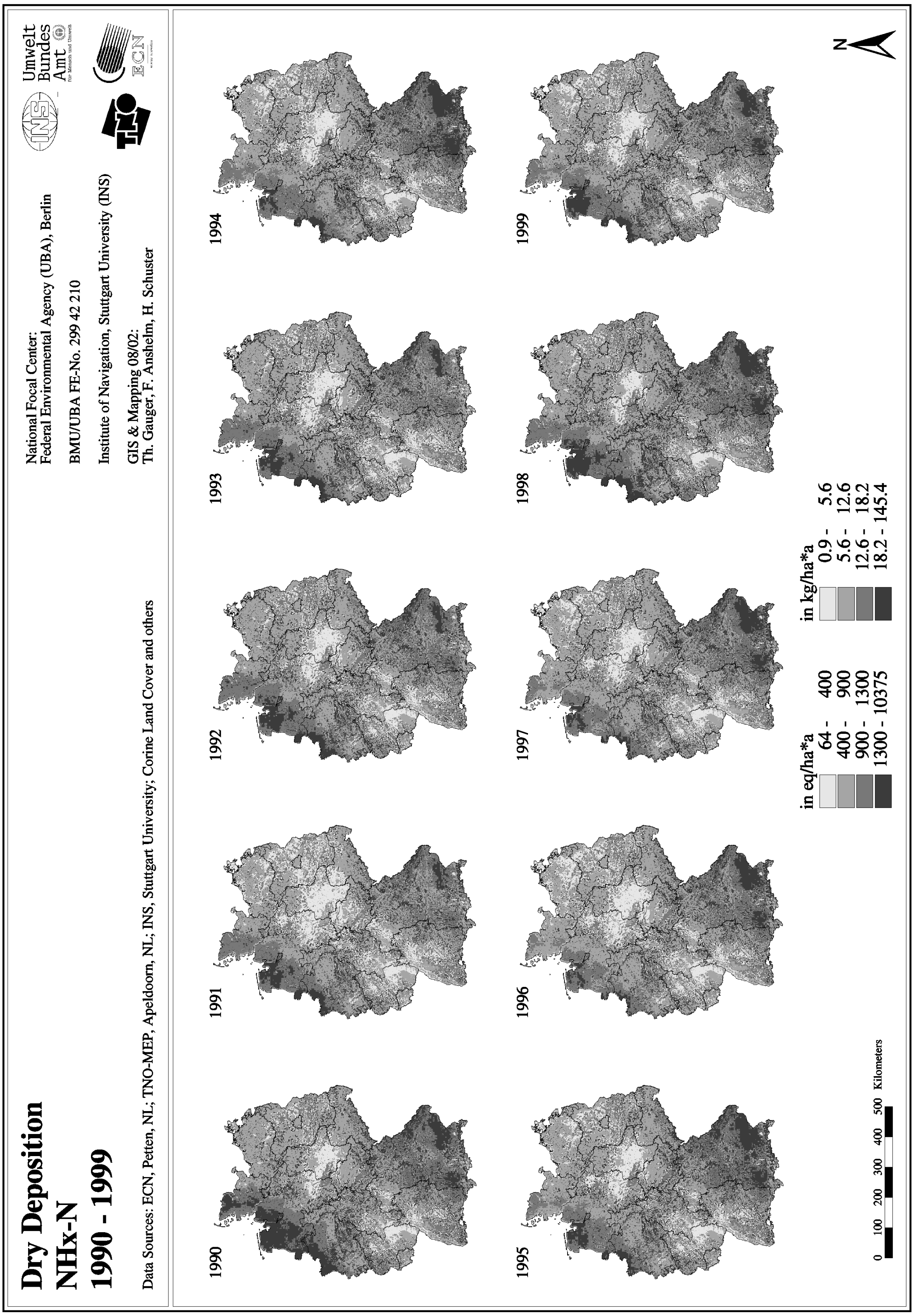

Map 5.3: Dry deposition of NH_X-N 1990-1999

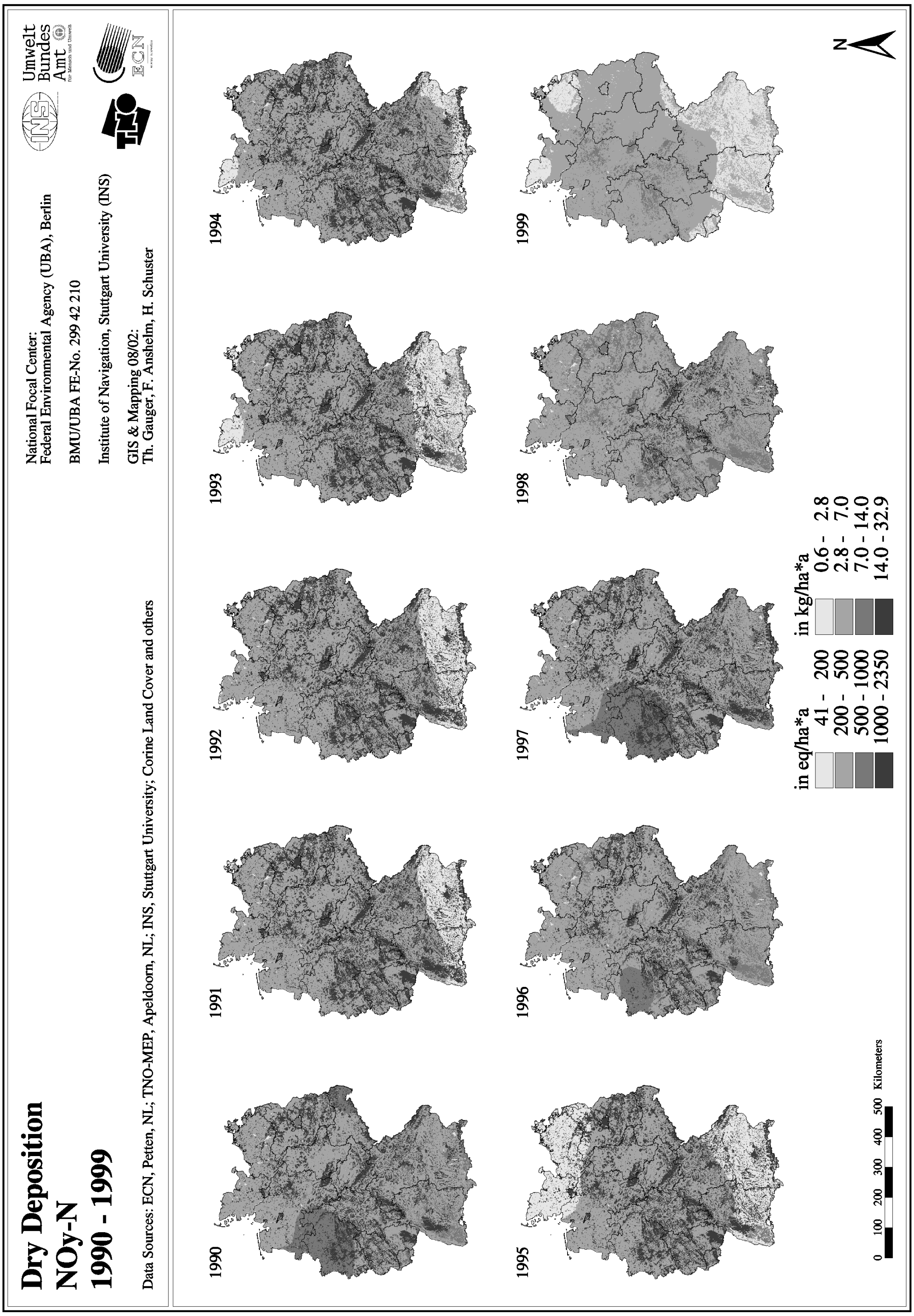

Map 5.4: Dry deposition of NO_Y-N 1990-1999

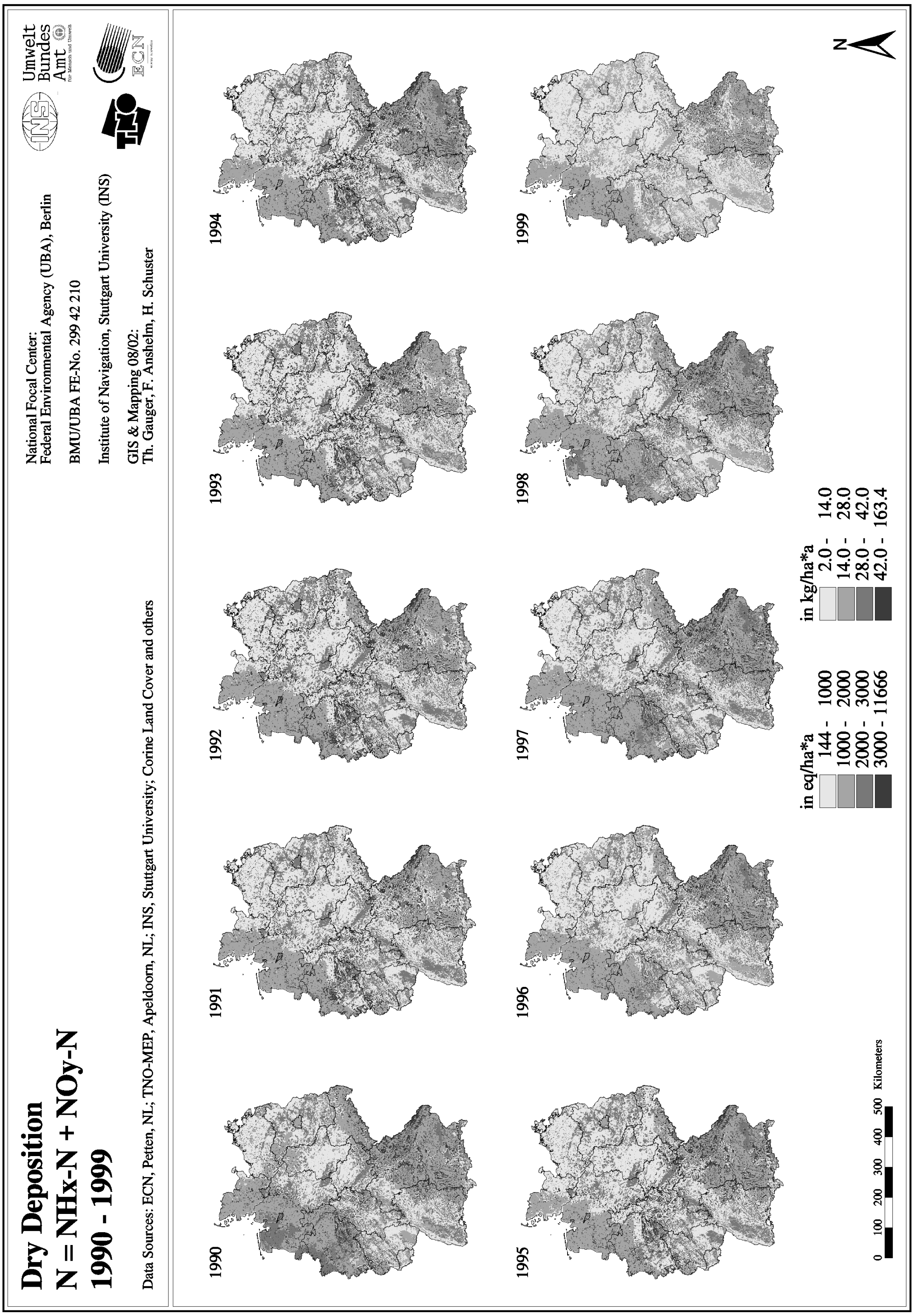

Map 5.5: Dry deposition of N 1990-1999

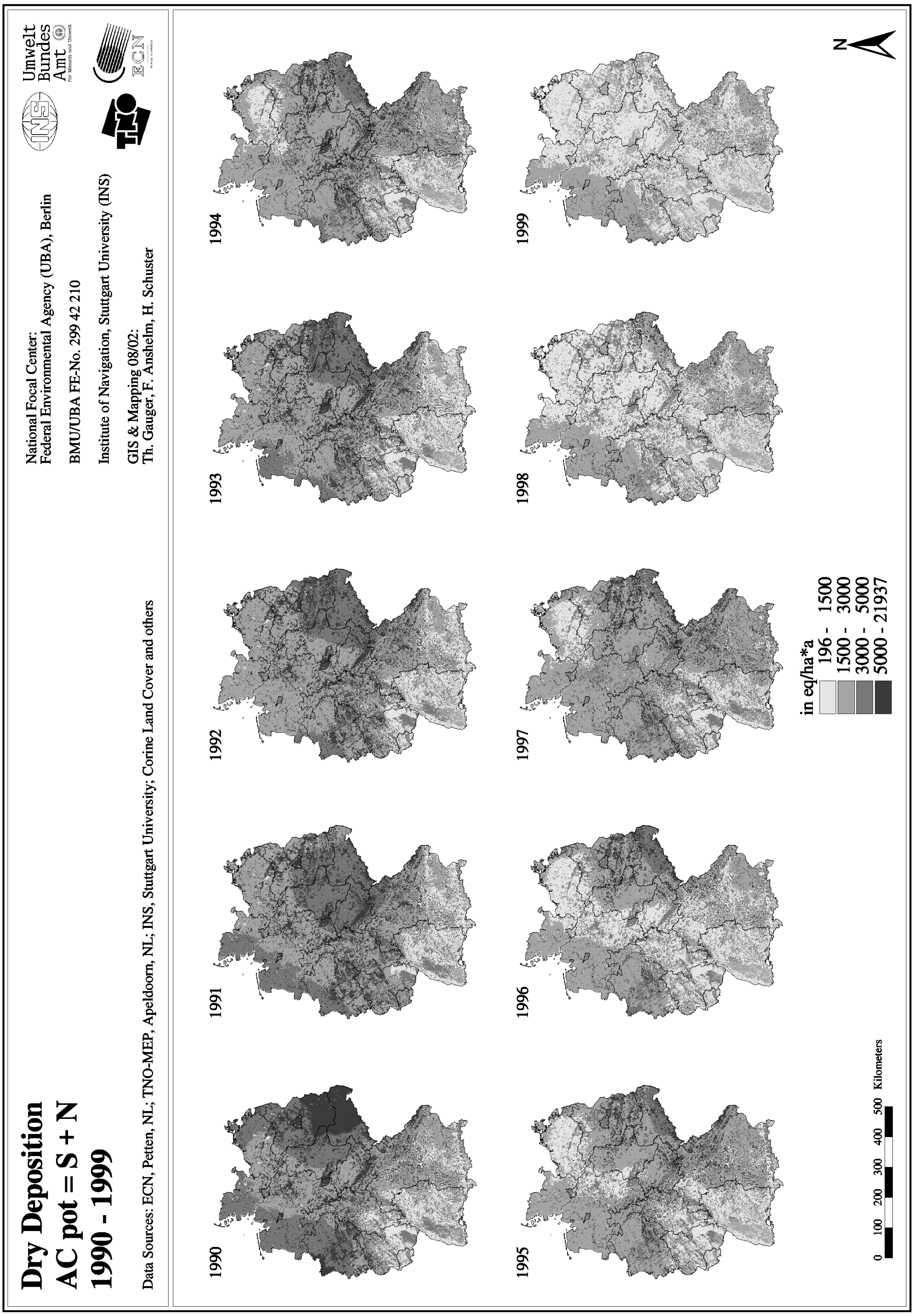

Map 5.6: Dry deposition of AC_{pot} 1990-1999

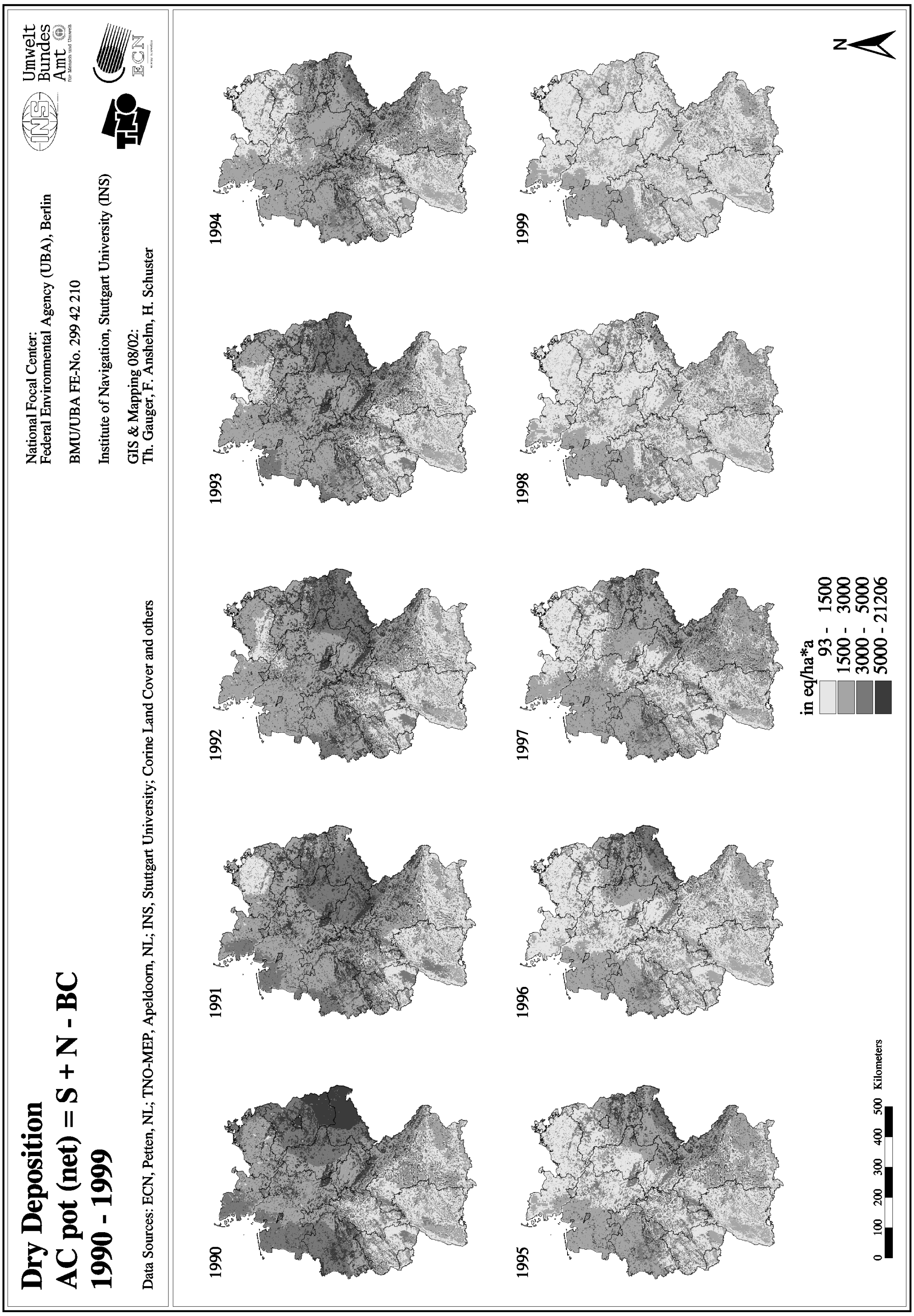

Map 5.7: Dry deposition of $AC_{pot(net)}$ 1990-1999

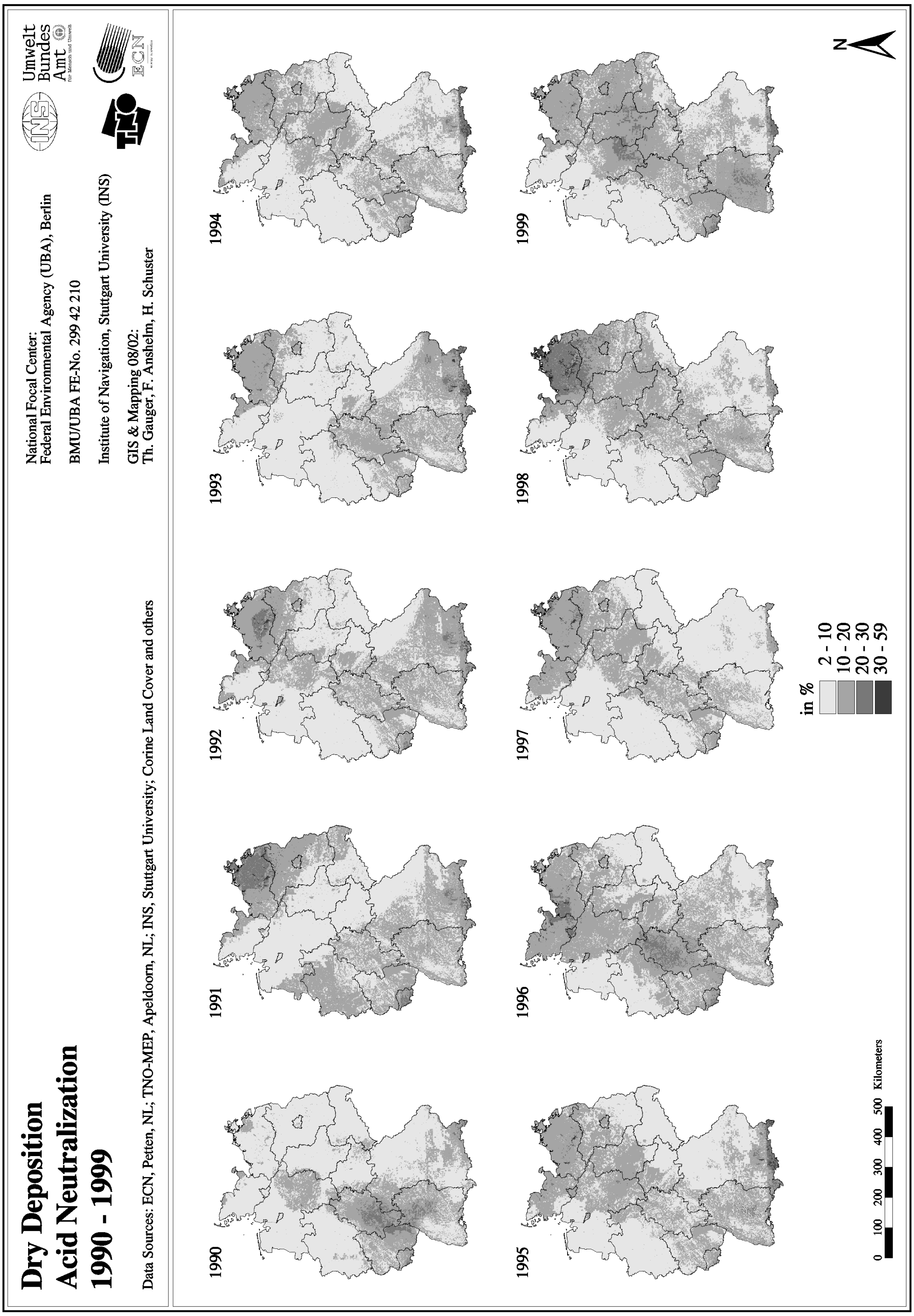

Map 5.8: Neutralisation of dry deposited AC_{pot} by $BC_{(nss)}$ 1990-1999

6 Total deposition 1990-1999

Maps of total deposition in this study is calculated as the sum of wet and dry deposition fluxes. Though a IDEM cloud deposition module has been developed and preliminary cloud deposition maps have been modelled, it was decided not to include cloud deposition for the calculation of 1990-1999 total deposition maps, because liquid water content (LWC) within this project could be made available only for the year 1998 (cf. Chapter 5.2).

6.1 Total deposition mapping results

An overview on all total deposition maps calculated for the period 1990-1999 within this study is given in Table 6.1. In order to calculate exceedances of Critical Loads for nutrient nitrogen, acidity and net acidity (cf. Chapter 2) it is necessary to calculate dry deposition fields of total nitrogen (N) of potential acidity (Ac_{pot}), the sum of base cations (BC, $BC_{(nss)}$), and potential net acidity ($AC_{pot(net)}$).

Table 6.1: Maps of Total deposition 1990-1999

Total Deposition	**1990**	**1991**	**1992**	**1993**	**1994**	**1995**	**1996**	**1997**	**1998**	**1999**
SO_X-$S_{(nss)}$	**X**	**X**	**X**	**X**	**X**	**X**	**X**	**X**	**X**	**X**
NO_Y-N	**X**	**X**	**X**	**X**	**X**	**X**	**X**	**X**	**X**	**X**
NH_X-N	**X**	**X**	**X**	**X**	**X**	**X**	**X**	**X**	**X**	**X**
Ca, $Ca_{(nss)}$	**X**	**X**	**X**	**X**	**X**	**X**	**X**	**X**	**X**	**X**
Mg, $Mg_{(nss)}$	**X**	**X**	**X**	**X**	**X**	**X**	**X**	**X**	**X**	**X**
K, $K_{(nss)}$	**X**	**X**	**X**	**X**	**X**	**X**	**X**	**X**	**X**	**X**
Na	**X**	**X**	**X**	**X**	**X**	**X**	**X**	**X**	**X**	**X**
N = $(NO_3\text{-}N + NH_4\text{-}N)$	**X**	**X**	**X**	**X**	**X**	**X**	**X**	**X**	**X**	**X**
Potential Acidity $AC_{pot} = (S_{(nss)} + N)$	**X**	**X**	**X**	**X**	**X**	**X**	**X**	**X**	**X**	**X**
BC = $(Ca + K + Mg)$, $BC_{(nss)} = (Ca_{(nss)} + K_{(nss)} + Mg_{(nss)})$	**X**	**X**	**X**	**X**	**X**	**X**	**X**	**X**	**X**	**X**
Potential Net Acidity $AC_{pot\ (net)} = ((S_{(nss)} + N) - BC_{(nss)})$	**X**	**X**	**X**	**X**	**X**	**X**	**X**	**X**	**X**	**X**
$_{(nss)}$ =non-seasalt (sea salt corrected)	**X = processed**									

The main results of the total deposition mapping calculations are presented in the following subchapters (Chapter 6.2 and 6.3) and are illustrated by the graphical representation of the modelled total deposition data sets (maps) in Chapter 6.4.

6.1.1 Total deposition and trends of base cations (BC = Ca + K + Mg)

Total deposition of base cations (BC) is calculated by summing up the wet and dry deposition fluxes of Ca, K and Mg. The annual average modelled total deposition of BC and its components 1990-1999 including percentage changes is listed in Table 6.2. Table 6.3 shows 1990-1999 annual average modelled total deposition and its changes for non-sea salt base cations ($BC_{(nss)}$).

Table 6.2: Budgets of average annual total deposition of Ca, Mg, K and BC in Germany 1990-1999

Total Deposition	**Ca [eq ha^{-1} a^{-1}]**	**% change from previous year**	**K [eq ha^{-1} a^{-1}]**	**% change from previous year**	**Mg [eq ha^{-1} a^{-1}]**	**% change from previous year**	**BC [eq ha^{-1} a^{-1}]**	**% change from previous year**
1990	411		175		163		749	
1991	453	+10,3	177	+1,0	149	-9,2	778	+3,9
1992	373	-17,6	179	+1,2	128	-14,1	680	-12,7
1993	380	+1,8	164	-8,3	140	+10,0	684	+0,7
1994	341	-10,3	142	-13,8	127	-9,8	609	-11,0
1995	280	-17,9	166	+17,2	129	+1,6	574	-5,7
1996	272	-2,5	154	-7,1	111	-13,8	538	-6,4
1997	277	+1,5	140	-9,2	105	-5,6	521	-3,0
1998	278	+0,5	140	-0,3	104	-1,1	521	-0,0
1999	251	-9,7	122	-12,7	105	+1,2	478	-8,3
% change from 1990 to 1999		-39		-30		-36		-36

Table 6.3: Budgets of average annual total deposition of $Ca_{(nss)}$, $Mg_{(nss)}$, $K_{(nss)}$ and $BC_{(nss)}$ in Germany 1990-1999

Total Deposition	**$Ca_{(nss)}$ [eq ha^{-1} a^{-1}]**	**% change from previous year**	**$K_{(nss)}$ [eq ha^{-1} a^{-1}]**	**% change from previous year**	**$Mg_{(nss)}$ [eq ha^{-1} a^{-1}]**	**% change from previous year**	**$BC_{(nss)}$ [eq ha^{-1} a^{-1}]**	**% change from previous year**
1990	381		146		39		566	
1991	433	+13,5	154	+5,9	44	-11,3	632	+11.6
1992	353	-18,4	158	+2,5	30	-12,8	541	-14.3
1993	359	+1,6	143	-9,7	32	+7,9	534	-1.3
1994	320	-10,8	120	-15,8	26	-18,5	467	-12.6
1995	257	-19,8	143	+18,5	22	-18,3	421	-9.8
1996	257	-0,0	137	-3,8	33	+50,8	426	+1.3
1997	260	+1,3	122	-10,8	24	-26,4	406	-4.7
1998	259	-0,3	121	-1,2	14	-41,7	394	-3.0
1999	231	-10,9	101	-16,7	14	-1,2	345	-12.3
% change from 1990 to 1999		-39		-31		-64		-39

A decline, both for BC and $BC_{(nss)}$ total deposition can be observed, starting in 1991 (Table 6.2 and 6.3). Figure 6.1 shows a graph of average $BC_{(nss)}$ total deposition and its compounds 1990 to 1999 in order to illustrate the trend of decline within this time period.

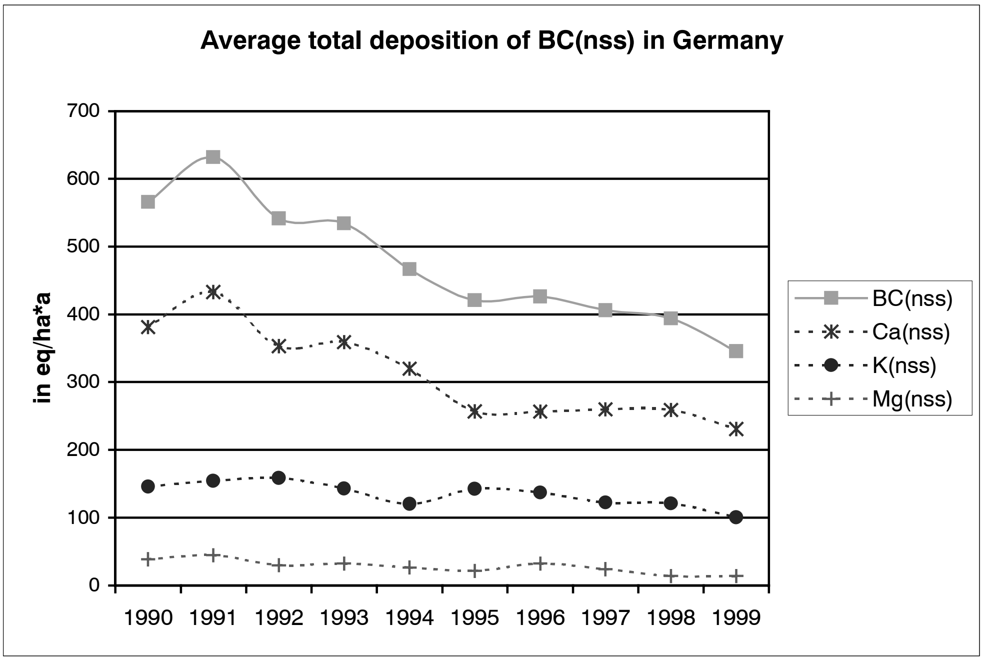

Figure 6.1: Average total deposition of non-seasalt base cations and its compounds ($BC_{(nss)} = Ca_{(nss)} + K_{(nss)} + Mg_{(nss)}$) in Germany 1990-1999

6.1.1.1 Total deposition of non-seasalt base cations (BC$_{(nss)}$)

Average total deposition of non-seasalt base cations (BC$_{(nss)}$) declined by 39% between 1990 and 1999. The absolute decrease was by 221 eq ha^{-1} a^{-1} from average 566 eq ha^{-1} a^{-1} in 1990 to 345 eq ha^{-1} a^{-1}in 1999 (Figure 6.2). The decline can not be observed continuously over the whole time period. From 1990 to 1991 rising average, minimum and maximum values, can be found, mainly due to rising Ca$_{(nss)}$ total deposition (cf. Figure 6.1). A stagnation can be observed in 1993 and again in 1996.

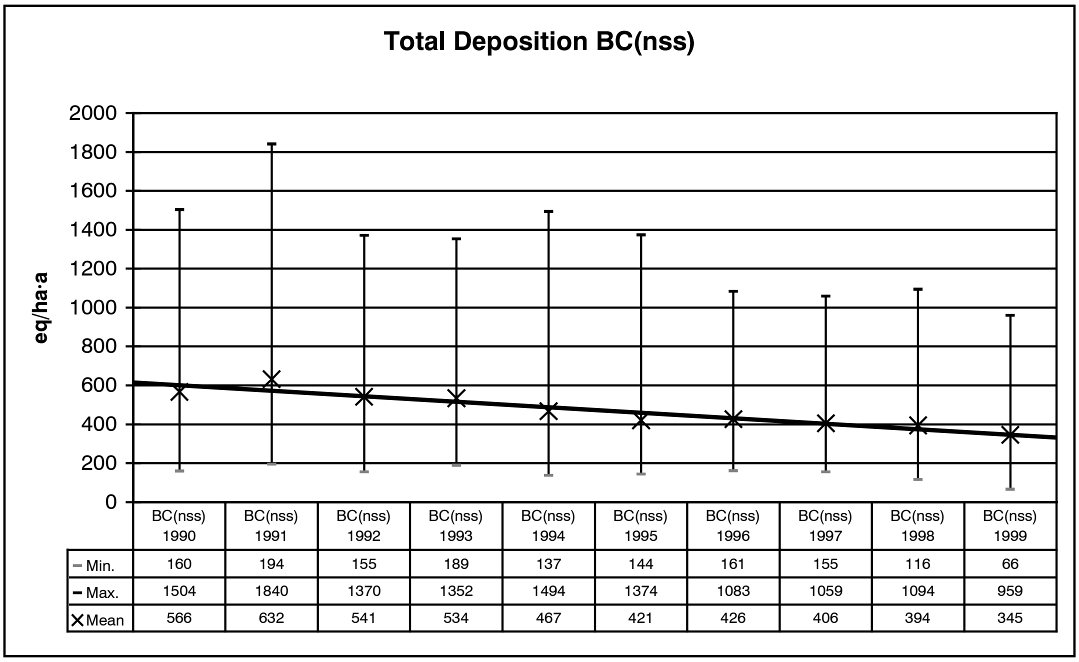

	BC(nss) 1990	BC(nss) 1991	BC(nss) 1992	BC(nss) 1993	BC(nss) 1994	BC(nss) 1995	BC(nss) 1996	BC(nss) 1997	BC(nss) 1998	BC(nss) 1999
– Min.	160	194	155	189	137	144	161	155	116	66
– Max.	1504	1840	1370	1352	1494	1374	1083	1059	1094	959
× Mean	566	632	541	534	467	421	426	406	394	345

Figure 6.2: Minimum, maximum and annual mean total deposition of non-seasalt base cations (BC$_{(nss)}$ = Ca$_{(nss)}$ + K$_{(nss)}$ + Mg$_{(nss)}$) 1990-1999

The average seasalt fraction of BC total deposition is shown in Table 6.4. Over the whole ten years period average 23% of BC total deposition are of marine origin.

Table 6.4: Average seasalt fraction of base cation total deposition 1990-1999

Average seasalt fraction of BC total deposition	**1990**	**1991**	**1992**	**1993**	**1994**	**1995**	**1996**	**1997**	**1998**	**1999**
in eq ha^{-1} a^{-1}	183	147	138	150	142	153	111	115	127	132
% of BC total deposition	24.5%	18.8%	20.3%	22.0%	23.3%	26.7%	20.7%	22.1%	24.4%	27.7%

The average fraction of wet and dry deposited $BC_{(nss)}$ total deposition is given in Table 6.5. On average over the whole period 1990 to1999 about 40% of $BC_{(nss)}$ are deposited with the wet deposition flux and about 60% are deposited dry.

Table 6.5: Average wet and dry fraction of non-seasalt base cation total deposition 1990-1999

Average wet and dry fraction of $BC_{(nss)}$ total deposition	**1990**	**1991**	**1992**	**1993**	**1994**	**1995**	**1996**	**1997**	**1998**	**1999**
$BC_{(nss)}$ wet deposition in eq ha^{-1} a^{-1}	235	250	217	227	199	161	154	151	163	135
BC wet deposition as % fraction of BC total deposition	*42%*	*40%*	*40%*	*42%*	*43%*	*38%*	*36%*	*37%*	*41%*	*39%*
$BC_{(nss)}$ dry deposition in eq ha^{-1} a^{-1}	331	382	325	307	268	260	273	255	231	211
BC dry deposition as % fraction of BC total deposition	*58%*	*60%*	*60%*	*58%*	*57%*	*62%*	*64%*	*63%*	*59%*	*61%*
$BC_{(nss)}$ total deposition in eq ha^{-1} a^{-1}	566	632	541	534	467	421	426	406	394	345
total %	*100%*	*100%*	*100%*	*100%*	*100%*	*100%*	*100%*	*100%*	*100%*	*100%*

In Germany Calcium contributes to average about 66% (1990-1999) to $BC_{(nss)}$, potassium to average 29% and magnesium to about 6%, respectively (cf. Table 6.6 and Figure 6.1).

Table 6.6: Average non-seasalt calcium ($Ca_{(nss)}$), potassium ($K_{(nss)}$) and magnesium ($Mg_{(nss)}$) fraction of the sum of total deposited base cations ($BC_{(nss)}$)

	1990	**1991**	**1992**	**1993**	**1994**	**1995**	**1996**	**1997**	**1998**	**1999**
fraction of $Ca_{(nss)}$	67%	69%	65%	67%	69%	61%	60%	64%	66%	67%
fraction of $K_{(nss)}$	26%	24%	29%	27%	26%	34%	32%	30%	31%	29%
fraction of $Mg_{(nss)}$	7%	7%	6%	6%	6%	5%	8%	6%	4%	4%
total %	*100%*	*100%*	*100%*	*100%*	*100%*	*100%*	*100%*	*100%*	*100%*	*100%*

The spatial pattern of non-seasalt base cations ($BC_{(nss)}$) from 1009 to 1999 are presented in Map 6.1. The overall decline of $BC_{(nss)}$ in the maps is obvious especially in the western, central and eastern part of Germany between the earlier and later years of the period. In all the years total deposition fluxes above the annual average values can be found in mountain areas, forested areas and urban areas.

6.1.2 Total deposition fluxes and trends of acidifying compounds and nitrogen

Eutrophication occurs due to atmospheric input of nitrogen, that causes nutrient imbalances, while acidification is caused by deposition loads of sulphur and nitrogen compounds (cf. Chapter 2). Average annual total deposition 1990 to 1999 and the percentage changes for sulphur (SO_X-$S_{(nss)}$), reduced, oxidised and total nitrogen (NH_X-N, NO_Y-N, N), respectively, are shown in Table 6.7. From 1990 to 1999 total deposition of all acidifying compounds declined. The greatest change can be observed in the 68% decline of sulphur total deposition (SO_X-$S_{(nss)}$), followed by the 41% decline of oxidised nitrogen (NO_Y-N), whereas reduced nitrogen total deposition declined by only 14%, and hence total nitrogen (N), calculated as the sum of NH_X-N and NO_Y-N declined by 24% (cf. Table 6.7).

Table 6.7: Budgets of average annual total deposition of SO_X-$S_{(nss)}$, NH_X-N, NO_Y-N and N in Germany 1990-1999

Total Deposition	SO_X-$S_{(nss)}$ [eq ha^{-1} a^{-1}]	% change from previous year	NH_X-N [eq ha^{-1} a^{-1}]	% change from previous year	NO_Y-N [eq ha^{-1} a^{-1}]	% change from previous year	N [eq ha^{-1} a^{-1}]	% change from previous year
1990	2901		1530		945		2475	
1991	2723	-6.1	1273	-16.8	924	-2.2	2197	-11.2
1992	2260	-17.0	1358	+6.7	951	+2.9	2309	+5.1
1993	2293	+1.5	1370	+0.9	937	-1.5	2307	-0.1
1994	1703	-25.7	1410	+2.9	946	+1.0	2356	+2.1
1995	1527	-10.4	1418	+0.6	895	-5.4	2313	-1.8
1996	1432	-6.2	1304	-8.0	833	-7.0	2136	-7.6
1997	1466	+2.4	1279	-1.9	936	+12.4	2214	+3.7
1998	927	-36.8	1419	+11.0	809	-13.5	2228	+0.6
1999	922	-0.4	1320	-7.0	562	-30.6	1882	-15.5
% change from 1990 to 1999		-68		-14		-41		-24

6.1.2.1 Total deposition of non-seasalt sulphur (SO_X-$S_{(nss)}$)

Average total deposition of non-seasalt sulphur (SO_X-$S_{(nss)}$) between 1990 and 1999 in Germany declined by 68% from 1659 kt a^{-1} (46.5 kg ha^{-1} a^{-1}; 2901 eq ha^{-1} a^{-1}) by 1132 kt (31.7 kg ha^{-1} a^{-1}; 1978 eq ha^{-1} a^{-1}) to 528 kt/a (14.8 kg ha^{-1} a^{-1}; 922 eq ha^{-1} a^{-1}) (Figure 6.3). In total deposition as well as in dry deposition of sulphur (Chapter 5.2.7.1) a stagnation in the average decline from 1992 to 1993 and from 1996 to 1997 can be found, while the maximum values still are falling. The peak values in 1995 and 1996 may indicate higher SO_2 emissions and air concentrations, due to colder winter temperatures and longer firing periods (cf. Chapter 3.1 in Part 2 of this report).

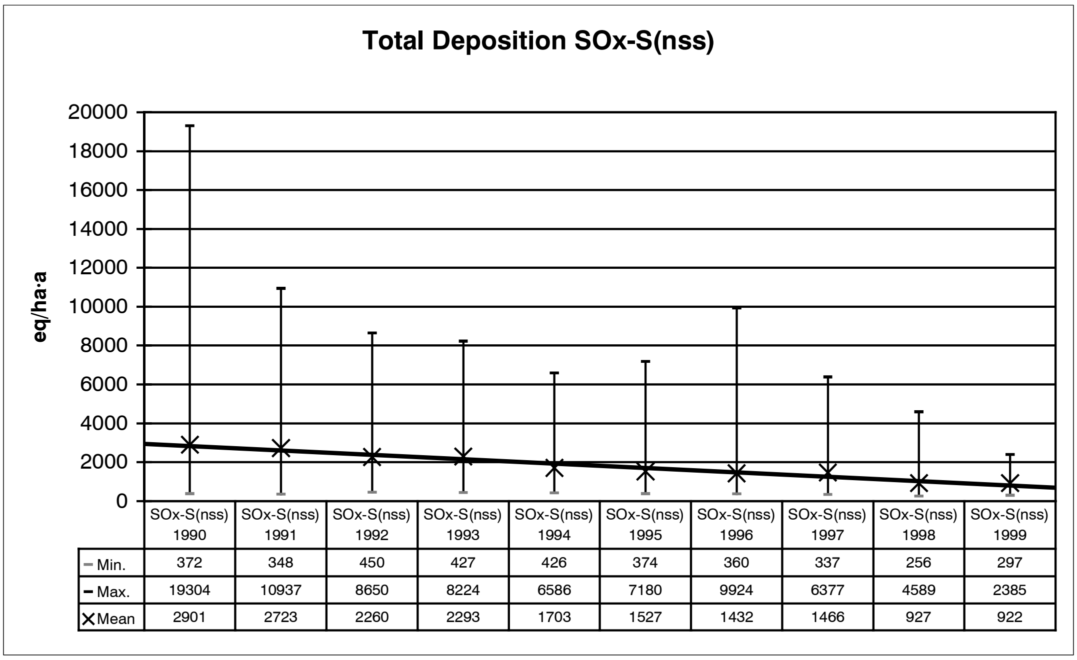

	SOx-S(nss) 1990	SOx-S(nss) 1991	SOx-S(nss) 1992	SOx-S(nss) 1993	SOx-S(nss) 1994	SOx-S(nss) 1995	SOx-S(nss) 1996	SOx-S(nss) 1997	SOx-S(nss) 1998	SOx-S(nss) 1999
– Min.	372	348	450	427	426	374	360	337	256	297
– Max.	19304	10937	8650	8224	6586	7180	9924	6377	4589	2385
× Mean	2901	2723	2260	2293	1703	1527	1432	1466	927	922

Figure 6.3: Minimum, maximum and annual mean total deposition of non-seasalt sulphur (SO_X-$S_{(nss)}$) 1990-1999

The spatial patterns of change in non-seasalt sulphur total deposition are presented in the 1990 to 1999 SO_X-$S_{(nss)}$ maps (Map 6.2). Especially in eastern Germany the decline from maximum value areas to average total deposition values can be observed. In 1998 and 1999 areas receiving sulphur total deposition at and above average values are found in larger areas of north-western and eastern Germany, and – visible in the maps as small patterns scattered over Germany – in forested mountain areas and in some urban agglomeration areas in the northern half of Germany (e.g. Berlin, Bremen, Hamburg, Hannover, Ruhrgebiet).

The average contribution of wet and dry deposition to total deposition of SO_X-$S_{(nss)}$ 1990-1999 is listed in Table 6.8. On average over all ten years 1990-1999 wet deposition contributes to about 26%, dry deposition to about 74% to total deposition of non-seasalt sulphur (SO_X-$S_{(nss)}$). The wet fraction of total deposition is rising over the time period considered, while the dry fraction is falling. This might be attributed to changes in the relative magnitude of in air SO_2 and SO_4 over the time period.

Table 6.8: Average wet and dry deposited fraction of total deposited SO_X-$S_{(nss)}$

Average fraction of SO_X-$S_{(nss)}$ total deposition	**1990**	**1991**	**1992**	**1993**	**1994**	**1995**	**1996**	**1997**	**1998**	**1999**
wet fraction of SO_X-$S_{(nss)}$	21,3%	19,0%	23,6%	24,4%	29,4%	29,2%	25,5%	21,4%	37,7%	30,8%
dry fraction of SO_X-$S_{(nss)}$	78,7%	81,0%	76,4%	75,6%	70,6%	70,8%	74,5%	78,6%	62,3%	69,2%
total	100%	100%	100%	100%	100%	100%	100%	100%	100%	100%

6.1.2.2 Total deposition of reduced nitrogen (NH_X-N)

No declining trend can be found in annual average total deposition of reduced nitrogen (NH_X-N) in Germany between 1990 and 1999 (cf. Figure 6.4). The 14% lower average total deposition in1999 compared to 1990, which is equal to an absolute reduction by 105 kt (210 eq ha^{-1} a^{-1}; 3.0 kg ha^{-1} a^{-1}) from 765 kt a^{-1} (1530 eq ha^{-1} a^{-1}; 21.4 kg ha^{-1} a^{-1}) in 1990 to 660 kt a^{-1} (1320 eq ha^{-1} a^{-1}; 18.5 kg ha^{-1} a^{-1}) in 1999, respectively, is more or less within the range of the changes (-16% to +11%) between the single years of the time period considered (cf. Table 6.7). From the maximum values (Figure 6.4) also no clear trend in time can be derived.

The spatial patterns of total deposition of (NH_X-N) 1990-1999 is presented in map 6.3. High fluxes above the annual average in all years can observed in the north-west and south east regions in Germany, where the regions with intensive animal husbandry can be found. Lower values regularly can be observed in the regions between south west Germany and the Baltic Sea. Locally high NH_X-N total deposition can be found in the small patterns of forested areas, which are receiving more dry deposited NH_X-N than neighbouring areas of other land use (cf. Chapter 5.7.2.2).

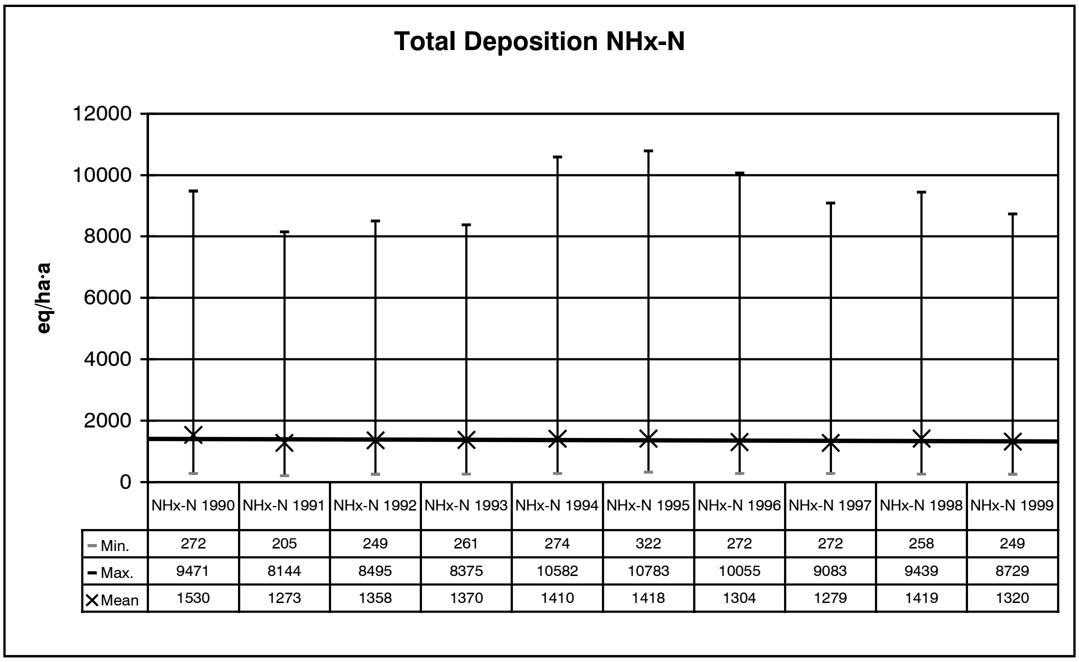

	NHx-N 1990	NHx-N 1991	NHx-N 1992	NHx-N 1993	NHx-N 1994	NHx-N 1995	NHx-N 1996	NHx-N 1997	NHx-N 1998	NHx-N 1999
− Min.	272	205	249	261	274	322	272	272	258	249
− Max.	9471	8144	8495	8375	10582	10783	10055	9083	9439	8729
× Mean	1530	1273	1358	1370	1410	1418	1304	1279	1419	1320

Figure 6.4: Minimum, maximum and annual mean total deposition of reduced nitrogen (NH_X-N) 1990-1999

Table 6.9 shows the average contribution of wet and dry deposition fluxes to total NH_X-N deposition 1990-1999 in Germany. Over the whole time period considered the mean fraction of wet deposition is about 29%, the dry fraction about 71%, respectively. It can be observed from the data in Table 6.9, that from 1990 to1999 the dry contribution to total deposition of NH_X-N is slightly rising, whereas the wet fraction is falling accordingly.

Table 6.9: Average wet and dry deposited fraction of total deposited NH_X-N

Average fraction of NH_X-N total deposition	**1990**	**1991**	**1992**	**1993**	**1994**	**1995**	**1996**	**1997**	**1998**	**1999**
wet fraction of NH_X-N	30.4%	30.3%	29.1%	30.8%	29.9%	29.0%	29.6%	26.9%	27.0%	28.7%
dry fraction of NH_X-N	69.6%	69.7%	70.9%	69.2%	70.1%	71.0%	70.4%	73.1%	73.0%	71.3%
total	100%	100%	100%	100%	100%	100%	100%	100%	100%	100%

6.1.2.3 Total deposition of oxidised nitrogen (NO_Y-N)

Average total deposition of oxidised nitrogen (NO_Y-N) declined by 41% between 1990 and 1999. This is equal to an absolute reduction by 192 kt (383 eq ha^{-1} a^{-1}; 5.4 kg ha^{-1} a^{-1}) from 472 kt a^{-1} (945 eq ha^{-1} a^{-1}; 13.2 kg ha^{-1} a^{-1}) in 1990 to 281 kt a^{-1} (562 eq ha^{-1} a^{-1}; 7.8 kg ha^{-1} a^{-1}) in 1999. The changes between the single years show decline as well as rising average and maximum values (Figure 6.5; cf. Table 6.7). The average changes are relatively small between 1990 to 1996. Then, after a rise of average 12% from 1996 to 1997, a sharp decline until 1999 can be observed. This decline is mainly due to air concentration data used as model input (cf. Chapter 5.5) and modelled dry deposition estimates, whereas changes in average wet deposition are relatively small (cf. Table 4.12 and Chapter 4.4.2.3).

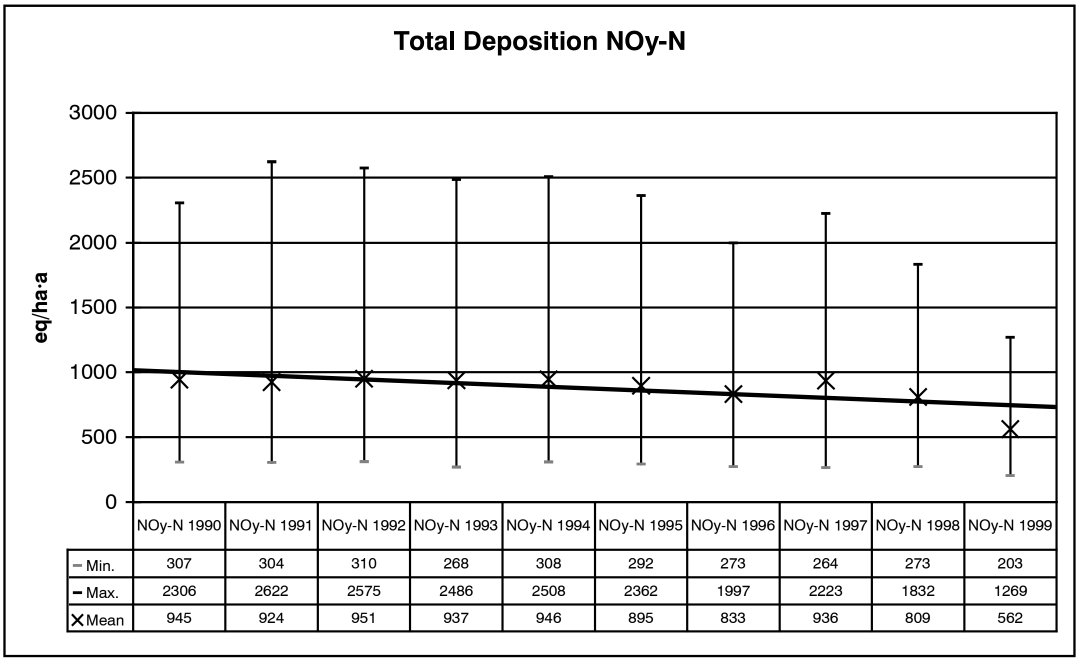

	NOy-N 1990	NOy-N 1991	NOy-N 1992	NOy-N 1993	NOy-N 1994	NOy-N 1995	NOy-N 1996	NOy-N 1997	NOy-N 1998	NOy-N 1999
- Min.	307	304	310	268	308	292	273	264	273	203
- Max.	2306	2622	2575	2486	2508	2362	1997	2223	1832	1269
× Mean	945	924	951	937	946	895	833	936	809	562

Figure 6.5: Minimum, maximum and annual mean total deposition of oxidised nitrogen (NO_Y-N) 1990-1999

The spatial patterns of NO_Y-N total deposition 1990-1999 are presented in Map 6.4. Total NO_Y-N deposition rates above the annual average makes the forested mountain areas appear as dark pattern in the maps for each year. Also some urban agglomeration areas (e.g. Hamburg, Bremen, Berlin, München) can be identified by higher total deposition rates than in their surrounding areas. The overall decline of total NO_Y-N deposition from 1997 to 1999 can be found in the colours becoming lighter.

The wet and dry deposition flux contribution to total deposition of NO_Y-N is shown in Table 6.10. The mean fraction of wet deposition over the whole time period is about 33%, the dry deposition flux contributes on average to about 67% to total deposition. A rising fraction of wet deposited NO_Y-N can be observed, especially between 1996 and 1999, at the same time when the NO_Y-N dry deposition estimates are sharply falling by about 58% (cf. Chapter 5.7.2.3).

Table 6.10: Average wet and dry deposited fraction of total deposited NO_Y-N

Average fraction of NO_Y-N total deposition	**1990**	**1991**	**1992**	**1993**	**1994**	**1995**	**1996**	**1997**	**1998**	**1999**
wet fraction of NO_Y-N	30.8%	29.6%	30.6%	33.3%	31.5%	32.3%	32.4%	26.4%	35.5%	48.0%
dry fraction of NO_Y-N	69.2%	70.4%	69.4%	66.7%	68.5%	67.7%	67.6%	73.6%	64.5%	52.0%
total	100%	100%	100%	100%	100%	100%	100%	100%	100%	100%

6.1.2.4 Total deposition of total nitrogen (N = NH_X-N + NO_Y-N)

Total deposition of nitrogen is calculated as sum of wet and dry deposited reduced and oxidised nitrogen (N= NH_X-N + NO_Y-N). The average total deposition of N in Germany declined by 24% between 1990 and 1999. The total amount of total deposited N in Germany declined from 1238 kt a^{-1} (2475 eq ha^{-1} a^{-1}; 34.7 kg ha^{-1} a^{-1}) in 1990 by 297 kt (594 eq ha^{-1} a^{-1}; 8.3 kg/ha·a) to 941 kt a^{-1} (1882 eq ha^{-1} a^{-1}; 26.4 kg ha^{-1} a^{-1}) in 1999 (Figure 6.6).

The spatial patterns of N total deposition in the single years 1990 to 1999 are presented in Map 6.5. In Map 6.6 the 1990 and 1999 total deposition of nitrogen is shown together with the changes, calculated as difference between 1990 and 1999 total deposition of nitrogen (in eq ha^{-1} a^{-1}) and as percentage difference from 1990 to 1999. Changes to higher N total deposition loads in 1999 compared to 1999 can be found in southern Bavaria, in some areas in Baden-Wurttemberg and in southern Rhineland-Palatinate. Whole regions showing a high decline of N total deposition of 30% to 54%, i.e. well above the average decline of 24% over Germany, can be observed over Schleswig-Holstein in the north, over Mecklenburg-West Pommerania, Brandenburg and Berlin in eastern Germany, while smaller areas are also scattered over most of the other states. Highest absolute fall of N total deposition can be found in areas within the regions of highest N total deposition loads, both in 1990 and in 1999, over eastern Bavaria and over north and north-western Germany.

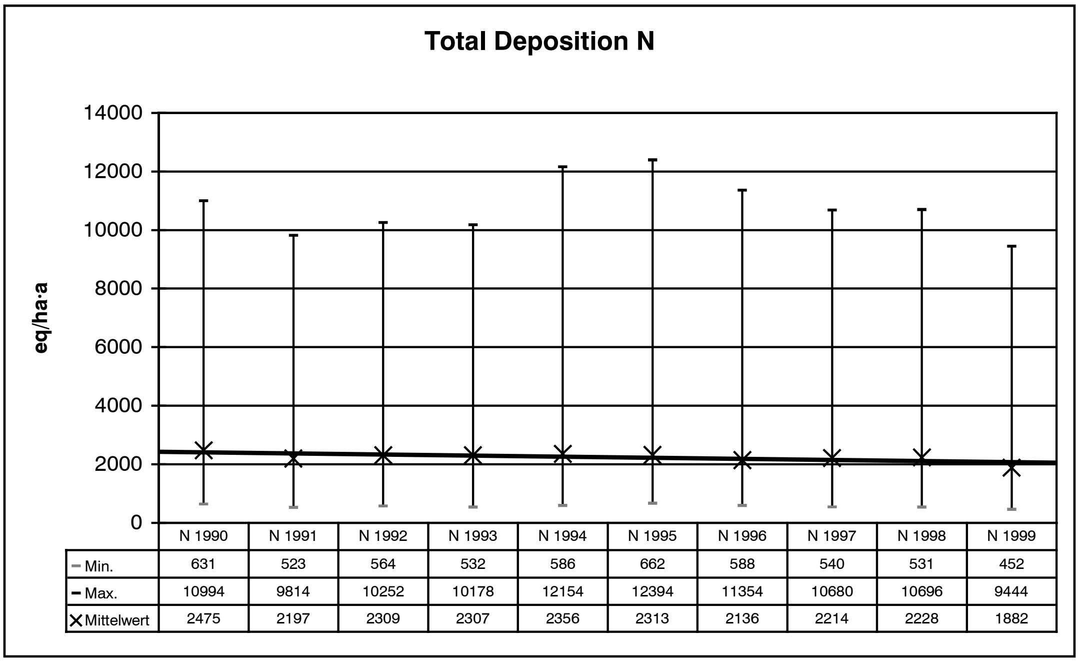

	N 1990	N 1991	N 1992	N 1993	N 1994	N 1995	N 1996	N 1997	N 1998	N 1999
– Min.	631	523	564	532	586	662	588	540	531	452
– Max.	10994	9814	10252	10178	12154	12394	11354	10680	10696	9444
× Mittelwert	2475	2197	2309	2307	2356	2313	2136	2214	2228	1882

Figure 6.6: Minimum, maximum and annual mean total deposition of total nitrogen (N) 1990-1999

The average wet and dry deposition fluxes of total N deposition 1990 to1999 are listed in Table 6.11. The mean wet deposited contribution to total N deposition over the whole period is about 30%, 70% are deposited by the dry N deposition flux, respectively.

Table 6.11: Average wet and dry deposited fraction of total deposited N

Average fraction of N total deposition	**1990**	**1991**	**1992**	**1993**	**1994**	**1995**	**1996**	**1997**	**1998**	**1999**
wet fraction of N	30.5%	30.0%	29.7%	31.8%	30.5%	30.3%	30.7%	26.7%	30.1%	34.4%
dry fraction of N	69.5%	70.0%	70.3%	68.2%	69.5%	69.7%	69.3%	73.3%	69.9%	65.6%
total	100%	100%	100%	100%	100%	100%	100%	100%	100%	100%

Reduced nitrogen (NH_X-N) contributes by an average portion of 61%, oxidised nitrogen (NO_Y-N) by average 39% to total N deposition, respectively. Annual average data (Table 6.12) are showing a trend to higher NH_X-N and lower NO_Y-N contribution over the period considered.

The contribution of the modelled total NO_Y-N deposition flux declined by 8.3% from 1990 to 1999.

Table 6.12: Average NH_X-N and NO_Y-N fraction of total deposited N

Average fraction of N total deposition	**1990**	**1991**	**1992**	**1993**	**1994**	**1995**	**1996**	**1997**	**1998**	**1999**
fraction of NH_X –N	61.8%	57.9%	58.8%	59.4%	59.8%	61.3%	61.0%	57.7%	63.7%	70.2%
fraction of NO_Y –N	38.2%	42.1%	41.2%	40.6%	40.2%	38.7%	39.0%	42.3%	36.3%	29.8%
total	100%	100%	100%	100%	100%	100%	100%	100%	100%	100%

6.1.2.5 Total deposition of potential acidity ($AC_{pot} = S_{(nss)} + N$)

Total deposition of potential acidity is calculated as the sum of wet and dry deposition of sulphur and nitrogen ($AC_{pot} = S_{(nss)} + N$). Chlorine non-seasalt wet deposition ($Cl_{(nss)}$), which is attributed to total deposition of anthropogenious HCl (cf. Chapter 4.4.2.5), also should be included in the calculation of AC_{pot} (UBA 1996). Since $Cl_{(nss)}$ only contributes to less than 1% to AC_{pot} total deposition (cf. Table6.14) this flux is neglected here.

Due to the decline of the contributing total deposition fluxes of sulphur and nitrogen (cf. Chapters 6.1.2.1 and 6.1.2.4), annual average AC_{pot} total deposition in Germany has fallen by 48% over the period from 1990 to 1999 (Figure 6.7, cf. Table 6.15).

Table 6.13 shows the average contribution of the wet and dry deposition fluxes to total deposition of AC_{pot}. Over the whole period wet deposition contributes to about 28% and dry deposition to about 72% to the total AC_{pot} deposition flux. From 1990 to1999 a shift of about 8% between the average dry and wet flux contribution to AC_{pot} total deposition can be observed .

Table 6.13: Average wet and dry deposited fraction of total deposited AC_{pot}

Average fraction of AC_{pot} total deposition	**1990**	**1991**	**1992**	**1993**	**1994**	**1995**	**1996**	**1997**	**1998**	**1999**
wet fraction of AC_{pot}	25.5%	23.9%	26.7%	28.1%	30.0%	29.9%	28.6%	24.6%	32.3%	33.2%
dry fraction of AC_{pot}	74.5%	76.1%	73.3%	71.9%	70.0%	70.1%	71.4%	75.4%	67.7%	66.8%
total	100%	100%	100%	100%	100%	100%	100%	100%	100%	100%

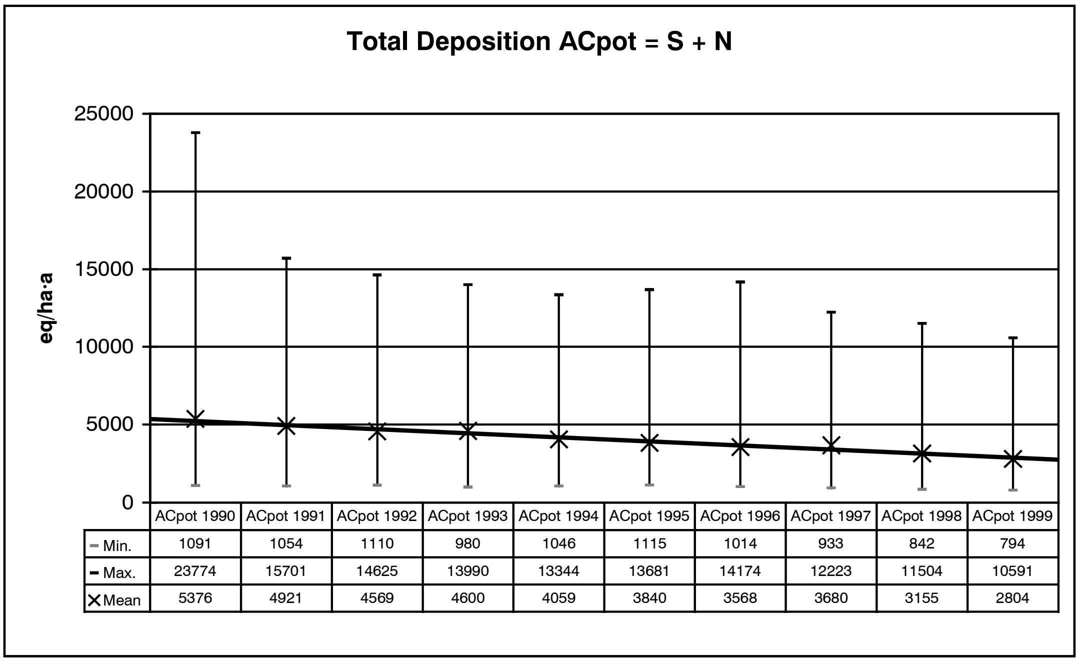

	ACpot 1990	ACpot 1991	ACpot 1992	ACpot 1993	ACpot 1994	ACpot 1995	ACpot 1996	ACpot 1997	ACpot 1998	ACpot 1999
- Min.	1091	1054	1110	980	1046	1115	1014	933	842	794
- Max.	23774	15701	14625	13990	13344	13681	14174	12223	11504	10591
× Mean	5376	4921	4569	4600	4059	3840	3568	3680	3155	2804

Figure 6.7: Minimum, maximum and annual mean total deposition of potential acidity (AC_{pot}) 1990-1999

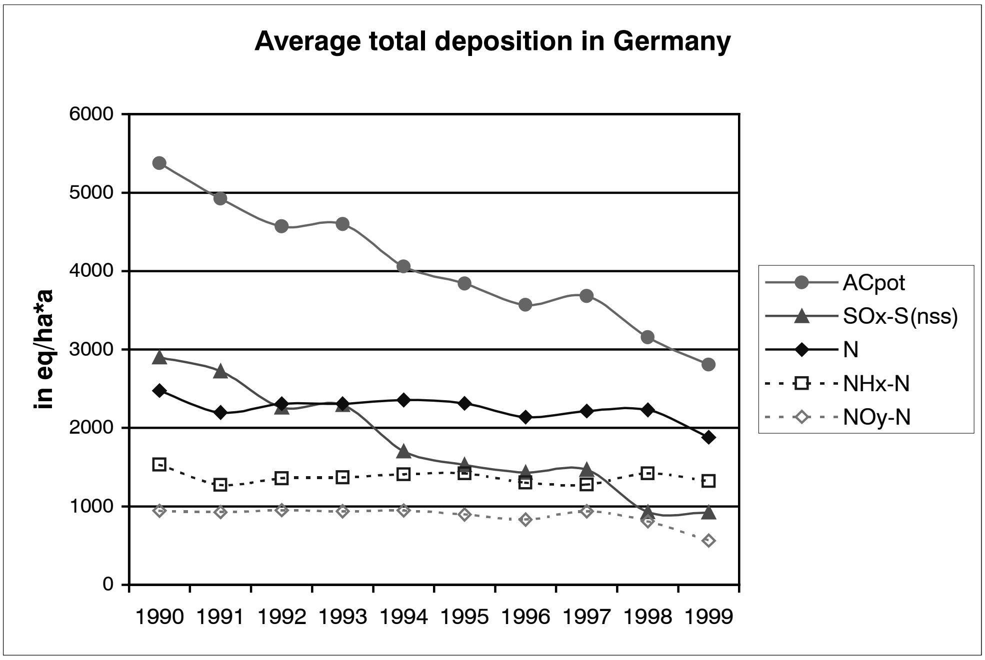

Figure 6.8: Average total deposition of AC_{pot} and its compounds in Germany 1990-1999

The annual average composition of total deposition of AC_{pot} in Germany 1990 to 1999 is shown in Figure 6.8, average fractions of the single compounds of AC_{pot} are listed in Table 6.14. From the curves in Figure 6.8 it clearly can be seen, that from 1994 on, due to the falling total deposition of SO_X-$S_{(nss)}$, N has taken over the role of the main acidifying compound, and in 1998 and 1999 the average estimates of NH_X-N are even higher than those of SO_X-$S_{(nss)}$.

Table 6.14: Average fractions of acidifying compounds of total deposition 1990-1999

Average fraction of...	**1990**	**1991**	**1992**	**1993**	**1994**	**1995**	**1996**	**1997**	**1998**	**1999**
SO_X-$S_{(nss)}$ in eq ha^{-1} a^{-1}	2901	2723	2260	2293	1703	1527	1432	1466	927	922
SO_X-$S_{(nss)}$ as % of the ACpot total deposition	54%	55%	49%	50%	42%	40%	40%	40%	29%	33%
N in eq ha^{-1} a^{-1}	2475	2197	2309	2307	2356	2313	2136	2214	2228	1882
N as % of the AC_{pot} total deposition	46%	45%	51%	50%	58%	60%	60%	60%	71%	67%
NH_X-N in eq ha^{-1} a^{-1}	1530	1273	1358	1370	1410	1418	1304	1279	1419	1320
NH_X-N as % of the AC_{pot} total deposition	28%	26%	30%	30%	35%	37%	37%	35%	45%	47%
NO_Y-N in eq ha^{-1} a^{-1}	945	924	951	937	946	895	833	936	809	562
NO_Y-N as % of the AC_{pot} total deposition	18%	19%	21%	20%	23%	23%	23%	25%	26%	20%
additional $Cl_{(nss)}$ in eq ha^{-1} a^{-1}	47	23	15	14	30	34	11	18	18	11
$Cl_{(nss)}$ as additional % to AC_{pot} total deposition	0.9%	0.5%	0.3%	0.3%	0.7%	0.9%	0.3%	0.5%	0.6%	0.4%

1990 to 1999 maps of total deposition of AC_{pot} showing the spatial pattern of the decline are presented in Map 6.7.

6.1.2.6 Total deposition of potential net acidity ($AC_{pot(net)} = AC_{pot} - BC_{(nss)}$)

Potential net acidity is calculated by subtracting the fluxes of non-seasalt base cations ($BC_{(nss)}$) from the sum of potential acidifying compounds (AC_{pot}) in order to account for potential acid neutralisation (cf. Chapter 2). Hence total deposition loads of $AC_{pot(net)}$ are lower than total deposition loads of AC_{pot}. The difference between the average total deposition of $AC_{pot(net)}$ in 1990 and in 1999 is a 49% (2351 eq ha^{-1} a^{-1}) lower total flux (Figure 6.9).

Budgets of average total deposition of AC_{pot}, $AC_{pot(net)}$ and acid neutralisation by $BC_{(nss)}$ within the ten years period considered are listed in Table 6.15.

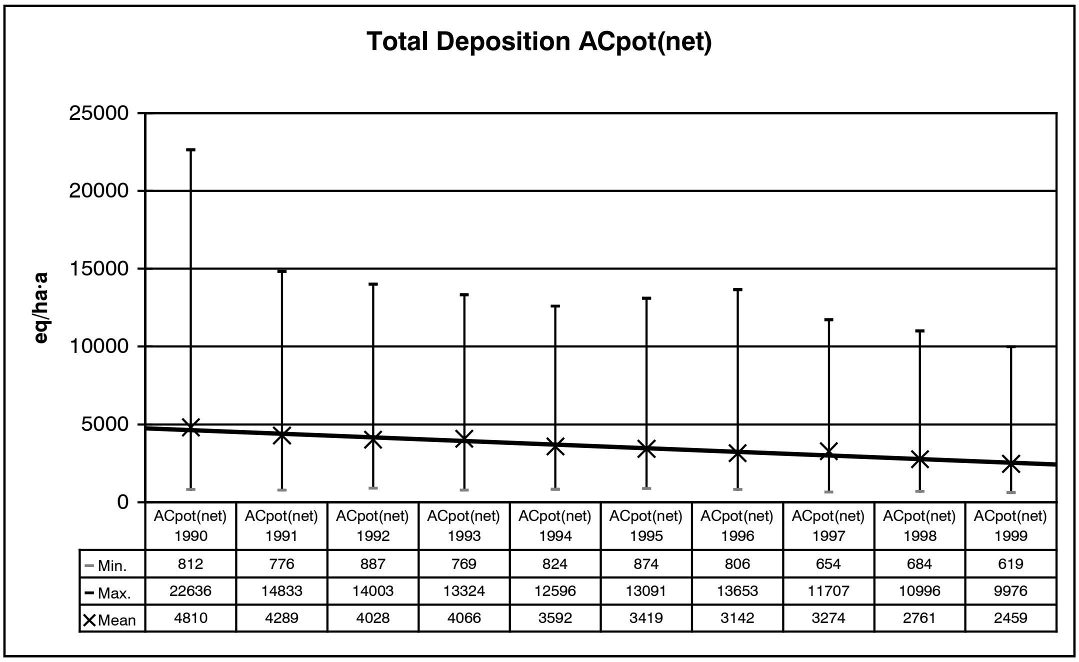

	ACpot(net) 1990	ACpot(net) 1991	ACpot(net) 1992	ACpot(net) 1993	ACpot(net) 1994	ACpot(net) 1995	ACpot(net) 1996	ACpot(net) 1997	ACpot(net) 1998	ACpot(net) 1999
– Min.	812	776	887	769	824	874	806	654	684	619
– Max.	22636	14833	14003	13324	12596	13091	13653	11707	10996	9976
× Mean	4810	4289	4028	4066	3592	3419	3142	3274	2761	2459

Figure 6.9: Minimum, maximum and annual mean total deposition of potential net acidity ($AC_{pot(net)}$) 1990-1999

Table 6.15: Budgets of average annual total deposition of AC_{pot}., $AC_{pot(net)}$ and Acid neutralisation in Germany 1990-1999

Total Deposition	AC_{pot} [eq ha^{-1} a^{-1}]	% change from previous year	$AC_{pot(net)}$ [eq ha^{-1} a^{-1}]	% change from previous year	$BC_{(nss)}$ [eq ha^{-1} a^{-1}]	% change from previous year	Acid neutralisation [%]
1990	5376		4810		566		11
1991	4921	-8.5	4289	-10.8	632	+11.6	11
1992	4569	-7.1	4028	-6.1	541	-14.3	13
1993	4600	+0.7	4066	+0.9	534	-1.3	12
1994	4059	-11.8	3592	-11.6	467	-12.6	12
1995	3840	-5.4	3419	-4.8	421	-9.8	11
1996	3568	-7.1	3142	-8.1	426	+1.3	13
1997	3680	+3.1	3274	+4.2	406	-4.7	12
1998	3155	-14.3	2761	-15.7	394	-3.0	13
1999	2804	-11.1	2459	-10.9	345	-12.3	13
% change from 1990 to 1999		-48		-49		-39	

Acid neutralisation by total deposition of non-seasalt base cations ($BC_{(nss)}$) in the period 1990-1999 is shown in Figure 6.10. The annual average values of acid neutralisation are slightly rising from 11% in 1990 to 13% in 1999. The spatial patterns of $AC_{pot(net)}$ are shown in Map 6.8, acid neutralisation by total deposition of $BC_{(nss)}$ 1990 to 1999 are presented in Map 6.9, respectively.

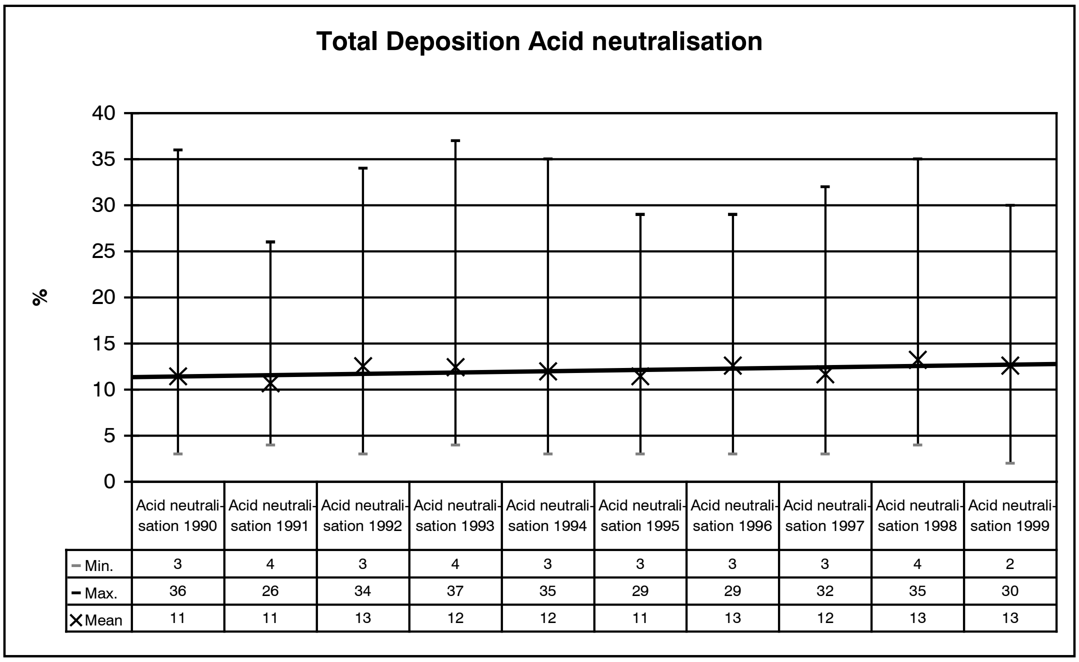

	Acid neutralisation 1990	Acid neutralisation 1991	Acid neutralisation 1992	Acid neutralisation 1993	Acid neutralisation 1994	Acid neutralisation 1995	Acid neutralisation 1996	Acid neutralisation 1997	Acid neutralisation 1998	Acid neutralisation 1999
− Min.	3	4	3	4	3	3	3	3	4	2
− Max.	36	26	34	37	35	29	29	32	35	30
× Mean	11	11	13	12	12	11	13	12	13	13

Figure 6.10: Minimum, maximum and annual mean total deposition of acid neutralisation 1990-1999

From the data presented in Table 6.15 it can be seen that the decline of average total deposition fluxes of potential Acidity (1990-99: -48%) is faster than the decline of non-seasalt base cations (-39%) over the same time period, hence the decline of potential net acidity (1990-99: -49%) is slightly faster than of potential acidity, since acid neutralisation is rising from 11% in 1990 to 13% in 1999 (cf. Figure 6.11).

The spatial patterns of $AC_{pot(net)}$ total deposition in all single years 1990 to 1999 are presented in Map 6.9. In Map 6.10 the 1990 and 1999 total deposition of $AC_{pot(net)}$ is shown together with the changes, calculated as difference between 1990 and 1999 total deposition of $AC_{pot(net)}$ (in eq ha^{-1} a^{-1}) and as percentage difference from 1990 to 1999. Reduction of $AC_{pot(net)}$ total deposition above the 49% average decline over Germany can be found over eastern Germany, Schleswig-Holstein and North Rhine-Westphalia. Rising $AC_{pot(net)}$ total deposition can be observed in some areas in Baden-Wurttemberg, central and southern Hesse, in southern Rhineland-Palatinate and a small area in southern Bavaria. Highest absolute changes with a 1990 to 1999 decline above 10 keq ha^{-1} a^{-1} can be found over forested areas in eastern Germany.

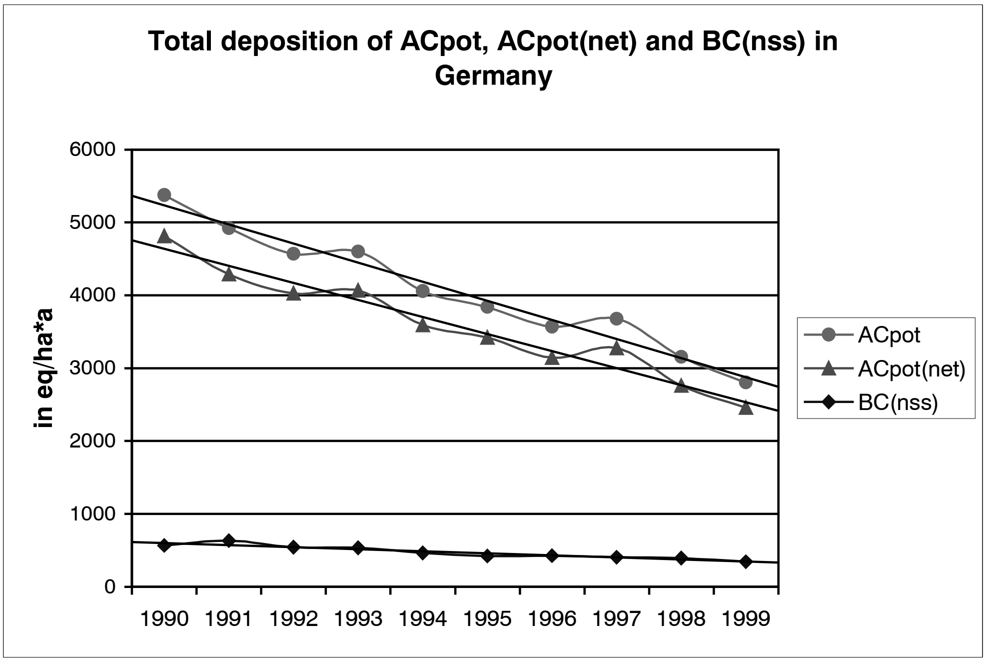

Figure 6.11: Average total deposition of AC_{pot}, $AC_{pot(net)}$, and $BC_{(nss)}$ in Germany 1990-1999

6.2 Quality of mapping results: errors & uncertainties

The methods applied to assess total deposition loads in Germany are based upon the coupling of measurements and models. The modelling and mapping procedures are used to predict deposition results in space and time. At present the use of models and modelled data, which is recommended by the mapping manual (UBA, 1996), is the only available technique to derive quantitative total deposition estimates o an ecosystem level over the whole area of Germany, which is the core subject to this research project, or across Europe, which in a coarser spatial resolution is carried out by EMEP.

Current knowledge of the emission, transport, transformation, dispersion and deposition processes is integrated in deposition modelling and mapping procedures. By their nature, the models can only be as good as the current understanding, and there is a time lag of model updates due to latest developments of the underlying science. Where possible measurements should be used in order to minimise and quantify uncertainties in the model output, respectively (cf. NEGTAP, 2001).

The methods applied to provide total deposition loads in Germany are based upon the coupling of measurements and models. Deposition measurement data in a relatively direct way are used for the processing of wet deposition fields (cf. Chapter 4). The resistance parameterisations of the dry and cloud deposition models are based upon measurements and implemented due to the current state of knowledge on underlying processes to derive deposition velocity and dry and cloud deposition fields (cf. Chapter 5). Emission, meteorology, air concentration fields and the respective models applied to derive deposition model input data generally are also based upon and validated with measurements.

There are, however, uncertainties in the modelling and mapping output, which, on the one hand are attributable to the quality of the input data used, the model calculations on the other. The quality of wet deposition mapping results is discussed in Chapter 4.3.2. The methodological approach and results of the quantification of uncertainties in total deposition using independent canopy budget model estimates at monitoring points is presented in the following Chapter 6.2.1.

A preliminary comparison of the German results with EMEP modelled SO_X-S, NH_X-N and NO_Y-N total deposition 1999 is shown in Chapter 6.3.

6.2.1 Validation, comparison with measured data/throughfall method results

The quality of the modelling and mapping results is judged by independent canopy budget model (CBM) calculation estimates, which are based upon deposition measurements. CBM are commonly used to estimate dry deposition (DD) and total deposition (TD) fluxes from long-term open field bulk deposition (bulk flux, BF), stemflow (SF) and throughfall (TF) measurements at certain forest stand monitoring points. A common way to derive dry and total deposition estimates into a forest stand is the use of a so called 'filtering approach', developed by ULRICH (1983), assuming a fixed relationship between wet (= BF) and dry deposition of particles by taking sodium (Na) as tracer (hence 'Na calibration approach'). Na particulates are assumed to be totally inert for canopy uptake and leaching. The relation of dry deposited Na particles (DD_{Na}) to wet deposited Na (BF_{Na}) is used to calculate the dry particulate deposition of Ca, Mg, K, Cl, NH_4, NO_3 and SO_4. The gaseous dry deposition (of HCl, SO_2, NH_3, NO_X) is calculated from the difference of canopy leaching (of Cl, SO_4, NH_4, NO_3), derived from the difference between TF+SF and BF, and particulate dry deposition. Canopy uptake of Cl, SO_4 and NO_3 is assumed negligible, uptake of H and NH_4 is taken equal to the total leaching of base cations (Ca, K, Mg) (cf. ULRICH 1983 and 1991, DRAAIERS ET AL. 1998). CBM calculations were found to be similar to deposition estimates from micrometeorological measurements, but its application supposed to be limited due to the basic assumptions (cf. SPRANGER 1992, DRAAIERS ET AL. 1994, DRAAIERS & ERISMAN 1995, ERISMAN & DRAAIERS 1995, DRAAIERS ET AL. 1998). Among others, the 'Na calibration approach' approximating dry deposition of all other particulates is questionable with respect to the particulate diameter (MMD) dependant deposition velocities. This holds especially for the, compared to Na, Cl, Mg and Ca and NO_3 (MMD > 3 to 2μm), relatively small K, SO_4 and NH_4 (MMD < 1μm) particles (cf. GRAVENHORST ET AL. 2000).

A comparison was made between mapped total deposition (dry + wet deposition) and site-specific total deposition derived from measured throughfall, stemflow and precipitation measurements using the CBM of DRAAIJERS AND ERISMAN (1995) in coniferous forest. In Table 6.16 some statistics on this comparison (T-test, coefficient of determination, slope of linear regression between model vs. measurement value and number of sites) are listed.

The comparison is performed on those coniferous forest sites where all main compounds were analysed and reported. This is prerequisite for the performance of an ion balance quality check using Equation (4.1). All measurements in excess of an ion imbalance of ± 20% are excluded from further processing. Moreover, only positive measured fluxes are used for the comparison in order to exclude unreliable CBM calculation results, and the calculated ratio between mapped and measured (CBM result) data falls within a ±4 times standard deviation range in order to exclude outliers.

The IDEM mapping results of total deposition at the coniferous forest sites were calculated from the sum of wet deposition fields and receptor specific dry deposition estimates. Detailed description on the methods applied are explained in Chapter 4 for wet deposition and in Chapter 5 for dry deposition, respectively. Main IDEM input data for dry deposition estimates of NH_X-N are EUTREND model calculations of ammonia air concentration calculated from recently revised German ammonia emission data on a 5x5km² grid resolution (cf. Chapter 5.3). Dry deposition estimates of NO_Y-N and SO_X-S for 1990 and 1996-1999 are calculated on the base of DEM/DEHM air concentration fields, whereas dry deposition of the years 1991 to 1995 are computed from EMEP air concentration fields. The dry deposition of Na and the base cations Ca, K and Mg are derived by IDEM using air concentration fields calculated from concentration in precipitation (cf. Chapter 5.4).

Overall, the comparison for the total deposition gives better results than those for dry deposition. The quality of the measurements, used for the comparison, and the subsequent use of the canopy budget model may cause a incorrect distinction between dry and wet deposition, thus hampering the comparison for the dry deposition fluxes.

The CEM and total deposition model results are comparing relatively good for Na and the base cations Mg and Ca, where on average more than 80% of the compared data points are within a ±50% range of deviation, while for K the matches are quite weak (cf. Table 6.16). Uncertainties are relatively high for K estimates based on measurements, since the magnitude of measured K wet deposition regularly is smaller than the deviation given as ‘not analysed’ fraction by ion balance calculations (cf. Table 4.10). The K comparison result may be attributed to a systematic overestimation of K in precipitation measurements, since most of the open space deposition samples used for the comparison are situated closely to forests, and K emission from the surrounding forest vegetation (e.g. by pollen), as a local effect, could be co-deposited into the bulk sampler funnels. Also nearby fertiliser application could have this effect. This would lead to underestimates of K dry and total deposition using CBM calculation. On the other hand interpolated wet deposition is input to derive K air concentration, which is used to calculate IDEM dry deposition (cf. Chapter 5.3). A systematic overestimation within the measurements due to the sampling method applied would yield too high air concentration and hence lead to overestimates of K dry deposition at those monitoring plots. The deviation for K, however, is quite high throughout all the years of the considered period, which gives reason to again check and correct the IDEM model calculations where necessary. The linear regression for the sum of the base cations Ca, K and Mg (BC) in the calculated comparison, however, shows reasonable agreements with significant relationships (T-Test $p > 0.05$) for almost every year's data and a tendency of overestimation of the CBM result by the mapping result ($m = 0.68$ to 0.90, cf. Table 6.16).

The mapped total deposition of the acidifying compounds SO_X-S, NO_Y-N and NH_X-N shows different degrees of overestimation in comparison with the CBM results. However, on average more than 50% of the compared data points are within a ±50% range of deviation. A remarkable positive exception from this are the mapping results of NO_Y-N in 1999: here the best mach can be found, with all points compared lying within a ±50% range of deviation and the linear regression shows a significant trend almost fitting an 1:1 agreement between mapped and CBM calculation result ($m = 1.01$, cf. Table 6.16). This is, according to information from the DEM/DEHM modelling team at NERI, caused by improvements in both the DEM/DEHM model and the emissions used for the calculations. Generally mapped total deposition in the years 1990 and 1996-1999, where DEM/DEHM air concentration data are used as input for NO_Y-N dry deposition modelling are comparing slightly better with CBM results than the ones (i.e. in 1991-1995) where EMEP Lagrangian LRT air concentration data are used.

The comparison for SO_X-S total deposition estimates do not show much difference whether EMEP or DEM/DEHM data are used to drive dry deposition. On average well above 50% of the data plots compared are lying within a ±50% range of deviation. In the later years 1994 to 1996, 1998 and 1999, a slightly better comparison result between modelled total deposition and CBM calculations can be found, though the mapping results generally are higher than the CBM results.

Modelled NH_X-N dry deposition within this project is based upon recently revised, and hence, due to current knowledge more reliable, small-scale emission data (cf. Chapter 5.3.4) and EUTREND modelled small-scale air concentration of ammonia. In the comparison of modelled total deposition with CBM calculations of NH_X-N the mapping results in all the years are higher than the CBM results, which at least partly can be can be attributed to uncertainties in the subsequent use of CBM calculations (see above).

Table 6.16: Information on the comparison between modelled and measured total deposition (wet + dry deposition) for the different components for the period 1990-1999

1990	**SO_X-S**	**NO_Y-N**	**NH_X-N**	**N**	**AC_{pot}**	**Ca**	**K**	**Mg**	**BC**	**Na**
n	66	67	67	67	67	65	67	65	67	65
m	0.46	0.53	0.40	0.45	0.47	0.87	0.45	0.94	0.81	0.64
R^2	0.57	0.03	0.16	0.05	0.35	0.41	0.28	0.59	0.42	0.59
T-Test	0.00	0.00	0.00	0.00	0.00	0.01	0.00	*0.16*	0.00	0.00
1991	**SO_X-S**	**NO_Y-N**	**NH_X-N**	**N**	**AC_{pot}**	**Ca**	**K**	**Mg**	**BC**	**Na**
n	42	42	41	41	42	42	41	42	42	42
m	0.36	0.45	0.51	0.48	0.43	0.74	0.33	0.84	0.68	0.69
R^2	0.44	0.01	0.30	0.16	0.27	0.11	0.16	0.66	0.21	0.86
T-Test	0.00	0.00	0.00	0.00	0.00	0.00	0.00	0.00	0.00	0.00
1992	**SO_X-S**	**NO_Y-N**	**NH_X-N**	**N**	**AC_{pot}**	**Ca**	**K**	**Mg**	**BC**	**Na**
n	56	56	55	56	56	56	54	56	56	55
m	0.44	0.46	0.48	0.47	0.47	1.03	0.45	1.16	0.90	0.85
R^2	0.41	0.07	0.31	0.18	0.16	0.37	0.07	0.61	0.35	0.55
T-Test	0.00	0.00	0.00	0.00	0.00	*0.17*	0.00	0.01	0.03	0.02
1993	**SO_X-S**	**NO_Y-N**	**NH_X-N**	**N**	**AC_{pot}**	**Ca**	**K**	**Mg**	**BC**	**Na**
n	62	63	62	63	63	62	63	61	61	63
m	0.39	0.43	0.42	0.43	0.43	0.92	0.43	0.93	0.79	0.73
R^2	0.36	0.07	0.16	0.11	0.17	0.27	0.12	0.51	0.22	0.73
T-Test	0.00	0.00	0.00	0.00	0.00	*0.15*	0.00	*0.13*	0.00	0.00
1994	**SO_X-S**	**NO_Y-N**	**NH_X-N**	**N**	**AC_{pot}**	**Ca**	**K**	**Mg**	**BC**	**Na**
n	60	59	60	60	60	59	60	57	59	60
m	0.58	0.46	0.48	0.48	0.52	0.95	0.50	1.05	0.85	0.77
R^2	0.31	0.07	0.40	0.27	0.25	0.06	0.22	0.35	0.09	0.72
T-Test	0.00	0.00	0.00	0.00	0.00	*0.25*	0.00	*0.34*	0.00	0.01
1995	**SO_X-S**	**NO_Y-N**	**NH_X-N**	**N**	**AC_{pot}**	**Ca**	**K**	**Mg**	**BC**	**Na**
n	58	60	60	60	57	59	59	57	59	58
m	0.54	0.43	0.42	2.10	0.48	0.84	0.40	0.87	0.72	0.76
R^2	0.57	0.14	0.32	0.21	0.31	0.00	0.08	0.18	0.03	0.59
T-Test	0.00	0.00	0.00	0.00	0.00	0.02	0.00	*0.32*	0.00	0.00
1996	**SO_X-S**	**NO_Y-N**	**NH_X-N**	**N**	**AC_{pot}**	**Ca**	**K**	**Mg**	**BC**	**Na**
n	62	66	66	66	62	66	64	64	66	66
m	0.54	0.56	0.53	0.56	0.57	0.82	0.37	1.00	0.73	0.63
R^2	0.32	0.11	0.12	0.04	0.07	0.03	0.12	0.48	0.20	0.50
T-Test	0.00	0.00	0.00	0.00	0.00	0.00	0.00	*0.24*	0.00	0.00
1997	**SO_X-S**	**NO_Y-N**	**NH_X-N**	**N**	**AC_{pot}**	**Ca**	**K**	**Mg**	**BC**	**Na**
n	69	68	67	66	67	69	68	68	68	69
m	0.39	0.48	0.44	0.49	0.46	0.85	0.39	0.96	0.74	0.74
R^2	0.50	0.14	0.02	0.01	0.17	0.01	0.05	0.51	0.06	0.52
T-Test	0.00	0.00	0.00	0.00	0.00	0.01	0.00	*0.17*	0.00	0.00
1998	**SO_X-S**	**NO_Y-N**	**NH_X-N**	**N**	**AC_{pot}**	**Ca**	**K**	**Mg**	**BC**	**Na**
n	55	55	54	54	54	55	53	53	55	55
m	0.61	0.62	0.48	0.54	0.57	0.92	0.48	0.97	0.82	0.84
R^2	0.39	0.17	0.25	0.08	0.16	0.00	0.16	0.20	0.01	0.69
T-Test	0.00	0.00	0.00	0.00	0.00	*0.22*	0.00	*0.46*	0.00	0.00
1999	**SO_X-S**	**NO_Y-N**	**NH_X-N**	**N**	**AC_{pot}**	**Ca**	**K**	**Mg**	**BC**	**Na**
n	45	43	43	43	44	44	43	42	45	45
m	0.55	1.01	0.45	0.62	0.59	0.80	0.36	0.72	0.71	0.85
R^2	0.23	0.17	0.11	0.02	0.05	0.02	0.00	0.00	0.07	0.54
T-Test	0.00	*0.35*	0.00	0.00	0.00	0.03	0.00	0.01	0.00	0.02

n = number of points
linear regression line between field estimate (y) and map (x); y = 0 when x = 0: y = m·x; **m** = slope
R^2 = coefficient of determination
italics: significant T-Test (p > 0.05)

6.3 German and EMEP total deposition data of NO_Y-N, NH_X-N and SO_X-S 1999

The German and international (EMEP) total deposition data sets for oxidised nitrogen (NO_Y-N), reduced nitrogen (NH_X-N) and oxidised sulphur (SO_X-S) 1999 are presented in the graphical synopsis of Figure 6.12 to 6.14. The graphical representation shown in this figures was produced by Öko-Data (NAGEL ET AL. 2002).

An obvious difference between all German and EMEP mapping results presented here is the different spatial differentiation, due to a grid resolution of 1x1km² of the German maps and the 50x50km² grid resolution of the EMEP Eulerian model. Apart from this fundamental difference in scale, which is most important as the deposition input on the ecosystem level is concerned, the 1999 data sets of oxidised nitrogen (NO_Y-N), reduced Nitrogen (NH_X-N) and sulphur (SO_X-S) to some extend are comparing, as the spatial distribution over Germany and the magnitudes, given by the use of identical legend classes of the total deposition fluxes are concerned.

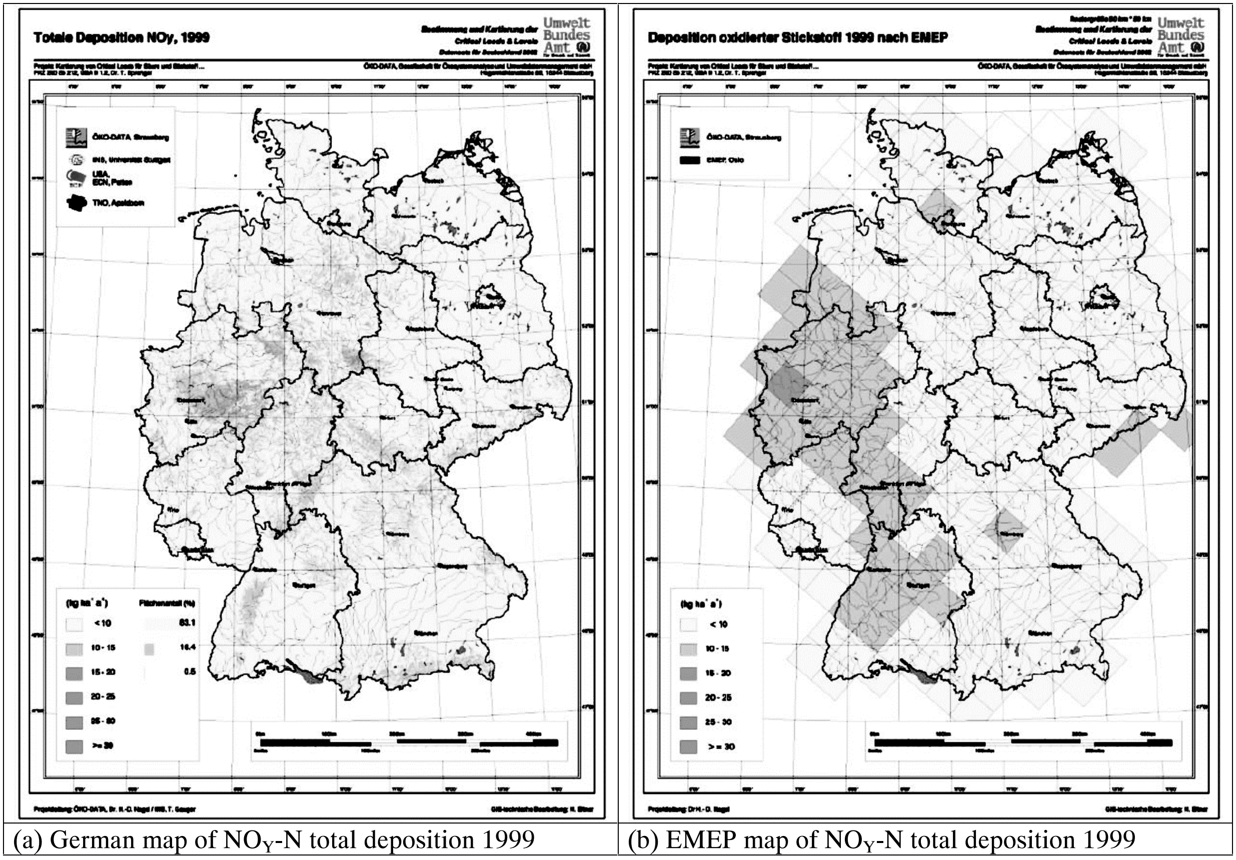

(a) German map of NO_Y-N total deposition 1999

(b) EMEP map of NO_Y-N total deposition 1999

Figure 6.12: German (a) and EMEP (b) total deposition of NO_Y-N 1999

The spatial trend of the German and EMEP NO_Y-N total deposition over Germany is presented in Figure 6.12 (a) and (b). High values (above 25 kg^{-1} ha^{-1} a^{-1}) in both maps can be found in the western part of Germany. In the German mapping result (Figure 6.12 (a)) these high deposition rates are mainly attributed to forested mountainous areas in North Rhine-Westphalia, southern Lower Saxony, Hesse, Rhineland-Palatinate, north-west Bavaria and Baden-Wurttemberg. An agreement in principle with the EMEP NO_Y-N map can be observed, since Figure 6.12 (b) shows contiguous grids above 25 kg^{-1} ha^{-1} a^{-1} over almost the same regions.

In contrast the NH_X-N maps (Figure 6.13 (a) and (b)) are showing rather different spatial trends.

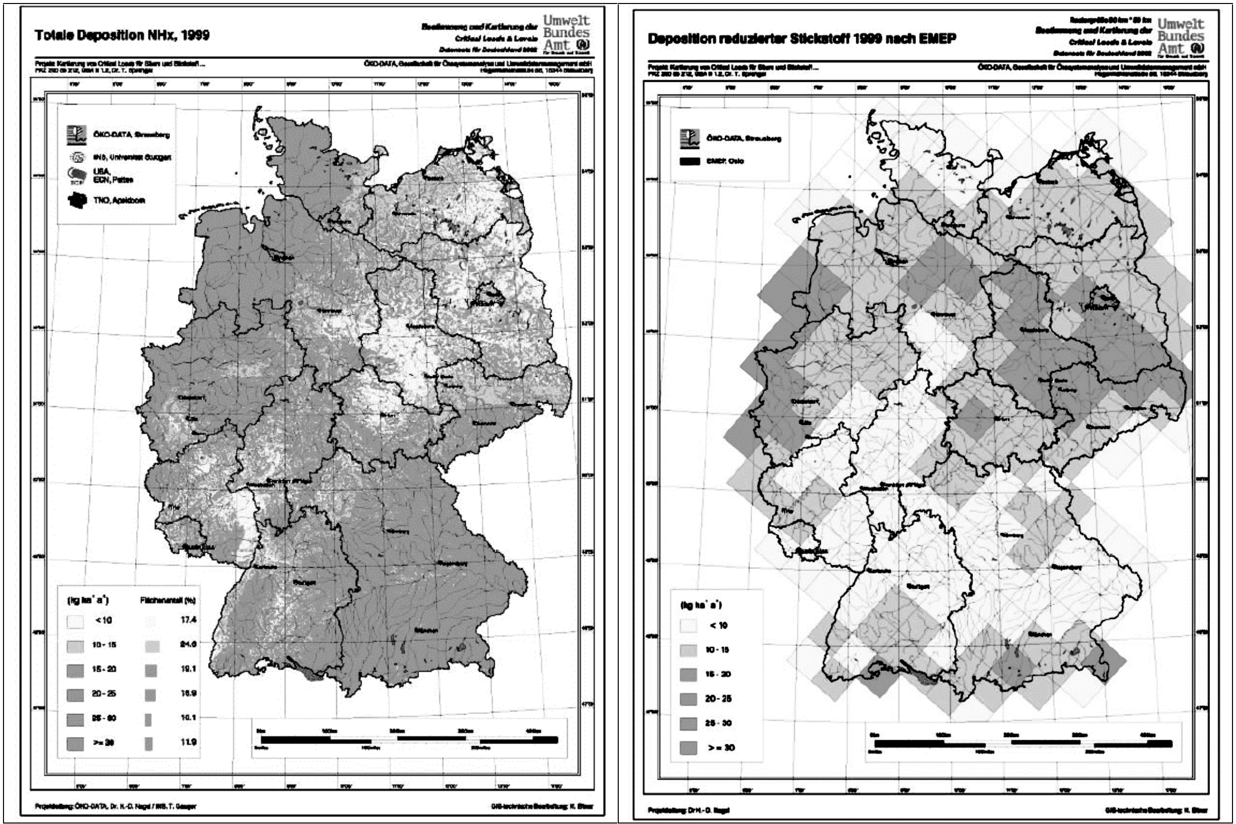

(a) German map of NH_X-N total deposition 1999

(b) EMEP map of NH_X -N total deposition 1999

Figure 6.13: German (a) and EMEP (b) total deposition of NH_X-N-1999

In the German map local scale ammonia emissions and local scale deposition is explicidly taken into account (cf. Chapter 5.3.2). In the EMEP model, mainly representing the NH_X-N long-range transport processes and their effects on the magnitude of total NH_X-N deposition fluxes, part of the emission within one EMEP grid cell is directly attributed to deposition within the same grid cell in order to account for local scale deposition (cf. Chapter 5.3.3).

Accordance between both, the German and EMEP NH_X-N mapping result (Figure 6.13 (a) and (b)), can be found in the matching total deposition flux above 25 kg^{-1} ha^{-1} a^{-1} at the north-western and southern border of Germany. The differences mainly can be found over eastern Germany, where the German mapping result is showing much lower fluxes than the EMEP map, and much lower fluxes over central and southern German regions in the EMEP NH_X-N map compared to the German result. The EMEP result here is not in line with the national Emission inventory (cf. Figure 5.10) and the spatial trend shown in the EMEP NH_X-N map may be interpreted as a too far eastward shift by the model's transport calculation.

The SO_X-S maps (Figure 6.14 (a) and (b)) are in relatively good agreement, as the overall magnitude and the maximum deposition areas are concerned. Again in the EMEP result the spatial distribution of forested areas receiving relatively high deposition rates (Figure 6.14 (a)), compared to other surrounding land use, must be taken as a sub-grid effect, which hides behind the 50x50km² grid resolution, and thus can not be found in those maps.

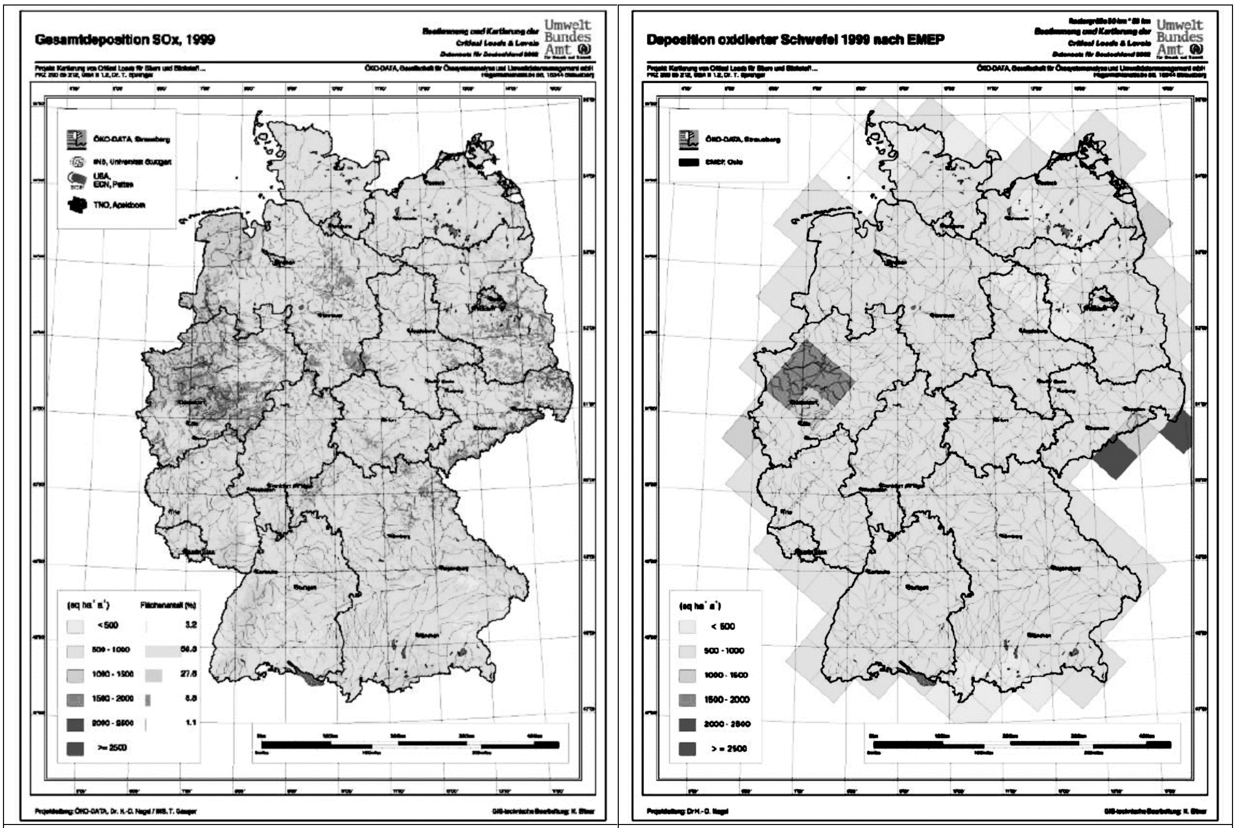

(a) German map of SO_X-S total deposition 1999

(b) EMEP map of SO_X-S total deposition 1999

Figure 6.14: German (a) and EMEP (b) total deposition of SO_X-S-1999

6.4 Maps of total deposition 1990-1999

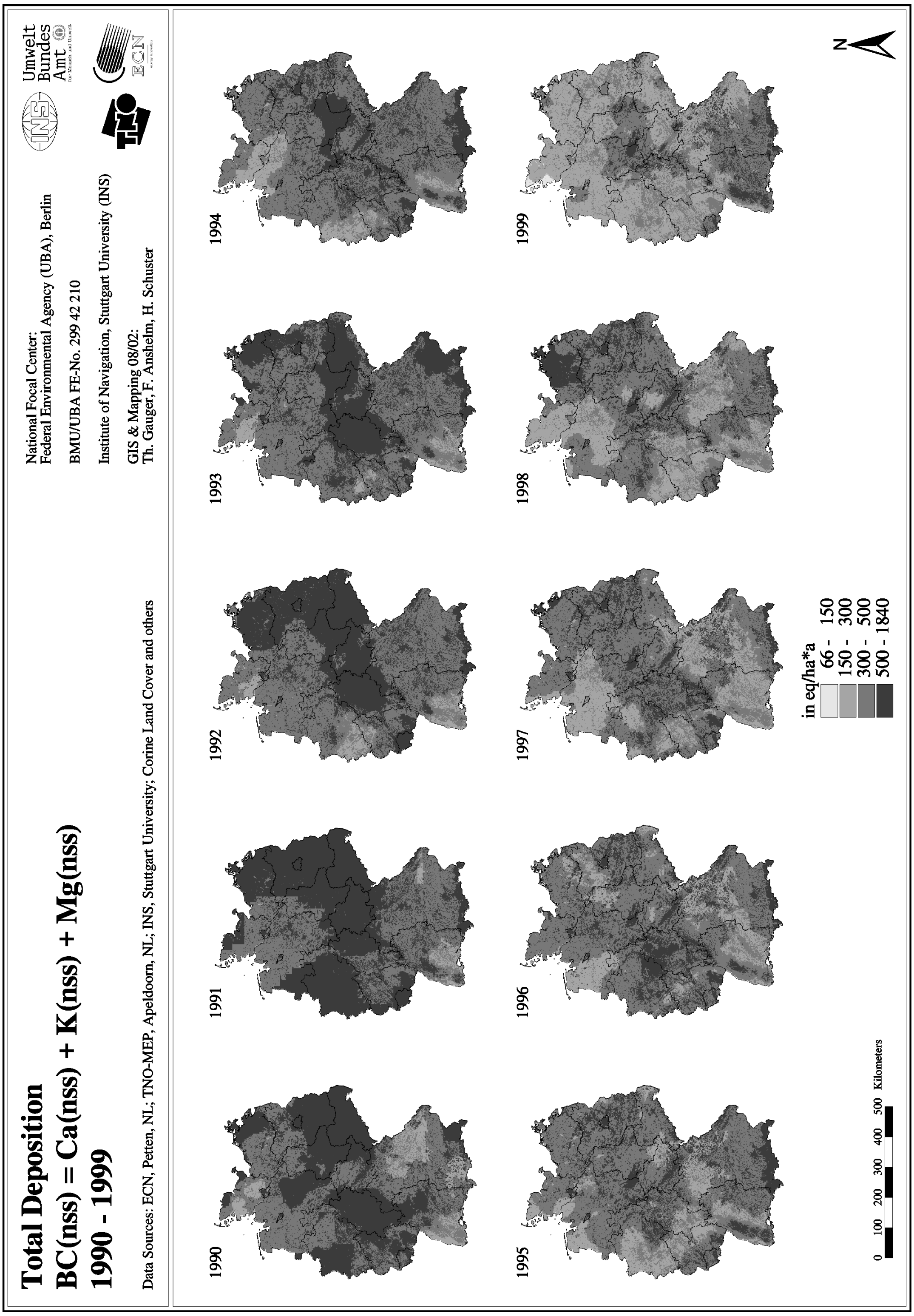

Map 6.1: Total deposition of $BC_{(nss)}$ 1990-1999

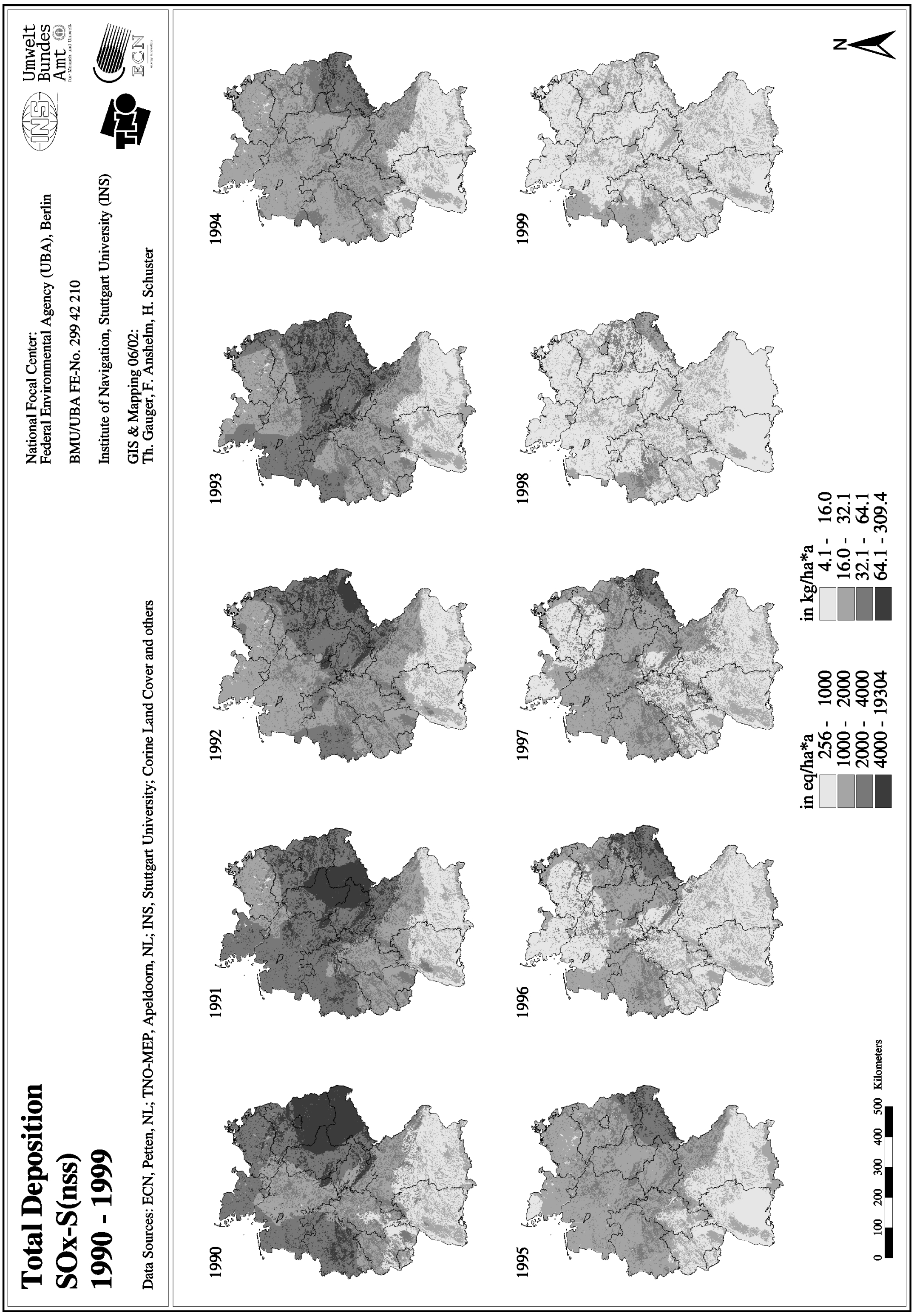

Map 6.2: Total deposition of SO_X-S 1990-1999

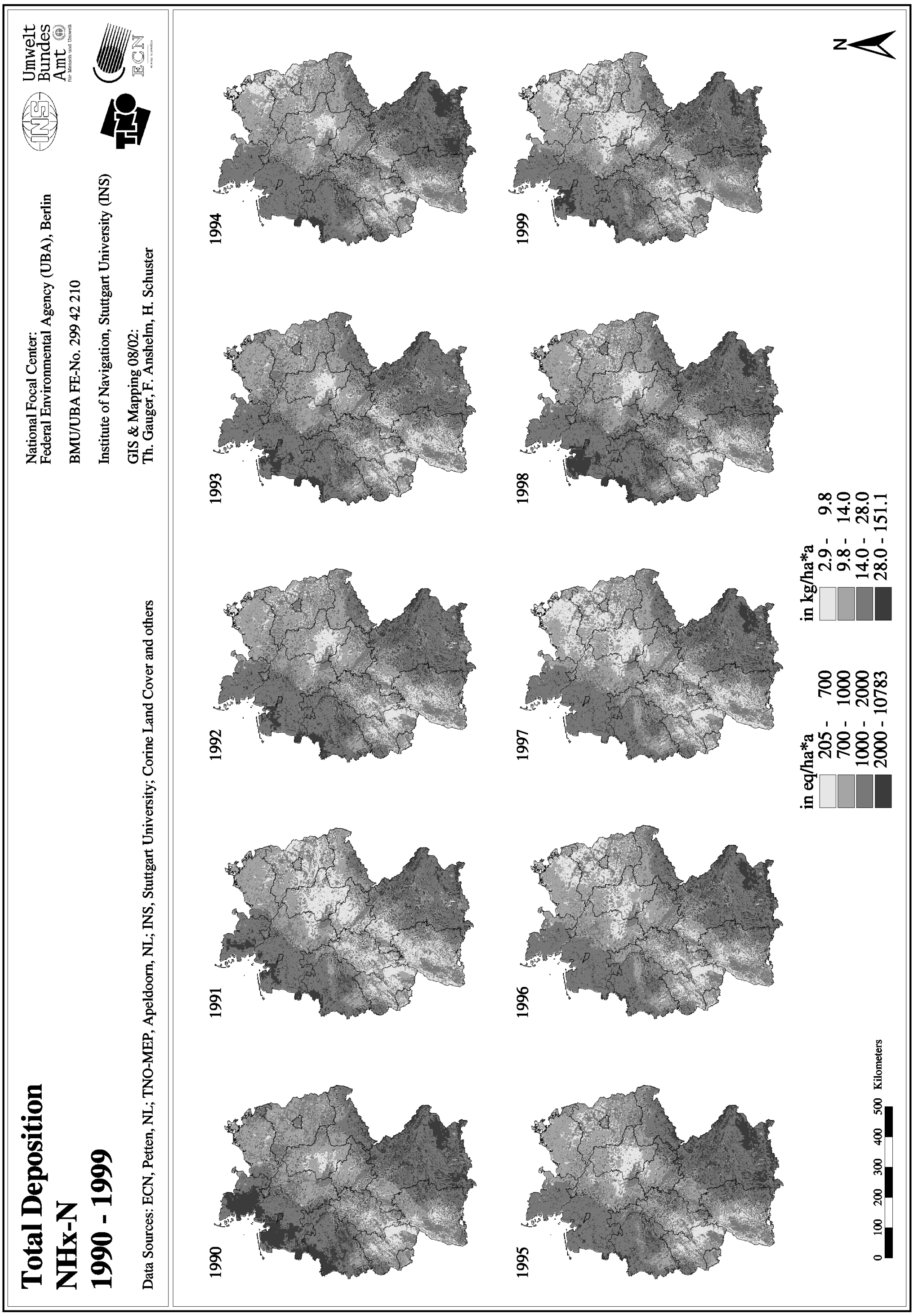

Map 6.3: Total deposition of NH_X-N 1990-1999

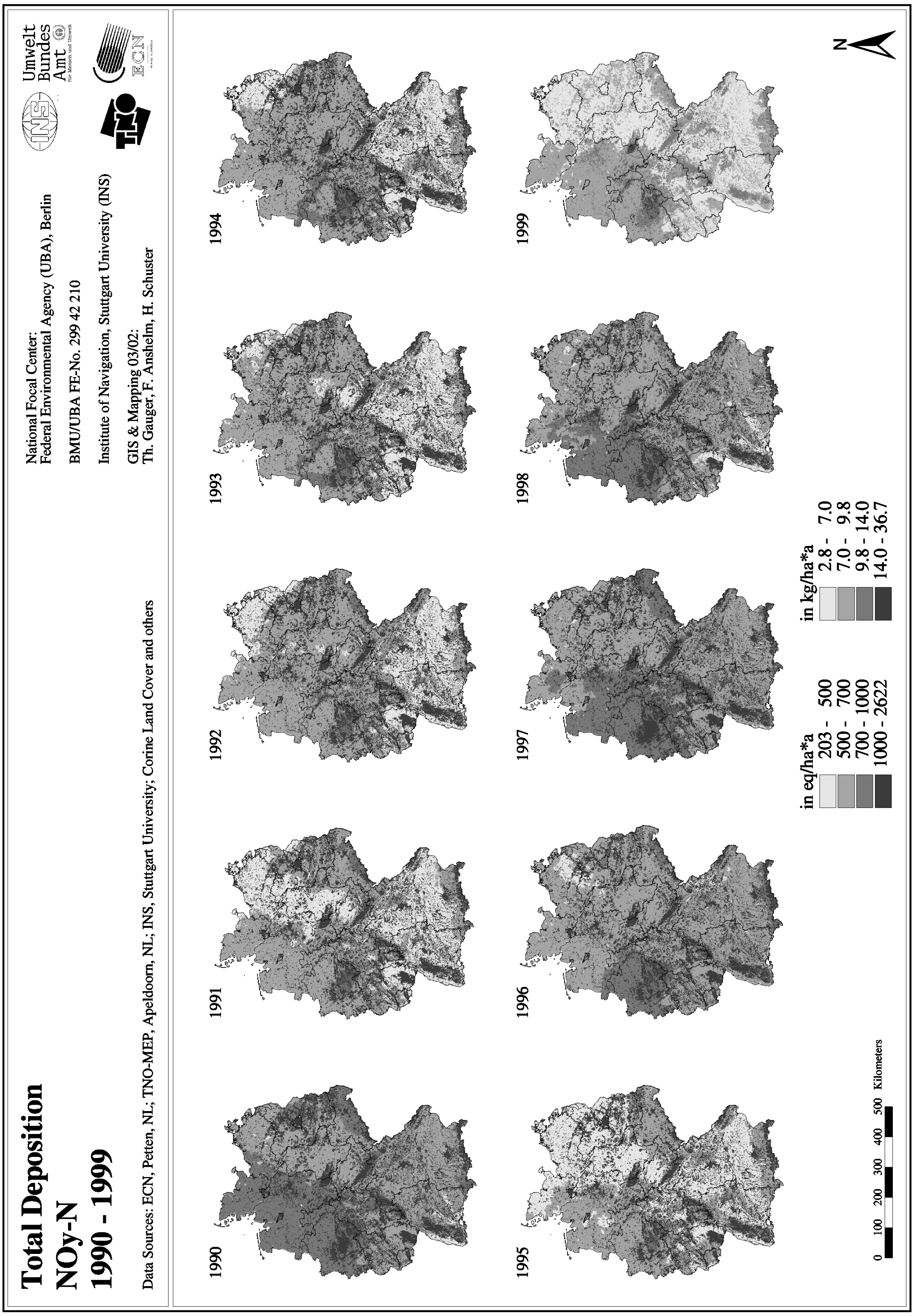

Map 6.4: Total deposition of NO$_Y$-N 1990-1999

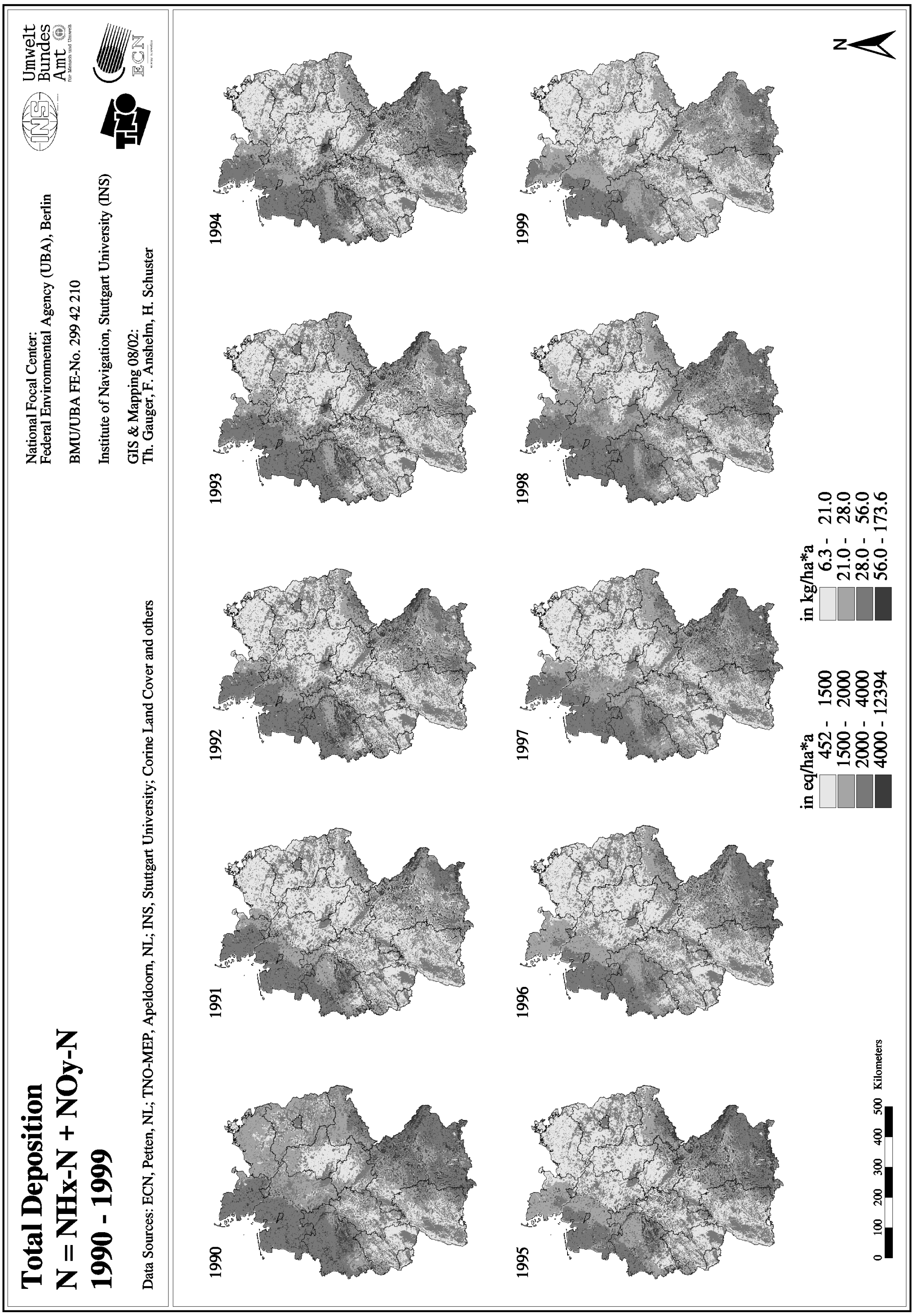

Map 6.5: Total deposition of N 1990-1999

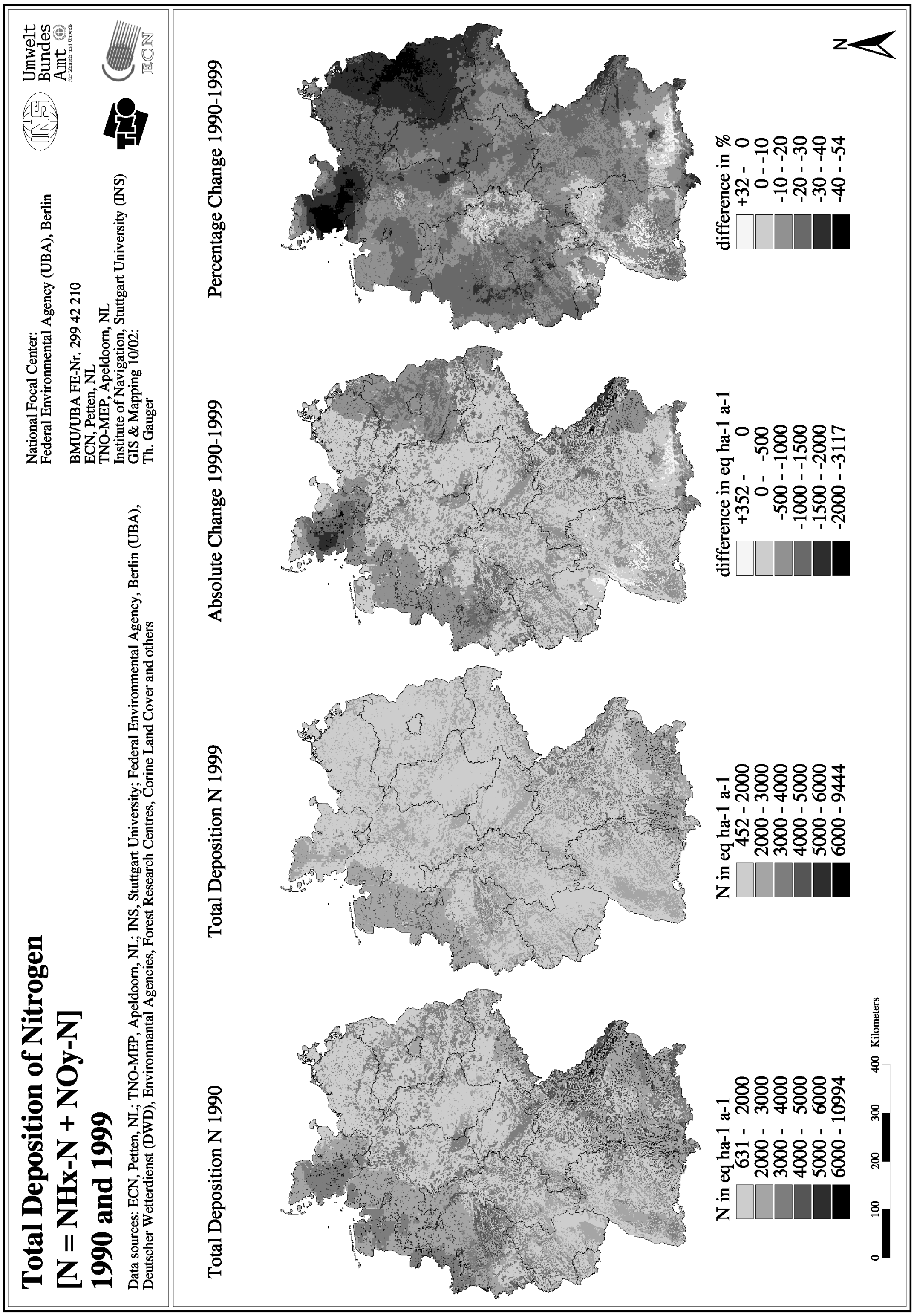

Map 6.6: Total deposition of nitrogen 1990 and 1999 and changes from 1990 to 1999

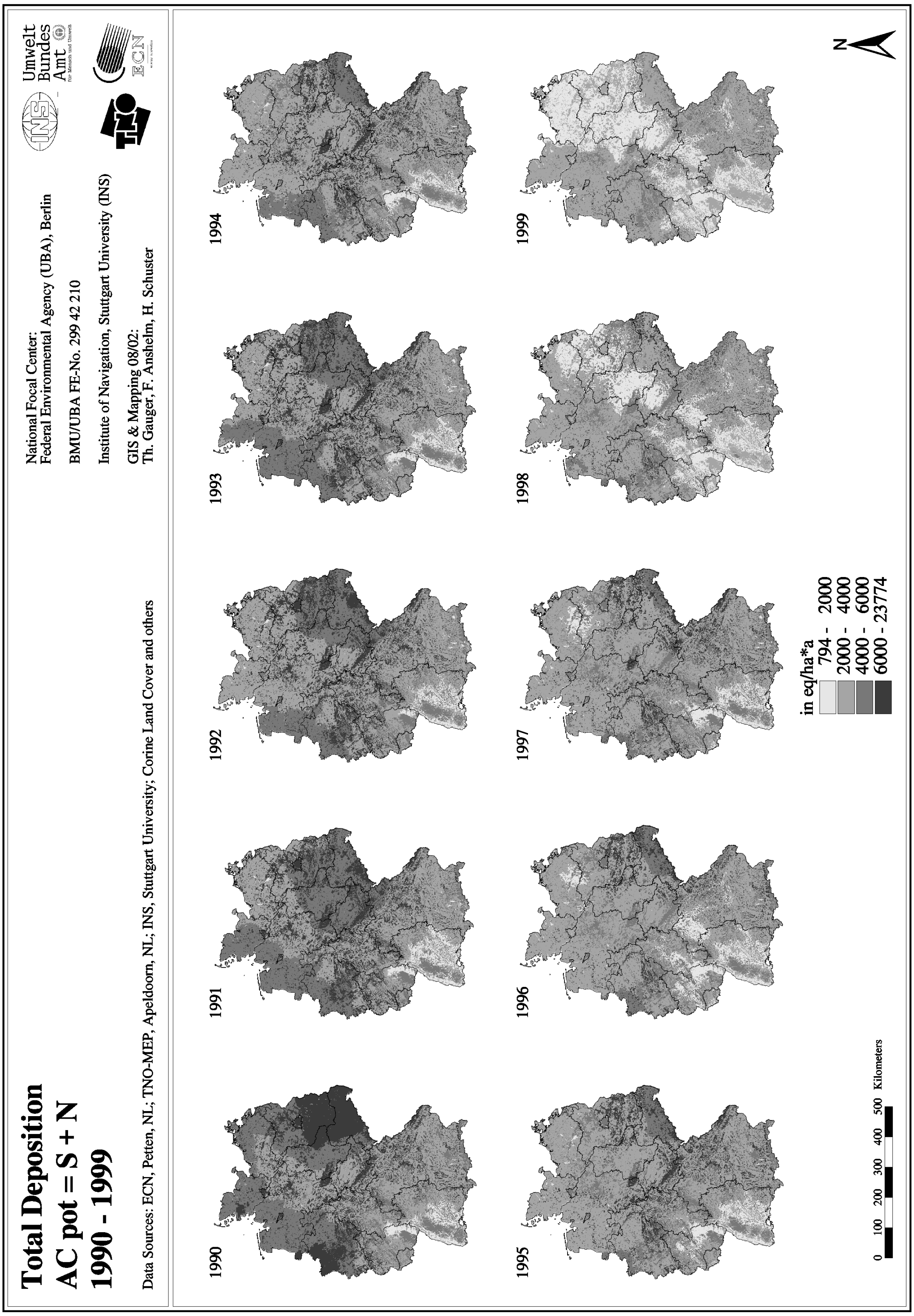

Map 6.7: Total deposition of AC_{pot} 1990-1999

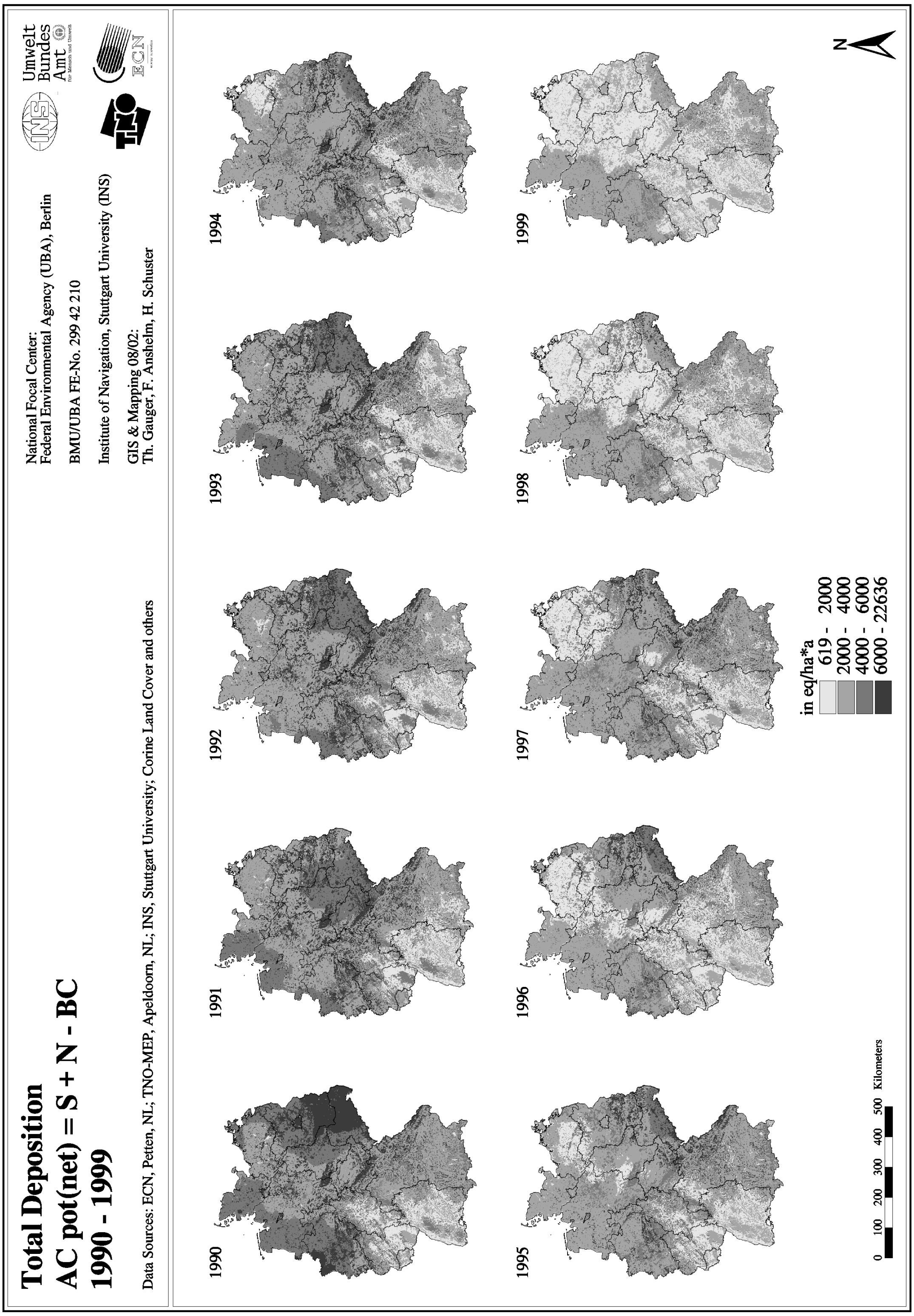

Map 6.8: Total deposition of $AC_{pot(net)}$ 1990-1999

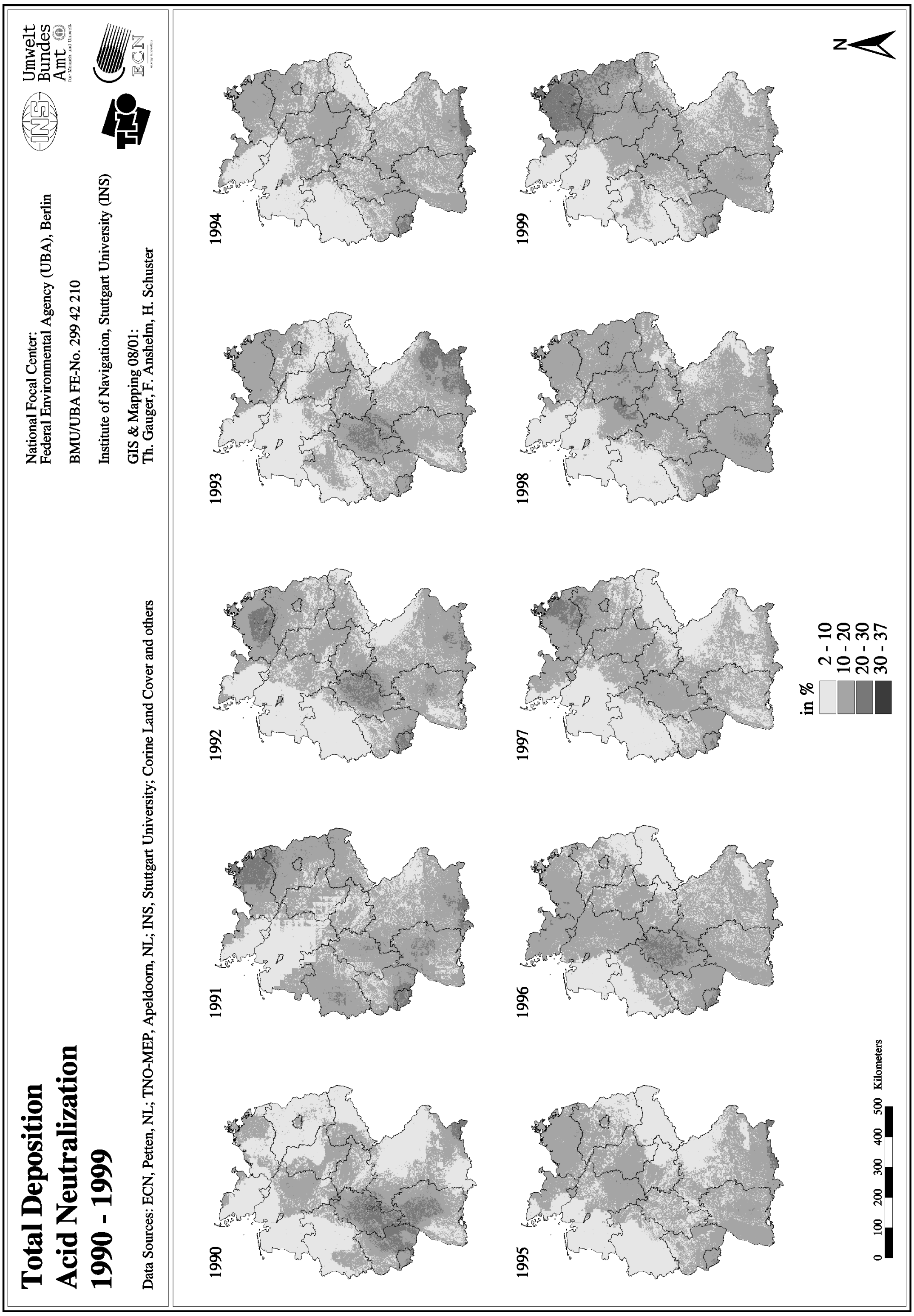

Map 6.9: Neutralisation of dry deposited AC_{pot} by $BC_{(nss)}$ 1990-1999

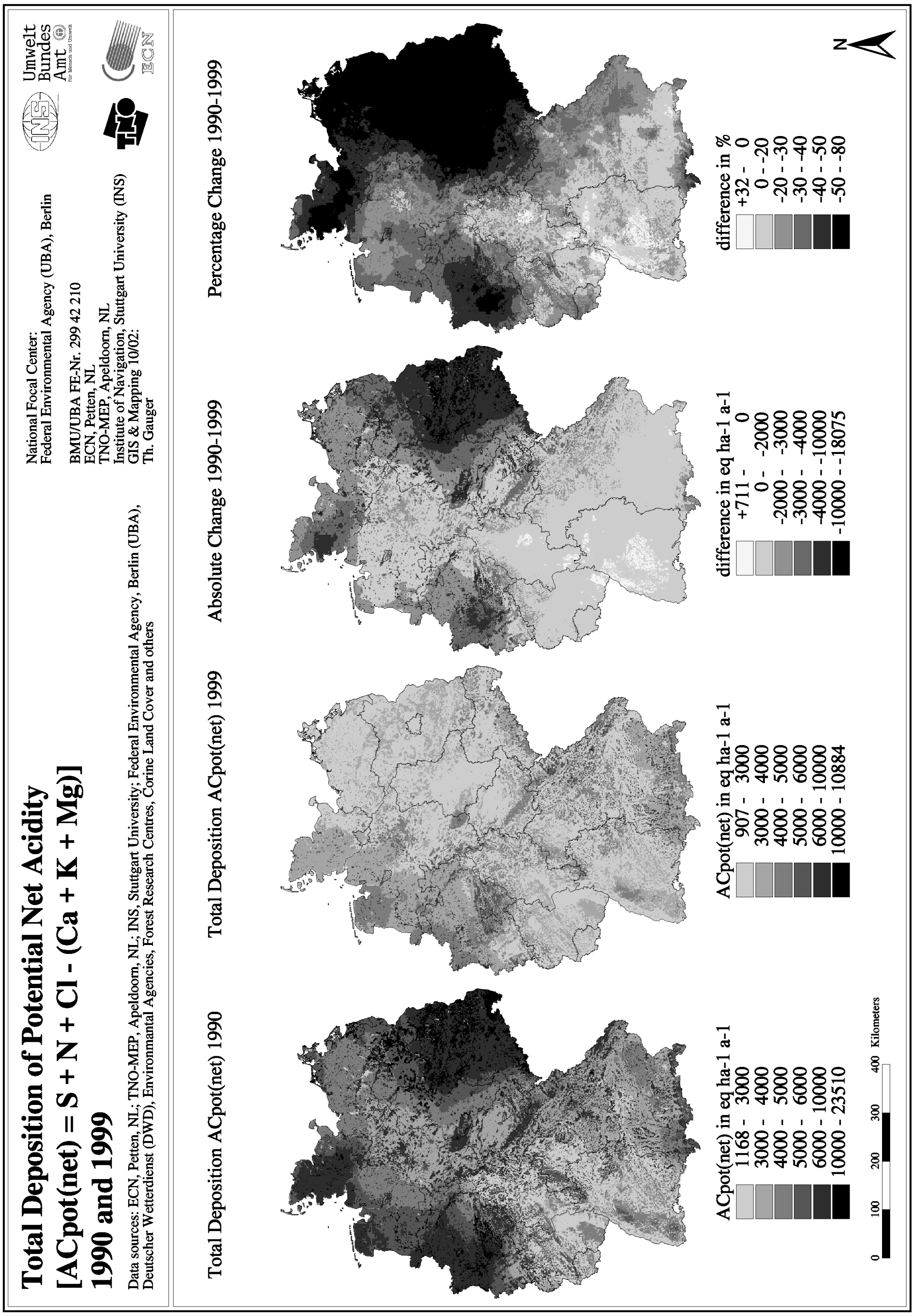

Map 6.10: Total deposition of $AC_{pot(net)}$ 1990 and 1999 and changes from 1990 to 1999

Conclusions and discussion

A main purpose of the work done within this research study is to derive long term trends of deposition loads in Germany. The time series of total deposition of oxidised sulphur (SO_X-S=SO_2-S+SO_4-S), oxidised nitrogen (NO_Y-N=NO_3-N+NO_2-N+NO-N+HNO_3-N), reduced nitrogen (NHX-N=NH_4-N+NH_3-N), base cations (BC=Ca+K+Mg), sodium (Na) and chlorine (Cl) presented in this report is covering the ten years period from 1990 to1999.

The deposition data sets modelled and mapped within this research project are primarily serving as input for critical loads and critical loads exceedance calculations for forest and seminatural non-forest ecosystems in Germany. Also other scientific projects, in which modelled deposition estimates covering Germany in a small scale are required, are provided with this deposition data sets. The basic method applied to derive total deposition consists in a combination of receptor independent wet deposition, derived by properly used kringing interpolation of wet deposition monitoring data (concentration of the main compounds in precipitation) and intersection with measurement based DWD modelled high resolution precipitation maps, with receptor specific dry deposition, derived by using the inferential models EUTREND (for NH_X-N) and IDEM (for SO_X-S, NO_Y-N, Ca, K, Mg, and Na). Thus the two most considerable deposition fluxes are included. The magnitude of cloud deposition also could be quantified by developing a cloud deposition module for the inferential model IDEM on the basis of findings within previous research projects. Those preliminary results of cloud deposition fluxes, however, are not yet implemented into the calculation of total deposition, since liquid water contents could only be made available for 1996 and not for the whole period from 1990 to 1999.

The progress and further development in modelling and mapping procedures within this research project mainly consists in

- a thorough update of the wet deposition database by comprehensive monitoring data acquisition, including provided revised data, which, compared to the previous project, allows an extension of wet deposition mapping for the years 1990 to 1992 and 1996 to 1999 and to recalculate wet deposition maps over the whole time period from 1990 to 1999
- acquisition of DWD modelled precipitation fields in 1x1km^2 grid resolution
- the development of the new IDEM dry deposition scheme by an update and modification of the EDACS dry deposition scheme, in terms of the horizontal resolution of meteorological

and air concentration input data (inverse distance weighting interpolation of coarse resolution data sets in order to derive 1x1km² grid resolution data with adequate horizontal continuity) and the retrieval of input data formats, improved (localised) parameterisation of atmospheric stability by calculation of local micrometeorological fluxes, and other corrections

- the development of an IDEM cloud deposition module and calculation of preliminary cloud deposition fields
- acquisition of ECMWF modelled 0,5°x0,5° grid meteorological data in six hourly time resolution
- acquisition of EMEP LRT 150x150km² grid air concentration fields for 1985 and 1990 to 1996 and of NERI DEM/DEHM 0,5°x0,5° grid air concentration fields for 1990 and 1996 to 2000 each in six hourly time resolution
- acquisition of revised NH_X emission data per German (Land-)Kreis for 1990 to 1998 from IER/UBA, reallocation of the emission data to agricultural area land use and modelling of NH_X air concentration using the EUTREND model
- modelling and mapping of wet, dry and total deposition for the period 1990 to 1999 in 1x1km² grid resolution for the six land use classes (1) urban areas, (2) agricultural areas, (3) deciduous forests, (4) coniferous forests, (5) mixed forests, and (6) inland water
- derivation of trends in deposition over the whole time period considered

Average total deposition of non-seasalt sulphur over Germany between 1990 and 1999 almost steadily declined by 68%. The magnitude of average total non-seasalt sulphur deposition fell from about 47 kg ha^{-1} a^{-1}1990 to about 15 kg ha^{-1} a^{-1} in 1999. Highest deposition rates, ranging between 175 up to more than 300 kg ha^{-1} a^{-1} can be found only in 1990 over forested areas in south-east Germany (Saxony, Saxony-Anhalt, Brandenburg). The peak values in 1999 are ranging between about 30 kg ha^{-1} a^{-1} and 38 kg ha^{-1} a^{-1} and can be observed in urban agglomeration areas and forested areas in western, north-western and eastern Germany. Lowest total deposition fluxes over the whole period can be observed in southern Germany, in 1999 in all regions except in north-western Germany and the eastern most part (Saxony, south-east Brandenburg).

Average total deposition of nitrogen, composed of reduced and oxidised nitrogen by average 61% and 39%, respectively, declined by 24% between 1990 and 1999. The average nitrogen total deposition load fell from almost 35 kg ha^{-1} a^{-1} in 1990 to 26 kg ha^{-1} a^{-1} in 1999. Highest deposition loads over 85 kg ha^{-1} a^{-1} can be observed in forested areas in north-western Germany, southern and eastern Bavaria. Minimum values are found between 6 kg ha^{-1} a^{-1} to 9 kg ha^{-1} a^{-1} over all Germany, over forested areas lowest values are ranging between 21 kg ha^{-1} a^{-1} and 33 kg ha^{-1} a^{-1}.

Total deposition of potential acid, calculated as the sum of nitrogen and non-seasalt sulphur total deposition, fell by about 48% from average 5.3 keq ha^{-1} a^{-1} in 1990 to 2.8 keq ha^{-1} a^{-1} in 1999. Maximum values over 20 keq ha^{-1} a^{-1} in 1990 can be observed over forested areas in Saxony. In 1999 the maximum values are above 7 keq ha^{-1} a^{-1} and can be found in forested areas in Lower Saxony, North Rhine-Westphalia and southern Bavaria, where the deposition rates of reduced nitrogen are highest. The minimum values of potential acid total deposition in Germany is about 1 keq ha^{-1} a^{-1}, in forested areas the minimum lies between 3 keq ha^{-1} a^{-1} in 1990 and 2 keq ha^{-1} a^{-1} in 1999. From 1994 onward average nitrogen total deposition is the main contributor to total deposition of potential acid, due to the faster decline of non-seasalt sulphur (-58%) compared to the decline of nitrogen total deposition (-24%) over the same time period. In 1998 and 1999 the average total deposition of reduced nitrogen alone is higher than average total deposition of non-seasalt sulphur.

Calcium contributes by average 66% to total deposition of non-seasalt base cations, whereas potassium contributes by 29% and magnesium only by about 6%. Average acid neutralisation by total deposition of non-saesalt base cations over the whole period ranges between 11% in 1990 and 13% in 1999. Average acid neutralisation 1990 to 1999 in forested areas ranges from about 7% to 11%, maximum values can be found between 17% and 32%, minimum values between 2% and 3%. Over the whole period from 1990 to 1999 average acid neutralisation is slightly rising. The changes, however, are relatively small, due to the decline of total deposition of potential acid as well as of total deposition of non-seasalt base cations.

The methods applied to assess total deposition loads in Germany are based upon the coupling of measurements and models. This modelling and mapping procedures are used to predict deposition results in space and time. There are, however, uncertainties in modelling and mapping results, and where ever possible measurement data are used. Deposition measurement data are in a more direct way used for the processing of wet deposition fields. The resistance parameterisations of the dry and cloud deposition models are based upon measurements and implemented due to the current state of knowledge to derive deposition velocity and dry and cloud deposition fields. Measurements and other measurement based independent estimates are also used to evaluate model results, both for data used as basic input for model calculations and for deposition estimates.

Compared to the results of the preliminary projects (BLEEKER ET AL 2000, GAUGER ET AL 2000) in some cases higher total deposition estimates were recalculated within this study. This mainly is due to the dry deposition model results and can to a certain degree be attributed to revised, and hence changed and more reliable air concentration data, which are basic input to the dry deposition model calculations.

In a comparative study between mapping results of total deposition at certain coniferous forest plots with canopy budged model calculations using measured deposition, the mapped total deposition of the single compounds to different degrees is higher than those canopy budget model results. Sodium, calcium and magnesium mapping results are comparing good with the canopy budget model results, while for potassium, oxidised sulphur, oxidised and reduced nitrogen the canopy model calculations yield lower estimates than the deposition model results. However, uncertainties in both model results compared must be taken into account when judging the modelling and mapping results by canopy budget model results. The remarkable good agreement in the 1999 comparison for oxidised nitrogen indicates the important role of basic input data quality with respect to the model output. The air concentration model as well as the emission data used have been changed and improved to derive the 1999 air concentration fields, which leads to obviously different results of the deposition model estimates compared to previous years.

The synopsis of the total deposition mapping results carried out in this project with actual EMEP total deposition maps over Germany obviously shows the different spatial scale due to the differentiation in a ecosystem specific 1x1km^2 grid and an ecosystem averaged 50x50km^2 EMEP grid. Aside this fundamental difference, the spatial trend and magnitude of total deposition of oxidised sulphur and oxidised nitrogen 1999 is comparing relatively good, whereas the mapping results for reduced nitrogen are quite different. The latter is due to the EMEP model approach, where only long-range transport is accounted for and the local scale deposition of ammonia, which on the ecosystem level is very important in magnitude, is not considered.

The deposition maps generated within this project are providing high spatial resolution on an ecosystem level to qualitatively and technically fulfil the given requirements to be used for

- calculating critical loads and critical loads exceedances for acidity and eutrophication for sensitive ecosystems in Germany
- deriving differentiated spatial trends of deposition over Germany and
- deriving trends in time within the ten year time period 1990 to 1999 considered

Furthermore the maps are providing a useful instrument for effect-based emission abatement evaluation.

Aside an actualisation of the deposition mapping in time, further work should aim at (1) further evaluation of the mapping results including a minimisation of errors and uncertainties and further qualitative optimisation, (2) acquisition of input data needed to fully integrate cloud water deposition into the mapping of total deposition, (3) acquisition of input data necessary to map and model total deposition of heavy metals, (4) the prediction of trends and calculation of scenarios to provide data which, among others, are needed for dynamic modelling and (5) providing mapping results for other research projects, where deposition data are in different spatial scale needed for e.g. risk assessment, planning purposes, sustainable development and the definition of environmental targets.

Zusammenfassung und Diskussion

Eine wesentliche Aufgebe in der Bearbeitung des Forschungsprojektes ist es, Langzeittrends der Depositionsraten in Deutschland zu erarbeiten. Der vorliegende Abschlußbericht umfasst die Dokumentation der Kartierung der Gesamtdeposition von oxidierten Schwefelverbindungen (SO_X-S=SO_2-S+SO_4-S), oxidiertem Stickstoff (NO_Y-N=NO_3-N+NO_2-N+NO-N+HNO_3-N), reduziertem Stickstoff (NHX-N=NH_4-N+NH_3-N), basischen Kationen (BC=Ca+K+Mg), Natrium (Na) und Chlor (Cl) im Zehnjahreszeitraum von 1990 bis 1999.

Die innerhalb des Forschungsprojektes modellierten und kartierten Depositionsdatensätze dienen als wesentlicher Input der Berechnung von Critical Loads und ihrer Überschreitung in Waldökosystemen und naturnahen waldfreien Ökosystemen in Deutschland. Daneben werden die Depositionsdatensätze auch weiteren Forschungsprojekten zur Verfügung gestellt, in welchen aufgrund unterschiedlicher Fragestellungen Bedarf an flächendeckenden Depositionsdaten besteht. Die methodische Grundlage der Kartierung der Gesamtdeposition besteht in er Kombination von rezeptorunabhängiger Nassdeposition, berechnet durch Verschneidung von hoch aufgelösten, aus Niederschlagsmessungen modellierten Niederschlagskarten des DWD mit kriging-interpolierten Messdaten der Stoffkonzentrationen der Hauptkomponenten im Niederschlag, und rezeptorspezifischer Trockendeposition, die mit Hilfe der Inferentilamodelle EUTREND (für NH_X-N) und IDEM (für SO_X-S, NO_Y-N, Ca, K, Mg, and Na) berechnet wird. Damit sind die beiden ihrer Größenordnung nach wesentlichen Depsoitionsflüsse einbezogen. Eine Quantifizierung der zusätzlichen Wolkenwasserdeposition konnte durch die Entwicklung eines Wolkenwasserdepositions-Moduls für das Inferentalmeodell IDEM auf Basis der Erkenntnisse und Entwicklungen der vorangegangenen Forschungsprojekte, erfolgen. Auf die Einbeziehung auch dieses Depositionsflusses in die Berechnung der Gesamtdeposition wird zunächst jedoch verzichtet, da Wolken-Flüssigwassergehalte nur für das Bezugsjahr 1996 verfügbar gemacht werden konnten und nicht für alle Jahre der betrachteten Zeitserie 1990 bis 1999.

Die innerhalb des Forschungsprojektes erfolgte Weiterentwicklung der Modellierungsverfahren und Kartierungsarbeiten besteht in

- wesentlicher Verbesserung der Datenbasis der Nassdeposition durch weitere umfangreiche Akquisition von Monitorigdaten, einschließlich gelieferter revidierter Daten, wodurch eine

Erweiterung der bisherigen Kartierung um die Jahre 1990 bis 1992 und 1996 bis 1999, und damit die Neuberechnung für den gesamten Zehnjahreszeitraum 1990-1999 erfolgen konnte

- der Akquisition von Niederschlagskarten des DWD im 1x1km² Raster
- der Entwicklung des neuen IDEM Trockendepositionsmodells durch Modifikationen und Verbesserungen des EDACS Modellprogramms hinsichtlich der horizontalen Auflösung der Eingangsdaten (Anpassung räumlicher Kontinuität im 1x1km² Grid bei grob aufgelösten Immissions- und Meteorologiedatensätzen durch Inverse Distance Weighting Interpolation), der Abfrage von Daten verschiedener Formate, verbesserter (lokalisierter) Parametrisierung atmosphärischer Stabilität, bzw. Berechnung lokaler mikrometeorologischer Flüsse und weiterer Korrekturen
- der Entwicklung eines Wolkenwasserdepositionsmoduls in IDEM und Berechnung vorläufiger Wolkenwasserdepositionskarten
- der Akquisition von ECMWF Meteorologiedatensätzen im 0,5°x0,5° Raster und in einer zeitlichen Auflösung von sechs Stunden
- der Datenakquisition von EMEP LRT modellierten Immissionskonzentrationen für 1985 und 1990 bis 1996 im 150x150km² Raster und von NERI DEM/DEHM Immissionskarten für 1990 und 1996 bis 2000 im 0,5°x0,5° Raster, jeweils in einer zeitlichen Auflösung von sechs Stunden
- der Akquisition von revidierten NH_X Emissionsdaten auf (Land-)Kreisbasis für die Jahre 1990 bis 1998 bei IER/UBA, Zuordnung der Emissionen zur landwirtschaftlichen Landnutzungsklasse und Modellierung der NH_X Immissionskonzentrationen mit dem EUTREND Modell
- der Modellierung und Kartierung der Nass-, Trocken- und Gesamtdeposition im Zeitraum 1990 bis 1999 im 1x1km² Raster differenziert in die sechs Landnutzungsklassen (1) bebaute Gebiete, (2) landwirtschaftliche Flächen, (3) Laubwald, (4) Nadelwald, (5) Mischwald, und (6) Binnengewässer
- der Darstellung der Entwicklung des Depositionsgeschehens im gesamten betrachteten Zehnjahreszeitraum

Die Gesamtdeposition von seesalzkorrigiertem Schwefel zeigt in dem Zeitraum zwischen 1990 und 1999 eine nahezu stetig verlaufende mittlere Verminderung um ca. 68% für die Gesamtfläche Deutschlands. 1990 lag der mittlere Eintrag bei ca. 47 kg ha^{-1} a^{-1}, 1999 bei etwa 15 kg ha^{-1} a^{-1}. Die höchsten Depositionsraten sind 1990 mit Werten zwischen ca. 175 bis über 300 kg ha^{-1} a^{-1} höher als in allen Folgejahren und sind in den Waldgebieten in Südostdeutschland (Sachsen, Sachsen-Anhalt, Brandenburg) zu beobachten. 1999 liegen die höchsten Werte bei ca. 30 kg ha^{-1} a^{-1} bis etwa 38 kg ha^{-1} a^{-1} in den städtischen Agglomerationen und Waldgebieten in West-, Nordwest- und Ostdeutschland. Niedrigste Gesamtdepositionsraten sind in allen Jahren in Süddeutschland zu finden, 1999 außer in Nordwestdeutschland und dem äußerten Osten (Sachsen, Südostbrandenburg) in allen übrigen Regionen.

Stickstoffgesamteinträge, die sich im Mittel zu etwa 61% aus reduzierten und zu ca. 39% aus oxidierten Stickstoffverbindungen zusammensetzen, haben sich im Zeitraum 1990 bis 1999 um ca. 24% vermindert. Der mittlere Eintrag verringerte sich damit von knapp 35 kg ha^{-1} a^{-1} auf ca. 26 kg ha^{-1} a^{-1}. Die höchsten Einträge liegen in Waldgebieten bei über 85 kg ha^{-1} a^{-1} und sind in Nordwestdeutschland sowie in Süd- und Ostbayern zu beobachten. Die niedrigsten beobachteten Eintragsraten liegen in Waldgebieten bei ca. 21-33 kg ha^{-1} a^{-1}, bezogen auf die Gesamtfläche Deutschlands bei etwa 6 bis 9 kg ha^{-1} a^{-1}.

Der potentielle Säureeintrag mit der Gesamtdeposition, berechnet als Summe der Stickstoff- und seesalzkorrigierten Schwefelverbindungen, nahm von 1990 (im Mittel ca. 5,4 keq ha^{-1} a^{-1}) bis 1999 (im Mittel ca. 2,8 keq ha^{-1} a^{-1}) um ca. 48% ab. Maximalwerte liegen 1990 in Waldgebieten über 20 keq ha^{-1} a^{-1} und sind in Sachsen zu beobachten. 1999 liegen maximale Werte in Waldgebieten über ca. 7 keq ha^{-1} a^{-1} und treten in einzelnen Gebieten hoher Deposition von reduziertem Stickstoff in Niedersachsen, Nordrhein-Westfalen und Südbayern auf. Bezogen auf die Gesamtfläche Deutschlands liegen die Minima potentieller Säureeinträge bei ca. 1 keq ha^{-1} a^{-1}, bezogen auf Waldgebiete bei ca. 3 keq ha^{-1} a^{-1}1990 und bei ca. 2 keq ha^{-1} a^{-1} 1999. Aufgrund des im Vergleich zu Stickstoff starken Rückgangs der Schwefeldepositionen sind seit 1994 die mittleren Anteile der Stickstoff-Gesamtdeposition an der potentiellen Säure in Deutschland höher als die mittleren seesalzkorrigierten Schwefelanteile. 1998 und 1999 sind sogar die mittleren Anteile der Gesamtdeposition reduzierter Stickstoffverbindungen an der Gesamtdeposition potentieller Säure größer als die mittlere Gesamtdeposition von seesalzkorrigiertem Schwefel.

Kalzium hat an der seesalzkorrigierten Summe basischer Kationen einen Anteil von etwa 66%, während der Kaliumanteil im Mittel ca. 29% und der Magnesiumabteil ca. 6% beträgt. Bei der Gegenüberstellung der Gesamteinträge von basischen Kationen und potentieller Säure ergibt sich im Mittel eine Säureneutralisationsrate zwischen 11% (1990) und 13% (1999). In Waldgebieten beträgt die mittlere Säureneutralisationsrate in allen betrachteten Jahren ca. 7% bis 11% mit Maxima zwischen 17% (1996) und 32% (1994) und Minima zwischen 2% und 3%. Die Veränderungen in der Säureneutralisation sind im zeitlichen Verlauf der betrachteten Jahre 1990 bis 1999 aufgrund der Verminderung sowohl der Säurebildner als auch der basischen Kationen in der Gesamtdeposition verhältnismäßig gering.

Bei der angewandten Methodik der Ermittlung der Gesamtdeposition in Deutschland werden Messungen und Modelle miteinander verknüpft. Bei den Modellierungen und Kartierungsarbeiten werden räumlich flächendeckende und zeitlich kontinuierliche Aussagen zum Depositionsgeschehen gemacht. Jedoch bestehen auch Unsicherheiten in den Modell- und Kartierungsergebnissen und soweit möglich wird auf direkte Messungen zurückgegriffen. Depositionsmessdaten werden in einem eher direkten Verfahren zur Kartierung der Nassdeposition verwendet. Die Widerstandsparameterisierung der Modelle basiert auf Messungen und wird, was durch die Modifikationen des IDEM Modells realisiert wird, entsprechend gegenwärtig verfügbarer Erkenntnisse angewendet, um Depositionsgeschwindigkeiten und Depositionskarten zu erstellen. Messwerte und andere aus Messwerten abgeleitete unabhängige Schätzungen werden außerdem zur Evaluation der Modellergebnisse, sowohl hinsichtlich des Dateninputs der Modellberechnungen, als auch für die Validierung Depositionskarten genutzt.

Im Vergleich mit dem vorangegangenen Projekten (BLEEKER ET AL 2000, GAUGER ET AL 2000) liefern die in diesem Projekt neu berechneten Kartierungsergebnisse in einigen Fällen höhere Gesamtdepositionen. Dies ist in erster Linie auf die Modellergebnisse der Trockendepositionsberechnung zurückzuführen. Hierbei lassen sich die höheren Trockendepositionsraten wiederum auf die als wesentliche Inputdaten verwendeten aktualisierten - und damit geänderten aber auch verlässlicheren - Immissionskonzentrationen zurückführen.

Die Gegenüberstellung der Kartenwerte mit Gesamtfrachten aus Kronenraumbilanzmodellberechnungen für Nadelwaldstandorte ergibt für die einzelnen Komponenten in unterschiedlichem Ausmaß vergleichsweise hohe Ergebnisse für die modellierten und kartierten Gesamtdepositionen. Die Kartierungsergebnisse für Natrium, Calcium und Magnesium weisen relativ gute Übereinstimmung mit den Berechnungen des Kronenraumbilanzmodells auf, während der Vergleich bei Kalium, oxidiertem Schwefel, oxidiertem und reduziertem Stickstoff niedrigere Kronenraumbilanzmodellergebnisse liefert. Bei der Beurteilung der Modell- bzw. Kartierungsergebnisse durch die Schätzungen mit Hilfe von Kronenraumbilanzmodellen sollten die beiden Ansätzen zugrundeliegenden Unsicherheiten berücksichtigt werden. Die im gezogenen Vergleich bemerkenswert gute Übereinstimmung der Ergebnisse bei oxidierem Stickstoff 1999 verweist auf die bestimmende Rolle der Qualität der verwendeten Inputdaten bezüglich der Modellergebnisse. Sowohl die Modellierung der Immissionsflder, als auch die dabei verwendeten Emissionsdaten wurden gegenüber den Vorjahren verändert und verbessert. Dies wirkt sich folglich auf die Ergebnisse der Depositionsmodellierung aus.

In der Gegenüberstellung der in diesem Forschungsprojekt kartierten Gesamtdeposition mit aktuellen EMEP Kartierungsergebnissen für Deutschland werden die Unterschiede der räumlichen Differenzierung, die durch die Auflösung im ökosystemspezifischen 1x1km^2 Raster und im für verschiedene Ökosysteme gemittelten 50x50km² EMEP-Raster gegeben sind, unmittelbar deutlich. Abgesehen von diesen grundsätzlichen Unterschieden weisen die Eintragshöhen und deren räumliche Verteilung bei oxidiertem Schwefel und oxidiertem Stickstoff 1999 relativ gute Übereinstimmungen auf. Dies ist bei der Gesamtdeposition von reduziertem Stickstoff nicht der Fall, da die EMEP Karte nur den weitreichenden ('long-range') Transport berücksichtigt und die in ihrer Größenordnung wesentlichen, ökosystemrelevanten Depositionen im Nahbereich von Emissionsquellen völlig vernachlässigt.

Die innerhalb des Forschungsprojektes erstellten Depositionskarten erfüllen die qualitativen und technischen Anforderungen

- der Berechnungen von Critical Loads und Critical Loads Überschreitungen für Säure und Eutrophierung sensitiver Ökosysteme in Deutschland
- der Darstellung von räumlich differenzierten Trends des Depositionsgeschehens in Deutschland und
- der Abbildung zeitlicher Trends innerhalb des betrachteten Zehnjahreszeitraumes von 1990 bis 1999

im Hinblick auf notwendige und hinreichende hohe räumliche und ökosystemspezifische Differenzierung. Sie sind damit auch als Instrument der wirkungsspezifischen Erfolgskontrolle von Emissionsminderungen nutzbar.

Abgesehen von einer zeitlichen Fortschreibung und notwendiger Aktualisierung der Kartierungen leiten sich Zukünftige Aufgaben, aus den im vorliegenden Abschlußbericht dargestellten Ergebnissen ab und liegen (1) im Bereich der weiteren Validierung der Kartierungsergebnisse, einschließlich einer Minimierung von Unsicherheiten und anzustrebender weiterer qualitativer Optimierung, (2) der Beschaffung notwendiger Inputdaten zur Integration der Wolkenwasserdeposition in die Kartierung der Gesamtdeposition, (3) der Beschaffung hinreichender Grundlagendaten zur Kartierung von Schwermetall-Gesamtdepositionen, (4) der gesicherten zeitlichen Fortschreibung von Trends bzw. Erweiterung der Kartierungsarbeiten um Szenarien, u.a. im Hinblick auf die Erfordernisse, die sich innerhalb der Entwicklungen von Dynamischen Modellierungen ergeben, sowie (5) der Aufbereitung und Bereitstellung der Kartierungsergebnisse für weitere Fragestellungen der Bewertung der Belastungssituation, der Risikoabschätzung, Planung, Sicherstellung nachhaltiger Entwicklung und Formulierung von Umweltqualitätszielen auf unterschiedlichem räumlichen Maßstab.

References

Asman W.A.H (1992). Ammonia emissions in Europe: Updated emission and emission variations. RIVM, Bilthoven, The Netherlands. Report no. 228471008.

Asman W.A.H. and van Jaarsveld J.A. (1992). A variable-resolution transport model applied for NH_X for Europe. *Atmospheric Environment 26A:* 445-464.

Baart A.C. and Diederen H.S.M.A.(1991). Calculation of the atmospheric deposition of 29 contaminants to the Rhine catchment area. *TNO, Delft, The Netherlands. TNO Report R 91/219.*

Baldocchi D.D., Hicks, B.B. and Camara, P. (1987). A canopy stomatal resistance model for gaseous deposition to vegetated surfaces. *Atmospheric Environment 21:* 91-101.

Baldocchi, D.D. (1988). A multi-layer model for estimating sulfur dioxide deposition to a deciduous oak forest canopy. *Atmospheric Environment 22:* 869-884.

Baldocchi, D.D. (1993). Deposition of gaseous sulfur compounds to vegetation. *In Sulfur Nutrition and Assimilation and Higher Plants (eds. Kok, L.J. et al.),* pp. 271-293, SGP Academic, The Hauge, Netherlands.

Beljaars A.C.M. and Holtslag A.A.M. (1990). Description of a software library for the calculation of surface fluxes. *Environmental Software, 5:* 60-68.

Benkovitz, C.M., Berkowitz, C.M., Easter, R.C., Nemesure, S., Wagner, R. and Schwartz, S.E. (1994). Sulfate over the North Atlantic and adjacent continental regions: evaluation for October and November 1986 using a three-dimensional model driven by observation-derived meteorology. *Journal of Geophysical Research 99:* 20725-20756.

BGR (1998). Digitales Höhenmodell. Bundesanstalt für Geologie und Rohstoffe, Hannover.

Bleeker A., Draaijers G.P.J., Klap J.M. & Jaarsveld J.A. van (2000). Deposition of acidifying components and base cations in Germany in the period 1987-1995. *Bilthoven, RIVM, report no. 722108027.* 124 p.

Branding, A. (1997). Die Bedeutung der atmosphärischen Deposition für die Forst- und Agrarökosysteme der Bornhöveder Seenkette. Dissertation im Geographischen Insitut d. Univ. Kiel. *EcoSys. Suppl. Bd. 14, Vorabdruck.* 117 p.

Brook, J.R., Zhang, L., Di-Giovanni, F. and Padro, J. (1999). Description and evaluation of a model of deposition velocities for routine estimates of air pollutant dry deposition over North America. Part I: model development. *Atmospheric Environment 33:* 5037-5051.

CCE (2001). Modelling and Mapping of Critical Thresholds in Europe. *Status Report 2001. Edited by: Posch, M., de Smet, P.A.M., HettelinghJ.P., Downing, R.J.. Coordination Center for Effects (CCE). National Institute of Public Health and the Environment, Bilthoven, Netherlands. RIVM Report No. 259101010.* ISBN No. 96-9690-092-7 [http://www.rivm.nl/cce/]

Chang, J.C., Brost, R.A., Isaksen, I.S.A., Madronich, P., Middleton, P., Stockwell, W.R. and Walcek, C.J. (1987). A three-dimensional Eulerian acid deposition model: physical concepts and formulation. *Journal of Geophysical Research 92:* 14681-14700.

Clarke, J.F., Edgerton, E.S. and Martin, B.E. (1997). Dry deposition calculations for the clean air status and trends network. *Atmospheric Environment 21:* 3667-3678.

Davidson, C.I. and Wu, Y.L. (1990). Dry deposition of particles and vapors. *In Acidic Precipitation (eds. S.E. Lindberg, A.L. Page and S.A. Norton), vol. 3. Springer-Verlag, New York.*

Dämmgen, U. (ed.) (1996). Untersuchungen zum chemischen Klima in Südostniedersachsen. Arbeiten des Teilprojektes A10 "Stoffflüsse in der bodennahen Atmosphäre" des Sonderforschungsbereichs 179 "Wasser- und Stoffdynamik in Agrar-Ökosystemen". *Landbauforschung Völkenrode, Sonderheft 170.* 333 p.

Dämmgen, U. (ed.) (2000). Versauernde und eutrophierende Luftvershmutzung in Nordost-Brandenburg. *Landbauforschung Völkenrode, Sonderheft 213.* 152 p.

Draaijers, G.P.J, Erisman, J.W (1995). A canopy budget model to estimate atmospheric deposition from throughfall measurements. *Water Air and Soil Pollution 85:* 122-134.

Draaijers, G.P.J., Van Ek, R. and Beuten, W. (1994). Atmospheric deposition in complex forest landscapes. *Boundary-Layer Meteorology 69:* 343-366.

Draaijers, G.P.J., van Leeuwen E.P., de Jong P.G.H. and Erisman J.W. (1996a). Deposition of base cations in Europe and its role in acid neutralization and forest nutrition. *RIVM, Bilthoven, The Netherlands. Report no. 722108017.*

Draaijers, G.P.J., Erisman, J.W., Spranger, T., Wyers, G.P. (1996b). The application of throughfall measurements for atmospheric deposition monitoring. *Athmospheric Environment 30(19):* 3349-3361.

Draaijers, G.P.J., Erisman, J.W., Spranger, T., Vel, E. (1998). Quality and uncertainty aspects of forest deposition estimation using throughfall, stemflow and precipitation measurements. *TNO-report TNO-MEP – R 98/093, Apeldoorn,* 73p.

Duyzer, J.H., Bouman, A.M.M., Aalst, R.M. van and Diederen, H.S.M.A. (1987). Assessment of dry deposition of NH3 and NH4+ over natural terrains. *In Proceedings of the EURASAP Symposium on Ammonia and Acidification. Bilthoven, The Netherlands, 13-15 April 1987.*

Duyzer, J.H., Verhagen, H.L.M., Westrate, J.H., Bosveld, F.C. and Vermetten, A.W.M. (1992). The dry deposition of ammonia onto a Douglas fir forest in the Netherlands. *Environmental Pollution 75:* 3-13.

Eugster, W. and Hesterberg, R. (1996). Transfer resistances of NO2 determined from eddy correlation flux measurements over a litter meadow at a rural site on the swiss plateau. *Atmospheric Environment 30(8):* 1247-1254.

Erisman, J.W. (1992). Atmospheric deposition of acidifying compounds in The Netherlands. *Ph.D. thesis, University of Utrecht, The Netherlands.*

Erisman, J.W. and D.D. Baldocchi (1994). Modelling dry deposition of SO_2. *Tellus, 46B:* 159-171.

Erisman, J.W. and G.P.J. Draaijers (1995). Atmospheric deposition in relation to acidification and eutrophication. *Studies in Environmental Science, 63, Elsevier, Amsterdam.*

Erisman, J.W. and Wyers G.P. (1993) On the interaction between deposition of SO_2 and NH_3. *Atmospheric Environment, 27A:* 1937-1949.

Erisman, J.W., van Elzakker, B.G. and Mennen, M. (1990). Dry deposition of SO_2 over grassland and heather vegetation in the Netherlands. *RIVM, Bilthoven, The Netherlands. Report no. 723001004.*

Erisman, J.W., Versluis, A.H., Verplanke, T.A.J.W., Haan, D. de, Anink, D., van Elzakker, B.G., Mennen, M.G. and van Aalst, R.M. (1993a). Monitoring dry deposition of SO2 in the Netherlands. *Atmospheric Environment, 27A:* 1153-1161.

Erisman, J.W., Mennen, M., Hogenkamp, J., Kemkers, E., Goedhart, D., Pul, A. and Boermans, J. (1993b). Dry deposition over the Speulder forest. *Proceedings of the CEC/BIATEX workshop, Aveiro, Portugal, 4-7 May 1993.*

Erisman, J.W., Potma C., Draaijers G.P.J., van Leeuwen E.P. and van Pul W.A.J. (1994a). A generalised description of the deposition of acidifying pollutants on a small scale in Europe. *Proceedings EUROTRAC symposium on Transport and transformation of pollutants in the Troposphere, Garmisch Partenkirchen, 11-15 April 1994.*

Erisman, J.W., Potma, C., Draaijers, G.P.J., Duyzer, J.H., Hofschreuder, P., van Leeuwen N., Römer, F.G., Ruijgrok W. and Wyers, G.P. (1994b). Contribution of aerosol deposition to atmospheric deposition and soil loads onto forests. Final Report of the Aerosol Project executed within the third phase of the Dutch Priority Programme on acidification. *RIVM Report no. 722108005. National Institute of Public Health and the Environment (RIVM), Bilthoven, TheNetherlands.*

Erisman, J.W., Mennen, M.G., Fowler, D., Flechard, C.R., Spindler, G., Grüner, Duyzer, J.H., Ruigrok, W. and Wyers, G.P. (1996). Towards development of a deposition monitoring network for air pollution of Europe. *RIVM Report no. 722108015, National Institute of Public Health and the Environment, Bilthoven, The Netherlands, April 1996.*

Erisman, J.W., Mennen, M.G., Fowler, D., Flechard, C.R., Spindler, G., Grüner, A., Duyzer, J.H., Ruigrok, W. and Wyers, G.P. (1997). Deposition monitoring in Europe. *Environ. Monit. and Assessment 53:* 279-295.

Farquhar, G.D., Firth, P.M., Wetselaar, R. and Wier, B. (1980). On the gaseous exchange of ammonia between leaves and the environment: determination of the ammonia compensation point. *Plant Physiol. 66:* 710-714.

Fowler, D. (1978). Dry deposition of SO2 on agricultural crops. *Atmospheric Environment, 12:* 369-373.

Fowler, D. (1985). Dry deposition of SO2 onto plant canopies. *In Sulfur dioxide and vegetation (Eds. Winner, W.E., Mooney, H.A. and Goldstein, R.A.). Stanford University Press, California*. pp. 75-95

Fowler, D. and Unsworth, M.H. (1979). Turbulent transfer of sulfur dioxide to wheat crop. *Quarterly Journal of the Royal Meteorological Society 105:* 767-784.

Fowler, D., Cape, J.N. and Unsworth, M.H. (1989). Deposition of atmospheric pollutants on forests. *Phil. Trans. R. Soc. Lond. B324:* 247-265.

Fowler, D., Duyzer, J.H. and Baldocchi, D.D. (1991). Inputs of trace gases, particles and cloud droplets to terrestrial surfaces. *Proc. R. Soc. Edinburgh 97B:* 35-59.

Franken, G., Puhlmann, M., Duijnisveld, W.H.M., Böttcher, J., Strebel, O. (1997). Auswirkungen saurer atmosphärischer Depositionen bei Nadelwald auf Stoffanlieferung an das Grundwasser und Stoffumsetzungen in einem Aquifer aus basenarmen Sanden (Fallstudie Modellgebiet Fuhrberger Feld). *Wasserforschung. Forschungsbericht 102 02 629. Im Auftrag des Umweltbundesamtes.* 272 S.

Garland, J.A. (1977). The dry deposition of sulfur dioxide to land and water surfaces. *Proc. R. Soc. Lond. A354:* 245-268.

Garland, J.A. (1978). Dry and wet removal of sulfur from the atmosphere. *Atmospheric Environment 12:* 349.

Garland, J.A. and Branson, J.R. (1977). The deposition of sulfur fioxide to pine forest assessed by a radioactive tracer method. Tellus 29, 445-454.

Ganzeveld, L. and Lelieveld, J. (1995). Dry deposition parameterization in a chemistry general circulation model and its influence on the distribution of reactive trace gases. *Journal of Geophysical Research 100:* 20999-21012.

Gauger, Th.; Köble, R. Smiatek, G. (1997). Kartierung kritischer Belastungskonzentrationen und –raten für empfindliche Ökosysteme in der Bundesrepublik Deutschland und anderen ECE-Ländern. *Endbericht zum Forschungsvorhaben 106 01 061 im Auftrag des Umweltbundesamtes. Institut für Navigation der Universität Stuttgart. - Teil 1: Deposition Loads.* 126 p. - *Teil 2: Critical Levels.* 75 p. - *Teil 3: Informationssystem CANDIS.* 27 p.

Gauger, Th.; Anshelm, F., Köble, R. (2000). Kritische Luftschadstoff-Konzentrationen und Eintragsraten sowie ihre Überschreitung für Wald und Agrarökosysteme sowie naturnahe waldfreie Ökosysteme. *Forschungsvorhaben im Auftrag des BMU/UBA, FE-Nr. 297 85 079. Institut für Navigation, Universität Stuttgart. Teil 1: Deposition Loads.* 140 p. - *Teil 2: Critical Levels.* 57 p. [http://www.nav.uni-stuttgart.de/German/Forschung/CriticalLoads/deutsch.html]

Gravenhorst G, Kreilein K, Schnitzler K-G, Ibrom A, Nützmann E (2000) Trockene und nasse Deposition von Spurenstoffen in der Atmosphäre. *In Gudreian G (ed.) Handbuch der Umweltveränderungen und Ökotoxikologie. Bd. 1B: Atmosphäre - Aerosol/ Multiphasenchemie – Ausbreitung und Deposition von Spurenstoffen – Auswirkungen auf Strahlung und Klima. Springer-Verlag. Berlin, Heidelberg, New York.* 147-247.

Harley, R.A., Russell, A.G., McRae, G.J., Cass, G.R. and Seinfeld, J.H. (1993). Photochemical modeling of the Southern California Air Quality Study. *Environmental Science and Technology 27:* 378-388.

Hass, H., Jakobs, H.J. and Memmesheimer, M. (1995). Analysis of a regional model (EURAD) near surface gas concentration predictions using observations from networks. *Meteorology and Atmospheric Physics 57:* 173-200.

Hicks, B.B. and Garland, J.A. (1983). Overview and suggestions for future research on dry deopsition. *Precipitation Scavenging, dry deposition and resuspension (ed. Pruppacher, Semonin and Slinn), Elsevier, New York:* 1429-1432.

Hicks B.B., Baldocchi D.D., Meyers T.P., Hosker R.P. Jr. and Matt D.R. (1987). A preliminary multiple resistance routine for deriving dry deposition velocities from measured quantities. *Water Air and Soil Pollution, 36:* 311-330.

Hicks, B.B. and Lenschow, D.H. (eds.) (1989). Global Tropospheric Chemistry, Chemical Fluxes in the Global Atmosphere. *Report prepared for the National Center for Atmospheric Research Boulder, CO.*

ICP Modelling and Mapping (2002). [http://www.oekodata.com/icpmapping/index.html]

Jarvis P.G., James G.B. and Landsberg J.J. (1976). Coniferous forest. *In J.L. Monteith (ed.), Vegetation and the atmosphere –2. Academic Press, New York.*

Jarvis, P.G. and Morison, J.I.L. (1981). The control of transpiration and photosynthesis by stomata. *In Stomatal Physiology (ed. Jarvis, P.G. and Mansfield, T.A.). Cambridge Univ. Press, Cambridge.* pp. 248-279

Jensen-Huß, K. (1990). Raumzeitliche Analyse atmospärischer Stoffeinträge in Schleswig-Holstein und deren ökologische Bewertung. *Dissertation an d. Math.-Naturwiss. Fakultät d. Chr.-Albr.-Universität zu Kiel.* 212 p.

Kane M.M., Rendell A.R. and Jickells T.D. (1994). Atmospheric scavenging processes over the North Sea. *Atmospheric Environment, 28:* 2523-2530.

Kallweit, D. (1997). Geeignete Sammelverfahren zur Erfassung von Depositionen und Anwendung im UBA-Messnetz. *In: LANDESANSTALT FÜR UMWELTSCHUTZ BADEN-WÜRTTEMBERG (HRSG.): Ermittlung atmosphärischer Stoffeinträge in den Boden. Nutzung neuer Sammel- und Nachweisverfahren. Fachgespräch am 27.11.1996 in Karlsruhe. Handbuch Boden 5:* 41-47.

Köble, R., Spranger, T. (1999). Definition und Kartierungsmethoden. *In Nagel, H.-D; Gregor, H.-D. [Hrsg.]: Ökologische Belastungsgrenzen – Critical Loads & Levels. Ein internationales Konzept für die Luftreinhaltepolitik.* Springer-Verlag.

Leucken, D.J., Berkowitz, C.M. and Easter, R.C. (1991). Use of a three-dimensional cloud-chemistry model to study the transatlantic transport of soluble sulfur species. *Journal of Geophysical Research 96:* 22477-22490.

Lovett, G.M. (1994). Atmospheric deposition of nutrients and pollutants in North America: An ecological perspective. *Ecological Applications 4:* 629-650.

Lövblad, G. and Erisman, J.W. (1992). Deposition of nitrogen in Europe. *In Proc. Critical Loads for Nitrogen, Lökeberg, Sweden, 6-10 April 1992 (eds. Grennfelt, P. and Thörnelöf, E.), Nordic Council of Ministers, Copenhagen, Denmark. Report no. Nord 1992:41*

Lövblad G., Erisman J.W. and Fowler D. (eds.) (1993). Models and methods for the quantification of atmospheric input to ecosystems. *Proceedings of an international workshop on the deposition of acidifying substances, Göteborg (Sweden), 3-6 November 1992. The Nordic Council of Ministers. Copenhagen. Report No. Nord 1993:573.*

Lux, W. (1993). Das PROGRAMM "Biologische Umweltkontrolle durch Waldökosysteme" (Teil 1). *Umweltbehörde Hamburg, Fachamt für ökologische Forst- u. Landwirtschaft. Institut für Bodenkunde, Hamburg.* 53 p.

Massman, W.J., Pederson, J., Delany, A., Grantz, D., den Hartog, G., Neumann, H.H., Oncley, S.P., Pearson Jr., R. and Shaw, R.H. (1994). An evaluation of the regional acid deposition model surface module for ozone uptake at three sites in the San Joaquin Valley of California. *Journal of Geophysical Research 99:* 8281-8294.

Meyers, T.P., Hicks, B.B., Hosker, R.P., Womack, J.D. and Satterfield, L.C. (1991). Dry deposition inferential measurement techniques-II. Seasonal and annual deposition rates of sulfur and nitrate. *Atmospheric Environment 25A:* 2361-2370.

Meyers, T.P., Finklestein, P., Clarke, J., Ellestad, T. and Sims, P.F. (1998). A multi-layer model for inferring dry deposition using standard meteorological measurements. *Journal of Geophysical Research 103:* 22645-22661.

Monteith, J.L. (1975). Vegetation and the atmosphere. *Academic Press, London, England.*

Müller-Westermeier, G. (1995). Numerisches Verfahren zur Erstellung klimatologischer Karten. *Berichte des Deutschen Wetterdienstes (DWD), Nr. 193.* Offenbach. 18 S.

NAGEL, H.-D; GREGOR, H.-D. [Eds.] (1999). Ökologische Belastungsgrenzen – Critical Loads & Levels. Ein internationales Konzept für die Luftreinhaltepolitik. *Springer-Verlag*. 320 p. (in German)

Nagel, H.-D., Becker, R., Eitner, H., Kunze, F., Schlutow, A. und Schütze, G. (2000). Kartierung von Critical Loads von Säure, eutrophierendem Stickstoff, POP's und Schwermetallen in Waldökosysteme und naturnahe waldfreie Ökosysteme zur Unterstützung von UN/ECE-Protokollen. *Abschlussbericht zum F/E-Vorhaben 29773011 des Umweltbundesamtes, Berlin.* [http://www.oekodata.com/eng/html/critical_loads_eng.html] [http://www.oekodata.com/deu/html/critical_loads.html] (in German)

Nagel, H.-D., Becker, R., Eitner, H., Kunze, F., Schlutow, A. und Schütze, G. (2002). Kartierung von Critical Loads für Säur und Stickstoff. Zwischenbericht zum F&E-Vorhaben 200 85 212 im Auftrag des Umweltbundesamtes.

NEGTAP (2001). Transboundary Air Pollutin: Acidification, Eutrophication and Ground-Level Ozone in the UK. *Report prepared by the National Expert Group on Transboundary Air Pollution at CEH Edinbourgh on behalf of the UK Department for Environment, Food and Rural Affairs, Scottish Executive, The National Assembly for Wales/Cynulliad Cenedlaethol Cymru, Department Of the Environment in North Ireland.*314 p. [http://www.nbu.ac.uk/negtap/]

NOAA (1997). NOAA library of input data for 'Big-leaf' and 'Multi-layer' models. *ATDD, NOAA, Oak Ridge, TN.*

Olson, J.S., J.A. Watts, and L.J. Allison, 1985. Major World Ecosystem Complexes Ranked by Carbon in Live Vegetation: A Database NDP-017*, Carbon Dioxide Information Center, Oak Ridge Laboratory, Oak Ridge, Tennessee.*

Padro, J., den Hartog, G. and Neumann, H.H. (1991). An investigation of the ADOM dry deposition module using summertime O3 measurements above a deciduous forest. *Atmospheric Environment 25A:* 1689-1704.

Pederson, J.R., Massman, W.J., Mahrt, L., Delany, A., Oncley, S., den Hartog, G., Neumann, H.H., Mickle, R.E., Shaw, R.H., Paw, U.K.T., Grantz, D.A., MacPherson, J.I., Desjardins, R., Schuepp, P.H., Pearson Jr., R. and Arcado, T.E. (1995). California Ozone Deposition Experiment: methods, results, and opportunities. *Atmospheric Environment 29:* 3115-3132.

Perry, J.H. (ed.) (1950). Chemical Engineers Handbook. *3rd edn. McGraw-Hill, New York.*

Pleim, J.E., Venkatram, A. and Yamartino, R. (1984). ADOM/TADAP Model Development Program. *The Dry Deposition Module, vol. 4. Ontario Ministry of the Environment, Rexdale, Canada.*

Reynolds, B., D. Fowler, R.I. Smith and Hall, J.R. (1997). Atmospheric inputs and catchment solute fluxes for major ions in five Welsh upland catchments. *Journal of Hydrology, 194:* 305-329.

Ruijgrok, W., Davidson, C.I. and Nicholson, K.W. (1995). Dry deposition of particles. Implications and recommendations for mapping of deposition over Europe. *Tellus 47B:* 587-601.

Ruijgrok, W., Tieben , H. and Eisinga, P. (1997). The dry deposition of particles to a forest canopy: a comparison of model and experimental results. *Atmospheric Environment 31:* 399-415.

Sachs, L. (1989). Angewandte Statistik. Anwendung statistischer Methoden. *Springer-Verlag. Berlin, Heidelberg, New York, Tokyo.* 552 S.

Sager (1997). Die Niedersclagsbeschaffenheits-Richtlinie der Länderarbeitsgemeinschaft Wasser (LAWA). *In Landesanstalt für Umweltschutz Baden-Württemberg (ed): Ermittlung atmosphärischer Stoffeinträge in den Boden. Nutzung neuer Sammel- und Nachweisverfahren. Fachgespräch am 27.11.1996 in Karlsruhe. Handbuch Boden 5*: pp. 49-54.

SAI (1996). User's Guide to the Variable-Grid Urban Airshed Model (UAM-V). *SYSAPP-96-95/27r, Systems Applications International, San Rafael, CA.*

Sandnes, H. (1993). Calculated budgets for airborne acidifying components in Europe, 1985, 1987, 1988. 1989, 1990, 1991 and 1992. *EMEP report 1/93. MSC-West, Oslo, Norway.*

Schimmig, C.-G. (1991). Wasser-, Luft-, Nähr- und Schadstoffdynamik charakteristischer Böden Schleswig-Holsteins. Dissertation. *Schriftenr. Nr. 13 aus dem Institut für Pflanzenern. und Bodenkunde der Chr.-Albr.-Universität zu Kiel.* 163 S.

Schulze, E.D. and Hall, A.E. (1982). Stomatal responses, water loss and CO2 assimilation rates of plants in contrasting environments. *In Encyclopedia of Plant Physiology, vol 12B (ed. Lange, O.L., Nobel, P.S., Osmond, C.B. and Ziegler, H.),* pp. 181-230. Springer, Berlin.

Sehmel, G.A. (1980). Particle and gas dry deposition: a review. *Atmospheric Environment 14:* 983-1011.

Simon, K.-H., Westendorff, K. (1991). Stoffeinträge mit dem Niederschlag in Kiefernbestände des norddeutschen Tieflandes in den Jahren 1985-1989. *Beitr. Forstwissenschaft 25, 4.* pp. 177-180

Slinn, W.G.N. (1982). Predictions of particle deposition to vegetative canopies. *Atmospheric Environment, 16:* 1785-1794.

Spranger, T. (1992). Erfassung und ökosystemare Bewertung der atmosphärischen Deposition und weiterer oberirdischer Stoffeinflüsse im Bereich der Bornhöveder Seenkette. *Eco-Sys, Beiträge zur Ökosystemforschung. Suppl. Bd. 4.* 153 S.

Spranger, T., Hollwurtel, E., Poetzsch-Heffter, F. and Branding, A. (1994). Dry deposition Estimates from Two Different Inferential Models as compared to Net Throughfall Measurements. A contribution to the subproject BIATEX. *In Proceedings of EUROTRAC Symposium '94 (ed. P.M. Borrell et al.), SPB Academic Publishing bv, The Hague, The Netherlands.* pp. 615-619.

Spranger, T., Kunze, F., Gauger, Th., Nagel, D., Bleeker, A., Draaijers, G.: (2001). Critical Loads Exceedances in Germany and their Difference on the Scale of Input Data. *Water, Air, and Soil Pollution. Focus 1. 2001:* 335-351.

Sutton, M.A. (1990). The surface-atmosphere exchange of ammonia. *Ph. D. thesis, University of Ëdinburgh, Scotland.*

Sutton, M.A., Moncrieff, J.B. and Fowler, D. (1992). Deposition of atmospheric ammonia to moorlands. *Environ. Pollut. 75:* 15-24.

Thom, A.S. (1975). Momentum, mass and heat exchange of plant communities. *In Vegetation and Atmosphere, (Ed. Monteith J.L), Academic Press, London.* pp. 58-109

Turner, N.C. and Begg, J.E. (1974). Stomatal behavior and water status of maize, sorghum and tobacco under field conditions. I: at high soil water potential. *Plant Physiol. 51:* 31-36.

Tuovinen, J.P., Aurela, M. and Laurila, T. (1998). Resistances to ozone deposition to flark fen in the northern aapa mire zone. *Journal of Geophysical Research 103:* 16953-16966.

UBA (1996). Manual on Methodologies and Criteria for Mapping Critical Levels/Loads and geographical areas where they are exceeded. *UBA-Texte 71/96.* [http://www.umweltbundesamt.de/mapping/] [http://www.oekodata.com/icpmapping/html/publication.html]

UBA (1997). Ergebnisse täglicher Niederschlagsanalysen in Deutschland von 1982 bis 1995. *UBA-Texte 10/97. Umweltbundesamt Berlin.* 452 S. und Anhang.

Ulrich, B. (1983). Interaction of forest canopies with atmospheric constituents: SO_2, alkali and earth alkali cations and chloride. *In Ulrich B. and J. Pankrath (eds), Effects of accumulation of air pollutants in forest ecosystems, Reidel, Dordrecht, The Netherlands:* 33-45.

Ulrich, B. (1991). Rechenweg zur Schätzung der Flüsse in Waldökosystemen. Identifizierung der sie bedingten Prozesse. *Berichte des Forschungszentrums Waldökosysteme, Reihe B, Bd. 24:* 204-210.

UN ECE and EC 2001. de Vries W., Reinds G.J., van der Salm C., Draaiers G.P.J., Bleeker A., Erisman J.W., Auée J, Gundersen P., Kristensen H.L., van Dobben H., de Zwart D., Derome J., Voogd J.C.M., Vel E.: Intensive Monitoring of Forest Ecosystems in Europe. *ICP Forest, FIMCI. Technical Report 2001. Brussels, Geneva 2001.* 177p. [http://www.fimci.nl/]

van den Hout K.D. (ed.) (1994). The Impact of atmospheric deposition of non-acidifying compounds on the air quality of European forest soils and the North Sea. *Main report of the ESQUAD project. Delft, The Netherlands. TNO report R93/329.*

van Jaarsveld J.A. (1989). A model approach for assessing transport and deposition of acidifying components on different spatial scales. *In: Changing composition of the Troposphere: Special environmental report no.17. Geneva, Swizerland. WMO-no. 724.* p. 197-204.

van Jaarsveld J.A. (1990). An Operational atmosferic transport model for Priority Substances; specification and instructions for use. *RIVM, Bilthoven, The Netherlands. Report no. 222501002.*

van Jaarsveld J.A. (1995). Modelling the long-term atmospheric behaviour of polluants on various spatial scales. *Ph.D. thesis. University of Utrecht, The Neterlands. RIVM, Bilthoven, The Netherlands. Report no. 722501005.*

van Jaarsveld J.A., van Aalst R.M. and Onderdelinden D. (1986). Deposition of metals from the atmosphere into the North Sea: model calculations. *RIVM, Bilthoven, The Netherlands. Report no. 842015002.*

van Pul, W.A.J. and Jacobs, A.F.G. (1993). The conductance of a maize crop and the underlying soil to ozone under various environmental conditions. *Boundary Layer Met.*

van Pul W.A.J., Erisman J.W., van Jaarsveld J.A. and de Leeuw F.A.A.M. (1992). High resolution assessment of acid deposition fluxes. *In Acidification Research, Evaluation and* *policy applications (edited by T. Schneider), Studies in Environmental Science, Elsevier, Amsterdam.*

van Pul W.A.J., Potma C., van Leeuwen E.P., Draaijers G.P.J. and Erisman J.W. (1995). EDACS: European Deposition maps of Acidifying Components on a Small scale. Model description and results. *RIVM report no. 722401005, National Institute of Public Health and the Environment, Bilthoven, The Netherlands.*

Veltkamp, A.C. and Wyers, G.P. (1997). The contribution of root-derived sulfur to sulfate in throughfall in a Douglas fir forest. *Atmospheric Environment 31:* 1385-1391.

Venkatram, A., Karamchandi, P.K. and Misra, P.K. (1988). Testing a comprehensive acid deposition model. *Atmospheric Environment 22:* 737-747.

Vermetten, A.W.M., Hofschreuder, P., Duyzer, J.H., Diederen, H.S.M.A., Bosveld, F.C. and Bouten, W. (1992). Dry deposition of SO2 onto a stand of Douglas fir: the influence of canopy wetness. *In Proceedings of the 5th IPSASEP-conference, Richland WA, USA, June 15-19, 1991 (eds. Schwartz, S.E. and Slinn, W.G.N.), Hemisphere Publishing Corporation, Washington.* pp. 1403-1414.

Voldner, E.C., Barrie, L.A. and Sirois, A. (1986). A literature review of dry deposition of oxides of sulphur and nitrogen with emphasis on long-range transport modeling in North America. *Atmospheric Environment 20:* 2101-2123.

Walmsley, J.L. and Wesely, M.L. (1996). Modification of coded parameterizations of surface resistances to gaseous dry deposition. *Atmospheric Environment 30:* 1181-1188.

Warmenhoven J.P., Duiser J.A., de Leu, L.Th. and Veldt C.(1989). The contribution of the input from the atmosphere to the contamination of the North Sea and the Dutch Wadden Sea. *TNO, Delft, The Netherlands. TNO Report R 89/349A.*

Wesely, M.L. (1989). Parametrization of surface resistances to gaseous dry deposition in regional-scale numerical models. *Atmospheric Environment, 23:* 1293-1304.

Wesely, M.L. and Hicks, B.B. (1977). Some factors that affect the deposition rates of sulfur dioxide and similar gases on vegetation. *J. Air Pollut. Control Assoc. 27:* 1110-1116.

Wesely, M.L. and Hicks, B.B. (2000). A review of the current status of knowledge on dry deposition. *Atmospheric Environment 34:* 2261-2282.

Wesely, M.L., Sisteron, D.L., Hart, R.L., Drapapcho, D.L. and Lee, I.Y. (1989). Observations of nitric oxide fluxes over grass. *J. atmos. Chem. 9:* 447-463.

Wilson, M.F., and A. Henderson-Sellers (1985). A Global Archive of Land Cover and Soils Data for Use in General Circulation Climate Models. *Journal of Climatology, vol. 5:* 119-143.

Yamartino, R.J., Scire, J.S., Carmichael, G.R. and Chang, Y.S. (1992). The CALGRID mesoscale photochemical grid model-I. Model evaluation. *Atmospheric Environment 26A:* 1493-1512.

Acronyms

ADOM: Acid Deposition and Oxidant Model.

BF: Bulk deposition Flux

CALGRID: California Photochemical Grid Model [http://www.arb.ca.gov/eos/soft.html#calgrid]

CBM: Canopy Budget Model calculaions. An overview of canopy model calculations can be found in DRAAIERS ET AL. 1998, an improved CBM can be found in UN ECE AND EC 2001.

CCE: Coordination Center for Effects, established at RIVM in Bilthoven, The Netherlands [http://www.rivm.nl/cce/], [http://arch.rivm.nl/cce/]

CLRTAP: UN/ECE Convention on Long-range Transboundary Air Pollution.
1979 Convention on long-range transboundary air pollution (1996). Published by the United Nations Economic Commissionfor Europe (UN ECE).
[http://www.unece.org/env/lrtap/]

CODE: California Ozone Deposition Experiment

CORINAIR: CORe INventory of AIR emissions. CORINAIR is a project performed since 1995 by the European Topic Centre on Air Emissions under contract to the European Environment Agency; European Union (EU) emission inventory programme [http://etc-acc.eionet.eu.int/databases/#emisdocdata]

CORINE Land Cover: The CORINE land cover database provides a pan-European inventory of biophysical land cover, using a 44 class nomenclature. It is made available on a 250m by 250m grid database which has been aggregated from the original vector data at 1:100 000. CORINE land cover is a key database for integrated environmental assessment. [http://dataservice.eea.eu.int/dataservice/metadetails.asp?table=landcover&i=1]

DEADM: Dutch Empirical Acid Deposition Model

DEHM: A new comprehensive 3-D air pollution model. This model will replace the DEOM model during the autumn 2002.
[http://www.dmu.dk/AtmosphericEnvironment/thor/intro_uk.html]

DEM: Danish Eulerian Model [http://www.dmu.dk/AtmosphericEnvironment/DEM/index.htm]

DEOM: Danish Eulerian Operational Model. DEOM is based on the DEM model.
[http://www.dmu.dk/AtmosphericEnvironment/thor/intro_uk.html]

DEPAC: DEPosition of Acidifying Components. The dry deposition sub-model that was built into IDEM is based on the DEPAC module.

DWD: Deutscher WetterDienst, the German meteorological survey [http//:www.dwd.de/]

ECHAM: European Centre HAmburg Model

ECMWF MARS: European Centre for Medium-Range Weather Forecasts
[http://www.ecmwf.int/] Meteorological Archival Retrieval System
[http://www.ecmwf.int/services/archive/]

ECMWF: European Centre for Medium-Range Weather Forecasts [http://www.ecmwf.int/]

ECN: Netherlands Energy Research Foundation, Petten [http://www.ecn.nl/index.en.html]

EDACS: European Deposition of Acidifying Components on Small scale (VAN PUL ET AL., 1995)

EMEP: The Cooperative Programme for Monitoring and Evaluation of the Long-range Transmission of Air Pollutants in Europe. EMEP is a scientifically based and policy driven program under the Convention on Long-Range Transboundary Air Pollution for international co-operation to solve transboundary air pollution problems. [http://www.unece.org/env/emep/welcome.html]

EURAD: EURopean Air Pollution Dispersion model system [http://www.eurad.uni-koeln.de/index_e.html]

EUTREND: European version of the OPS model (VAN JAARSVELD, 1990, 1995)

GChM: Global CHemistry Model [http://www.pnl.gov/atmos_sciences/as_acp3.html]

GIS: Geographic Information System

GrADS Grid Analysis and Display System [http://grads.iges.org/grads/grads.html]

GRIB (GRId in Binary format) is the new gridded data standard from the World Meteorological Organization (WMO). [http://www-imk.fzk.de/imk2/kasima/aktuelles/grib/]

ICP Modelling and Mapping: UN ECE International Co-operative Program on Modelling and Mapping of Critical Loads & Levels and Air Pollution Effects, Risks and Trends (ICP M&M) [http://www.oekodata.com/icpmapping/index.html]

ICP: UN ECE International Co-operative Program

IDEM: Integrated DEposition Model. The dry deposition of the components considered in this project is calculated by a model called IDEM using the so called dry deposition inference method (ERISMAN, 1992; ERISMAN & BALDOCCHI, 1994; VAN PUL ET AL, 1992, 1995).

IER: Institute of Energy Economics and the Rational Use of Energy, University of Stuttgart [http://www.ier.uni-stuttgart.de]

INS: Institute of Navigation, Stuttgart University [http://www.nav.uni-stuttgart.de]

KNMI: Netherlands Meteorological Institute [http://www.knmi.nl/]

LRT: Long-range transport (models, modelled air concentration)

NCAR: American National Centre for Atmospheric Research [http://www.ncar.ucar.edu/ncar/]

NEGTAP: National Expert Group on Transboundary Air Pollution at Centre for Ecology and Hydrology Edinburgh (CEH), UK.

NERI: National Environmental Research Institute, Denmark. The regional and hemispheric air pollution models DEM, DEOM and DEHM, have been developed at NERI, Department of Atmospheric Environment (ATMI). [http://www.dmu.dk/forside_en.asp]

NFC: National Focal Center [http://arch.rivm.nl/cce/collaborators.html]

ÖKO-DATA: Gesellschaft für Ökosystemanalyse und Umweltdatenmanagement mbH, Strausberg [http://www.oekodata.com/eng/index_eng.html]

OPS: Operational Priority Substances model. (VAN JAARSVELD, 1990)

RADM: Regional Acid Deposition Model [http://www.epa.gov/asmdnerl/radm.html]

RIVM: the National Institute of Public Health and the Environment (RijksInstituut voor Volksgezondheid en Milieu) in Bilthoven, The Netherlands [http://www.rivm.nl]

SF: StemFlow deposition flux

TF: ThroughFall deposition flux

TNO: Netherlands Organization for Applied Scientific Research [http://www.tno.nl]

TNO-MEP: TNO Institute of Environmental Sciences, Energy Research and Process Innovation, Appeldoorn [http://www.mep.tno.nl/homepage_eng_mep.html]

UAM: Urban Airshed Model [http://www.epa.gov/asmdnerl/urban.html]

UBA: Federal Environmental Agency (Umweltbundesamt), Berlin [http://www.umweltbundesamt.de]

WF: Wet-only deposition Flux

WGE: UN ECE Working Group on Effects

Acronyms of wet deposition data sources

BFH-EB: Bundesforschungsanstalt für Holz- und Forstwirtschaft; Eberswalde (Simon&Westendorff)

BGR: Bundesanstalt für Geowissenschaften und Rohstoffe; Hannover (Franken et.al)

BLFU: Bayerische Landesanstalt für Umweltschutz; München

BLFW: Bayerisches Landesamt für Wasserwirtschaft; München

BLWF: Bayerische Landesanstalt für Wald- und Forstwirtschaft, Abt. Forsthydrologie, Freising

CHMI: Czech Hydrometeorological Institute (Data provided via SLUG)

DDR-MD: Meteorologischer Dienst der DDR (via SLUG)

DWD: Deutscher Wetterdienst, Meteorologisches Observatorium Hohenpeißenberg

FAL: Bundesforschundsanstalt für Landwirtschaft BS-Völkenrode, FAL-AOE, Braunschweig (former Institut für agrarrelevante Klimaforschung; Müncheberg und Braunschweig) (DÄMMGEN)

FhG:.Fraunhofer gesellschaft für Umweltchemie und Ökotoxikologie, Schmallenberg, Grafschaft

FPA-SB: Forstplanungsanstalt des Saarlandes; Saarbrücken/Univ. des Saarlandes, ZFU, AG-Forst; Duttweiler/Saarbrücken

FVA-BW: Forstliche Versuchs- und Forschungsanstalt Baden-Württemberg; Freiburg i. B.

FVA-RP: Forstliche Versuchsanstalt Rheinland-Pfalz, Abt. Waldschutz; Trippstadt

FVFA-ST: Forstliche Versuchs- und Forschungsanstalt; Flechtingen

HLFWW: Hessische Landesanstalt f. Forsteinrichtung, Waldforschung und Waldökologie; Hannoversch Münden

IFT: Institut für Troposphärenforschung e.V., Abt. Chemie; Leipzig

LAFOP-BB: Landesanstalt für Forstplanung, Brandenburg; Potsdam

LAFOP-MV: Landesamt für Forstplanung; Schwerin

LANU-SH: Landesamt für Natur und Umwelt des Landes Schleswig-Holstein, Abteilung Gewässer; Flintbeck

LAUN-MV: Landesamt für Umwelt und Natur, Abt. Immissionsschutz; Güstrow-Gülzow

LFU-BW: Landesanstalt für Umweltschutz Baden-Württemberg, Ref. 31 Luftreinhaltung Klima; Karlsruhe

LfU-ST: Landesamt für Umweltschutz Sachsen-Anhalt, Abt.5, Halle

LÖBF/LAFAO-NW: Landesanstalt für Ökologie, Bodenordnung und Forsten/Landesamt für Agrarordnung (former LÖLF), Dez. Bioindikation, Biomonitoring; Recklinghausen

LUA-BB: Landesumweltamt Brandenburg, Nebenstelle Lauchhammer

LUA-NW: Landesanstalt für Umweltschutz (LUA, former LIS), Nordrhein-Westfalen, Abt. 3; Essen

LWF-TN: Landesanstalt für Wald und Forstwirtschaft, Thüringen; Gotha

NFVA: Niedersächsische Forstliche Versuchsanstalt, Abt. Umweltkontrolle; Göttingen

NLÖ-H: Niedersächsisches Landesamt für Ökologie, Dez.63 Luftreinhaltung, Dr. K.-P. Giesen; Hannover

NLÖ-HI: Niedersächsisches Landesamt für Ökologie, Abt. 6 Immissionsschutz; Hildesheim

SenV-B.: Senatsverwaltung für Stadtentwicklung und Umweltschutz, Abt. III A 31; Berlin

SLAF: Sächsische Landesanstalt für Forsten; Graupa

SLUG: Sächsische Landesanstalt für Umwelt und Geologie, Abt. L1 Luft-Lärm-Strahlen; Radebeul

STUA-SH (former GAA-SH): Staatliches Umweltamt Itzehoe, Lufthygienische Überwachung Schleswig-Holstein, former Gewerbeaufsichtsamt Schleswig-Holstein, Dez. Luftqualitätsüberwachung

TU Wien: Technische Universität Wien, Institut für Analytische Chemie, Abt. Umweltanalytik

TU-DD: Technische Universität Dresden, Institut für Pflanzen- und Holzchemie; Tharandt

UBA-b (bulk): Umweltbundesamt, Fg. II 6,5 Meßnetz-Datenzentrale; Langen (former in Berlin)

UBA-wo (wet-only): Umweltbundesamt, Fg. II 6.5; Meßnetz-Datenzentrale; Langen

UFZ: Umweltforschungszentrum Leipzig-Halle GmbH, Sektion Analytik; Leipzig

Univ. F: Universität Frankfurt, Zentrum für Umweltforschung (ZUF)

Univ. HH: Freie und Hansestadt Hamburg - Umweltbehörde, Amt für Naturschutz und Landschaftspflege / Universität Hamburg, Institut für Bodenkunde (LUX)

Univ. KI: Christian-Albrechts-Universität Kiel, Öklologie-Zentrum (JENSEN-HUß; SCHIMMING; SPRANGER; BRANDING)

List of Authors

Dipl.-Geogr. Thomas Gauger	tel.: ++49-711-121-4177 fax: ++49-711-121-2755 gauger@nav.uni-stuttgart.de http://www.nav.uni-stuttgart.de	Institute of Navigation Stuttgart University (INS) Geschwister-Scholl-Str. 24 D D-70174 Stuttgart
Dipl.-Geogr. Frank Anshelm	tel.: ++49-711-121-3412 fax: ++49-711-121-2755 anshelm@nav.uni-stuttgart.de http://www.nav.uni-stuttgart.de	Institute of Navigation Stuttgart University (INS) Geschwister-Scholl-Str. 24 D D-70174 Stuttgart
Dipl.-Geogr. Hartmut Schuster	tel.: ++49-711-121-4177 fax: ++49-711-121-2755 schuster@nav.uni-stuttgart.de http://www.nav.uni-stuttgart.de	Institute of Navigation Stuttgart University (INS) Geschwister-Scholl-Str. 24 D D-70174 Stuttgart
Dr. Jan Willem Erisman	tel.: ++31-224-564-155 fax: ++31-224-568-488 erisman@ecn.nl http://www.ecn.nl/main	Energy research Center of the Netherlands, ECN P.O.Box 1 NL-1755 ZG Petten
MSc. Alex T. Vermeulen	tel.: ++31-224-564-194 fax: ++31-224-563-488 a.vermeulen@ecn.nl http://www.ecn.nl/main.html	Netherlands Energy Research Center, ECN P.O.Box 1 NL-1755 ZG Petten
Dr. Geert P.J. Draaijers	tel.: ++31-55-549-3233 fax. ++31-55-549-3252 g.p.j.draaiers@mep.tno.nl http://www.mep.tno.nl	TNO Institute of Environmental Sciences, Energy Research and Process Innovation, TNO-MEP P.O.Box 342 NL-7300 AH Apeldoorn
MSc. Albert Bleeker	tel.: ++31-55-549-3037 fax. ++31-55-549-3252 a.bleeker@mep.tno.nl http://www.mep.tno.nl	TNO Institute of Environmental Sciences, Energy Research and Process Innovation, TNO-MEP P.O.Box 342 NL-7300 AH Apeldoorn
Dr. Hans-Dieter Nagel	tel. ++49-3341-390-1920 fax: ++49-3341-390-1926 hans.dieter.nagel@oekodata.com http://www.oekodata.com/	ÖKO-DATA, Strausberg, Ecosystem Analysis and Environmental Data Management Hegermühlenstr. 58 D-15344 Strausberg